Contrast-Enhanced Mammography

Marc Lobbes
Maxine S. Jochelson
Editors

Springer

Contrast-Enhanced Mammography

Marc Lobbes • Maxine S. Jochelson
Editors

Contrast-Enhanced Mammography

Springer

Editors
Marc Lobbes
Department of Radiology and Nuclear Medicine
Maastricht University Medical Centre
Maastricht
Limburg
The Netherlands

Maxine S. Jochelson
Department of Radiology
Memorial Sloan Kettering Cancer Center
New York
NY
USA

ISBN 978-3-030-11062-8 ISBN 978-3-030-11063-5 (eBook)
https://doi.org/10.1007/978-3-030-11063-5

This Springer imprint is published by the registered company Springer Nature Switzerland AG
The registered company address is: Gewerbestrasse 11, 6330 Cham, Switzerland

Contents

A History of Contrast-Enhanced Mammography

1

John M. Lewin and Martin J. Yaffe

1.1 Full-Field Digital Mammography

When the first *full-field* digital mammography (FFDM) systems were introduced around 2000, there was great hope that they would significantly outperform the standard mammography technology of the time, film mammography (technically "screen-film" since a phosphorescent screen was used to convert the X-ray energy to visible light, which was then recorded on the film). Physics testing confirmed that digital mammography had better contrast resolution than film, an advantage that, it was hoped, would lead to better detection of breast cancers, especially in dense tissue. Unfortunately, clinical trials comparing digital to film mammography for screening showed, at best, only a limited advantage for digital mammography, mainly in premenopausal women and those with dense breasts [1, 2]. Cancers were still missed due to the masking effects of the overlap of dense breast tissue and also because some cancers simply did not provide inherent X-ray contrast from their surroundings. Researchers were motivated to build upon the platform of digital mammography technology to extend its capabilities and overcome these two limitations. Digital breast tomosynthesis addressed the overlap problem by reconstructing quasi 3D image sets from a set of digital projection images acquired over a range of

J. M. Lewin (✉)
The Women's Imaging Center, Denver, CO, USA
e-mail: John.Lewin@thewomensimagingcenter.net

M. J. Yaffe
Department Medical Biophysics, Sunnybrook Research Institute, University of Toronto, Toronto, ON, Canada

Department of Medical Imaging, Sunnybrook Research Institute, University of Toronto, Toronto, ON, Canada

Imaging Research Program, Ontario Institute for Cancer Research, Toronto, ON, Canada
e-mail: martin.yaffe@sri.utoronto.ca

M. Lobbes, M. S. Jochelson (eds.), *Contrast-Enhanced Mammography*,
https://doi.org/10.1007/978-3-030-11063-5_1

angles about the breast. Contrast-enhanced mammography (CEM) attacked both problems by providing contrast only where iodinated agent was concentrated, primarily in areas of tumor angiogenesis. Fortunately work on these technologies had started even before the results of the large clinical trials of digital versus film had been published.

1.2 Concepts/Background/Stimulus

1.2.1 Breast Angiography

The concept of using intravenous contrast with mammography was discussed in print long before the introduction of digital mammography made it feasible. Some of the early evidence that iodine contrast imaging would be useful in detecting breast cancers was provided by clinical studies on CT scanning of the breast, using a dedicated breast CT device, performed as early as 1975 at the Mayo Clinic [3] and by Chang et al. at the University of Kansas [4, 5]. On these early systems, the CT slices were 1 cm thick, the pixels were 1.56 mm in dimension, and doses were over 30 mGy. Breast CT was further validated at other centers in Europe and Asia in the 1990s [6, 7]. These studies demonstrated that intravenous iodinated contrast enhancement of breast cancers could be readily depicted on CT. These early scanners were used primarily as a proof of principle for computed tomography. In subsequent years emphasis in CT shifted to whole body systems, whose geometrical design was less suitable for imaging the breast.

Fritz et al. at the University of Kansas wrote a paper on optimizing beam quality for iodine contrast in 1983 [8]. Successful contrast enhancement with film mammography was not really practical, however, due to the fixed dynamic range of film compared to digital detectors as well as the cumbersome nature of performing image subtraction using film. Watt et al. in 1985 performed digital subtraction angiography (DSA) on 18 pre-biopsy patients at Henry Ford Hospital in Detroit using a standard body DSA system following an intravenous injection of ionic iodinated contrast. [9] Imaging was performed in the MLO projection with the patient prone and her breast compressed within a custom built device. The criteria for malignancy were the presence of tumor "blush" and of abnormal feeding vessels. DSA performed well, demonstrating seven out of the eight malignancies in the group and having only two false-positive results, a fibroadenoma and an area of fat necrosis.

1.2.2 Breast MRI

Breast MRI was introduced in the 1990s as the first practical contrast-enhanced imaging technique for breast cancer detection. It was immediately apparent that breast cancers would enhance with gadolinium-based contrast agents. It was also apparent, however, that benign tumors as well as normal tissue would often enhance, causing the technique to gain a reputation for low specificity. Breast MRI was also time-consuming, with scans lasting around one hour, and expensive, due to the high

cost of MRI machines. With technical improvements, primarily to the MRI equipment, but also to the technique itself, MRI has become a practical and useful tool, with extremely high sensitivity, although the high expense and claustrophobia in some women due to the confined magnet bore remain an issue.

It was initially not clear whether iodinated contrast, as would be used for breast CT, would work as well as gadolinium does with MRI. Because free gadolinium is toxic, gadolinium-based agents require the gadolinium to be chelated to a large anion. Iodinated agents differ in that it is only required that the iodine atoms be ionically bound to a medium-sized ion. Hence the diameter of a molecule of gadolinium chelate, such as is used in MRI contrast agents, is about five to ten times that of iodinated contrast agents. Additionally, a much smaller number of gadolinium atoms are needed to concentrate in a tumor for a detectible MRI signal change compared with the number of iodine atoms needed to for a detectible change in X-ray absorption. Whether or not iodinated contrast would work as well as gadolinium-based contrast was an open question.

1.3 Temporal Subtraction CEM

Although digital mammography had superior contrast resolution and effective dynamic range to film mammography, it was still a projection radiography technique, and its contrast resolution was inferior to that of CT or MRI. To improve the detection of small cancers radiologically, it was necessary to make use of new types of signals such as angiogenesis. The phenomenon of tumor angiogenesis had been noted as early as 1971 by Folkman [10] who observed that in malignant neoplasia, the tumors grow rapidly without the normal control mechanisms associated with healthy tissue. Upon reaching a size of 2–3 mm, they rapidly outgrow their supply of nutrients and oxygen and, in response, send out growth factors such as vascular endothelial growth factor (VEGF) which promotes the development of new microvasculature. These new vessels, which sprout from existing nearby vasculature, tend to be poorly constructed with loose intercellular junctions causing leakage of blood into the interstitial space. If an iodinated contrast agent has been injected into the bloodstream, it will also leak, and the increased local concentration of iodine can be imaged radiographically. The concentration of interstitially pooled iodine is related both to the microvascular density and the increased permeability associated with angiogenesis [11, 12].

Around 2000, at Sunnybrook Research Institute in Toronto, Martin Yaffe's group, aware of the successful application of digital subtraction angiography and having read the earlier reports of Watt, Ackerman, Chang, and Fritz in imaging the breast as described above [8, 9], asked if the improved imaging performance (spatial resolution and dynamic range) of the new digital mammography systems could be used effectively for contrast-enhanced detection of breast cancers.

The first question was—how much intravenous iodine was required to obtain adequate uptake in breast lesions. This question was addressed by reviewing a large number of CT examinations in which women had received contrast-enhanced thoracic CT. The researchers looked for focal areas of enhancement in the breast (mainly representative of benign lesions) on these scans and measured the elevation in CT

number in these areas. From this information it was possible to estimate the concentration of iodine in these lesions. With knowledge of the amount of injected iodine, it was possible to develop a quantitative relationship between the two. Maria Skarpathiotakis, working as a graduate student in the lab, developed a theoretical model and performed benchtop experiments to ascertain the required concentrations of iodine to reliably visualize simulated lesions in a two-dimensional imaging system [13]. CEM was then implemented by making some in-house modifications to an early clinical digital mammography system, the General Electric Senographe 2000D.

Although the presence of iodine increases radiographic contrast, this may not be adequate to visualize subtle areas of uptake, especially if there is superposition of signal from layers of attenuating surrounding soft tissue. For this reason, radiographic excretory urography, for example, does not show lesions in the kidneys and liver to the same degree that abdominal CT (where overlapping signals are not present) does. To enhance contrast and suppress tissue superposition effects, the approach used was temporal subtraction, similar to that used in other contrast imaging, such as contrast-enhanced breast MRI. A digital image of the breast was acquired prior to injection of the contrast agent. This was then subtracted from an image, acquired ideally under identical positioning, after administration of the contrast. Signals in common to the two images would then be canceled by the subtraction, while differences, presumably due to the iodine contrast signal, would remain. In a digital presentation, the displayed contrast of the residual iodine signal could be amplified by manipulation of "window" and "level" adjustments on the computer display.

Because X-rays are attenuated exponentially in passing through any object such as the breast, a more effective isolation of the iodine signal could be obtained by transforming the pixel signal values in both the mask and post-contrast images to their natural logarithms before subtraction. This is essentially equivalent to dividing one of the images by the other.

There are key differences between the techniques of angiography and contrast-enhanced mammography however. In angiography, multiple arterial injections are used to allow depiction of the anatomy in multiple projections. In CEM, because the injection is intravenous, repeat injections are not an option. Only a single (pre-contrast) mask image can be obtained to use for subtraction, and, as in angiography, any patient motion between the pre- and post-contrast images results in misregistration artifacts when the two images are subtracted.

These two limitations, the inability to obtain a second projection and the need to have the breast immobilized during the injection, limited the practicality of this exam. Without the ability to obtain a second projection, it is not possible to localize enhancing lesions in the orthogonal plane. It is also not possible to image the other breast, something that is routine in MRI. Immobilizing the breast during the injection poses its own problems. The way to immobilize the breast is to compress it, but the compression, which causes pressures above that of venous return, would be expected to decrease contrast uptake to the breast. This effect has been noted anecdotally, such as in MRI biopsies, and was recently confirmed in a formal study [14]. To avoid this problem, it would be necessary to use lighter than normal compression, but this raises the likelihood of movement, a problem exacerbated by a

relatively long injection time (about 30 s using a power injection), as compared to either angiography or MRI (typically less than 10 s). Lighter compression also provides less tissue separation, important for standard mammography, although of unknown importance to CEM. Additionally, the increased tissue thickness resulting from decreased compression increases both the dose to the breast and the amount of X-rays scattered in the breast that are recorded by the imaging detector.

John Lewin's group at the University of Colorado experimented with breast immobilization using clear adhesive plastic (shelf liner) and found that it provided fairly good non-contrast images (Fig. 1.1). Another alternative, used in Toronto, was to use light compression with standard compression paddles and correct for misregistration during post-processing (Fig. 1.2).

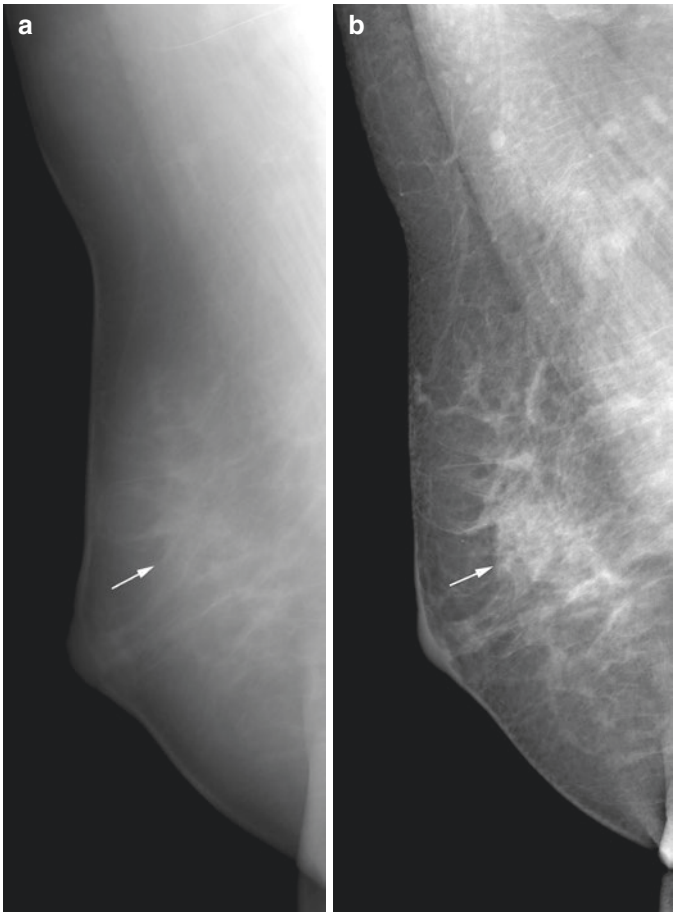

Fig. 1.1 (**a**) Unenhanced MLO view mammogram using adhesive sheet immobilization instead of paddle compression. Positioning is reasonable, but the lack of compression decreases the overall contrast, due to increased scatter, and decreases the conspicuity of the malignant mass in the central breast (arrow). (**b**) Standard compressed mammogram has higher contrast and better shows the mass (arrow)

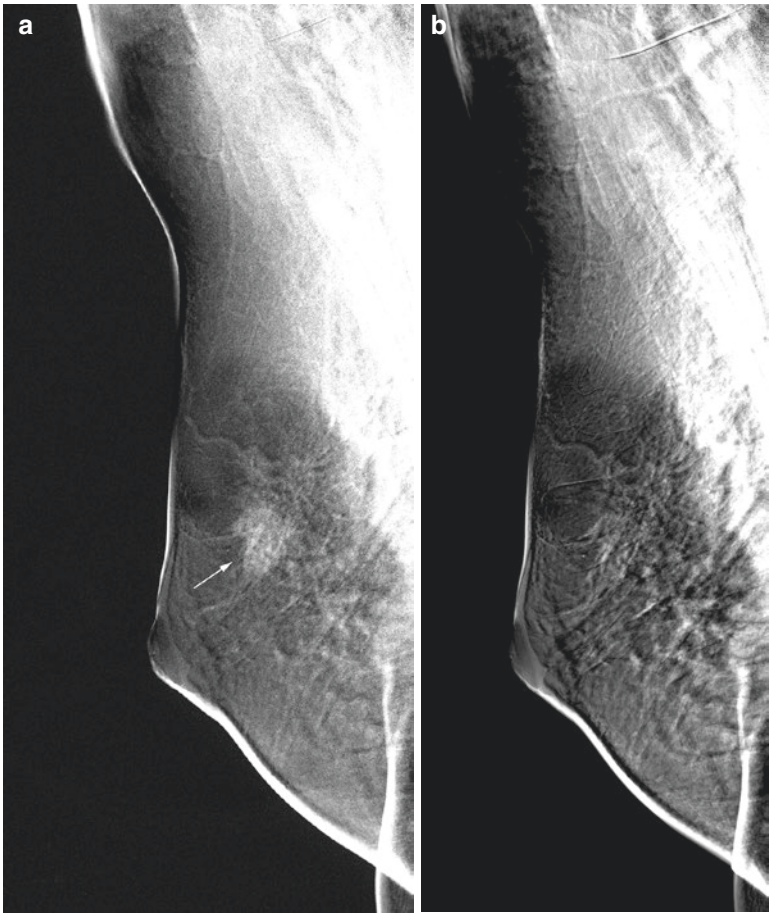

Fig. 1.2 Same case as in Fig. 1.1. Temporally subtracted images obtained at two energies. The source images were acquired without breast compression before and 2 min after contrast agent administration. (**a**) High-energy subtracted image shows the cancer as an enhancing mass (arrow). (**b**) Low-energy subtracted image does not the show enhancement of the cancer due to decreased visibility of iodine at lower X-ray energies

Along with light compression, the key to depicting iodine enhancement using mammography lies in optimizing the X-ray beam for iodine absorption rather than tissue absorption. The goal of optimization is to increase the relative absorption of iodine, as compared to tissue, in order to increase the conspicuity of iodine. Because the absorption curve of iodine increases sharply at 33.2 keV, the *k-edge* of iodine, the optimal beam is one that where as many photons as possible has an energy just above 33.2 keV. This optimum is achieved by increasing the kV to a higher value, usually 44–49, and adding filtration to the beam to filter out the low-energy photons [15]. In Toronto a thin (5 mm) layer of copper was added to the filter wheel, while in Colorado a thicker (8 mm) layer of aluminum was used, due to easy availability

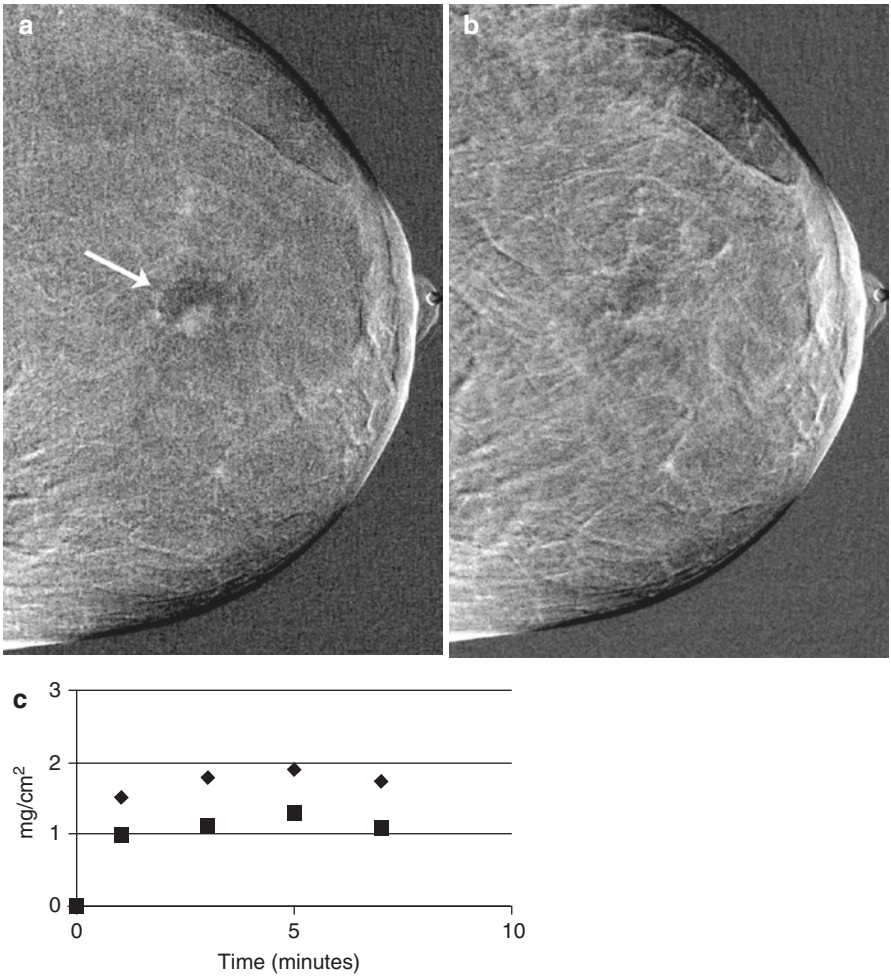

Fig. 1.3 Infiltrating ductal carcinoma CEM subtraction (**a**) CC image obtained 1 min after the start of contrast injection showing small nodule with rim enhancement of entire mass (arrow). (**b**) CEM subtraction CC image obtained 10 min after start of contrast injection showing washout of contrast from mass. (**c**) Kinetic curves for the mass and an area of normal tissue adjacent to the mass. Curve for carcinoma shows early enhancement with a decrease over time, while the curve for normal tissue continues to rise at 10 min. *Reproduced with permission from Ref.* [23]

of aluminum sheets used for half-value layer physics testing. The aluminum was manually placed in the beam prior to each high-energy exposure.

Combining beam optimization; light compression, either with the paddle or the shelf liner; and subtraction led to the technical success of temporal subtraction (Fig. 1.2). Cancers could be shown to enhance with iodine. If serial exposures were made, a kinetic curve could be constructed (Fig. 1.3). Still, the single breast/single view limitations explained above put CEM at a big disadvantage to contrast-enhanced MRI, which allowed bilateral imaging and provided 3D positional

information with a single injection. Interestingly, contrast-enhanced breast MRI started as a single breast technique, due to limitations in breast coils and acquisition speed, but by the early 2000s was typically a bilateral technique.

1.4 Dual-Energy Subtraction CEM

1.4.1 Development of Dual-Energy CEM

To overcome the limitations of temporally subtracted CEM, Lewin and colleagues developed a dual-energy subtraction technique. In dual-energy contrast imaging, contrast agent administration is completed before positioning is started so that the compression effect on contrast uptake is not an issue. Imaging can, therefore, be performed in full compression.

The principle of dual-energy imaging relies on the X-ray attenuation properties of the component materials to be imaged. Overall the X-ray attenuation by any material tends to be strong at low energies and progressively weaker with increasing energy. Therefore, these materials tend to become more transparent to X-rays as energy increases. At the same time, image contrast, which depends on the difference in X-ray attenuation of two materials, tends to fall with increasing energy. Therefore, in general, a compromise exists between imaging at low or at higher energies. At low energies good contrast is achieved, but the increased opacity of the material necessitates that a higher radiation dose be given to get enough X-rays through the body to obtain an acceptable signal-to-noise ratio. The alternative of imaging at high energy allows doses to be reduced but with a loss of contrast. When the goal is to image a high atomic number metal, such as iodine, however, the best result is obtained by combining both a high-energy and a low-energy image. As mentioned above, the attenuation coefficient of iodine increases dramatically at the *k*-edge energy of 33.2 keV. The attenuation remains high for a range of energies above 33.2 keV. Therefore, if the breast is imaged with a spectrum rich in X-rays above 33 keV, there will be strong absorption in areas where there is iodine, but the breast will be quite transparent to X-rays elsewhere. This makes it feasible to obtain a strong iodine signal at reasonably low dose. For the soft tissue in the breast, the attenuation coefficient decreases slowly and smoothly with increasing energy. Therefore images acquired with X-rays at energies just below and just above the iodine *k*-edge will be similar in areas of soft tissue and differ mainly where there is iodine. The dual-energy procedure utilizes two images, one at an energy optimized for iodine (high energy) as described above and one with the kV set below the *k*-edge (low energy), acquired in a single compression. A weighted logarithmic subtraction of the low-energy image from the high-energy image is then performed to create the final iodine-enhanced image. The physics of dual-energy CEM is described more fully in the next chapter.

Because dual-energy subtraction does not rely on a mask image for subtraction, multiple acquisitions can be obtained of both breasts in multiple projections, limited only by the length of time until the contrast “washes out” of the lesion, i.e., equalizes between the lesion and the normal tissue.

1.4.2 History of Dual Energy in Radiology

The concept of using dual-energy subtraction was new to contrast-enhanced mammography, but it had a long history in other aspects of radiology. Dual-energy digital subtraction angiography was developed by William Brody and colleagues at Stanford in the 1980s as a way to perform angiography with an intravenous injection [16]. It was later incorporated into a "hybrid" technique combining both dual-energy and temporal subtraction in order to improve the iodine visibility [17]. Although the technique was an improvement on temporal subtraction, it could not compete with standard arterial angiography and never came into routine clinical use.

Dual-energy subtraction tuned for calcium has also been studied and has been included in some commercial chest radiography equipment to improve pulmonary nodule detection by subtracting out overlapping ribs or, alternatively, to evaluate for calcification in a nodule by subtracting out soft tissues [18, 19]. Calcium dual-energy subtraction was studied for use with digital mammography to enhance the visibility of calcifications [20, 21] but was not shown to be a significant improvement over standard single-energy digital mammography, which is already quite good at calcium detection. Today, in addition to its use with contrast-enhanced mammography, dual-energy is used with contrast-enhanced CT for applications such as evaluating organ perfusion [22].

1.4.3 The Colorado Dual-Energy CEM Clinical Trial

In Colorado the CEM project was started in 1998 using a prototype digital mammography unit. The technology was transitioned to a commercial digital unit after FDA approval for digital in 2000. After phantom studies to optimize the technique factors, a clinical trial was started to evaluate both temporal subtraction and dual-energy subtraction CEM on a series of subjects with suspicious mammographic or palpable lesions scheduled for biopsy. Phantom studies led to a choice of 44 kV Rh/Rh with an additional 8 mm of Al filtration for the high-energy beam and 30 kV Mo/Mo for the low-energy beam (changed to 33 kV Rh/Rh for the last few subjects to place the beam closer to the *k*-edge). Iohexol, at a concentration of 350 mgI/ml, was selected as the contrast agent.

The protocol provided contrast-enhanced MLO views of the breast of interest obtained using both temporal and dual-energy subtraction, the former acquired with immobilization but no compression and the latter with full compression.

The imaging sequence was as follows:

- Breast placed in full compression (MLO view).
  - Low-energy image obtained.
  - High-energy image obtained.
- Compression released.
- Breast immobilized with shelf liner (MLO view).
  - High-energy image obtained.

- *100 ml of contrast injected using a power injector*
  - High-energy image obtained.
- Shelf liner removed.
- Breast place in full compression (MLO view).
  - Low-energy image obtained.
  - High-energy image obtained.
- Compression released.

The first two exposures were used to create a pre-contrast dual-energy image (helpful for comparison to the post-contrast image); the next two exposures, straddling the injection, were subtracted to create a temporal subtraction image, and the last two, both obtained after contrast administration, were used to create a post-contrast dual-energy image. Figures 1.4 and 1.5 show temporal and dual-energy subtracted images from the study. Even though temporal subtraction should give perfect subtraction and therefore a stronger iodine signal, in practice the dual-energy

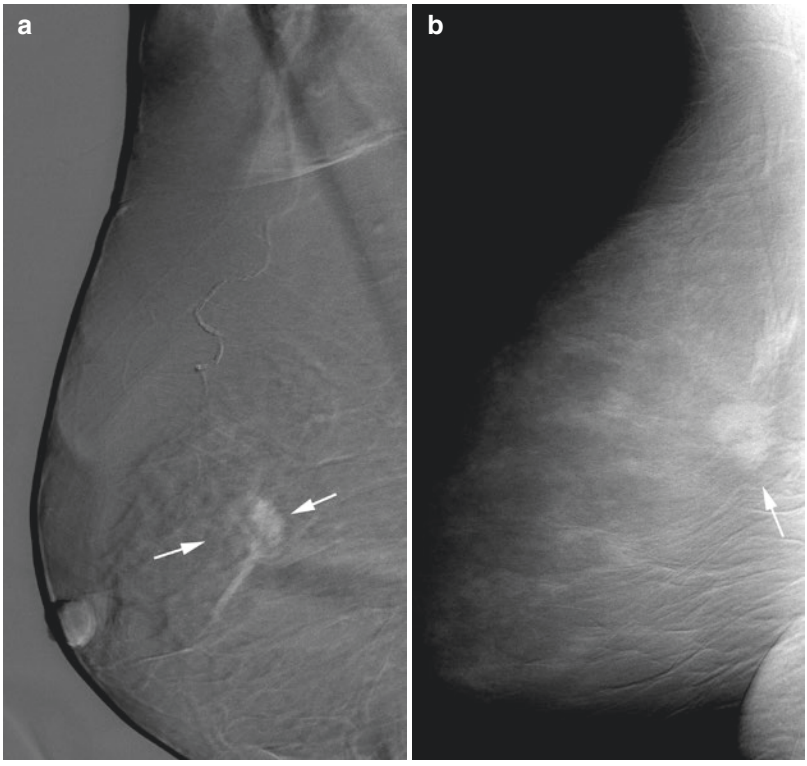

Fig. 1.4 Subject with invasive ductal carcinoma studied a protocol producing both temporal and dual-energy subtraction CEM. (**a**) High-energy temporal subtraction, performed without breast compression, shows the cancer (arrows). (**b**) Dual-energy subtraction without breast compression gives better delineation of the entire mass (arrow). (**c**) Dual-energy subtraction with breast compression shows the entire lesion (arrow) and better delineates its margins

Fig. 1.4 (continued)

images were usually superior due to the use of full compression. For this reason, in the second half of the study, the temporal portion was eliminated, and serial dual-energy imaging was performed instead (Fig. 1.6). Following completion of the initial cohort, in 2003, a second series was started using bilateral dual-energy imaging. That year the technique was also evaluated for ductography in two patients but was not deemed worth pursuing given the excellent visibility of contrast in standard ductography. In one of the two subjects, the technique did allow for the detection of additional lesions not shown by standard ductography in a patient with multiple central papillomas (Fig. 1.7).

1.5 Early CEM Literature

The first temporal subtraction paper was published by Jong et al., from the group in Toronto in 2003 [23]. Imaging was performed both on GE Senographe 2000D systems and a Fischer Senoscan unit. Neither system was designed specifically for contrast imaging; modifications to the systems were implemented by the research team.

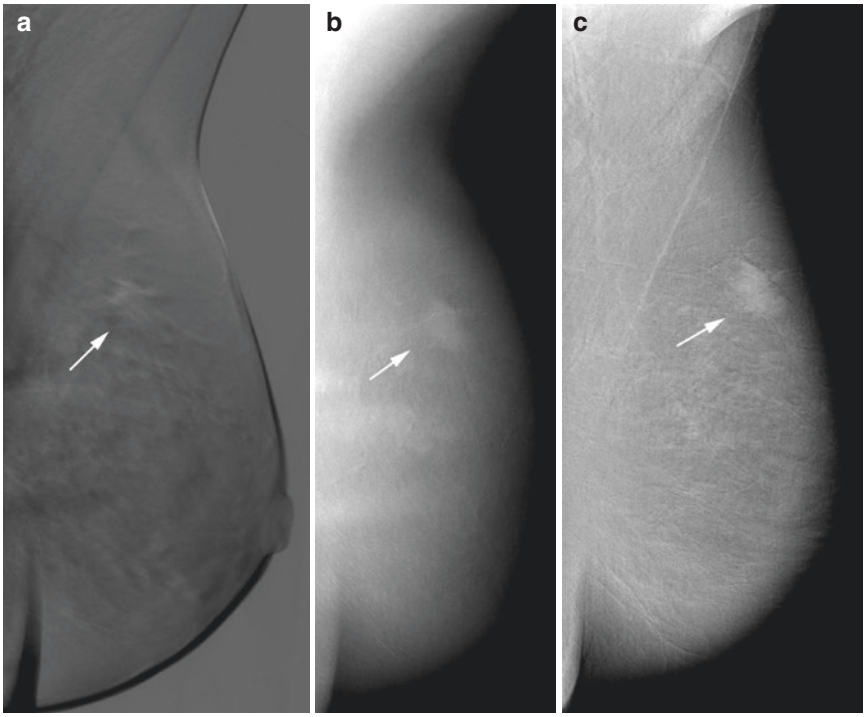

Fig. 1.5 Invasive ductal carcinoma. (**a**) High-energy temporal subtraction shows the cancer (arrow) as only a faint blush. (**b**) Dual-energy subtraction without breast compression shows the cancer (arrow) with moderately higher contrast. (**c**) Dual-energy subtraction with breast compression best shows the cancer (arrow) and best delineates its margins

In that study of 22 subjects, ten with breast cancers were studied with single-energy contrast mammography. All but 1 of the 9 invasive cancers showed iodine enhancement, while 7 of the 12 benign lesions that were originally of concern on ultrasound or mammography did not enhance. The results suggested that CEM may be more specific than contrast-enhanced breast MRI. Low-dose contrast images were obtained at six time points allowing construction of kinetic curves. In some cases, enhancement characteristics were similar to those from malignant and benign lesions as observed in breast MRI, but this was not consistent. One of the limitations in this study was the use of manual injection of the contrast agent. The time required for the administration of contrast limited the temporal resolution of the imaging procedure, likely diminishing the quality of the kinetic information.

The following month the first dual-energy subtraction paper was published by Lewin et al. in Colorado [24]. Starting in 2000, 26 subjects scheduled for biopsy and were studied with both single-energy and dual-energy CEM on a GE Senographe 2000D digital mammography system, approved that year for clinical use, using the technique and protocol described above with manual insertion of aluminum filtration to generate the high-energy beam. Thirteen of the 26 subjects were shown at

subsequent biopsy to have invasive cancer, 1 had DCIS, and the other 12 had benign lesions. For simplicity, only the dual-energy results were reported in the paper. Eleven of the 13 invasive cancers enhanced strongly on DE CEM, 1 enhanced moderately, and 1 weakly. The one case of DCIS showed up as a mildly enhancing duct containing calcifications. Two of the benign cases showed diffuse enhancement, what we would now call background parenchymal enhancement [25]. Two others showed weak focal enhancement and were considered false positives.

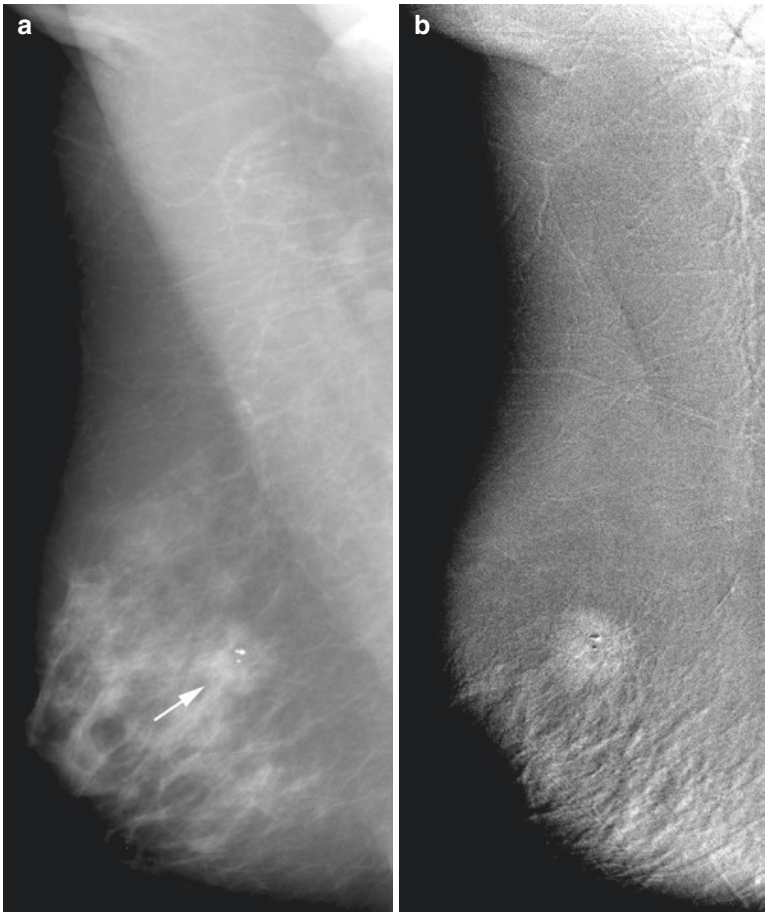

Fig. 1.6 Serial dual-energy contrast-enhanced mammography. (**a**) Pre-contrast standard energy mammogram shows an invasive ductal carcinoma presenting as a 2 cm mass with coarse calcifications (arrow). (**b**) Dual-energy subtracted image at 3 min shows bright enhancement of the cancer. (**c**) Dual-energy subtracted image at 6 min shows less bright enhancement of the mass. (**d**) Dual-energy subtracted image at 9 min shows even less contrast difference between the mass and the background. The 9-min image in this case is degraded by misregistration artifact caused by patient movement between the low-energy and high-energy images. Note that each acquisition of each high- and low-energy image pair is obtained under a separate compression; compression is released between image pairs

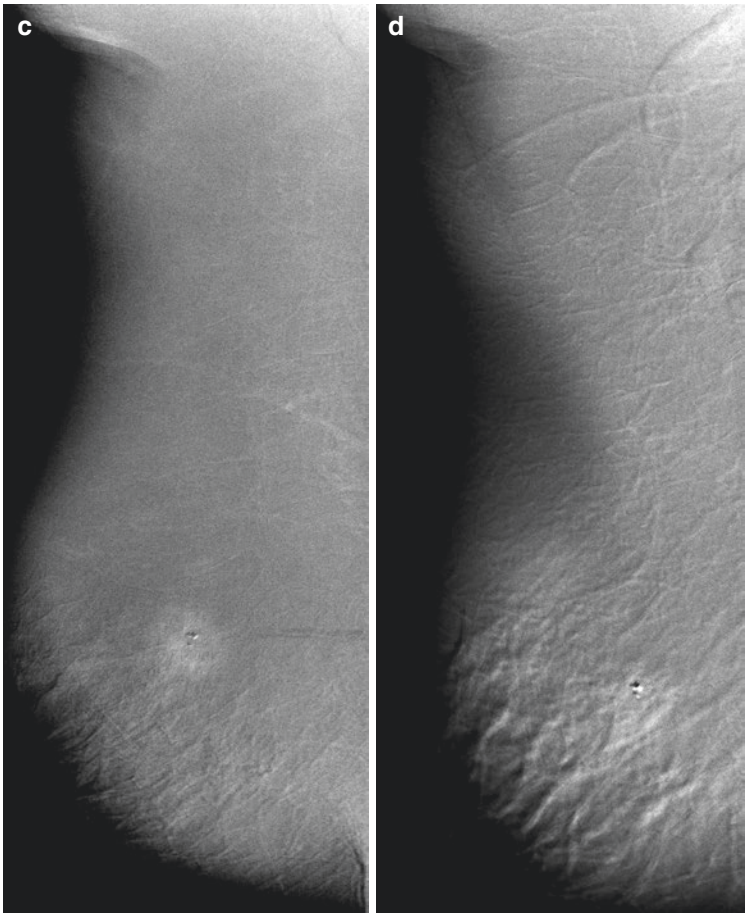

Fig. 1.6 (continued)

Two additional temporal subtraction studies were published in 2005 and 2006. Both studies were performed on commercial GE digital units. Diekmann et al., at Charite Hospital in Berlin, studied 25 lesions, 14 malignant [26]. Dromain et al., at the Institut Gustave Roussy outside Paris, studied 20 lesions, all malignant [27]. All of the malignant lesions enhanced in the former study, and all but two enhanced in the latter; the two false-negative cases were cancers not included on the image due to positioning issues. Both trials included serial imaging and resulted in kinetic curves similar to those seen in contrast-enhanced breast MRI. As with MRI, however, the curve shapes were highly variable among the cancers and, therefore, not especially useful for discriminating between benign and malignant lesions.

By this point, GE had decided to invest in building a prototype unit to perform dual-energy CEM. The GE system employed a copper filter in the filter wheel and allowed for automatic switching of the filter and the kilovoltage between the

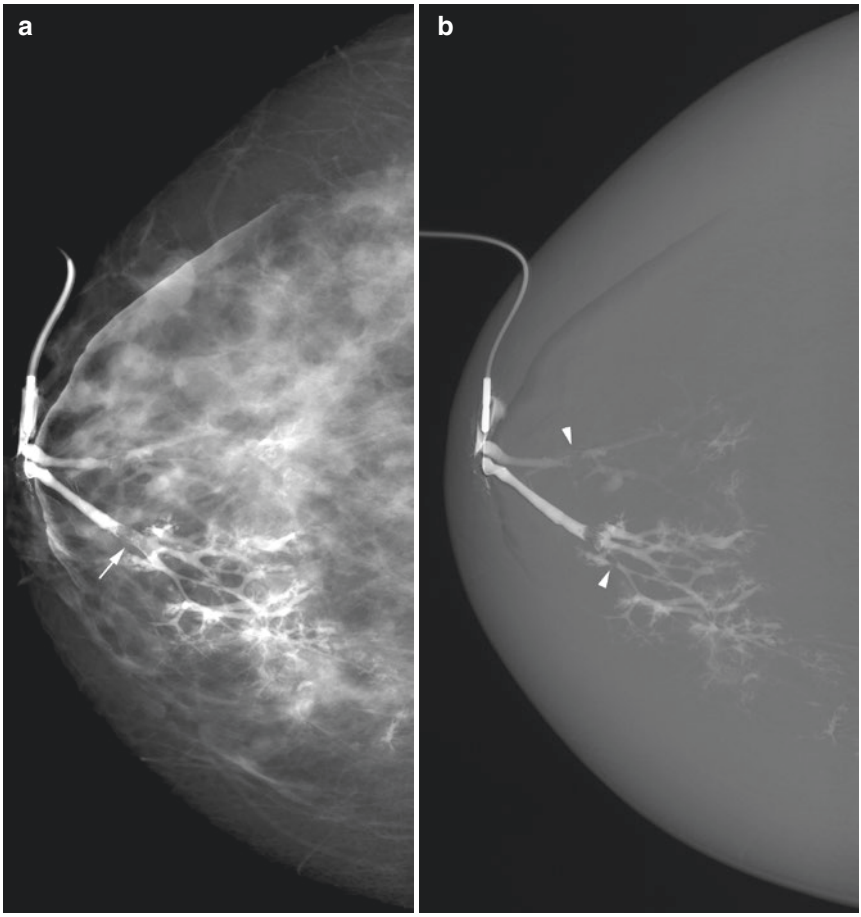

Fig. 1.7 Patient with nipple discharge. (**a**) Standard ductogram shows an intraductal lesion (arrow). (**b**) Dual-energy subtraction ductogram subtracts out the background breast tissue, allowing detection of additional smaller lesions (arrowheads). Papillomas were found at surgery

high- and low-energy image acquisitions. The first dual-energy CEM paper using this prototype system was published by Dromain et al. in 2011 [28]. In this study 120 patients with 142 suspicious lesions, some palpable and others detected by mammography and/or ultrasound, were studied with two-view dual-energy CEM. As in the earlier papers, only the affected breast was studied. The data set included 80 cancers and 62 benign lesions. Seventy-four of the 80 cancers enhanced. The six non-enhancing lesions included two cases of DCIS and four invasive ductal cancers. Thirteen benign lesions also enhanced. The primary outcome of the study was area under the receiver operating characteristic (ROC) curve generated based on a single radiologist reading of mammography alone, mammography plus CEM, and mammography plus ultrasound. As expected, the ROC curve for CEM plus mammography was significantly better than that for mammography alone or

mammography plus ultrasound. The same results were obtained when the image set was evaluated in a multi-reader study [29].

Given the obvious superiority of CEM to standard mammography, work then switched to comparisons of CEM to contrast-enhanced MRI. Prospective trials, using a GE-designed prototype unit, at Charite and at Sloan Kettering in New York, compared bilateral CEM to MRI in patients with known cancers [30, 31]. These trials showed MRI and CEM to have similar levels of performance, with each modality slightly outperforming the other by some measures. The results of trials comparing CEM to MRI are discussed more fully in a later chapter of this book.

The idea of combining the benefits of contrast-enhanced mammography with the quasi-3D imaging of tomosynthesis is a logical conclusion of the successful demonstration of the two individual modalities. A limited amount of preliminary data has been published on both a temporal [32] and a dual-energy [33] approach to contrast-enhanced digital breast tomosynthesis. The first trial comparing CEM to MRI using a prototype device from Hologic was conducted in Taiwan and Colorado and included both 2D CEM and contrast-enhanced tomosynthesis. The results of that study showed that CEM, contrast-enhanced tomosynthesis, and MRI were all superior to unenhanced mammography and unenhanced tomosynthesis based on ROC analysis from a multi-reader study. The three contrast-enhanced modalities were not significantly different. Notably, the addition of contrast-enhanced tomosynthesis to 2D CEM did not improve performance [34]. Fig. 1.8 shows an example from that study.

1.6 Clinical Introduction/Commercialization

The first commercial CEM system was introduced by General Electric in 2010. It obtained CE mark approval for sale in Europe at that time and received FDA 510(k) approval in 2011. Hologic obtained CE mark and FDA 510(k) approval for their system in 2012. Their first commercial units were installed in 2014. Units from both companies included the typical ease of use features found on clinical mammography units, such as autoexposure methods, to make the technique practical in a standard clinical environment. The Hologic unit also included the ability to perform a low-energy tomosynthesis view in the same compression. As of this writing, these are the only two commercial systems approved for use in the United States. A system made by Siemens is available for use outside the United States. Working research systems have been developed, Fuji and Philips, and have been used in clinical trials but have not yet been commercialized. The introduction of commercial systems allows both clinical adoption and clinical research to proceed more rapidly. The use of CEM in clinical settings allows for expanded experience in a variety of settings, not just the academic settings common to research. Additional techniques not easily adapted to a clinical protocol, such as the use of spot compression or special projections, can be employed and their usefulness evaluated. To date there are an estimated 800 commercial units installed worldwide and an estimated 500,000 CEM examinations have been performed [35].

Note that, as manufacturers have introduced dual-energy CEM systems, they have also introduced new names for the procedure. For example GE coined the term *contrast-enhanced spectral mammography* (CESM) when it introduced its commercial system. Other synonyms for the technique include contrast-enhanced digital mammography (CEDM), contrast media mammography (CMM), and contrast-enhanced 2D (CE2D) used by Hologic to differentiate its 2D system from any future contrast-enhanced tomosynthesis product. Siemens uses TiCEM for their system, reflecting the use of a titanium filter for the high-energy beam. Among these names, CEM, CEDM, and CESM are the most commonly used in the literature.

Fig. 1.8 Invasive ductal carcinoma studied with both CEM and contrast-enhanced tomosynthesis using a prototype research system. A metallic ribbon-shaped mark was placed anterior to the mass at the time of biopsy. (**a**) Standard mammogram. (**b**) 2D CEM. (**c**) Tomosynthesis slice. (**d**) Dual-energy contrast-enhanced tomosynthesis slice. Note that the 2D CEM and the contrast-enhanced tomosynthesis slice are equally good at showing the lesion

Fig. 1.8 (continued)

1.7 Conclusion

The demonstration of CEM occurred fairly rapidly after the development and dissemination of the first full-field digital mammography systems, with the first research subjects being imaged less than 1 year after FDA approval of FFDM. The introduction of dual-energy subtraction to the technique made it clinically viable. Nonetheless, it took many years and the interest/effort/commitment of a large company to bring the technology to market. More than a decade later, adoption of the technique remains modest, due to competition with the well-established technique of MRI, which has had a 20 year head start. A major barrier to CEM's ability to compete with MRI, especially in the United States, is a lack of appropriate reimbursement codes. Without the ability to get adequately reimbursed for CEM, centers have no incentive to switch patients from MRI, which is highly profitable on a

per-case bases, to this more cost-effective (and, therefore, less profitable) technique. An absence of robust data on screening with CEM is also in issue. Hopefully these hurdles will be crossed in the next few years, and adoption of CEM will accelerate, so that its benefits can be fully realized.

References

1. Lewin JM, Hendrick RE, D'Orsi CJ, Isaacs PK, Moss LJ, Karellas A, Sisney GA, Kuni CC, Cutter GR. Comparison of full-field digital mammography with screen-film mammography for cancer detection: results of 4,945 paired examinations. Radiology. 2001;218(3):873–80. PubMed PMID: 11230669.
2. Pisano ED, Gatsonis C, Hendrick E, Yaffe M, Baum JK, Acharyya S, Conant EF, Fajardo LL, Bassett L, D'Orsi C, Jong R, Rebner M, Digital Mammographic Imaging Screening Trial (DMIST) Investigators Group. Diagnostic performance of digital versus film mammography for breast-cancer screening. N Engl J Med. 2005;353(17):1773–83. Erratum in: N Engl J Med 2006;355(17):1840. PubMed PMID: 16169887.
3. Gisvold JJ, Reese DF, Karsell PR. Computed tomographic mammography (CTM). AJR Am J Roentgenol. 1979;133(6):1143–9. PubMed PMID: 116508.
4. Chang CH, Sibala JL, Fritz SL, Dwyer SJ III, Templeton AW, Lin F, Jewell WR. Computed tomography in detection and diagnosis of breast cancer. Cancer. 1980;46(4 Suppl):939–46. PubMed PMID: 7397672.
5. Chang CH, Nesbit DE, Fisher DR, Fritz SL, Dwyer SJ 3rd, Templeton AW, Lin F, Jewell WR. Computed tomographic mammography using a conventional body scanner. AJR Am J Roentgenol. 1982;138(3):553–8. PubMed PMID: 6978009.
6. Hagay C, Cherel PJ, de Maulmont CE, Plantet MM, Gilles R, Floiras JL, Garbay JR, Pallud CM. Contrast-enhanced CT: value for diagnosing local breast cancer recurrence after conservative treatment. Radiology. 1996;200(3):631–8. PubMed PMID: 8756908.
7. SA FT, Miyakawa K, Uchiyama N, Nanasawa T, Tsuda H. Clinical use of contrast-enhanced computed tomography for decision making in breast conserving surgery. Breast Cancer. 1997;4(4):280–4. PubMed PMID: 11091615.
8. Fritz SL, Chang CH, Livingston WH. Scatter/primary ratios for x-ray spectra modified to enhance iodine contrast in screen-film mammography. Med Phys. 1983;10(6):866–70. PubMed PMID: 6656696.
9. Watt AC, Ackerman LV, Shetty PC, Burke M, Flynn M, Grodsinsky C, Fine G, Wilderman S. Differentiation between benign and malignant disease of the breast using digital subtraction angiography of the breast. Cancer. 1985;56(6):1287–92. PubMed PMID: 3896454.
10. Folkman J. Tumor angiogenesis: therapeutic implications. N Engl J Med. 1971;285:1182–6.
11. Dean PB, Plewes, DB. Contrast media in computed tomography. In: Soval M Radiocontrast agents. Berlin: Springer-Verlag. 1984; 497–508.
12. Hill ML, Liu K, Mainprize JG, Levitin RB, Shojaii R, Yaffe MJ. Pre-clinical evaluation of tumour angiogenesis with contrast-enhanced breast tomosynthesis. 11th international workshop on breast imaging. Philadelphia, 8 Jul 2012.
13. Skarpathiotakis M, Yaffe MJ, Bloomquist AK, Rico D, Muller S, Rick A, Jeunehomme F. Development of contrast digital mammography. Med Phys. 2002;29(10):2419–26.
14. Castillo-Lopez JP, Cruz-Rodríguez JC, Galván-Espinoza HA, Berumen F, Villaseñor-Navarro Y, Brandan ME. Optimization of acquisition parameters for the detection of secondary breast lesions applying temporal contrast enhanced digital mammography, Proceedings of the SPIE 10718, 14th international workshop on breast imaging (IWBI 2018), 107181Y, 6 July 2018. https://doi.org/10.1117/12.2318672.
15. Ullman G, Sandborg M, Dance DR, Yaffe MJ, Skarpathiotakis M, Alm Carlsson G. A search for optimal x-ray spectra in iodine contrast media mammography. Phys Med Biol. 2005;50:3143–52.

16. Brody WR, Macovski A, Lehmann L, DiBianca FA, Volz D, Edelheit LS. Intravenous angiography using scanned projection radiography: preliminary investigation of a new method. Investig Radiol. 1980;15(3):220–3. PubMed PMID: 6995395.
17. Brody WR. Hybrid subtraction for improved arteriography. Radiology. 1981;141(3):828–31. PubMed PMID: 7029620.
18. Kruger RA, Armstrong JD, Sorenson JA, Niklason LT. Dual energy film subtraction technique for detecting calcification in solitary pulmonary nodules. Radiology. 1981;140(1):213–9. PubMed PMID: 7017812.
19. Ishigaki T, Sakuma S, Ikeda M. One-shot dual-energy subtraction chest imaging with computed radiography: clinical evaluation of film images. Radiology. 1988;168(1):67–72. PubMed PMID: 3289096.
20. Johns PC, Yaffe MJ. Theoretical optimization of dual-energy x-ray imaging with application to mammography. Med Phys. 1985;12(3):289–96.
21. Lemacks MR, Kappadath SC, Shaw CC, Liu X, Whitman GJ. A dual-energy subtraction technique for microcalcification imaging in digital mammography—a signal-to-noise analysis. Med Phys. 2002;29(8):1739–51. PubMed PMID: 12201421.
22. Marin D, Boll DT, Mileto A, Nelson RC. State of the art: dual-energy CT of the abdomen. Radiology. 2014;271(2):327–42. https://doi.org/10.1148/radiol.14131480. Review. PubMed PMID: 24761954.
23. Jong RA, Yaffe MJ, Skarpathiotakis M, Shumak RS, Danjoux NM, Gunesekara A, Plewes DB. Contrast-enhanced digital mammography: initial clinical experience. Radiology. 2003;228(3):842–50. PubMed PMID: 12881585.
24. Lewin JM, Isaacs PK, Vance V, Larke FJ. Dual-energy contrast-enhanced digital subtraction mammography: feasibility. Radiology. 2003;229(1):261–8. PubMed PMID: 12888621.
25. Jochelson MS, Dershaw DD, Sung JS, et al. Bilateral contrast-enhanced dual-energy digital mammography: feasibility and comparison with conventional digital mammography and MR imaging in women with known breast carcinoma. Radiology. 2013;266(3):743–51.
26. Diekmann F, Diekmann S, Jeunehomme F, Muller S, Hamm B, Bick U. Digital mammography using iodine-based contrast media: initial clinical experience with dynamic contrast medium enhancement. Investig Radiol. 2005;40(7):397–404. PubMed PMID: 15973130.
27. Dromain C, Balleyguier C, Muller S, Mathieu MC, Rochard F, Opolon P, Sigal R. Evaluation of tumor angiogenesis of breast carcinoma using contrast-enhanced digital mammography. AJR Am J Roentgenol. 2006;187(5):W528–37. PubMed PMID: 17056886.
28. Dromain C, Thibault F, Muller S, Rimareix F, Delaloge S, Tardivon A, Balleyguier C. Dual-energy contrast-enhanced digital mammography: initial clinical results. Eur Radiol. 2011;21(3):565–74. https://doi.org/10.1007/s00330-010-1944-y. PubMed PMID: 20839001.
29. Dromain C, Thibault F, Diekmann F, Fallenberg EM, Jong RA, Koomen M, Hendrick RE, Tardivon A, Toledano A. Dual-energy contrast-enhanced digital mammography: initial clinical results of a multireader, multicase study. Breast Cancer Res. 2012;14(3):R94. PubMed PMID: 22697607; PubMed Central PMCID: PMC3446357.
30. Fallenberg EM, Dromain C, Diekmann F, Engelken F, Krohn M, Singh JM, Ingold-Heppner B, Winzer KJ, Bick U, Renz DM. Contrast-enhanced spectral mammography versus MRI: initial results in the detection of breast cancer and assessment of tumour size. Eur Radiol. 2014;24(1):256–64. https://doi.org/10.1007/s00330-013-3007-7. PubMed PMID: 24048724.
31. Jochelson MS, Dershaw DD, Sung JS, Heerdt AS, Thornton C, Moskowitz CS, Ferrara J, Morris EA. Bilateral contrast-enhanced dual-energy digital mammography: feasibility and comparison with conventional digital mammography and MR imaging in women with known breast carcinoma. Radiology. 2013;266(3):743–51. https://doi.org/10.1148/radiol.12121084. PubMed PMID: 23220903; PubMed Central PMCID: PMC5673037.
32. Chen SC, Carton A-K, Albert M, Conant EF, Schnall MD, Maidment ADA. Initial clinical experience with contrast-enhanced digital breast tomosynthesis. Acad Radiol. 2007;14:229–38.
33. Carton A-K, Gavenonis SC, Currivan JA, Conant EF, Schnall MD, Maidment ADA. Dual-energy contrast-enhanced digital breast tomosynthesis – a feasibility study. Br J Radiol.

2010;83(988):344–50. https://doi.org/10.1259/bjr/80279516. PMCID: PMC3473453 PMID: 19505964.
34. Chou CP, Lewin JM, Chiang CL, Hung BH, Yang TL, Huang JS, Liao JB, Pan HB. Clinical evaluation of contrast-enhanced digital mammography and contrast enhanced tomosynthesis – comparison to contrast-enhanced breast MRI. Eur J Radiol. 2015;84(12):2501–8. https://doi.org/10.1016/j.ejrad.2015.09.019. PubMed PMID: 26456307.
35. Katz L, GE Healthcare. Personal communication, 26 Jul 2018. PubMed PMID: 26456307.

Physics of Contrast-Enhanced Mammography

2

Cécile R. L. P. N. Jeukens

2.1 Image Formation in Mammography

To acquire a mammogram, the breast is compressed by a paddle to make the breast uniform in thickness and to minimize superimposition of fibroglandular tissue, which could mimic breast lesions. X-rays produced in the X-ray tube of the mammography unit are directed to the breast below which the detector is located (Fig. 2.1).

2.1.1 Generation of X-Rays

In the X-ray tube, the X-rays are generated as follows (Fig. 2.2a). The cathode is heated by the tube current, resulting in the release of electrons. The electrons are accelerated toward the anode by the tube voltage and hit the anode, also called the target. In the anode, the electrons interact with nuclei of the anode material, and bremsstrahlung is released, which in fact is the X-ray radiation used for imaging (Fig. 2.2b). The energy of the photons depends on the strength of the interaction: the closer the electron approaches the nucleus, the stronger the interaction becomes. The interaction strength varies per electron hitting the anode, and consequently the X-ray photons have many different energies resulting in an X-ray spectrum rather than a single photon energy. The maximum energy is determined by the maximal acceleration of the electrons which is dictated by the tube voltage. By adding a filter in the X-ray beam, the low-energy X-ray photons are absorbed. This is beneficial for the dose to the breast as the low-energy photons are so strongly attenuated in the breast that they are completely absorbed in the breast before reaching the detector.

C. R. L. P. N. Jeukens (✉)
Department of Radiology and Nuclear Medicine, Maastricht University Medical Center, Maastricht, The Netherlands
e-mail: cecile.jeukens@mumc.nl

M. Lobbes, M. S. Jochelson (eds.), *Contrast-Enhanced Mammography*,
https://doi.org/10.1007/978-3-030-11063-5_2

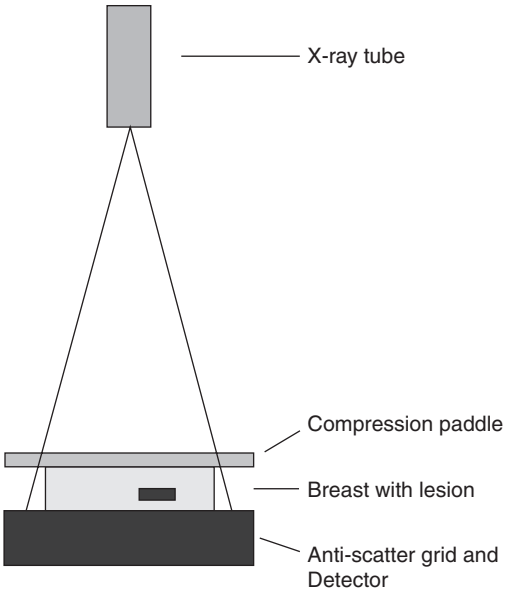

Fig. 2.1 Schematic set-up of a mammography system

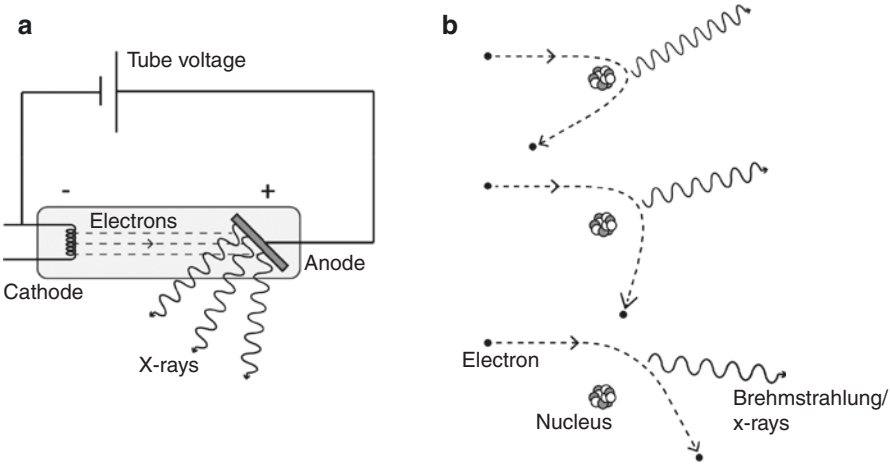

Fig. 2.2 (**a**) Schematic of an X-ray tube showing the cathode where the electrons are released and attracted towards the positively charged anode. X-rays are generated in the anode during the interaction of electrons with the nuclei of the anode atoms. The cathode and anode are positioned in a vacuum indicated by the grey shaded area. (**b**) Depending on the distance the electron approaches the nucleus a stronger or less strong interaction takes place resulting in higher and lower energy photons. This is the reason that an X-ray tube emits a multi-energetic spectrum of photons

As such, these low-energy photons do not contribute to image formation, while they do contribute to the radiation dose of the breast. The final X-ray spectrum is determined by the combination of tube voltage, anode material, and filter material.

2.1.2 Attenuation of X-Rays in the Breast

In the breast the X-rays are partly absorbed and partly transmitted. The transmitted X-rays reach the detector to form the image. The challenge is to visualize both benign and malignant breast structures. Differences between attenuation properties of the glandular, adipose, and cancerous tissue lead to image contrast. The attenuation of tissue (or any material in fact) is characterized by the linear attenuation coefficient indicated by the symbol μ, which describes how much the tissue attenuates radiation per cm of tissue. The value of the attenuation coefficient depends on the type of tissue and the energy of the X-ray radiation.

The attenuation properties of glandular, adipose, and cancerous tissue are comparable (Fig. 2.3). This makes it challenging to achieve sufficient contrast in mammographic images. For lower photon energies, the differences between the attenuation coefficient of the different tissues increase leading to improved contrast between these tissues [5]. This is the reason for using very low tube voltages (range 25–34 kV) in mammography when compared to other radiological applications (typically 50–140 kV). However, for low photon energies, increasing attenuation results in increasing photon absorption in the breast, decreasing the number of photons reaching the detector and noisier images while increasing the dose to the breast. The choice of the most ideal X-ray spectrum is therefore a trade-off. With modern full-field digital mammography (FFDM) units employing low-energy X-ray spectra (kVp ~25–34 kV, with additional filtration), advanced digital detectors, anti-scatter grids, proper breast compression, and advanced post-processing algorithms, high-quality diagnostic images can be obtained with low dose to the breasts.

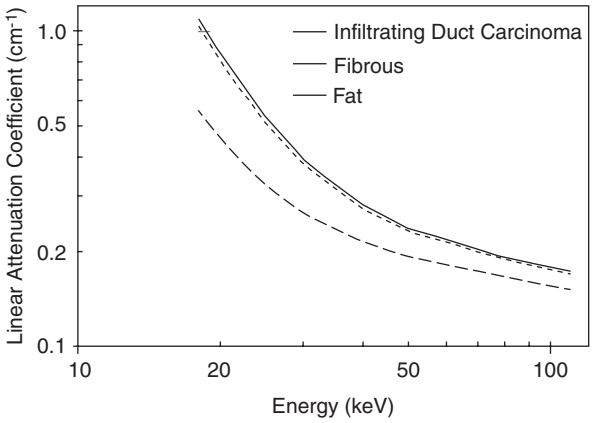

Fig. 2.3 Linear attenuation coefficient as a function of energy for adipose and glandular breast tissue and infiltrating ductal carcinoma [5]. The attenuation of the carcinoma and glandular tissue is very similar making it difficult to obtain sufficient contrast. Image is based on data published in ref. [5]

2.2 Enhancement by Iodine Contrast Agent

Iodinated contrast enhances the contrast between malignant lesions and normal breast tissue enabling improved breast cancer detection: When tumors grow, they develop blood vessels to provide nutrients and oxygen to the tumor in a process called "angiogenesis." These new blood vessels are rapidly formed and therefore "leaky," which allows contrast agent to extravasate from these vessels into the tumor itself, causing it to enhance when dedicated imaging protocols are used [6]. The attenuation coefficient μ of the iodine shows a discontinuity called the *k*-edge at an energy level of 33.2 keV, while the attenuation coefficient μ of the breast tissue continues to gradually decrease (Fig. 2.4). These differences in attenuation between the iodine contrast agent containing breast lesion and the surrounding breast tissue are exploited in dual-energy mammography to visualize the iodine contrast enhancement.

2.2.1 The *k*-Edge of Iodine

The X-ray radiation is absorbed in the iodinated contrast agent primarily by the photoelectric effect. This is a process in which an X-ray photon interacts with the innermost electron shells of the iodine atom (Fig. 2.5). The incoming X-ray photon is completely absorbed, and an electron is ejected from the atom. Depending on its energy, the X-ray photon interacts with the first (K), second (L), third (M), etc. electron shell. A higher energy is required for the lower, innermost shells. The

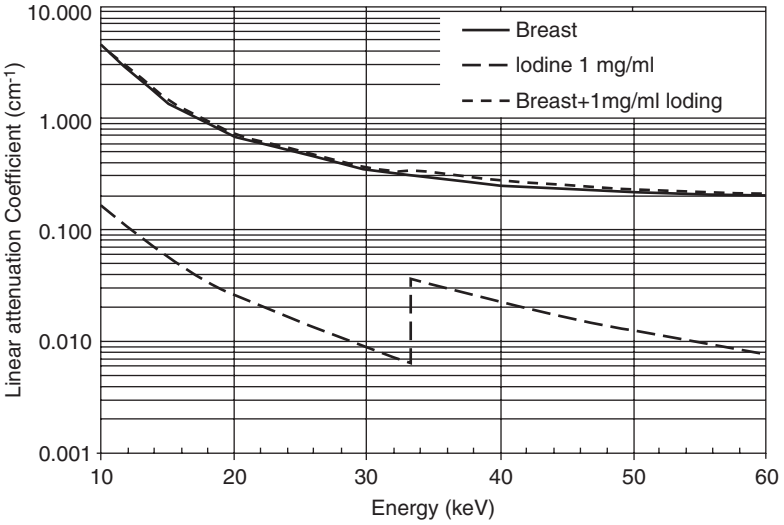

Fig. 2.4 Attenuation coefficient as a function of photon energy for breast tissue and 1 mg/ml iodine [7], where the latter shows a *k*-edge at 33.2 keV. Note the logarithmic scale on the *y*-axis. To appreciate the small contribution of the iodine to the total attenuation the sum of the breast and 1 mg/ml iodine attenuation is shown

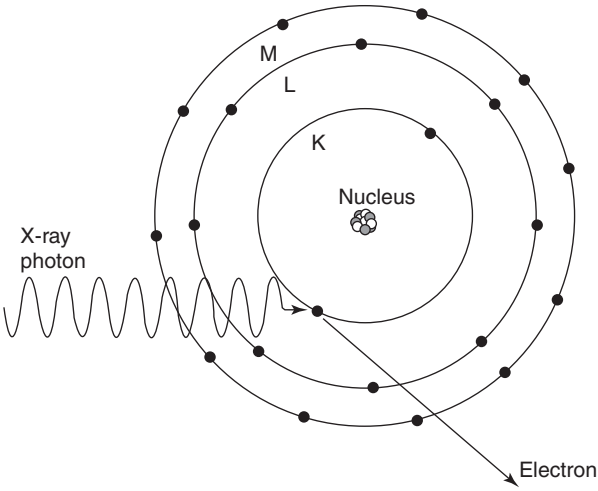

Fig. 2.5 Illustration of the photoeffect: an X-ray photon interacts with an electron from the inner shells. The energy of the photon is completely absorbed and the electron is ejected from the atom

probability that the X-ray photons are absorbed decreases with increasing photon energy. However, when the photon energy is high enough to match the energy required for ejecting an electron from the innermost shell, the so-called K-shell, the X-ray photon absorption probability suddenly increases (about five times for iodine [7], Fig. 2.4), after which it gradually decreases again with increasing photon energy. This sudden increase is called the *k*-edge, and the energy value at which it occurs is specific for the atom with which the incoming photon interacts. For iodine, the *k*-edge is at 33.2 keV. In analogy, also a L- and M-edge occurs, but for iodine these are observed at much lower photon energies to be clinically relevant.

2.2.2 Visualizing Iodine in the Breast

Although the iodine has a much higher attenuation coefficient per unit mass than the breast tissue, it is not visible in a regular mammogram because the iodine concentration in breast lesions is very low. For the standard injection protocol used in CEM (1.5 ml/kg body weight, iodine concentration: 300–350 mg/ml), the concentration in low to normal enhancing lesions is in the order of 1–4 mg/ml [8]. To illustrate, Fig. 2.4 also shows the sum of the breast and iodine attenuation where 1 mg/ml iodine leads to only a small increase of the total attenuation.

The iodine can be visualized by acquiring two images, taken with sufficiently different photon energies and subsequently performing post-processing on these images. Iodine shows a *k*-edge in the photon energy range used in mammography, and this sudden increase in absorption can be exploited to enhance differences between iodine-enhanced lesions and non-iodinated normal breast tissue. To this extent, it is important to choose the spectra of the two images properly: one with an X-ray spectrum below the *k*-edge of iodine and one with a spectrum above. These two CEM images are called low-energy and high-energy images, respectively.

2.2.3 Spectra of the Low-Energy and High-Energy Image

The X-ray spectrum of the low-energy image is equal to that of a FFDM image. Typically, a tube voltage of 25–34 kV is used, tungsten (W), rhodium (Rh), or molybdenum (Mo) as anode material and silver (Ag), Rh, or Mo as filter material. The low-energy image spectrum is below the *k*-edge of iodine (see, e.g., spectrum Fig. 2.6), and although iodine is present in the breast (as it is injected approximately 2 min prior to image acquisition), it is invisible on the low-energy image. Recent studies have shown that the low-energy CEM images are diagnostically equal to "regular" FFDM images [9–11].

For the high-energy image, the X-ray spectrum is generated with a higher tube voltage of 45–49 kV and a titanium (Ti) or copper (Cu) filter, with the same anode materials (see, e.g., Fig. 2.6). The filter is chosen to remove as many X-ray photons as possible with energies below the *k*-edge of iodine and to separate the high-energy spectrum from the low-energy spectrum.

2.2.4 Acquisition of CEM Images

To begin the CEM exam, patients are injected intravenously with a nonionic, monomeric, low-osmolar iodine contrast agent at a dose of 1.5 ml/kg of body weight. The most frequently used dose is 300 mg/ml iodine or more. The use of an automated injector is recommended (flow rate of 2–3 ml/s, followed by a saline bolus) using at least a 20 G needle. After an at least 2-min delay to allow the contrast agent to disperse in the breast, acquisition of mammographic images can commence ideally in

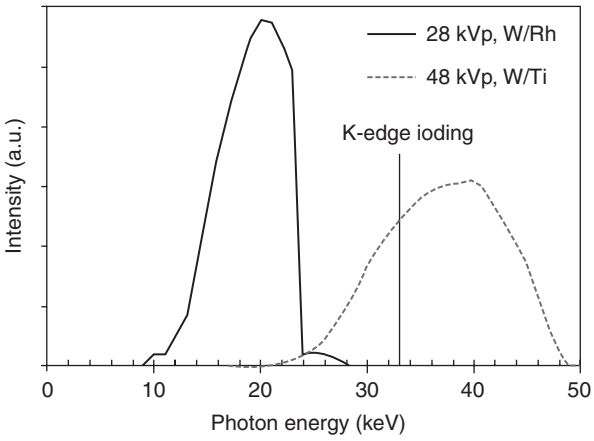

Fig. 2.6 Example of a low-energy (solid line) and high-energy (dotted line) spectrum used in clinical practice. The vertical line indicates the iodine *k*-edge at 33.2 keV showing that the low-energy spectrum is well below the kedge, while the high-energy spectrum is largly above. For visualization, the spectra are normalized to the same area under the curve. In practice the high-energy spectrum delivers a lower dose than the low-energy spectrum

the same order as is normally used in FFDM. The image acquisition usually takes 5–8 min postinjection which is well within the generally accepted time window of 10 min after contrast administration in which the image acquisition needs to be completed [12].

During each CEM acquisition, the low- and high-energy images are acquired directly after each other during the same breast compression: after the first acquisition, the mammography system rapidly switches the filter and the tube voltage to minimize the time between the two acquisitions. The total breast compression time of a single CEM exposure is typically 2–22 s, depending on the breast composition and thickness.

2.3 Post-processing to Obtain the Contrast-Enhanced (Recombined) Image

2.3.1 Concept of Post-processing

To obtain the contrast-enhanced image (also called the recombined image), the low- and high-energy images are processed using a weighted subtraction [13–16]. This involves three steps (Fig. 2.7). First, the images are log-transformed using the natural logarithm. The reason for this step is that X-ray radiation is exponentially attenuated when passing through the breast and the natural logarithm is the mathematical

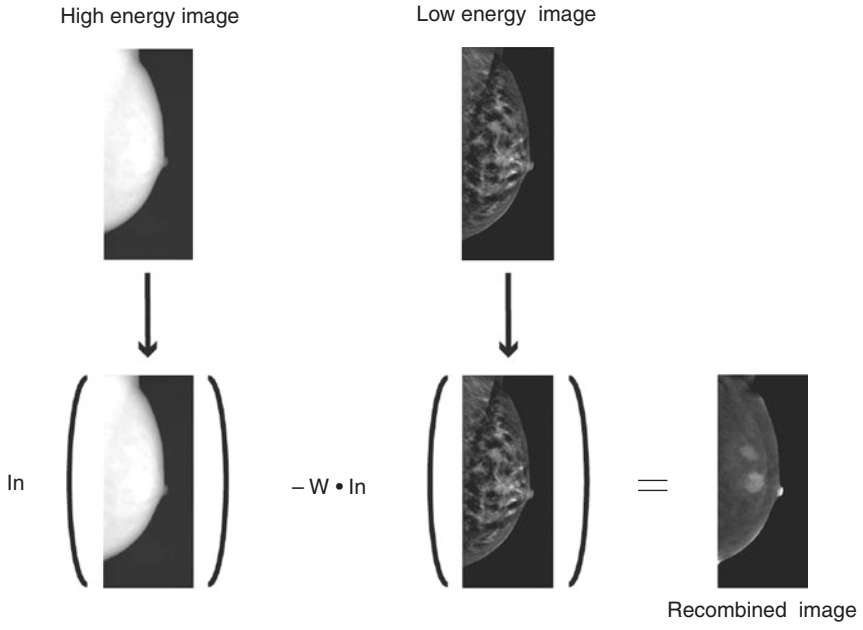

Fig. 2.7 Visual presentation of the postprocessing to obtain the contrast-enhanced recombined image from the low- and high-energy acquisition

counterpart of an exponential function. Second, the log-transformed low-energy image is multiplied by the weighting factor *w*, which is a number that depends on the low- and high-energy attenuation coefficients of normal breast tissue, which in turn depends on the used spectra. Finally, the weighted log-transformed low-energy image is subtracted from the log-transformed high-energy image. The resulting image, which shows areas of iodine accumulation or "enhancement," is called the recombined image.

It is important that in the second step the weighting factor *w* is chosen so that the normal tissue is canceled out, while the iodine contrast agent is not. In choosing the weighting factor, the *k*-edge of iodine is exploited. For the breast tissue, the attenuation coefficient gradually decreases for increasing photon energy (Fig. 2.4), while for the iodine a marked increase at the *k*-edge is present. These differences in attenuation coefficients between low- and high-energy for tissue and iodine allow to further enhance the iodine signal resulting in an image that is dominated by the iodine signal.

2.3.2 Mathematical Description of the Post-processing

For simplification, it is assumed that images are obtained with monoenergetic X-rays, i.e., not a poly-energetic X-ray spectrum as in clinical practice but a single X-ray energy. Although the attenuation coefficients of the glandular and adipose tissue are energy dependent (Fig. 2.3), they are also assumed to be represented by a single attenuation coefficient.

To explain the principle, the attenuation in the breast is considered in a single voxel (Fig. 2.8). The voxel is a 2D projection of a volume and contains a lesion with iodine contrast agent and normal breast tissue. The thickness of the lesion is denoted by *T*, and the thickness of the normal breast tissue is denoted by *t*, which equals the total compressed breast thickness (CBT) minus the lesion thickness. Both the lesion and the normal tissue absorb the X-rays. The absorption is given by an attenuation coefficient μ which is different for the lesion and the normal tissue. Moreover, the attenuation coefficient is different for the low- and high-energy X-rays. Four μ-values are involved: lesion low- and high-energy (denoted by $\mu_{\mathrm{l}}^{\mathrm{LE}}$ and $\mu_{\mathrm{l}}^{\mathrm{HE}}$, where l indicates lesion and LE and HE indicate low-energy and high-energy) and normal tissue low- and high-energy ($\mu_{\mathrm{t}}^{\mathrm{LE}}$ and $\mu_{\mathrm{t}}^{\mathrm{HE}}$, where t denotes tissue). The X-ray radiation is attenuated by the lesion and the normal tissue. How much attenuation takes place is determined by the attenuation coefficient of the material multiplied by the thickness: ($\mu_{\mathrm{t}}^{\mathrm{LE}} \cdot t + \mu_{\mathrm{l}}^{\mathrm{LE}} \cdot T$) and ($\mu_{\mathrm{t}}^{\mathrm{HE}} \cdot t + \mu_{\mathrm{l}}^{\mathrm{HE}} \cdot T$) for the low- and high-energy image, respectively. According to the Lambert-Beer law, the intensity of the incoming X-rays is attenuated exponentially when passing through the tissue and the lesion. The X-ray intensity reaching the detector can be described by the following equation:

$$I_{\mathrm{d}}^{\mathrm{LE}} = I_{0}^{\mathrm{LE}} \cdot \mathrm{e}^{-\left(\mu_{\mathrm{t}}^{\mathrm{LE}} \cdot t + \mu_{\mathrm{l}}^{\mathrm{LE}} \cdot T\right)} \quad \textit{and} \quad I_{\mathrm{d}}^{\mathrm{HE}} = I_{0}^{\mathrm{HE}} \cdot \mathrm{e}^{-\left(\mu_{\mathrm{t}}^{\mathrm{HE}} \cdot t + \mu_{\mathrm{l}}^{\mathrm{LE}} \cdot T\right)} \tag{2.1}$$

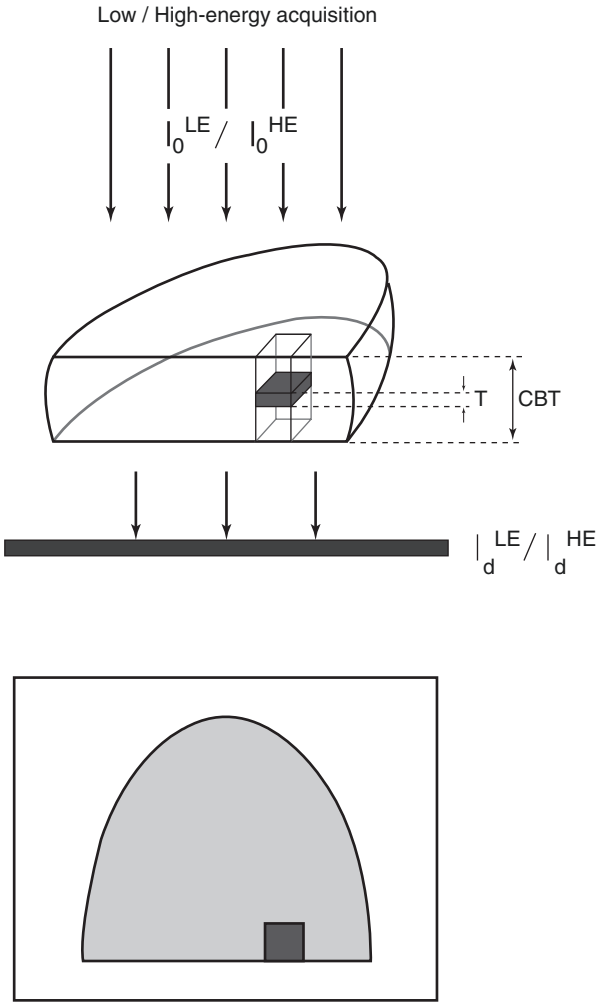

Fig. 2.8 Schematic representation of the breast for the mathematical description of the postprocessing. *I* indicates the intensity of the incoming (0) and transmitted (*d*) low- (LE) and high- (HE) energy X-rays, CBT is the total compressed breast thickness and *T* is the lesion thickness

where I_0^{LE} and I_0^{HE} are the intensities of the incoming X-rays for the low- and high-energy image, respectively; $I_{\mathrm{d}}^{\mathrm{LE}}$ and $I_{\mathrm{d}}^{\mathrm{HE}}$ are the intensities of the X-rays reaching the detector for the low- and high-energy image, respectively; μ denotes the attenuation coefficient; the sub- and superscripts are explained above; and T and t are the thickness of the lesion and normal tissue, respectively.

Each voxel in both the low- and high-energy image contains information of the lesion and the normal tissue. Because two images are acquired with different energies, the iodine attenuation from the lesion can be unraveled by manipulating the two equations above [13–16].

The first mathematical step is to transform the intensities using the natural logarithm. This removes the exponential function from the equations making them easier to handle:

$$\begin{aligned}\ln\left(I_{\mathrm{d}}^{\mathrm{LE}}\right) &= \ln\left(I_0^{\mathrm{LE}} \cdot \mathrm{e}^{-\left(\mu_{\mathrm{t}}^{\mathrm{LE}} \cdot t + \mu_{\mathrm{l}}^{\mathrm{LE}} \cdot T\right)}\right) \\ &= \ln\left(I_0^{\mathrm{LE}}\right) - \left(\mu_{\mathrm{t}}^{\mathrm{LE}} \cdot t + \mu_{\mathrm{l}}^{\mathrm{LE}} \cdot T\right)\end{aligned} \tag{2.2a}$$

$$\begin{aligned}\ln\left(I_{\mathrm{d}}^{\mathrm{HE}}\right) &= \ln\left(I_0^{\mathrm{HE}} \cdot \mathrm{e}^{-\left(\mu_{\mathrm{t}}^{\mathrm{HE}} \cdot t + \mu_{\mathrm{l}}^{\mathrm{HE}} \cdot T\right)}\right) \\ &= \ln\left(I_0^{\mathrm{HE}}\right) - \left(\mu_{\mathrm{t}}^{\mathrm{HE}} \cdot t + \mu_{\mathrm{l}}^{\mathrm{HE}} \cdot T\right)\end{aligned} \tag{2.2b}$$

It should be noted that the natural logarithm of the incoming intensity ($\ln\left(I_0^{\mathrm{LE}}\right)$ and $\ln\left(I_0^{\mathrm{HE}}\right)$) is a constant in Eq. (2.2b).

The second step is to subtract the logarithmic low-energy intensity from the logarithmic high-energy intensity using a specifically chosen weighting factor *w*. This *w* has a certain value and is chosen to cancel out the attenuation due to the normal tissue in the final contrast-enhanced recombined image. The subtraction can be mathematically written as:

$$\begin{aligned}\ln\left(I_{\mathrm{d}}^{\mathrm{HE}}\right) - w \cdot \ln\left(I_{\mathrm{d}}^{\mathrm{LE}}\right) &= \left[\ln\left(I_0^{\mathrm{HE}}\right) - \left(\mu_{\mathrm{t}}^{\mathrm{HE}} \cdot t + \mu_{\mathrm{l}}^{\mathrm{HE}} \cdot T\right)\right] - w \\ &\cdot \left[\ln\left(I_0^{\mathrm{LE}}\right) - \left(\mu_{\mathrm{t}}^{\mathrm{LE}} \cdot t + \mu_{\mathrm{l}}^{\mathrm{LE}} \cdot T\right)\right]\end{aligned} \tag{2.3}$$

This equation can be reshuffled to group the constant values, the tissue thickness (*t*)-dependent terms, and lesion thickness (*T*)-dependent terms together. This results in:

$$\begin{aligned}\ln\left(I_{\mathrm{d}}^{\mathrm{HE}}\right) - w \cdot \ln\left(I_{\mathrm{d}}^{\mathrm{LE}}\right) &= \left[\ln\left(I_0^{\mathrm{HE}}\right) - w \cdot \ln\left(I_0^{\mathrm{LE}}\right)\right] - \left[\mu_{\mathrm{t}}^{\mathrm{HE}} - w \cdot \mu_{\mathrm{t}}^{\mathrm{LE}}\right] \cdot t \\ &- \left[\mu_{\mathrm{l}}^{\mathrm{HE}} - w \cdot \mu_{\mathrm{l}}^{\mathrm{LE}}\right] \cdot T\end{aligned} \tag{2.4}$$

In this equation, there is only one term that contains the thickness of the normal tissue *t* and one term containing the thickness of the lesion *T*. Again, the natural logarithm of the incoming intensities is a constant value, indicated by *C* in the next equations.

The third step is to choose the weighting factor *w* such that the term containing the tissue thickness *t* becomes zero. This can be achieved by making $\left[\mu_{\mathrm{t}}^{\mathrm{HE}} - w \cdot \mu_{\mathrm{t}}^{\mathrm{LE}}\right]$ to become zero, namely, by taking $w = \mu_{\mathrm{t}}^{\mathrm{HE}} / \mu_{\mathrm{t}}^{\mathrm{LE}}$. The used low- and high-energy X-ray radiation determine the value of $\mu_{\mathrm{t}}^{\mathrm{LE}}$ and $\mu_{\mathrm{t}}^{\mathrm{HE}}$ and consequently the numerical value of the weighting factor *w*.

The resulting equation shows only a dependency on the lesion thickness:

$$\ln\left(I_{\mathrm{d}}^{\mathrm{HE}}\right) - w \cdot \ln\left(I_{\mathrm{d}}^{\mathrm{LE}}\right) = C - \left[\mu_{\mathrm{l}}^{\mathrm{HE}} - w \cdot \mu_{\mathrm{l}}^{\mathrm{LE}}\right] \cdot T \tag{2.5}$$

Finally, because of the *k*-edge present in the iodine attenuation coefficient curve (Fig. 2.4), the low- and high-energy X-ray radiation can be chosen such that

$\mu_l^{LE} \sim< \mu_l^{HE}$, while the attenuation of the tissue gradually decreases: $\mu_t^{LE} > \mu_t^{HE}$ and thus $w = \mu_t^{HE} / \mu_t^{LE} < 1$. This reduces Eq. (2.5) further to:

$$\begin{aligned} \ln\left(I_d^{HE}\right) - w \cdot \ln\left(I_d^{LE}\right) &= C - \mu_l^{HE}\left[1 - w \cdot \frac{\mu_l^{LE}}{\mu_l^{HE}}\right] \cdot T \\ &\sim C - \mu_l^{HE} \cdot T \end{aligned} \tag{2.6}$$

This image that is the result of the weighted subtraction is mainly dominated by the iodine attenuation factor for the high-energy X-ray radiation.

2.3.3 Post-processing for Poly-energetic X-Ray Spectra

The above mathematics that produce the iodine contrast-enhanced image simplifies the process by assuming that a monoenergetic X-ray source is used, e.g., the low- and high-energy X-ray radiations consist of a single energy or a very narrow spectrum. In practice, a *poly-energetic* low- and high-energy spectrum is used, which contains a wider range of energies, even to the extent that the tails of the spectrum may cross the *k*-edge (Fig. 2.6). In this case, the monoenergetic approximation method may introduce errors in the recombined image, such as an increase of visible residual background structures [17].

In literature, poly-energetic solutions are presented that have practical disadvantages such as the requirement of calibrations [17, 18]. One vendor has implemented a practically feasible poly-energetic solution that in the basis expands the monoenergetic weighted subtraction with so-called second-order terms [17]:

$$T_{\text{Iodine}} \sim w_1 \cdot \ln I_d^{HE} - w_2 \cdot \ln I_d^{LE} - w_3 \cdot \left(\ln I_d^{HE}\right)^2 - w_4 \cdot \left(\ln I_d^{LE}\right) - w_5 \cdot \ln I_d^{HE} \cdot \ln I_d^{LE} \tag{2.7}$$

In this equation, T is the iodine thickness present in the voxel and I is defined as in Fig. 2.8. The constant C and the weighting factors w_1–w_5 are determined for each combination of breast thickness and low- and high-energy spectra. This is done by performing simulations using a detailed model of the imaging chain of the mammograph (tube, anode/filter material, breast, anti-scatter grid, detector). Puong et al. [17] show that this indeed leads to a significant background texture removal. Another vendor has implemented a slightly different approach using modeling based on a poly-energetic spectrum to derive the optimal weighting factor used in Eqs. (2.3–2.6).

2.3.4 Further Steps in Post-processing

Besides the calculation to produce the contrast-enhanced image, the post-processing may entail other steps, such as a correction for movement of the breast between the two acquisitions and a correction for the reduced breast thickness toward the edge of the breast. Although the time between the two acquisitions is kept short (typically 0.6–20 s) and the breast remains compressed during the whole CEM acquisition,

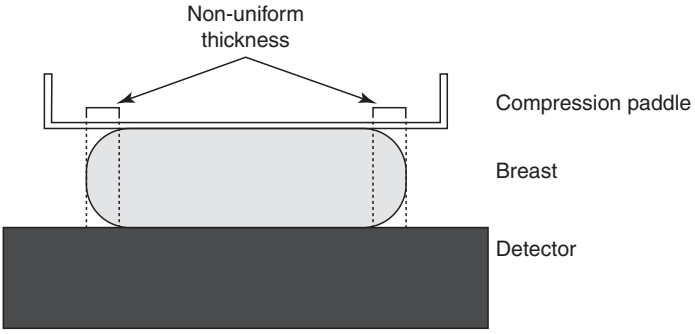

Fig. 2.9 During compression the breast has a uniform thickness, except at the edges as is illustrated here

there may be some movement which may lead to ripple artifacts if unaccounted for [19]. To circumvent this, the low- and high-energy image can be co-registered before further post-processing takes place.

The post-processing algorithm assumes the breast thickness to be uniform which is the case when the breast is compressed except for the edges (see Fig. 2.9). As a result, the total attenuation at the edges is lower which may lead to errors in the calculation of the iodine content in those voxels. The post-processing incorporates corrections for this [17, 20].

2.3.5 Interpretation of Gray Values in Iodine Contrast-Enhanced Image

For each voxel in the image, the calculated iodine contrast enhancement is displayed as a gray value. Since CEM is a two-dimensional technique, each voxel is the result of a projection along a line through the breast (Fig. 2.8) and only the cumulative iodine content along that line can be determined. Consequently, no distinction can be made between a thick lesion with a low iodine concentration (low attenuation μ) and a thin lesion with a high iodine concentration (high attenuation μ) (Fig. 2.10). Therefore, it should be realized that the gray values never represent absolute iodine concentrations (mg/ml or mg/cm^3) but represent the so-called iodine mass thickness (IMT, mg/cm^2) [21, 22]. IMT is a cumulative value of the iodine present in the projection line of a voxel.

2.4 Commercial Implementation

At the time of writing this chapter, three vendors have four commercially available CEM systems. CEM is integrated in their FFDM units that are adapted to allow a rapidly switch to the HE spectrum, read out two acquisitions in a short time period, and perform the necessary post-processing. For the patient, CEM acquisition is

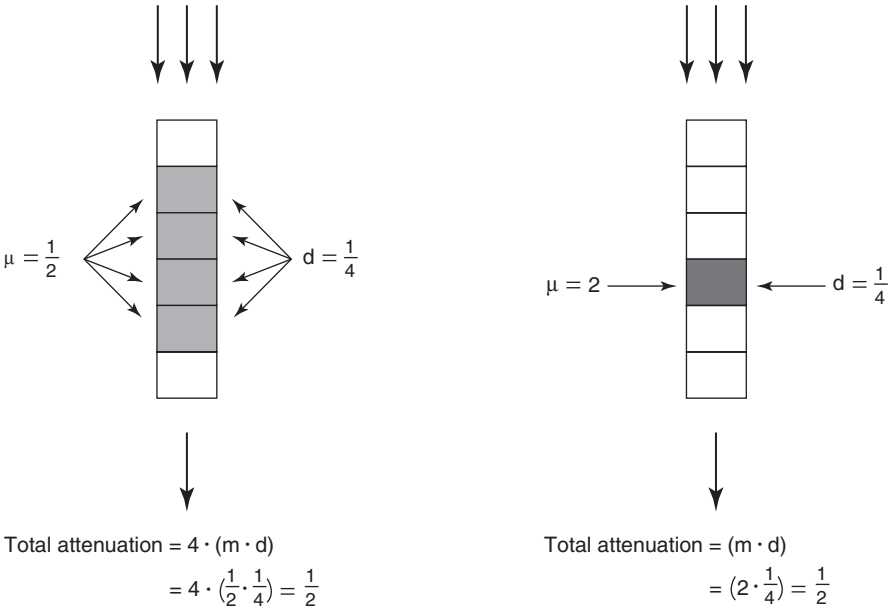

Fig. 2.10 As CEM is a 2D projection technique only the cummulative iodine content along the projection line can be determined. A low concentration but thicker lesion can result in the same grey value as a high concentration thinner lesion

similar to a regular FFDM acquisition: the machine has the same appearance and the same method of compression and positioning, and there is no additional movement of the X-ray tube such as in digital breast tomosynthesis. The main difference during the acquisition is that the total acquisition time of the CEM is a few seconds longer than a FFDM acquisition.

As indicated in Sect. 2.2.3, the high-energy X-ray spectrum needs to be above the iodine *k*-edge and in addition as narrow or monoenergetic as possible. This can be achieved by choosing a higher tube voltage and inserting a filter that absorbs the low-energy photons thoroughly. By choosing a thicker filter, the spectrum becomes narrower, but to maintain enough X-ray intensity for imaging the X-ray, tube output needs to increase. In this respect, vendors have made a trade-off. The high-energy spectrum is generated by using the same anode material as in the low-energy acquisition. For one vendor there are two available anode materials for the low-energy acquisition, and one is chosen based on breast thickness and composition. The same anode material is also always used for the high-energy acquisition. The filter material and tube voltage are switched after the low-energy acquisition to obtain the high-energy spectrum for the second acquisition. The typical switching time ranges from 0.6 to 20 s depending on the vendor. The total acquisition time depends on breast thickness and composition and ranges from 2 to 22 s for the different vendors. Table 2.1 shows the technical specification of the low- and high-energy spectra used in the commercial systems.

Table 2.1 Settings for the low-energy and high-energy CEM acquisition for the four currently commercially available CEM systems

	GE Healthcare		Hologic	Siemens Healthineers
	Senographe Essential SenoBright	Senographe Pristina SenoBright HD	Selenia Dimensions/ 3Dimensions I-View	MAMMOMAT Revelation TiCEM
Low-energy acquisition				
Anode/filter material	Mo/Mo; Mo/Rh; Rh/Rh	Mo/Mo; Rh/Ag	W/Rh; W/Ag	W/Rh
Thickness filter (mm)	Mo: 0.03; Rh 0.025	Mo: 0.03; Ag 0.03	0.050	0.050
Tube voltage range (kV)	26–31	Mo/Mo: 26 Rh/Ag: 34[a]	25–33	28–34
High-energy acquisition				
Anode/filter material	Mo/Al + Cu; Rh/Al + Cu	Rh/Cu	W/Cu	W/Ti
Thickness filter (mm)	Al: 0.3; Cu: 0.3	0.25	0.3	1.0
kV range	45–49	49[a]	45–49	49
Total acquisition time (s)	2.5–7.5	2.5–7.5	<2	<22

Source: Personal communication with J. Korporaal, Siemens Healthineers; S. Muller, GE Healthcare; A. Smith, Hologic; May–Oct 2018
Mo molybdenum, *Rh* rhodium, *Ag* silver; *W* tungsten, *Cu* copper, *Ti* titanium
[a]When the automated exposure control is not used, a larger kV range is possible: LE 22–50 kVp; HE 40–49 kV

2.5 Breast Dose: Mean Glandular Dose Calculation

During a mammographic acquisition, the breast is exposed to radiation which is partly absorbed. As the glandular tissue is the most radiosensitive tissue present in the breast, the mean dose to the glandular tissue or mean glandular dose (MGD) is recommended as a dosimetric quantity [23]. The MGD can be related to the carcinogenic risk. The MGD cannot be measured directly; however, it can be calculated from the incident dose or air kerma at the top surface of the compressed breast using appropriate conversion factors [23, 24]. The conversion factors are based on Monte Carlo computer simulations and are tabulated for a range of breast thicknesses, glandularity, and, initially, low-energy FFDM spectra [25–27]. To accommodate MGD calculation for high-energy spectra in CEM, later on also conversion factors were published for spectra in this energy range [28].

CEM acquires a high-energy acquisition in addition to the low-energy acquisition that is equal to an FFDM acquisition [9–11]. Therefore, it is to be expected that the MGD for CEM is higher compared to FFDM. Only a few studies have been reported regarding the MGD for a commercially implemented CEM. The reported mean MGD values for unilateral single-view CEM acquisition are in the range of 2.49–3.0 mGy for a mean compressed breast thickness in the study population of

56–63 mm [29–32] (Table 2.2). Although the reported MGD values for CEM are very similar, the percentage increase with respect to FFDM varies considerably, ranging from 42% to 81%, due to variations in the reported MGD values for FFDM. It is therefore important also to consider both the CEM and FFDM dose values and not only the percentage increase. Both Badr et al. and Jeukens et al. found that the high-energy acquisition contributes 24–25% to the total MGD of a CEM acquisition. All reported doses are below the acceptable limits set by regulatory institutions [24, 33].

The MGD can be used to relate the radiation exposure to risk of health detriment being the incidence of (non-)fatal cancer. To this extent age-dependent lifetime attributable risk (LAR) factors are published by the Biological Effects of Ionizing Radiation VII committee [34]. For a unilateral, single-view CEM acquisition having an MGD of 2.8 mGy, the LAR for cancer incidence is 2 (age = 40 years), 0.4 (age = 60 years), and <0.1 (age = 80 years) cases out of 100,000 persons. The LAR values for cancer mortality are about 2–3 times lower. From these data one can conclude that CEM exposure poses only a small additional risk compared to the lifetime risk for breast cancer incidence and mortality of 12,000 and 3000 cases per 100,000 women, respectively [34].

Table 2.2 Comparison of MGD for unilateral single-view CEM and FFDM acquisitions reported in literature

	CEM			FFDM		
	Study population (images/patients)	MGD (mean ± SD[a]) [mGy]	Mean (±SD[a]) compressed breast thickness (mm)	Study population (images/patients)	MGD (mean ± SD[a]) [mGy]	Mean (±SD[a]) compressed breast thickness (mm)
Badr et al. [29] (system 1)	391/104	2.65 ± 0.78	56	360/104	1.72 ± 0.96	57
Jeukens et al. [30] (system 1)	193/47	2.80 ± 0.88	58 ± 14	2577/715	1.55 ± 0.48	56 ± 14
James et al. [31] (system 2)	173/173	3.0 ± 1.1	63	6214/6214	1.8 ± 0.9	47[b]
Phillips et al. [32] (systems 1 and 2)	180/45	2.49[c]	56	180/45	1.40 (system 1)[c] 2.16 (system 2)[c]	56

System 1 indicates the GE Healthcare Senographe Essential, system 2 the Hologic Selenia Dimensions

[a]Not all studies report the SD

[b]James et al. report in addition that the CEM MGD is 42% higher than the FFDM MGD for a 63 mm compressed breast thickness

[c]The study reports MGD values for CEM of system 1 and for FFDM for systems 1 and 2

References

1. Alvarez RE, Macovski A. Energy-selective reconstructions in X-ray computerized tomography. Phys Med Biol. 1976;21(5):733–44. PMID: 967922.
2. Brody WR, Butt G, Hall A, Macovski A. A method for selective tissue and bone visualization using dual energy scanned projection radiography. Med Phys. 1981;8(3):353–7. PMID: 7033756.
3. Lehmann LA, Alvarez RE, Macovski A, Brody WR, Pelc NJ, Riederer SJ, Hall AL. Generalized image combinations in dual KVP digital radiography. Med Phys. 1981;8(5):659–67. PMID: 7290019.
4. Johns PC, Drost DJ, Yaffe MJ, Fenster A. Dual-energy mammography: initial experimental results. Med Phys. 1985;12(3):297–304. PMID: 4010634.
5. Johns PC, Yaffe MJ. X-ray characterisation of normal and neoplastic breast tissues. Phys Med Biol. 1987;32(6):675–95. PMID: 3039542.
6. Lalji U, Lobbes M. Contrast-enhanced dual-energy mammography: a promising new imaging tool in breast cancer detection. Womens Health. 2014;10(3):289–98. PMID: 24956295.
7. ICRU. Tissue substitutes in radiation dosimetry and measurement, report 44 of the international commission on radiation units and measurements. Bethesda, MD: ICRU; 1989. https://physics.nist.gov/PhysRefData/XrayMassCoef/tab4.html. Accessed 13 Sept 2018.
8. Dromain C, Canale S, Saab-Puong S, Carton AK, Muller S, Fallenberg EM. Optimization of contrast-enhanced spectral mammography depending on clinical indication. J Med Imaging (Bellingham). 2014;1(3):033506. PMID: 26158058.
9. Fallenberg EM, Dromain C, Diekmann F, Renz DM, Amer H, Ingold-Heppner B, Neumann AU, Winzer KJ, Bick U, Hamm B, Engelken F. Contrast-enhanced spectral mammography: does mammography provide additional clinical benefits, or can some radiation exposure be avoided? Breast Cancer Res Treat. 2014;146(2):371–81. PMID: 24986697.
10. Francescone MA, Jochelson MS, Dershaw DD, Sung JS, Hughes MC, Zheng J, Moskowitz C, Morris EA. Low energy mammogram obtained in contrast-enhanced digital mammography (CEDM) is comparable to routine full-field digital mammography (FFDM). Eur J Radiol. 2014;83(8):1350–5. PMID: 24932846.
11. Lalji UC, Jeukens CR, Houben I, Nelemans PJ, van Engen RE, van Wylick E, Beets-Tan RG, Wildberger JE, Paulis LE, Lobbes MB. Evaluation of low-energy contrast-enhanced spectral mammography images by comparing them to full-field digital mammography using EUREF image quality criteria. Eur Radiol. 2015;25(10):2813–20. PMID: 25813015.
12. Lobbes MB, Smidt ML, Houwers J, Tjan-Heijnen VC, Wildberger JE. Contrast enhanced mammography: techniques, current results, and potential indications. Clin Radiol. 2013;68(9):935–44. PMID: 23790689.
13. Richard S, Siewerdsen JH. Cascaded systems analysis of noise reduction algorithms in dual-energy imaging. Med Phys. 2008;35(2):586–601. PMID: 18383680.
14. Markay MK. Physics of mammographic imaging. Boca Raton, FL: CRC Press; 2013. ISBN: 978-1–4398-7544-5.
15. Hill ML, Mainprize JG, Carton AK, Saab-Puong S, Iordache R, Muller S, Jong RA, Dromain C, Yaffe MJ. Anatomical noise in contrast-enhanced digital mammography. Part II. Dual-energy imaging. Med Phys. 2013;40(8):081907. PMID: 23927321.
16. Hu YH, Scaduto DA, Zhao W. Optimization of contrast-enhanced breast imaging: analysis using a cascaded linear system model. Med Phys. 2017;44(1):43–56. PMID: 28044312.
17. Puong S, Bouchevreau X, Paoureaux F, Iordache R, Muller S. Dual-energy contrast enhanced digital mammography using a new approach for breast tissue canceling. 2007 Medical imaging proceedings of SPIE, vol 6510 65102H/Proceedings volume 6510, medical imaging 2007: physics of medical imaging; 65102H. 2007. https://doi.org/10.1117/12.710133.
18. Contillo A, Di Domenico G, Cardarelli P, Gambaccini M, Taibi A. A novel approach to background subtraction in contrast-enhanced dual-energy digital mammography with commercially

available mammography devices: polychromaticity correction. Med Phys. 2015;42(11):6641–50. PMID: 26520754
19. Yagil Y, Shalmon A, Rundstein A, Servadio Y, Halshtok O, Gotlieb M, Sklair-Levy M. Challenges in contrast-enhanced spectral mammography interpretation: artefacts lexicon. Clin Radiol. 2016;71(5):450–7. PMID: 26897335
20. Korporaal JG, Hörnig MD, Mertelmeier T, Hebecker A. Titanium contrast-enhanced mammography (TiCEM). White paper. Erlangen: Siemens Healthineers; 2018.
21. Hwang YS, Cheung YC, Lin YY, Hsu HL, Tsai HY. Susceptibility of iodine concentration map of dual-energy contrast-enhanced digital mammography for quantitative and tumor enhancement assessment. Acta Radiol. 2018;59(8):893–901. PMID: 29117707.
22. Lobbes MBI, Mulder HKP, Rousch M, Backes WH, Wildberger JE, Jeukens CRLPN. Quantification of enhancement in contrast-enhanced spectral mammography using a custom-made quantifier tool (I-STRIP): a proof-of-concept study. Eur J Radiol. 2018;106:114–21. PMID: 30150032.
23. Dance DR. Monte Carlo calculation of conversion factors for the estimation of mean glandular breast dose. Phys Med Biol. 1990;35(9):1211–9. PMID: 2236205.
24. European Communities. European guidelines for quality assurance in breast cancer screening and diagnosis. 4th ed. Luxembourg: Office for Official Publications of the European Communities; 2006.
25. Wu X, Gingold EL, Barnes GT, Tucker DM. Normalized average glandular dose in molybdenum target-rhodium filter and rhodium target-rhodium filter mammography. Radiology. 1994;193(1):83–9. PMID: 8090926.
26. Boone JM. Glandular breast dose for monoenergetic and high-energy X-ray beams: Monte Carlo assessment. Radiology. 1999;213(1):23–37. PMID: 10540637.
27. Dance DR, Skinner CL, Young KC, Beckett JR, Kotre CJ. Additional factors for the estimation of mean glandular breast dose using the UK mammography dosimetry protocol. Phys Med Biol. 2000;45(11):3225–40. PMID: 11098900.
28. Dance DR, Young KC. Estimation of mean glandular dose for contrast enhanced digital mammography: factors for use with the UK, European and IAEA breast dosimetry protocols. Phys Med Biol. 2014;59(9):2127–37. PMID: 24699200.
29. Badr S, Laurent N, Régis C, Boulanger L, Lemaille S, Poncelet E. Dual-energy contrast-enhanced digital mammography in routine clinical practice in 2013. Diagn Interv Imaging. 2014;95(3):245–58. PMID: 24238816.
30. Jeukens CR, Lalji UC, Meijer E, Bakija B, Theunissen R, Wildberger JE, Lobbes MB. Radiation exposure of contrast-enhanced spectral mammography compared with full-field digital mammography. Investig Radiol. 2014;49(10):659–65. PMID: 24872005.
31. James JR, Pavlicek W, Hanson JA, Boltz TF, Patel BK. Breast radiation dose with CESM compared with 2D FFDM and 3D tomosynthesis mammography. AJR Am J Roentgenol. 2017;208(2):362–72. PMID: 28112559.
32. Phillips J, Mihai G, Hassonjee SE, Raj SD, Palmer MR, Brook A, Zhang D. Comparative dose of contrast-enhanced spectral mammography (CESM), digital mammography, and digital breast tomosynthesis. AJR. 2018;211:839–46.
33. Food and Drug Administration. Mammography quality standards act regulations. https://www.fda.gov/Radiation-EmittingProducts/MammographyQualityStandardsActandProgram/Regulations/ucm110906.htm#s90012. Accessed 13 Sept 2018.
34. National Research Council. Health risks from exposure to low levels of ionizing radiation: BEIR VII phase 2. Washington, DC: National Academic Press; 2006.

Setting Up a CEM Program

3

Jordana Phillips and Tejas S. Mehta

3.1 CEM Overview

A CEM is a four-view bilateral mammogram acquired using a dual-energy technique in standard craniocaudal and medial lateral oblique projections performed entirely after intravenous injection of nonionic low-osmolar iodinated contrast. During each compression, low-energy images are acquired that provide morphologic and density information similar to a conventional mammogram [1], and high-energy images are acquired that provide vascular information similar to breast MRI. Recombined images are generated from subtracting and post-processing the low- and high-energy images, highlighting areas of contrast uptake. A combination of any findings seen on low-energy and/or recombined images is included in exam interpretation (Fig. 3.1). The added information on enhancement allows CEM to identify cancers that would otherwise be obscured on conventional mammography due to tissue density. As a result, CEM in the diagnostic setting has shown improved performance relative to full-field digital mammography (FFDM) and similar performance to breast MRI [2–7]. The Food and Drug Administration (FDA) approved its use as an adjunct to mammography and ultrasound to localize a known or suspected lesion in 2011 [8]. Since that time, there has been increased interest in CEM primarily as a less costly and more accessible alternative to breast MRI.

3.2 Equipment Requirements

One of the perceived strengths of CEM is the relatively few equipment requirements necessary to perform the imaging exam. The minimum requirement includes a mammography unit capable of performing dual-energy imaging. Some older

J. Phillips (✉) · T. S. Mehta
Beth Israel Deaconess Medical Center, Boston, MA, USA
e-mail: jphilli2@bidmc.harvard.edu

M. Lobbes, M. S. Jochelson (eds.), *Contrast-Enhanced Mammography*,
https://doi.org/10.1007/978-3-030-11063-5_3

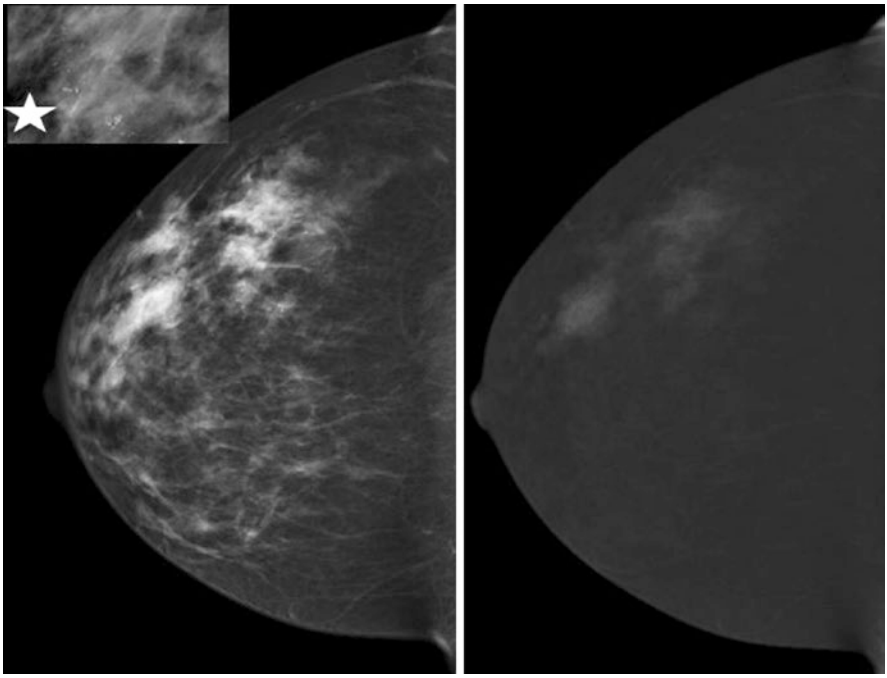

Fig. 3.1 Interpretation of a contrast-enhanced mammogram (CEM) includes a low-energy image (left) and a recombined image (right). Pleomorphic calcifications (star) with associated density are noted throughout the outer right breast (left) with associated non-mass enhancement on the recombined image (right)

mammography units can be upgraded to allow for the acquisition of dual-energy images. This upgrade includes the addition of software and firmware that includes new dose tables to allow for the correct display of dose for the low- and high-energy images. In addition, a copper filter is added to the mammography unit's filter wheel (Fig. 3.2). This copper filter selects high-energy X-rays to be used for the high-energy image acquisition. Once the mammography unit has been upgraded, the physicists must test it to ensure it is functioning appropriately. The process of upgrading the mammography unit and undergoing physicist testing takes approximately 2 days. Practices will need to account for the time this unit will be out of use when planning the clinical schedule.

CEM can be viewed on many vendors' digital workstations with varying functionality. It is worthwhile to contact the vendor managing your imaging display to determine whether CEM can be viewed and what is required to allow viewing. A common method of viewing the CEM study is with the low-energy and recombined images stacked on top of one another. This allows the radiologist to flip between the two images for direct correlation of findings seen on low-energy and recombined images. Vendors distributing CEM mammography equipment typically have viewing workstations with added functionality, such as fading of the low-energy image

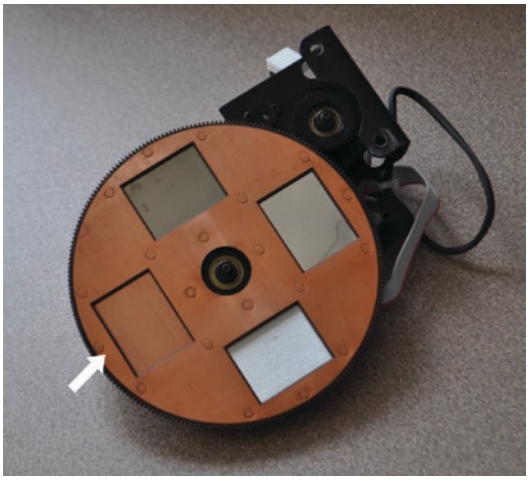

Fig. 3.2 Filter wheel of a mammography unit. The copper filter (white arrow) is added to the filter wheel to enable the mammography unit to acquire high-energy images for the CEM

into the recombined image or the ability to co-register the contrast mammography images with tomosynthesis images, but this added functionality is not required for implementation. Setting up a workstation to be able to view CEM images may take up to a few hours, and this should be accounted for during the implementation schedule.

Lastly, a power injector is a worthwhile consideration for injection of the contrast agent. Although not required, the power injector allows the contrast to be injected more easily than using a manual technique. If using an injector, it must be able to inject the contrast material at a rate of 3 mL/s.

3.3 Physical Space Requirements

The CEM study takes place within the mammography room using CEM-capable mammography equipment. There are a few items that should be close at hand when preparing for the study. These items include a power injector and emergency supplies should the patient develop a contrast reaction. Although it is possible to inject the intravenous line (IV line) outside the mammography unit, it is recommended to perform the injection in the room. This allows for appropriate timing of the CEM study while minimizing the possibility for interruption. It is also preferable to have the patient seated while injecting. This is not only more comfortable for the patient but also safer should the patient have a vasovagal or contrast reaction during, or immediately following, the injection.

To prepare for a possible contrast reaction, it is vital to have emergency supplies readily available. In our department, we keep a small emergency supply box within the contrast mammography room that contains medications used for treating contrast reactions. We also have a crash cart that includes an automated external defibrillator (AED) device and pacer pads close by on the floor. In addition, practices

should have policies for how to manage a contrast reaction and who will manage it, should one occur. For hospital-based practices, this can include utilizing the hospital medicine resources. For outpatient sites, an arrangement can be made with local medicine practices, otherwise emergency services will need to be called. The recommended contrast training for technologists and radiologists will be discussed in more depth later in the chapter.

The final component for the CEM room that is worth considering is a scale. At the time of this writing, it is common practice to administer the contrast agent at a dose of 1.5 mL/kg. To determine the correct amount of contrast to administer, practices can choose to ask the patient to provide her weight or can directly weigh the patient. It is worthwhile to first discuss these options with radiology colleagues in the institution's CT department to see if there are departmental standards for contrast administration.

In addition to preparing the CEM room, it is important to set up a space for placing the IV line. Ideally, this will be a separate room from where the CEM will be performed. It is also helpful to have someone place the IV who has experience performing this task, such as an experienced technologist or nurse. Doing so unlinks IV placement from the performance of the CEM which, in turn, will decrease technologist and mammography room utilization times [9]. A few items are needed to adequately prepare the IV placement room. This includes a chair for the patient to sit in while the IV is placed, IV placement supplies, a sharps container for the needles after they are used, and a point-of-care (POC) test kit for rapid bedside evaluation of renal function (further discussion in contrast safety section). It is worthwhile to consider a reclining chair for IV placement. This may be helpful should the patient have a vasovagal response during IV placement and needs to be laid down.

3.4 Storage Considerations

As reviewed earlier, the standard images for a CEM include standard craniocaudal and mediolateral oblique projections for each breast. Low-energy and high-energy images are acquired during each compression for a total of eight images. The mammography unit automatically processes the low- and high-energy images into a recombined image. The processed recombined images and the processed low-energy images are sent to the imaging workstation for radiologist interpretation and long-term storage. At our institution, the low- and high-energy raw images, of which there are eight, are also sent for storage; however they are not used for interpretation.

The size of each low-energy, high-energy, and recombined image that is acquired and stored is roughly equivalent to a conventional mammographic 2D image. Therefore, the average storage size for a CEM is just a multiple of the average storage size of a conventional 2D mammogram. The storage size will vary depending on whether your institution chooses to store the high-energy images in addition to low-energy and recombined images.

The necessary storage space will increase if additional images are acquired. Additional imaging, such as 90° lateral views, magnification, or spot compression views, can be performed as requested by the interpreting radiologist. These additional images can be acquired using a dual-energy technique highlighting contrast uptake or using only FFDM or tomosynthesis. Should these images be performed using dual-energy, they must be obtained within the 10-min window after contrast administration as contrast is still visible during this time.

It is important to recognize these storage considerations when implementing CEM into your practice as the ability to store the images will depend on the capacity for your PACS.

3.5 Patient Selection

3.5.1 Study Indication

Since receiving FDA approval, CEM has been utilized and studied in many different clinical settings. In non-cancer patients, it has been used to evaluate abnormalities detected on screening mammography or ultrasound, as a follow-up to inconclusive imaging findings, to assess patients with clinical symptoms, and to better detect breast cancer in high-risk women and/or women in whom mammography is of limited value (e.g., dense breast tissue) [2, 3, 10–15]. In patients with suspected or known cancer, CEM has been used to evaluate extent of disease, better define mammographically occult cancers, and monitor response to neoadjuvant chemotherapy [16–18].

When incorporating CEM into practice, a group must first decide for which cases they will be using the modality, i.e., screening callbacks or palpable lumps or to allow each radiologist to choose when they think CEM would be useful. A good population to learn from could be patients with known cancers. For the imager, the recombined images parallel findings seen on breast MRI, as both are technologies assessing vascularity and tumor angiogenesis. In fact, prior MRI can be used for comparison if there are no prior CEM examinations.

Moving forward, practices may opt to use CEM as an alternative to breast MRI given that it is a lower-cost, faster, more accessible option to breast MRI [9, 19]. Using CEM in this setting may also be more palatable to practitioners and patients given that an IV line is placed and contrast injected with both exams, and therefore no added discomfort or risk is being introduced with the CEM. CEM is particularly useful for patients with relative or absolute contraindications to MRI, including pacemakers, metal devices such as aneurysm clips and cochlear implants, increased body habitus limiting MRI scanner capacity, inability to lay prone, or claustrophobia.

As we gain experience with CEM in our practice, we are transitioning to using CEM as the first-line imaging tool for disease extent in women with newly diagnosed breast cancer who would otherwise be getting contrast-enhanced imaging with breast MRI. The most frequently imaged are those who are young (less than

50 years old), have invasive lobular carcinoma, or have mammographically occult malignancy. Should the CEM be difficult to interpret, such as when there is moderate to marked background enhancement or the malignancy is near the chest wall, we will then recommend breast MRI. Using CEM in this way not only minimizes the wait time for the advanced imaging information but also allows greater interaction between the radiologists throughout the staging process. Often with breast MRI, the exam is interpreted after the patient leaves the department, and in some practices the referring clinician rather than the breast imager may transmit the results to the patient. In our practice, the CEM is performed similarly to a diagnostic mammogram, where the patient waits in the department until all necessary imaging is completed. The results are then immediately transmitted to the patient by the radiologist who also can show the images and answer any questions.

Once the imagers and the rest of the breast care team have gained some familiarity with CEM as a new technology, the practice can consider expanding indications for which CEM is performed.

3.5.2 Contrast Safety

In addition to choosing the indications for use, the practice must establish guidelines for determining who can safely receive the contrast agent. In general, the main concerns relate to allergic-like and physiologic reactions as well as other nonallergic reactions, such as contrast-induced nephropathy (CIN), that may develop after contrast administration. Per the American College of Radiology (ACR) Contrast Manual, acute contrast reactions are rare, occurring in less than 1% of patients, and when occur they tend to be mild and self-limiting. Severe reactions to low-osmolar nonionic contrast agents are extremely rare, reported at 0.04%. Fatalities are also extremely rare with a conservative estimate of 1 fatality per 170,000 contrast-enhanced exams. Delayed allergic-like reactions occur in 0.5–14% of patients and are often cutaneous and self-limited [20].

Contrast-induced nephropathy (CIN) is defined as an acute deterioration of renal function caused by intravascular iodinated contrast administration. Unfortunately, there is very little data on the true incidence of CIN as few studies were designed to allow for differentiation of CIN from other causes of post-contrast acute kidney injury. Despite this, the ACR still supports this diagnosis but states that it is a rare entity.

When determining a patient's risk for a contrast-related event, it is often necessary to review the patient's medical history. The ACR Contrast Manual indicates that patients with a history of prior reaction to iodinated contrast media have a five-fold increased risk for developing a subsequent reaction [20]. This is the greatest predictor for subsequent contrast reaction. Beyond that, the manual identifies other medical conditions that may increase the likelihood of an acute reaction; however, the degree of this added risk is not clear. These conditions include asthma, multiple severe allergies, significant cardiovascular disease including aortic stenosis or severe congestive heart failure, anxiety, and renal insufficiency. Acute thyroid storm,

recent radioactive iodine therapy or imaging, or use of beta-blockers may also impact a patient's response to the contrast. Given that the risks for acute contrast reactions are not well-defined, there may be some variability in how practices identify patients at risk for a contrast-related event and who they deem appropriate to receive contrast.

Consensus among all studies evaluating CIN is that underlying severe renal insufficiency is the main risk for development of CIN. However, there is no agreed upon cutoff for serum creatinine of estimated GFR measures to determine when the risk of CIN significantly increases. As a result, practices vary significantly in their guidelines for contrast administration in patients with underlying renal disease. Groups that use renal function measures to determine risk for CIN most commonly use serum creatinine. Increasingly, however, the calculated estimated glomerular filtration rate (eGFR) is being used due to limitations of using the serum creatinine alone. Both measures are limited in patients with acute renal insufficiency [20]. Renal function can be tested in a lab or at the bedside using a point-of-care (POC) test kit (Fig. 3.3). It is important to note that these POC tools may overestimate renal function [21, 22]. Therefore, while they may be an attractive option, it is worthwhile considering formal lab testing, if available.

Fig. 3.3 Example of a point-of-care (POC) testing tool. This allows the radiology practice to evaluate the patient's renal function in the radiology department at the time of their visit rather than sending the patient to a lab

If your breast imaging group is part of a hospital system or large radiology practice, guidelines for safe contrast administration are often predetermined by the CT section. Otherwise, the ACR Contrast Manual is a valuable resource for understanding the risks of contrast agents, determining screening guidelines, as well as reviewing treatment strategies should a reaction occur [20].

Ultimately, the benefit of imaging must always be weighed with the risk of any contrast-related event. Often CEM is not critical to a patient's care, and therefore our practice has opted to only offer CEM to those patients without any risk factors for a contrast-related event. Otherwise, conversations are had with the referring staff regarding the medical need for the study.

Once you determine that a patient is safe to receive contrast, there is still the small possibility for a contrast reaction. Therefore, it is vital that staff, primarily the technologists and radiologists, be prepared to address a reaction should it occur. Staff training will be discussed in more depth later in the chapter. There is also the small chance (0.1–1.2%) that the contrast agent will extravasate into the surrounding tissue while being administered [20]. The patient may experience swelling, tightness, or burning at the IV site. When treated appropriately, extravasations often resolve without significant injury. Rarely, however, serious complications may occur. Your practice should have a formal system in place for managing extravasation when it happens.

Overall, determining that a patient is safe to receive contrast is a critical component of the implementation process. Although contrast reactions can happen, significant reactions are uncommon, and this should not deter a practice from implementing CEM.

3.6 Workflow Considerations

There are many aspects to consider when incorporating CEM into clinical workflow. To sufficiently address key components of implementation, we have chosen to divide the clinical experience into three stages: before the patient arrives in the department, while the patient is in the department, and after the patient has left the department (Table 3.1).

3.6.1 Prior to Patient Arrival in the Department

3.6.1.1 Appointment Times

A practice should decide the time that will be allotted for a CEM appointment. The image acquisition time for CEM is similar to that of a diagnostic mammogram; however, the preparation for the study including IV placement requires additional time [9]. Ideally, IV line placement will be performed outside the mammography room and therefore will not impact the appointment time slot, which is often based on mammography room and technologist utilization. In this scenario, the CEM can be scheduled in a routine diagnostic mammogram appointment slot. Should the

Table 3.1 Workflow considerations before, during, and after the patient is in the department

Prior to patient arrival
Appointment times
Ordering
Scheduling
Validating appropriateness and protocoling
While patient in department
Screening for contrast contraindications
IV line placement
Contrast administration
Performing CEM and additional imaging if needed
Managing results
After patient departure
Coding and billing

practice decide to use the mammography room or the mammography technologist for IV placement, it may be worth lengthening the appointment slot to account for this added use of mammography resources. Given that each practice has different available resources, individual groups will have to determine how much time to allocate to the appointment to complete these tasks.

3.6.1.2 Ordering

Once a practice routinely performs CEM, orders may originate from several parties. Many requests for CEM will originate from within the radiology department, such as in the setting of callbacks for abnormal screening studies or to further evaluate inconclusive findings on FFDM, tomosynthesis, and/or ultrasound. Other requests will originate from primary care providers or the breast care team of referrers (surgeons, breast nurse practitioners, medical oncologists, radiation oncologists). A practice must decide whether they will require radiologist approval prior to the clinician placing an order for the study, to ensure the CEM is ordered for the correct indication and is safe to perform, or whether they will allow referrers to place the order without radiologist input. In the latter scenario, it is vital that the breast practice employs a clinical decision support tool or creates an alternate protocoling system, whereby the practice can ensure that the CEM has been appropriately ordered. As with any diagnostic study, if a general practitioner is given the option to order a specific exam, it is important he/she have some knowledge of the indications.

3.6.1.3 Scheduling

Our academic center offers various breast imaging and intervention services at numerous sites throughout our network. Some sites are screening only, others offer diagnostic mammography and ultrasound services with ultrasound interventions only, and our main academic site offers all diagnostic imaging and interventions, including breast MRI and MRI-guided biopsies. Therefore, if a patient at one of these satellite sites needs an MRI biopsy, she would be instructed to go to the main campus for the procedure. Similarly, CEM is only offered at our main campus due

to equipment availability. As a result, patients must be appropriately scheduled at the main campus and clearly instructed to arrive at the main site for the imaging exam. For multisite practices like ours, it is important to create a system for how patients from one site will be scheduled at another site. Education of the administrative staff at the different sites is critical.

3.6.1.4 Validating Appropriateness and Protocoling

It is important to make sure that patients who are scheduled for CEM are appropriate candidates for the study before their visit. This is especially true when having patients travel to a satellite office to have the CEM. It is suboptimal for a patient to travel to a distant site only to later discover she cannot have the CEM. As mentioned above, practices with sophisticated ordering programs and IT support can use a decision support platform and incorporate a series of contrast screening questions into the order entry process. Screening can also take place after the CEM has been scheduled by a radiologist or radiologist-in-training.

Once a patient is deemed an appropriate candidate for CEM, a protocol should be provided that indicates three aspects: confirmation that it is safe for the patient to receive a CEM, whether any additional testing is necessary to prove it is safe for the patient to receive contrast (i.e., renal function testing), and what images should be performed at the time of the imaging exam.

There is no agreed upon ordering of images for a CEM. Jochelson and colleagues showed that the order of image acquisition did not impact a radiologist's ability to identify breast cancer [5]. Some practices begin with one view of the affected side and alternate with the non-affected side, while others do both projections for the affected breast first. Still others will begin with the same projection for both breasts. For example, they will perform craniocaudal views for each breast first followed by the mediolateral oblique views. Lastly, some practices simply have their mammography technologists perform the CEM similarly to how they would perform the diagnostic mammogram in order to keep the mammography technologists comfortable. Each practice should decide how they will acquire the images, and this will be part of their standing protocol for CEM.

Practices may also create protocols for CEM performed for specific indications. For example, a practice offering conventional FFDM may have a "lump protocol" for their technologist that includes routine CC and MLO views with additional images such as a lateral or spot compression or tangential view. If this patient could have CEM, the "lump protocol" may differ, with fewer or no additional images given the benefit of dual-energy imaging offering higher diagnostic capabilities.

3.6.2 During Patient Visit in the Department

When the patient arrives for a CEM, she interfaces with many different members of the breast imaging team. Figure 3.4 outlines the parallel steps involved by the patient, technologist, radiologist, and other staff during the CEM study. This is discussed in detail below.

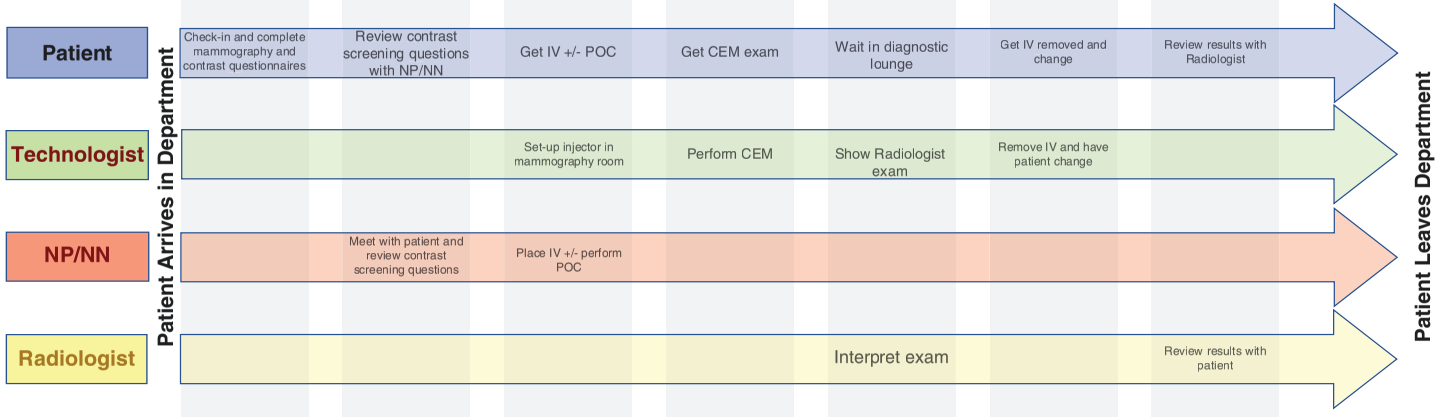

Fig. 3.4 The parallel steps involved by the patient, technologist, radiologist, and other support staff during the CEM study are outlined below. *NP* nurse practitioner, *NN* nurse navigator, *POC* point-of-care testing

3.6.2.1 Screening for Contrast Contraindications

Patients receiving IV contrast for CT are commonly given a questionnaire to evaluate for contrast risk at the time of check-in. This questionnaire is reviewed by the technologist before performing the study and allows the technologist to identify any possible contraindications to contrast administration. Given that the contrast agent used for a CEM is the same as what is used for CT scans, patients receiving CEM should similarly complete these forms, per department protocol, in addition to any conventional mammography questionnaires. The screening questions should include identification of any allergies, any prior history of IV contrast administration or reaction, and questions related to renal function or conditions that may cause renal insufficiency. Breast imaging groups can either use the CT questionnaire itself or make their own based on accepted department guidelines. In our practice, this serves as the second safety check to make sure that the patient is an appropriate candidate for the CEM exam. (The first check occurs before the patient arrives in the department.)

After check-in but before the exam, our practice has opted to have a member of the breast imaging team (nurse, nurse practitioner, or physician) briefly speak to the patient about CEM. We discuss how the exam is performed and the added benefits of this imaging technique. We also ask the patients a series of questions related to contrast risk (Table 3.2). This serves as the third safety check for CEM.

Some practices may opt to perform a time-out procedure immediately prior to contrast administration, similar to what is performed for other imaging-guided procedures and surgical cases. This would serve as the final check before the exam is performed.

3.6.2.2 IV Placement

Although this may appear to be a simple task, IV placement may be one of the more challenging components of CEM implementation. Unlike MRI or CT technologists, mammography technologists may not be familiar with IV line placement and therefore may not embrace this new task. As a result, practices may need to identify other

Table 3.2 Quick checklist to screen for contraindications to contrast administration

Checklist for contrast administration
Prior history of allergic reaction to contrast?
Significant allergies to food/medicine?
Severe asthma?
Diabetes?
Hypertension?
Renal disease?
Multiple myeloma?
Myasthenia gravis?
Actively treated thyroid disease?

Answering yes to any of these may not preclude CEM however would provide an alert to further investigate if contrast can be safely administered

members of the breast imaging team who can comfortably and safely place the IV line. Practices can utilize preexisting resources, such as other CT/MRI technologists, who routinely place IV lines. The feasibility of this is related to how accessible the other services are to the breast imaging suite. Another option is to train other members of the team, such as a nurse navigator or nurse practitioner, if either is available. Lastly, a hospital-based practice may opt to use a specialized IV team; however, this may result in suboptimal efficiency depending on the travel distance required.

The person placing the IV line must learn the gauge of the angiocatheter and location for IV placement. Ideally, a 20 G angiocatheter will be used in the antecubital fossa. However, smaller angiocatheters can be used, if needed. Most importantly, the angiocatheter must be able to support the flow rate of 3 cc/s from the power injector. It is worthwhile to reference the power injector for minimal gauge required for use. It is also important to have a system in place for handling technically challenging IV placements or those patients with chest wall ports.

Ideally, the person placing the IV line should also be trained to perform POC renal function testing, if being used. Not all patients will require this testing, and this should be determined ahead of time based on department guidelines for contrast administration. Independent breast practices should consult the ACR Contrast Manual and other local radiology groups to develop a formal practice guideline.

If the practice opts to have members of the breast imaging team perform IV placement and POC testing, it is useful to train at least two people for this task. This ensures that there is a backup person available should the main person be unavailable. If a second person is not available, then it is worthwhile to create a backup plan with the CT/MRI department or the IV team.

In addition to identifying the staff to place the IV line, it is important to also identify a room for IV line placement. Ideally, the IV line should be placed in a separate room from the mammography unit in order to minimize mammography room utilization times.

3.6.2.3 Contrast Administration

While the patient is having her IV line placed, the technologist can be preparing the mammography room and injector for contrast administration. As the CEM study is sensitive to timing of contrast, we suggest the patient receive the contrast in the same room that the mammography images are performed. Standard practice is to administer the nonionic iodinated contrast agent at a dose of 1.5 mL/kg and at a rate of 3 mL/s. Our group weighs each patient for accurate dosing but this is not universal practice. In addition, a power injector is recommended to administer the contrast agent at the abovementioned rate. It is also recommended that the technologists wear gloves when administering contrast to prevent contamination on the breast or detector.

Although the contrast is being administered by the technologist, all members of the breast imaging team (technologists, nurses, nurse practitioners, physicians-in-training, and physicians) should be trained to manage contrast reactions and extravasation.

This training should be performed at routine intervals. In addition, it is worthwhile to have a designated location to observe patients who may have a contrast-related event. This location should be separated from the mammography room to have minimal impact on workflow and other patients presenting for imaging evaluation.

3.6.2.4 Performing CEM (and Any Additional Imaging)

Once the patient has received the contrast, the IV line is disconnected, and the patient is ready for imaging. It is imperative that the dual-energy images be obtained within a 10-minute period to maintain the benefits of contrast enhancement [5]. It is conventional to obtain bilateral craniocaudal and mediolateral oblique dual-energy views, even if there is only one affected symptomatic or abnormal side. However, there is no set standard of which order the images should be acquired. In our practice, following a (minimum) 2-min delay, we alternate imaging of each breast, starting with the craniocaudal view of the affected breast (Fig. 3.5).

Depending on the indication for the exam, additional dual-energy or conventional views can be obtained following the initial four dual-energy views to assist in diagnosis. These views are often determined by the practice's protocols, although may also be requested by the interpreting radiologist based on the individual case. Having established protocols helps streamline workflow so that any additional images can be obtained while the patient is in the mammography room for the CEM study. This is especially important if additional dual-energy images are being obtained as these should be performed within the 10-min window following contrast injection. Alternatively, the radiologist can stay in the mammography room while the CEM is being performed such that a quick decision can made as to whether additional images should be obtained. Often these additional dual-energy images are acquired *after* the standard four views are obtained.

Like any diagnostic mammogram, once the initial images are completed, the patient is asked to wait in the diagnostic lounge, and the study is reviewed by the radiologist. Any findings identified by the radiologist are then worked up with mammography, tomosynthesis, or ultrasound, while the patient waits in the department.

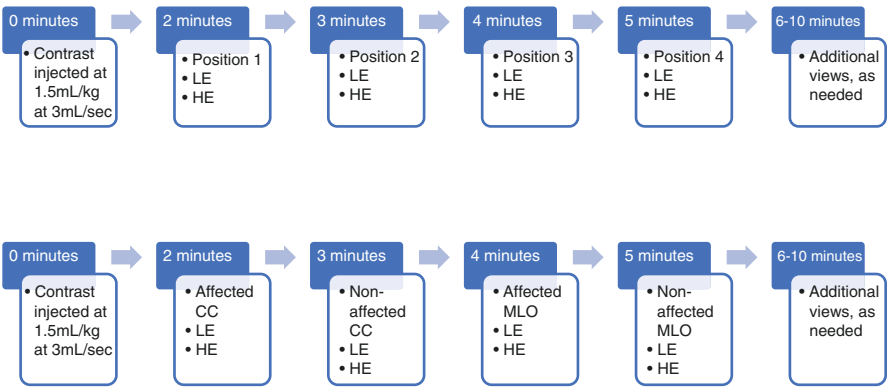

Fig. 3.5 General (**a**) and institutional specific (**b**) image acquisition protocols for CEM

3.6.2.5 Management of Results

Once the diagnostic workup is complete, the radiologist must provide an appropriate BI-RADS code (to be discussed in depth in a later chapter) and associated management plan. In many scenarios, conventional mammography, tomosynthesis, and ultrasound may be used for any follow-up or interventional procedures that are necessary. It is important to recognize, however, that there may be CEM-only findings for which mammography, tomosynthesis, and/or ultrasound cannot resolve. At present, MRI is commonly used in this scenario with subsequent MRI biopsy if an MRI correlate is found. Practices without immediate access to breast MRI should connect with local groups who do have MRI. Alternatively, CEM follow-up can be pursued, or CEM-guided biopsy can be attempted using conventional mammography equipment as there is currently no formal method for performing a CEM-guided biopsy.

Regardless of the final recommendation, it is critical for the breast imaging practice to have a plan to ensure that any recommended imaging occurs. For example, if an MRI is going to be recommended, it is important that the practice have a plan for how this will be communicated to the patient and referring physician and how the MRI will be ordered and scheduled.

3.6.3 After Patient Leaves the Department

3.6.3.1 Coding and Billing

Although CEM requires additional time of screening and speaking to the patient about contrast administration, placing the IV line, and administering contrast [9, 23], there is no billing code specific to this study yet. Thus, our practice, like others performing CEM, is billing this procedure as a diagnostic mammogram with IV contrast. As CEM becomes more routinely used, we suspect there will be separate CPT (current procedural terminology) codes taking the additional factors associated with CEM into account. The use of CEM in lieu of MRI can result in a significant cost savings [19], and a practice may be able to elicit institutional support for some of the nonreimbursed time and personnel to build a CEM program.

3.7 Staff Training

Staff training largely involves the technologists, who will be performing the CEM, and the radiologists who will be interpreting the exam (Table 3.3). These two groups will be the focus of this chapter; however, there are others involved in the clinical workflow that should be identified and included in the implementation process. This includes the technical support staff helping with CEM workflow, front desk staff checking patients in, nursing staff helping with IV placement and/or monitoring, and the schedulers and coordinators who are booking the exams. These people are all part of the CEM team. By involving them early you can ensure they understand their role and can successfully perform it.

Table 3.3 Elements of preparation for technologists and radiologists

Staff	Training recommendations
Technologists	Identification of 2–3 technologists
	Educational overview of CEM, including dose
	Practical review of how to perform CEM and QA (including phantoms and patients)
	Review of contrast contraindications, eligibility tests, and management of complications
	IV placement training
	Review CEM workflow
Radiologists	Educational overview of CEM, including dose
	Review of CEM indications for practice
	Review CEM workflow
	Review of contrast contraindications, eligibility tests, and management of complications
	Training how to interpret, manage, and report on CEM findings

3.8 Technologists

The technologists play a large role in preparing for and performing CEM. In fact, in our institution the technologists are the main interface with patients during this exam. As a result, it is important that they not only understand how to physically perform the exam, but it is also important they understand the value of the study. This begins with someone from the team providing an educational overview of the modality to include the history of the exam, the data supporting its use, and examples of how CEM can benefit patients. At the beginning, it is also worthwhile to identify two to three technologists who will learn to perform the CEM and who can train additional staff as needed. These technologists will be the first members of the CEM team, so it is vital to choose technologists who can embrace innovation and change. Getting the technologists invested in CEM is a top priority and will allow for a smoother implementation process.

Once the CEM technologists are identified and have received basic training on the background of the technology, they must be trained to perform the exam by an application specialist. This training includes how to perform the exam on both a phantom and a patient, as well as all quality control requirements. This training takes approximately 2 days. The clinical workflow should consider the absence of these technologists and the mammography room when planning for the training.

As mentioned above, the technologists' role is not isolated to simply performing the CEM. They must also be trained as to which patients are acceptable candidates for the study and who might be at risk for a contrast-related event. As with CT and MRI at our institution, our patients complete a safety form before their CEM to make sure they can safely undergo the imaging exam. This form is the same form used for CT studies, as the risks related to a contrast-related event and radiation are the same. The technologists review these forms before performing the study. Given that not all mammography technologists are acquainted with the risks of iodinated

contrast or these forms, they must be trained in the institutional guidelines on who can receive iodinated contrast, who cannot receive contrast, and any required testing that must be performed to determine whether the patient can receive contrast agent.

Depending on your clinical workflow, the technologists may also need to be trained on how to place IV lines and perform bedside renal function testing using a POC test kit. Part of this training includes learning the minimal gauge requirements to handle the power injector flow rate of 3 cc/s. Twenty and twenty-two gauge angiocatheters are commonly used. Chest wall ports often have specific rules for access and training should include these. When using a power injector, it is important that the port is power-injectable and can handle the high flow rates. It is also important to make sure that the injection is performed in a way to preserve the port function, such as using heparin before and after injection to ensure port patency. Lastly, it is worthwhile to have a system in place for those patients that are technically challenging for IV placement.

Once the CEM is performed, the technologists must be aware of how to identify and manage the preliminary phases of a contrast-related event should one occur. These include contrast-related reactions and extravasation. Often breast divisions can use policies already in place for managing contrast reactions and extravasation; however, stand-alone breast imaging practices may need to formulate these from scratch. Overall, CEM training should include training on contrast-related events so all staff can act appropriately in this circumstance. This training should occur at routine intervals. At our institution, training includes an annual lecture followed by clinical scenarios. Simulation has also been shown to be useful for contrast reaction training and should be considered [24, 25].

Lastly, technologists should be knowledgeable about the radiation dose of a CEM, like conventional mammography or tomosynthesis. In our experience, it is not uncommon for patients to ask about radiation dose when an exam is being performed. To aid the technologists, it may be worthwhile to create an educational handout for patients discussing the benefits of CEM while addressing questions related to dose and contrast administration.

3.9 Radiologists

Like technologists, radiologists must first understand the role and value of CEM in their clinical practice. This is vital for ultimate acceptance of this new modality. Often this will involve discussions among the clinical group regarding how best to implement the technology so as to incur minimal disruptions to the clinical workflow. Radiologists must then be trained in two primary areas which include management of contrast-related events and CEM interpretation and reporting.

Along with their technologist colleagues, radiologists must learn how to screen patients for risk factors for contrast administration, identify contrast-related events, and learn how to manage them. This is especially important given that contrast is not routinely administered in breast imaging divisions, and therefore some breast radiologists, particularly those without exposure to breast MRI, may be less

comfortable managing contrast-related events than their colleagues in general radiology. Training should be a formal process and can include simulation exercises to maximize radiologist comfort. Given that contrast reactions can also occur with breast MRI, although less frequently, this training serves to prepare breast imagers for adverse events with both modalities.

Radiologists must also learn how to interpret and report CEM cases. Overall, it is a relatively straightforward modality to learn to interpret given that image interpretation is similar to other modalities commonly interpreted by breast imagers. This includes the low-energy images which are similar to conventional mammography and the recombined images which are similar to subtraction images on MRI without kinetics. Lalji and colleagues demonstrated that radiologists with no experience interpreting CEM performed nearly as well as those with 2 years of experience [2].That being said, there is training that is involved to teach radiologists how to appropriately view and hang the CEM images, as well as how to interpret CEM findings. This includes the imaging appearance and management of benign and malignant breast disease on CEM. Radiologists must also be taught how to report CEM, highlighting the fact that CEM interpretations and reports include findings seen on both low-energy and recombined images. As of this writing, there is no formal training requirement for CEM interpretation; however, one study suggested that radiologist performance improved from 80% to 92.4% after diagnosing 100 lesions [3]. Therefore, it is recommended that radiologists have an opportunity to view CEM cases before incorporating CEM into clinical practice.

3.10 Marketing

Having your technologists and radiologists excited about CEM is important, but it is also important to have referring providers and patients on board as well. This can be accomplished through educational conferences, letters to providers, pamphlets, and posters. Showing a few relevant cases at tumor boards may also encourage clinicians to order CEM. Practices should also embrace social media as a platform for advertising their new use of CEM. Finally, radiologists should talk to patients directly, informing them of the new service that the group is offering.

References

1. Lalji UC, Jeukens CR, Houben I, Nelemans PJ, van Engen RE, van Wylick E, et al. Evaluation of low-energy contrast-enhanced spectral mammography images by comparing them to full-field digital mammography using EUREF image quality criteria. Eur Radiol. 2015;25(10):2813–20.
2. Lalji UC, Houben IP, Prevos R, Gommers S, van Goethem M, Vanwetswinkel S, et al. Contrast-enhanced spectral mammography in recalls from the Dutch breast cancer screening program: validation of results in a large multireader, multicase study. Eur Radiol. 2016;26(12):4371–9.
3. Cheung YC, Lin YC, Wan YL, Yeow KM, Huang PC, Lo YF, et al. Diagnostic performance of dual-energy contrast-enhanced subtracted mammography in dense breasts compared to mammography alone: interobserver blind-reading analysis. Eur Radiol. 2014;24(10):2394–403.

4. Fallenberg EM, Schmitzberger FF, Amer H, Ingold-Heppner B, Balleyguier C, Diekmann F, et al. Contrast-enhanced spectral mammography vs. mammography and MRI – clinical performance in a multi-reader evaluation. Eur Radiol. 2017;27(7):2752–64.
5. Jochelson MS, Dershaw DD, Sung JS, Heerdt AS, Thornton C, Moskowitz CS, et al. Bilateral contrast-enhanced dual-energy digital mammography: feasibility and comparison with conventional digital mammography and MR imaging in women with known breast carcinoma. Radiology. 2013;266(3):743–51.
6. Tagliafico AS, Bignotti B, Rossi F, Signori A, Sormani MP, Valdora F, et al. Diagnostic performance of contrast-enhanced spectral mammography: systematic review and meta-analysis. Breast. 2016;28:13–9.
7. Lee-Felker SA, Tekchandani L, Thomas M, Gupta E, Andrews-Tang D, Roth A, et al. Newly diagnosed breast cancer: comparison of contrast-enhanced spectral mammography and breast MR imaging in the evaluation of extent of disease. Radiology. 2017;285(2):389–400.
8. GE Healthcare 510(k) premarket notification submission. [Available from: https://www.accessdata.fda.gov/cdrh_docs/pdf10/k103485.pdf]. Accessed February 19, 2019.
9. Phillips J, Steinkeler J, Talati K, Brook A, Dialani V, Fishman M, et al. Workflow considerations for incorporation of contrast-enhanced spectral mammography into a breast imaging practice. J Am Coll Radiol. 2018;15(6):881–5.
10. Jochelson MS, Pinker K, Dershaw DD, Hughes M, Gibbons GF, Rahbar K, et al. Comparison of screening CEDM and MRI for women at increased risk for breast cancer: a pilot study. Eur J Radiol. 2017;97:37–43.
11. Lobbes MB, Lalji U, Houwers J, Nijssen EC, Nelemans PJ, van Roozendaal L, et al. Contrast-enhanced spectral mammography in patients referred from the breast cancer screening programme. Eur Radiol. 2014;24(7):1668–76.
12. Mori M, Akashi-Tanaka S, Suzuki S, Daniels MI, Watanabe C, Hirose M, et al. Diagnostic accuracy of contrast-enhanced spectral mammography in comparison to conventional full-field digital mammography in a population of women with dense breasts. Breast Cancer. 2017;24(1):104–10.
13. Phillips J, Miller MM, Mehta TS, Fein-Zachary V, Nathanson A, Hori W, et al. Contrast-enhanced spectral mammography (CESM) versus MRI in the high-risk screening setting: patient preferences and attitudes. Clin Imaging. 2017;42:193–7.
14. Fallenberg EM, Dromain C, Diekmann F, Renz DM, Amer H, Ingold-Heppner B, et al. Contrast-enhanced spectral mammography: does mammography provide additional clinical benefits or can some radiation exposure be avoided? Breast Cancer Res Treat. 2014;146(2):371–81.
15. Tennant SL, James JJ, Cornford EJ, Chen Y, Burrell HC, Hamilton LJ, et al. Contrast-enhanced spectral mammography improves diagnostic accuracy in the symptomatic setting. Clin Radiol. 2016;71(11):1148–55.
16. Iotti V, Ravaioli S, Vacondio R, Coriani C, Caffarri S, Sghedoni R, et al. Contrast-enhanced spectral mammography in neoadjuvant chemotherapy monitoring: a comparison with breast magnetic resonance imaging. Breast Cancer Res. 2017;19(1):106.
17. Fallenberg EM, Dromain C, Diekmann F, Engelken F, Krohn M, Singh JM, et al. Contrast-enhanced spectral mammography versus MRI: initial results in the detection of breast cancer and assessment of tumour size. Eur Radiol. 2014;24(1):256–64.
18. Lobbes MB, Lalji UC, Nelemans PJ, Houben I, Smidt ML, Heuts E, et al. The quality of tumor size assessment by contrast-enhanced spectral mammography and the benefit of additional breast MRI. J Cancer. 2015;6(2):144–50.
19. Patel BK, Gray RJ, Pockaj BA. Potential cost savings of contrast-enhanced digital mammography. AJR Am J Roentgenol. 2017;208(6):W231–W7.
20. American College of Radiology, ACR Committee on Drugs and Contrast Media ACR manual on contrast media, version 10.3. 2018. https://www.acr.org/-/media/ACR/Files/Clinical-Resources/Contrast_Media.pdf
21. Houben IPL, van Berlo CJLY, Bekers O, Nijssen EC, Lobbes MBI, Wildberger JE. Assessing the risk of contrast-induced nephropathy using a finger stick analysis in recalls from breast screening: the CINFIBS explorative study. Contrast Media Mol Imaging. 2017;2017:5670384.

22. Snaith B, Harris MA, Shinkins B, Jordaan M, Messenger M, Lewington A. Point-of-care creatinine testing for kidney function measurement prior to contrast-enhanced diagnostic imaging: evaluation of the performance of three systems for clinical utility. Clin Chem Lab Med. 2018;56(8):1269–76.
23. Patel BK, Garza SA, Eversman S, Lopez-Alvarez Y, Kosiorek H, Pockaj BA. Assessing tumor extent on contrast-enhanced spectral mammography versus full-field digital mammography and ultrasound. Clin Imaging. 2017;46:78–84.
24. Pfeifer K, Staib L, Arango J, Kirsch J, Arici M, Kappus L, et al. High-fidelity contrast reaction simulation training: performance comparison of faculty, fellows, and residents. J Am Coll Radiol. 2016;13(1):81–7.
25. Wang CL, Chinnugounder S, Hippe DS, Zaidi S, O'Malley RB, Bhargava P, et al. Comparative effectiveness of hands-on versus computer simulation-based training for contrast media reactions and teamwork skills. J Am Coll Radiol. 2017;14(1):103–10.e3.

Interpretation of Contrast-Enhanced Mammography

4

Marc Lobbes

4.1 Introduction

Contrast-enhanced mammography (CEM) is most commonly performed in women who have clinical symptoms, a contraindication for breast MRI, or abnormal screening mammograms requiring additional imaging. A typical CEM exam consists of three different images per breast and per view: low-energy, high-energy, and recombined. As in conventional full-field digital mammography (FFDM), both breasts should be imaged in two standard views (i.e., craniocaudal and mediolateral oblique views). Additional views (e.g., magnification, spot compression, and rolled views) can be requested by the radiologist if necessary and can be acquired when performing CEM. A typical example of a standard CEM exam is presented in Fig. 4.1.

4.2 Contrast-Enhanced Mammography Images

4.2.1 Low-Energy Images

The low-energy images are acquired at least 2 min after the completion of intravenous administration of an iodine-based contrast agent, usually at a dose of ≥300 mg/ml. Although the breast tissue already contains contrast, it cannot be appreciated visually as these images are acquired at keV levels below the *k*-edge of iodine. Several studies have compared low-energy images with conventional FFDM images.

Fallenberg et al. compared FFDM and CEM in 118 women with histologically proven breast cancer [1]. Sensitivity across readers increased from 77.9% for FFDM

M. Lobbes (✉)
Department of Radiology and Nuclear Medicine, Maastricht University Medical Center, Maastricht, The Netherlands
e-mail: marc.lobbes@mumc.nl

M. Lobbes, M. S. Jochelson (eds.), *Contrast-Enhanced Mammography*,
https://doi.org/10.1007/978-3-030-11063-5_4

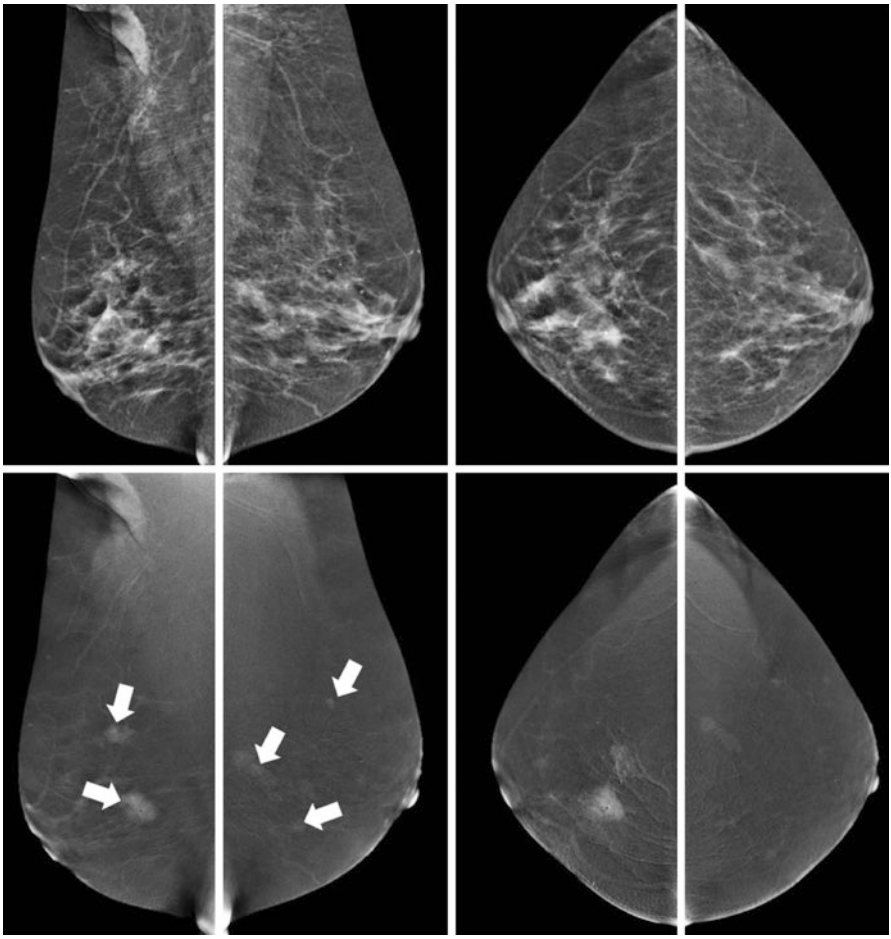

Fig. 4.1 Typical example of a standard contrast-enhanced mammography exam, consisting of low-energy images (top row) and recombined images (bottom row). Images are acquired from both breasts in the standard mammographic views (craniocaudal and mediolateral oblique). In this case, bilateral multifocal invasive breast cancer was diagnosed (arrows)

to 94.7% for CEM. This did not improve any further by adding a separate mammogram. Regarding tumor size, CEM resulted in a slight overestimation of 0.6 mm, whereas the combination of CEM and FFDM resulted in an overestimation of 4.5 mm. Hence, the authors concluded that FFDM is not necessary if CEM has been performed.

Francescone et al. compared low-energy CEM with FFDM images of 170 breasts. In this study, 88 women had both CEM and FFDM within 6 months of each other while undergoing evaluation for newly diagnosed breast cancer or screening [2]. The study parameters included mammographic findings such as calcifications and masses, distance from the nipple to chest wall, compression

thickness, and compression force on the mediolateral oblique view. The authors concluded that the low-energy CEM images were equivalent to the FFDM images, as they did not observe any statistically significant differences regarding the study parameters.

Lastly, Lalji et al. studied the similarity of low-energy CEM and FFDM on both a breast phantom and in clinical cases [3]. For the phantom experiments, they did not find any significant difference between detection thresholds for CEM and FFDM at different phantom thicknesses using a CDMAM phantom and by applying CEM settings commonly used in clinical cases. After the phantom study, two experienced radiologists compared the quality of CEM and FFDM images in 147 women who underwent both CEM and FFDM within 2 weeks of each other. Images were scored according to the European Reference Organization for Quality Assured Breast Screening and Diagnostic Services [4]. Of the 20 scoring criteria, no statistically significant differences were found in 17 criteria. Two criteria determined that there was superior visualization of (micro)calcifications on the low-energy images, although these differences were small ($p = 0.042$). These differences were also not confirmed by the previous study by Francescone et al. [2]. The delineation of the pectoral muscle on mediolateral oblique views was considered worse on low-energy CEM exams ($p < 0.001$), but the authors concluded that this would not cause any clinically relevant limitations.

Based on these three studies, it is safe to conclude that low-energy images are equivalent to FFDM.

4.2.2 High-Energy Images

The high-energy images are acquired within seconds of the low-energy images and primarily used for imaging the areas of iodine uptake, as these are acquired with keV levels above the *k*-edge of iodine. As the energy of the X-ray spectrum used is much higher, less radiation is absorbed when passing through the breast tissue. The high-energy images result in only a small additional radiation dose to the breast. The high-energy images are white and not suitable for any form of interpretation. The data in these images are used in conjunction with that of low-energy images to construct the recombined CEM images.

4.2.3 Recombined Images

The recombined images provide images of areas of enhancement enabled by increased perfusion of the breast tissue at the site of a malignant or occasionally benign neoplasm. In clinical practice, the radiologist views the low-energy and recombined images of both breasts in at least two views. Although the recombined images are reconstructed from images which are acquired only seconds apart, some artifacts can be observed. The radiologist evaluating CEM images should be aware of these artifacts, as knowledge of them reduces clinical dilemmas.

4.2.4 Artifacts on Recombined Images

The most common artifacts on recombined images are "breast-in-breast" artifacts; artifacts caused by breast implants, medical devices, or jewelry; ripple or motion artifacts; axillary line artifacts; and skin line enhancement artifacts.

The "breast-in-breast" artifact consists of a band of lower gray values at the periphery of the breast, simulating a double breast contour (Fig. 4.2). The artifact is observed in approximately 95% of images but usually does not result in difficulties in image interpretation [5]. This artifact is produced by different patterns of scatter radiation in low- and high-energy CEM images. These are assumed to be similar during reconstruction to form a recombined image, but this is not entirely true. The artifact is most pronounced in larger breasts and is commonly seen with first-generation CEM units, as the anti-scatter grids used then were not specifically designed for high-energy acquisitions. With next-generation CEM units, this artifact is less pronounced.

Women with breast implants are difficult to image with CEM. The implants create extensive artifacts on recombined images. The physics behind CEM is based on the presence of breast tissue (i.e., fat and fibroglandular tissue) and iodine.

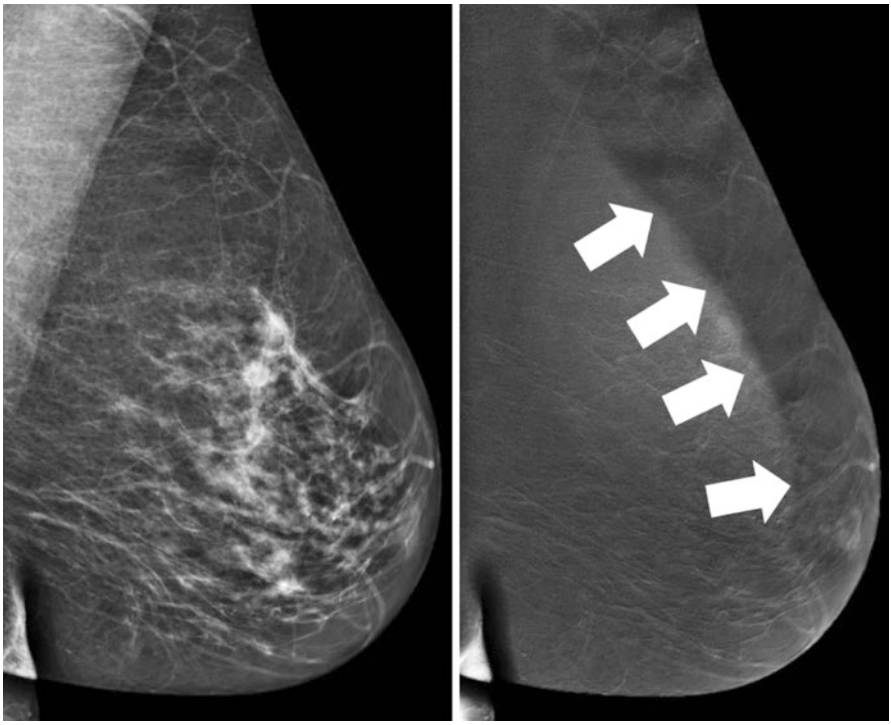

Fig. 4.2 Example of the "breast-in-breast" artifact. On the recombined images, a band of lower gray values can be observed at the periphery of the breast, suggesting a double breast contour (arrows)

Consequently, the distinction of breast tissue with material of any other composition, such as silicone or metal, would require an extra third acquisition with a different X-ray spectrum, leading to more noise in the recombined images. Similarly, other medical devices or jewelry (such as piercings) create artifacts on the recombined images (Fig. 4.3). Although CEM can be performed in women with medical devices or jewelry, the breast tissue surrounding these can only be evaluated on low-energy images. Hence, women with jewelry should be encouraged to remove these prior to CEM if possible.

The ripple artifact consists of fine black and white lines arranged in a ripple-like fashion layered upon the breast tissue (Fig. 4.4). It is observed in approximately 32% of cases [5]. Jeukens et al. found that although low- and high-energy images are acquired within seconds apart, the (mean) image acquisition time is 1.4 s for low-energy images compared with 4.2 s for high-energy images [6]. Therefore, in this time frame, slight motion from a patient could create a "mismatch" between the images in the post-processing of the recombined image. As a result, ripple artifacts are most often seen in the mediolateral oblique view, since the compression of the breast is then more centered on the upper part of the breast and the pectoral muscle,

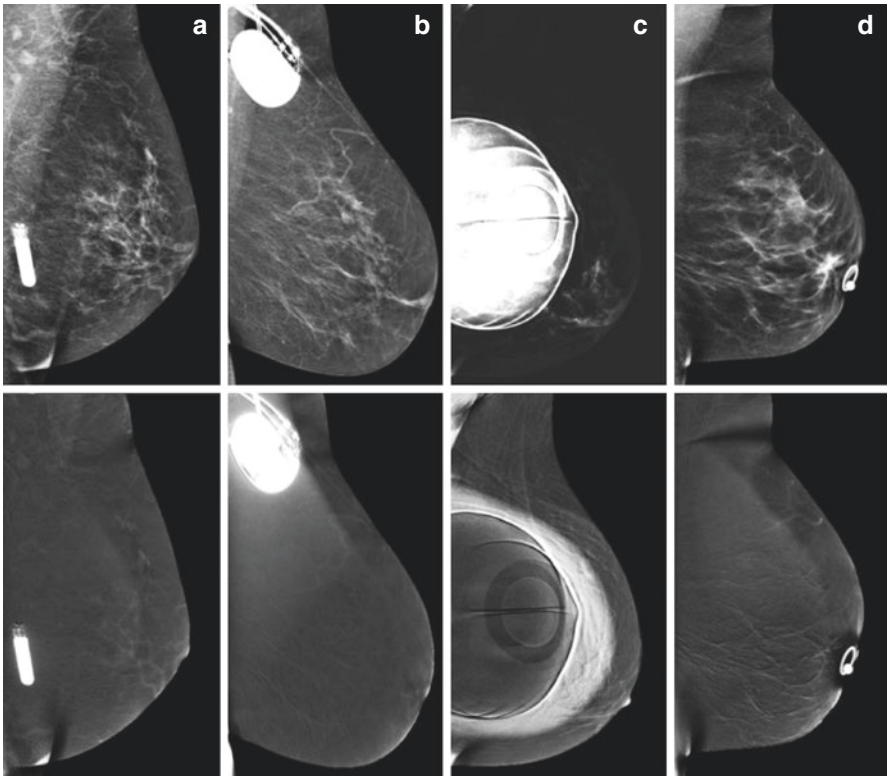

Fig. 4.3 Artifacts caused by cardiac devices, breast implants, or jewelry. Examples of (**a**) implantable cardiac monitoring device, (**b**) cardiac pacemaker, (**c**) breast implant, and (**d**) nipple piercing

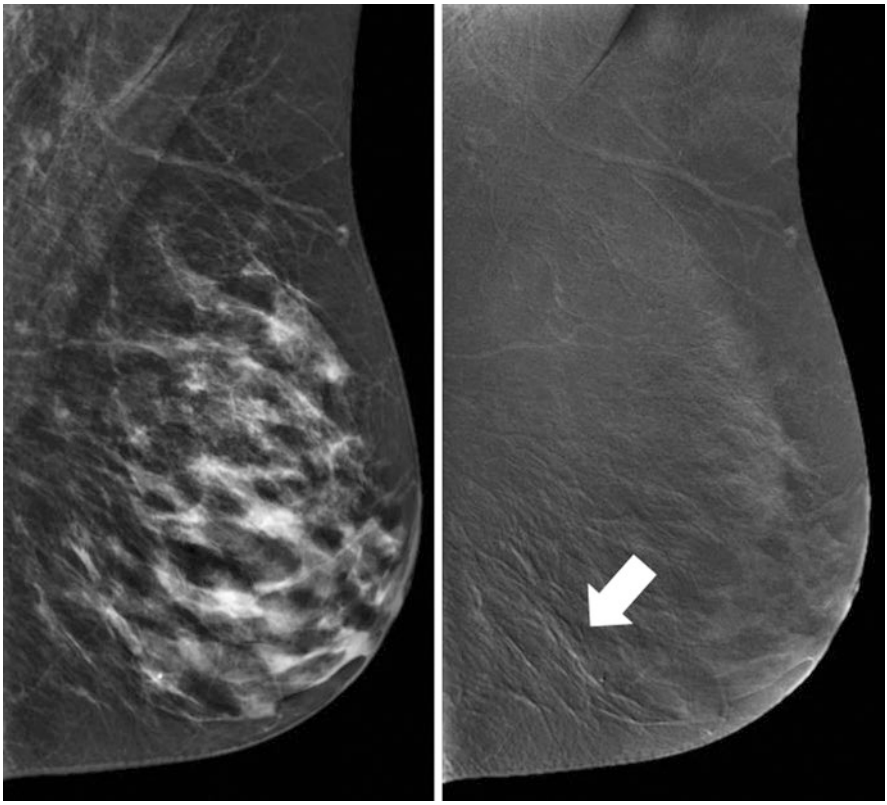

Fig. 4.4 Example of the ripple artifact. The ripple artifact consists of fine black and white lines in a ripple-like fashion layered upon the breast tissue and is caused by slight motion of the patient between the acquisition of the low-energy and high-energy CEM image

while the lower parts of the breast are usually less effectively compressed, rendering them susceptible to slight motion. To reduce ripple artifacts, some institutes recommend breath-holding instructions during the image acquisition phase.

The axillary line artifact consists of a well-defined line extending across the axillae and occurs in approximately 32% of images (Fig. 4.5). It is only observed on mediolateral oblique views and is always bilateral [5]. Usually, there is no interference with image interpretation. This artifact occurs due to the high sensitivity of high-energy images to lag. The line corresponds to the collimator position in previously acquired collimated images.

The skin line enhancement artifact consists of a segmental area of skin contour highlighting (Fig. 4.6). It does not involve the entire skin. It is presumably caused by image filtration which is applied to the recombined image to equalize breast thickness. When no apparent skin abnormalities are present, such as skin thickening, the skin line enhancement artifact is the most probable cause of the finding. It occurs in approximately 32% of cases and is mostly seen in the craniocaudal views [5].

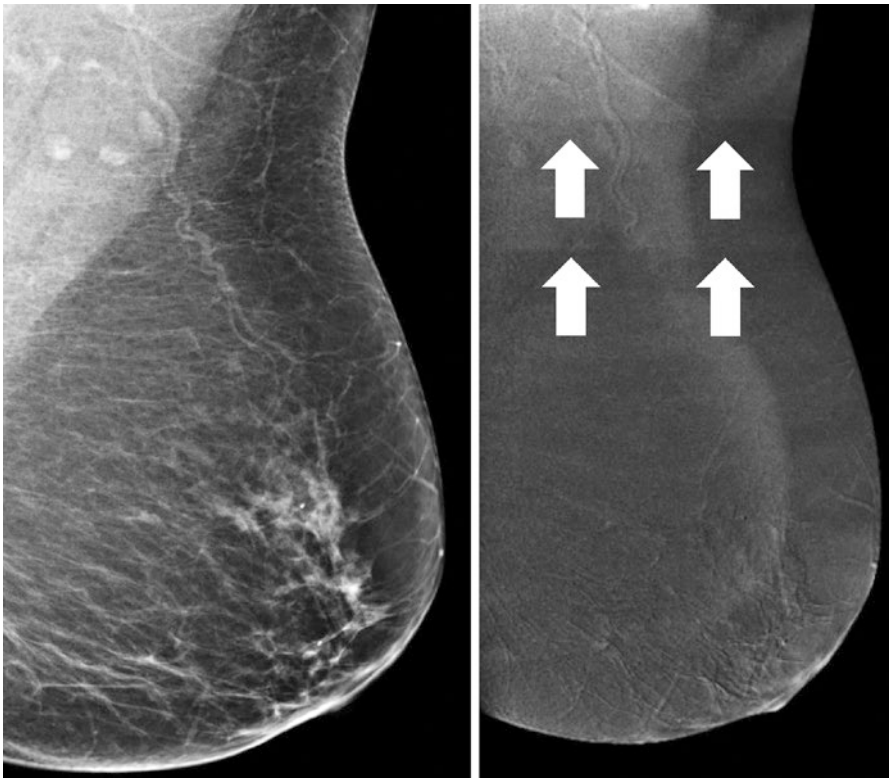

Fig. 4.5 Example of the axillary line artifact (arrows). An ill-defined line is present extended through the axilla. Images courtesy of Miriam Sklair-Levy, MD

In general, these artifacts do not present any relevant difficulties in image interpretation when the radiologist is familiar with them. It should also be noted that these artifacts are largely based on initial experiences with the first available CEM unit (SenoBright*) brought to market by GE Healthcare. In other commercially available units or newer generation models, these artifacts might be less prominent or even absent due to improvements in both hardware and software.

4.3 Image Interpretation

4.3.1 How to Read the Low-Energy Image

As discussed above, low-energy images are the CEM counterpart of FFDM images. Hence, they can be evaluated using a similar approach and terminology as suggested in the American College of Radiology Breast Imaging Reporting and Data System (BI-RADS) lexicon [7]. Although a detailed description of this evaluation is beyond the scope of this chapter, a summary is provided below.

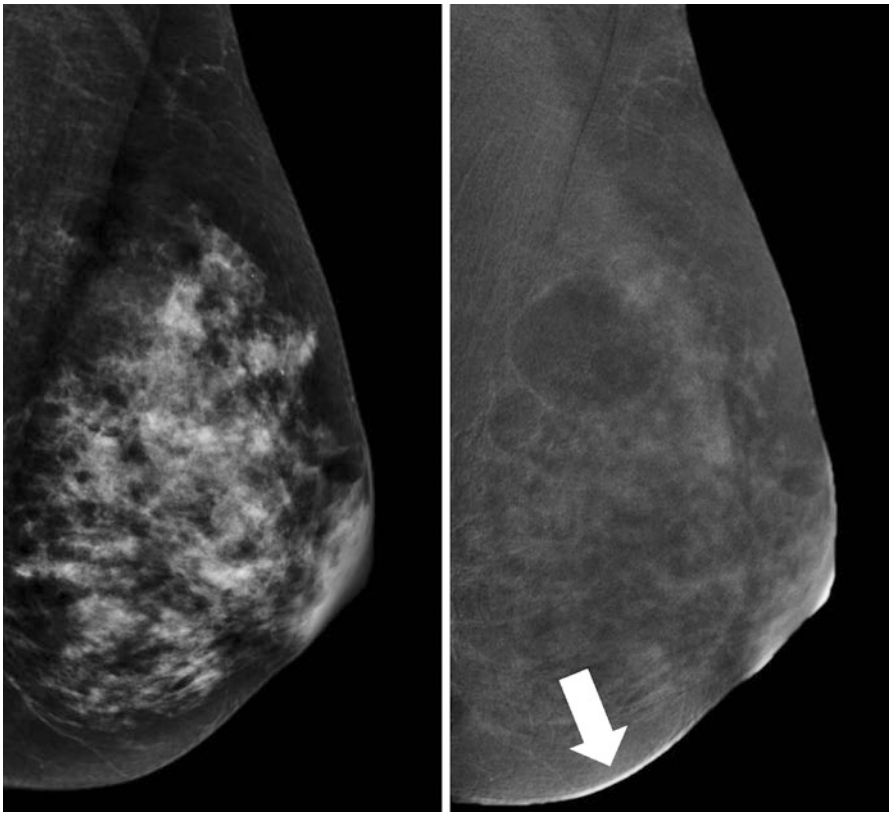

Fig. 4.6 Example of skin line enhancement artifact (arrow). There is a focal skin contour highlighting present on the recombined images (only left mediolateral oblique view shown) without any accompanying skin thickening or abnormality present on the low-energy image

As in any mammographic exam, an overview of the exams performed and the quality of the image acquisition (in terms of positioning, etc.) should be described, including the availability of any prior exams. As a first step, a description of the breast density should be provided in the report according to four different categories: (1) almost entirely fat, (2) scattered fibroglandular tissue, (3) heterogeneous fibroglandular tissue, or (4) extreme fibroglandular tissue. Although the accuracy of CEM is less influenced by breast density than FFDM, it remains important to report on breast density as this is reflective of the risk of developing breast cancer. In addition to the subjective classification of breast density ("eyeballing") which is less reliable [8], different (semi-)automated classification tools have been developed.

For the detection of breast abnormalities, four main categories can be distinguished: masses, architectural distortion, asymmetry, and (micro)calcifications. For each of these items, the nomenclature of the BI-RADS lexicon should be applied for the report. In addition, the lesion size and location within the breast should be reported. Finally, any clinically relevant additional findings such as benign

calcifications, vascular calcifications, skin abnormalities, axillary lymphadenopathy, etc. may be reported. For more specific details on state-of-the-art reporting of mammographic images, the BI-RADS lexicon can be consulted [7].

4.3.2 How to Read the Recombined Image

The recombined image should be evaluated in conjunction with the low-energy image. The recombined image is an adjunct to the low-energy image rather than a replacement.

As with breast MRI, background parenchymal enhancement (BPE) also occurs with CEM and should be evaluated. Sogani et al. performed a retrospective study of 278 women (aged 25–76 years) comparing BPE on CEM with that on breast magnetic resonance imaging (MRI) [9]. Three readers independently scored BPE as minimal, mild, moderate, or marked on CEM and MRI in the same patients. Most women had minimal or mild BPE on both CEM (68–76%) and breast MRI (69–76%), and there was good agreement between CEM and MRI. Both modalities showed a significant association between BPE and menopausal status, prior breast radiation therapy, hormonal treatment, and breast density.

Although no studies to date have studied the effect of BPE on CEM accuracy, one might consider that for elective CEM exams, i.e., screening, similar guidelines should be applied as breast MRI to reduce the presence of BPE [10]. For breast MRI, the exam is ideally performed in the first phase of the menstrual cycle (i.e., days 3–14), with day 1 being the first day of menstruation [11]. Institutes that adhere to these guidelines for MRI would probably apply the same for CEM. However, evidence of improved breast MRI with these guidelines are conflicting. As DeMartini et al. showed, although increased BPE in breast MRI is associated with a younger patient age and a higher abnormal interpretation rate, it was not related to significant differences in positive biopsy rates, cancer yield, sensitivity, or specificity [12]. Hence, some institutes might prefer not to consider the menstrual cycle when planning elective (screening) CEM exams. In other CEM indications, the exam should be performed at the earliest opportunity. In these cases, rapid clarification through imaging is preferred over optimal BPE in CEM.

Finally, regarding the evaluation of BPE, the report of the recombined images should include a description of the BPE with special focus on the symmetry of BPE, as asymmetrical BPE could be caused by underlying invasive (lobular) breast cancer or ductal carcinoma in situ (without accompanying calcifications) (Fig. 4.7).

Any relevant enhancement on recombined images should be matched with findings on low-energy images. In some cases, no mammographic counterpart can be observed for areas of enhancement. Enhancement should be described as enhancement associated with an underlying mass or architectural distortion or as non-mass enhancement. In contrast to breast MRI, the term “focus” may not be applicable to CEM as enhancing lesions observed in two views should be called a mass, even if they are very small. For non-mass enhancement, similar terminology as breast MRI

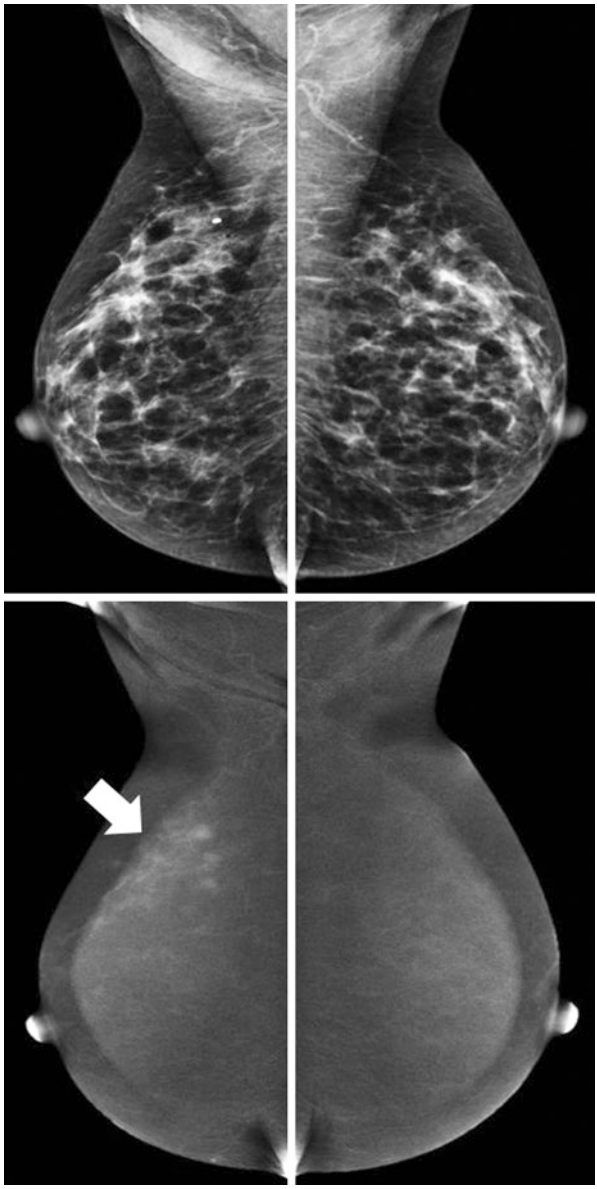

Fig. 4.7 Asymmetric enhancement might be the only sign of underlying breast cancer. In this case, asymmetrical non-mass enhancement in a segmental orientation was observed. Final diagnosis was a 6 mm invasive breast cancer with extensive ductal carcinoma in situ up to 60 mm

can be used to describe the orientation of the enhancement [7]. Non-mass enhancement can thus be focal, linear, segmental, regional, multiple regions, or diffuse.

Enhancement should also be assessed qualitatively, but there is not yet a single accepted classification for this purpose. Some institutes prefer a "yes/no" classification. Others prefer a more detailed classification and use "no/mild/moderate/marked." However, progress is being made to quantitatively assess CEM enhancement. Hwang et al. used a tool filled with fluid chambers on a known contrast agent

concentration [13]. Based on the linear relationship between contrast-to-noise levels measured and iodine concentrations, iodine overlay maps could be generated for the recombined images. In a single clinical case of a multifocal breast cancer, they calculated the enhancement of CEM (expressed as iodine mass thickness (IMT) in mg l/cm^2) for three different foci: 2.8, 1.5, and 1.3 mg l/cm^2. Parallel to this study, Lobbes et al. used a similar approach and calculated a mean IMT of 2.1 mg l/cm^2 (range 1.3–3.4 mg l/cm^2) for breast cancers [14]. In addition, they showed that malignant lesions enhanced more intensely than benign lesions. Therefore, it is expected that the rate of enhancement of lesions, when it can be accurately assessed, can be used to further improve the diagnostic accuracy of CEM, potentially even discriminating between breast cancer subtypes as Van Nijnatten et al. has shown that invasive lobular carcinomas more often show very weak enhancement [15]. Artificial intelligence and computer-aided decision systems could boost the accuracy of CEM potentially even more (see also Sect. 4.4).

When there is a significant discrepancy regarding the maximum diameter of the lesion between the low-energy and recombined images, this discrepancy should also be reported.

4.3.3 False-Negative Findings in CEM

Since the introduction of CEM in 2011, many studies have shown that the diagnostic accuracy of CEM is consistently superior to that of FFDM. These findings were summarized in a systematic review by Tagliafico et al., showing that the estimated sensitivity of CEM was 98%, with only a moderate specificity of 58% [16]. The latter could be explained by the overrepresentation of papers of a single study group within this review. Jochelson and Lobbes recalculated the results of this review and observed a specificity of 78% [17]. In an updated review, Zhu et al. reported a pooled sensitivity and specificity of 89% and 84%, respectively [18].

Prior studies have reported on "missed cancer diagnosis" when using CEM. Thibault et al. reported six missed cancers in their population of 54 patients, which were mostly invasive lobular cancers or cancer located outside of the mammographic field of view (caused by suboptimal patient positioning) [19]. Fallenberg et al. reported one cancer missed by all three readers (in a study population of 118 women) [1]. Lalji et al. reported ten missed cancers (overlooked by more than one reader in a study of ten readers in total) [20]. The main causes for the missed diagnosis were weak enhancement and location outside of the mammographic field of view.

4.3.4 CEM in the Evaluation of Suspicious Breast Calcifications

The diagnostic accuracy of CEM with respect to pathological calcifications was studied by Cheung et al. who reported a sensitivity and specificity of 89% and 87%, respectively [21]. These findings are like the findings by Houben et al. Of note,

Houben et al. found that the diagnostic accuracy of the complete CEM exam did not differ significantly from that of only low-energy images [22]. The sensitivity and specificity using only low-energy images were 91% and 39%, respectively. For the complete CEM exam, the sensitivity was 94%, while the specificity was 37%. In addition, Houben et al. evaluated the impact of using CEM to evaluate breast calcifications on surgical decision-making; they observed no relevant differences between low-energy images and a complete CEM exam. Hence, the added value of CEM for the evaluation of suspicious calcifications is limited and can only be used for upgrading lesions: when calcifications show enhancement, the likelihood of an underlying cancer increases, but biopsy of suspicious calcifications should be performed regardless of the lack of enhancement, just as with breast MRI.

4.3.5 Contamination Artifacts

Contamination artifacts mimicking suspicious breast calcifications have been reported by Gluskin et al. [23]. Contrast can be transported on the hands of the technologist, especially if gloves are not worn or if the line is not properly connected. Although the low-energy image does not demonstrate the presence of iodine within the breast, contamination of the skin with contrast might mimic calcifications due to the higher concentration of contrast agent, producing a greater attenuation of photons relative to the intravenous contrast distributed throughout the breast. The artifact can be recognized by viewing the recombined image in overlay of the low-energy image. Due to the subtraction algorithm used for the recombined images, "true" calcifications will appear black on recombined images. In case of contrast splatter, the "calcifications" will remain white on the recombined images (Fig. 4.8). This latter observation should trigger the radiologist to consider contrast contamination. Other warning signs are as follows: (1) the findings are observed in only one view or the mirror image of findings seen in another view or breast; (2) the abnormality does not persist on high-quality magnification views; and (3) the findings do not persist on repeat CEM studies [23]. Contrast contamination can be easily managed by cleansing, but technologists should be aware that contamination could occur on either the breast or the detector. Also, the risk of encountering this artifact is reduced by wearing gloves during patient handling, handwashing, and/or having contrast administration and mammographic positioning done by two different technologists.

4.4 Outlook and Future Perspectives

Reading CEM images does not require an extended training. When the radiologist viewing CEM exams is also experienced with reading both FFDM and breast MRI, there is no difference between the performance of expert CEM readers or experienced breast radiologists. This was demonstrated by a study by Lalji et al., who showed that the diagnostic accuracy among four experienced CEM readers was comparable to that of experienced breast radiologists [20]. Nevertheless, a

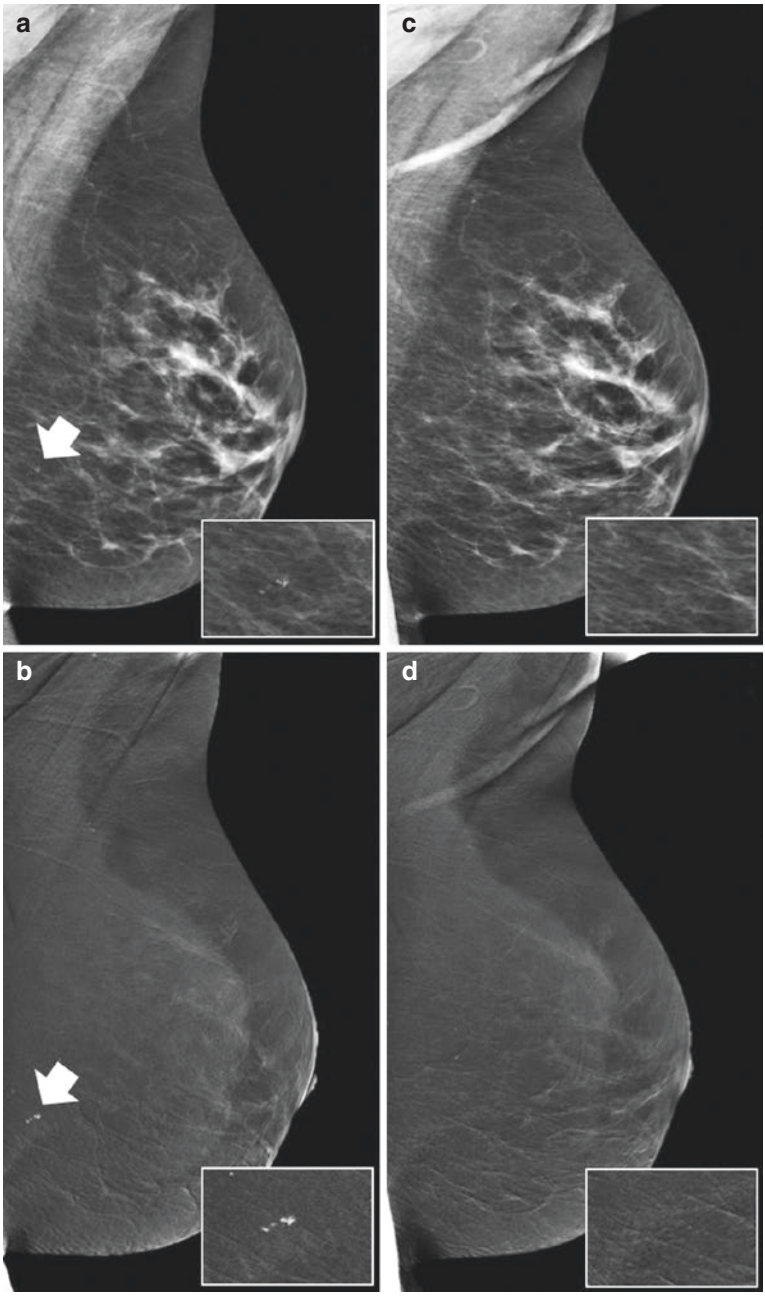

Fig. 4.8 Example of iodine contamination artifact. During this CESM exam, an area suspicious for pathologic micro calcifications was observed on the low-energy images of the left breast (**a**, white arrow). However, this area was high in opacity on the recombined images (**b**), not compatible with micro calcifications (which are black in the recombined images), but suggestive of iodine contamination on the detector. Next, the detector was cleaned and the exam repeated (**c**, **d**), confirming that this abnormality was indeed caused by iodine contamination during the exam

consistency in terminology is required. Although many descriptors of conventional mammography and breast MRI can be applied to CEM exams, there are some phenomena that are exclusive to CEM. Efforts should be made on introducing consistency in terminology.

We are only touching the surface of CEM applications, as it provides a window of opportunity for advanced imaging analyses (e.g., using computer-aided diagnosis (CAD), radiomic feature analysis, and artificial intelligence). For example, Patel et al. were the first to study the application of CAD-CEM on 50 breast lesions [24]. Their algorithm could correctly identify 45 out of these 50 lesions (accuracy 90%), while the radiologists in this study achieved an accuracy of 78% and 86%, respectively. Preliminary data from our own institute applying deep learning algorithms and radiomics to CEM showed promising results. In 112 patients, the deep learning algorithm achieved an AUC of 0.67 (95% confidence interval (CI) 0.51–0.82), with radiomic feature analysis achieving an AUC of 0.90 (95% CI 0.84–0.96) (Van Wijk, unpublished data). These examples show that the superior diagnostic accuracy of CEM over FFDM can be further enhanced when using advanced computer programs. This is a very exciting field of research which can only make the promising technique of CEM even more robust.

References

1. Fallenberg EM, Dromain C, Diekmann F, et al. Contrast-enhanced spectral mammography: does mammography provide additional clinical benefits or can some radiation exposure be avoided? Breast Cancer Res Treat. 2014;146:371–81.
2. Francescone MA, Jochelson MS, Dershaw DD, et al. Low energy mammogram obtained in contrast-enhanced digital mammography (CEDM) is comparable to routine full-field digital mammography (FFDM). Eur J Radiol. 2014;83:1350–5.
3. Lalji UC, Jeukens CR, Houben I, et al. Evaluation of low-energy contrast-enhanced spectral mammography images by comparing them to full-field digital mammography using EUREF image quality criteria. Eur Radiol. 2015;25:2813–20.
4. European Reference Organisation for Quality Assured Breast Screening and Diagnostic Services. EUREF European guidelines. 4th ed; 2013. http://www.euref.org/european-guidelines
5. Yagil Y, Shalmon A, Rundstein A, et al. Challenges in contrast-enhanced spectral mammography interpretation: artefacts lexicon. Clin Radiol. 2016;71:450–7.
6. Jeukens CR, Lalji UC, Meijer E, et al. Radiation exposure of contrast-enhanced spectral mammography compared with full-field digital mammography. Investig Radiol. 2014;49:659–65.
7. D'Orsi CJ, et al. ACR BI-RADS Atlas, breast imaging reporting and data system. Reston, VA: American College of Radiology; 2013.
8. Lobbes MB, Cleutjens JP, Lima Passos V, et al. Density is in the eye of the beholder: visual versus semi-automated assessment of breast density on standard mammograms. Insights Imaging. 2012;3:91–9.
9. Sogani J, Morris EA, Kaplan JB, et al. Comparison of background parenchymal enhancement at contrast-enhanced spectral mammography and breast MR imaging. Radiology. 2017;282:63–73.
10. Mann RM, Kuhl CK, Kinkel K, Boetes C. Breast MRI: guidelines from the European Society of Breast Imaging. Eur Radiol. 2008;18:1307–18.
11. Delille JP, Slanetz PJ, Yeh ED, et al. Physiologic changes in breast magnetic resonance imaging during the menstrual cycle: perfusion imaging, signal enhancement, and influence of the T1 relaxation time of breast tissue. Breast J. 2005;4:236–41.

12. DeMartini WB, Liu F, Peacock S, et al. Background parenchymal enhancement on breast MRI: impact on diagnostic performance. AJR Am J Roentgenol. 2012;198:W373–80.
13. Hwang YS, Cheung YC, Lin YY, Hsu HL, Tsai HY. Susceptibility of iodine concentration map of dual-energy contrast-enhanced digital mammography for quantitative and tumor enhancement assessment. Acta Radiol. 2018;59:893–901.
14. Lobbes MBI, Mulder H, Rousch M, et al. Quantification of enhancement in contrast-enhanced spectral mammography using a custom-made quantifier tool (I-STRIP): a proof-of-concept study. Eur J Radiol. 2018;106:114–21.
15. Van Nijnatten TJA, Jochelson MS, Pinker K, et al. Differences in degree of lesion enhancement on contrast-enhanced mammography between invasive lobular and ductal carcinoma. BMJ Open. 2019; Under review.
16. Tagliafico AS, Bignotti B, Rossi F, et al. Diagnostic performance of contrast-enhanced spectral mammography: systematic review and meta-analysis. Breast. 2016;28:13–9.
17. Jochelson M, Lobbes MBI, Bernard-Davila B. Reply to Tagliafico AS, Bignotti B, Rossi F, et al. Breast. 2017;32:267.
18. Zhu X, Huang JM, Zhang K, et al. Diagnostic value of contrast-enhanced spectral mammography for screening breast cancer: systematic review and meta-analysis. Clin Breast Cancer. 2018;18(5):e985–95.
19. Thibault F, Balleyguier C, Tardivon A, Dromain C. Contrast enhanced spectral mammography: better than MRI? Eur J Radiol. 2013;81(Suppl 1):S162–4.
20. Lalji UC, Houben IPL, Prevos R, et al. Contrast-enhanced spectral mammography in recalls from the Dutch breast cancer screening program: validation of results in a large multireader, multicase study. Eur Radiol. 2016;12:4371–9.
21. Cheung YC, Juan YH, Lin YC, et al. Dual-energy contrast-enhanced spectral mammography: enhancement analysis on BI-RADS 4 non-mass microcalcifications in screened women. PLoS One. 2016;11:e0162740.
22. Houben IPL, Vanwetswinkel S, Kalia V, et al. Contrast-enhanced spectral mammography in the evaluation of breast suspicious calcifications:diagnostic accuracy and impact on surgical management. Acta Radiologica. 2019; Jan 24, Epub ahead of print.
23. Gluskin J, Click M, Fleischman R, et al. Contamination artifact that mimics in-situ carcinoma on contrast-enhanced digital mammography. Eur J Radiol. 2017;95:147–54.
24. Patel BK, Ranjbar S, Wu T, et al. Computer-aided diagnosis of contrast-enhanced spectral mammography: a feasibility study. Eur J Radiol. 2018;98:207–13.

5 Comparison of Contrast-Enhanced Mammography and Contrast-Enhanced Breast MRI

Bhavika K. Patel and John M. Lewin

5.1 Introduction

Screening mammography remains the only test that has been shown to reduce breast cancer mortality in randomized clinical trials [1–3]. Mammography is a rapid and low-cost test, making it a well-suited screening examination. The sensitivity of mammography for the detection of breast cancer in screening populations ranges from as low as 35% up to 90%, primarily depending on breast density [4]. Contrast-enhanced breast MRI, on the other hand, consistently has a much higher sensitivity, approaching 98–100% [5]. The high sensitivity of MRI is due to the added information gained by contrast enhancement of tumor neovascularity; non-contrast MRI performs very poorly for cancer detection [6, 7]. The success of contrast-enhanced breast MRI was one of the primary stimuli for the development of contrast-enhanced mammography (CEM). The hope was that CEM would combine the low cost, speed, and convenience of mammography with the high sensitivity of contrast-enhanced breast MRI.

In order to compete with MRI, a technique that allowed imaging of both breasts in multiple projections was needed. These requirements are met by use of the dual-energy subtraction technique for CEM [8]. Initial studies of dual-energy CEM consistently demonstrated superiority to standard unenhanced mammography [9–11]. Given the added expense, discomfort, and risk of CEM due to IV placement and contrast injection, however, it is not enough for the technique to outperform mammography. In order to be clinically relevant, CEM needs to show sensitivity and specificity comparable to, or better than, contrast-enhanced MRI.

B. K. Patel (✉)
Mayo Clinic Arizona, Phoenix, AZ, USA
e-mail: patel.bhavika@mayo.edu

J. M. Lewin
The Women's Imaging Center, Denver, CO, USA

M. Lobbes, M. S. Jochelson (eds.), *Contrast-Enhanced Mammography*,
https://doi.org/10.1007/978-3-030-11063-5_5

5.2 Imaging Technique

As described in other chapters, in dual-energy contrast-enhanced mammography, the only commercially available technique, two images are taken at different energy levels and subtracted from one another. Dual-energy imaging allows imaging of both breasts in multiple projections after a single contrast injection. The dual-energy image is obtained by using a weighted logarithmic subtraction of two images, taken one right after the other, where one is acquired at a high-energy (typically 45–49 kVp) and low-energy image (at that of standard mammography, typically 28–32 kVp). To further increase the energy separation of the two images, the high-energy beam is filtered with copper, whereas the low-energy beam is filtered using filtration typical of standard mammography (molybdenum, rhodium, or silver).

CEM utilizes the concept of imaging tumor neovascularity, based on the basic principle that invasive cancers are associated with increased vascularity. A standard low-osmolar contrast agent, typically with a concentration of 300–370 mgI/ml, is administered intravenously using a power injector. The contrast volume is similar to that used for abdominal CT, typically 90–150 ml, depending on body weight. The patient is seated for the injection, which typically takes place in the mammography exam room. Approximately 2 min after the injection, dual-energy image pairs are acquired of each breast in standard mammography projections and, if needed, additional projections. The number of images that can be acquired depends entirely on the speed of positioning; the actual image acquisition takes only about 3–4 s. For each dual-energy image pair, a contrast-enhanced subtraction image is computed for use in clinical interpretation.

About 10 min are available for imaging after the injection until which the enhancement fades and is no longer considered adequate for diagnosis. The currently used protocol is timed such that the first images are optimized at peak enhancement.

5.3 Clinical Studies Comparing CEM and MRI

5.3.1 Extent of Disease

Many patients with newly diagnosed breast cancers undergo MRI to define extent of disease. Although MRI is excellent at determining lesion size and detecting additional lesions, it is expensive, not always clinically accessible in a timely matter and difficult for some patients due to claustrophobia and prolonged exam time in a prone position. CEM is a potential alternate method for defining disease extent. Several modest-sized clinical studies have been performed comparing CEM to MRI in subjects with a newly diagnosed cancer (Table 5.1). These studies have compared the two modalities for their ability to detect the index lesion, accurately depict its size and extent of disease, and depict additional, separate lesions.

Table 5.1 Clinical studies comparing CEM and MRI

Study	No. of subjects/ lesions	Primary outcome	Result: CEM vs. MRI	Statistical result
Fallenberg et al. [12]	80	Sensitivity[a]	100% vs. 98%	No difference
Jochelson et al. [13]	52	Sensitivity[a]	96% vs. 96%	No difference
Chou et al. [15]	185	Accuracy (AUC)[b]	0.878 vs. 0.897	No difference
Li et al. [37]	48	Sensitivity	100% vs. 100%	No difference
Luczynska et al. [38]	102/118	Sensitivity Accuracy	100% vs. 93% 79% vs. 73%	Statistically significant No difference

[a]Defined as percentage of index cancers detected on each modality
[b]AUC, area under the receiver operating characteristic curve

A European study, in which both CEM and MRI were performed on 80 subjects with a newly diagnosed breast cancer, showed statistically equivalent performance between CEM and MRI for detection of the index lesion, with the trend favoring CEM (80/80 cancers detected for CEM vs. 77/80 for MRI). Both CEM and MRI outperformed conventional mammography (66/80 cancer detected) [12]. In a similar prospective study at Memorial Sloan Kettering, by Jochelson et al., 52 subjects with newly diagnosed cancer were studied by both CEM and MRI [13]. This study also showed an equal sensitivity of 96% for CEM and MRI, with each modality detecting 50 out of 52 index cancers. By comparison, conventional mammography only detected 81% (42/52). Twenty-five additional malignant foci were found in the study. Of these, MRI found more than CEM, 22 (88%) vs. 14 (56%). The increase in detection of these additional lesions by MRI came at the expense of more false positives, 13 vs. 2 for CEM.

In 2017, Lee-Felker et al. published a retrospective study comparing the performance of CEM to that of breast MRI in the detection of index and secondary cancers in women with newly diagnosed breast cancer in 52 consecutive subjects who had both tests over a 20-month period [14]. The study was somewhat biased toward MRI in terms of sensitivity toward detection of secondary lesions since most of the patients in the study (46/52) were included because they underwent CEM to evaluate additional findings detected on MRI. There were 61 index cancers, defined as lesions already biopsy-proven at the time of MRI. MRI demonstrated all 61 of these cancers (100%), while CEM demonstrated 58/61 (95%) (Fig. 5.1). Secondary cancers were defined as those first detected on the staging MRI or on the CEM. Despite the bias toward MRI, CEM demonstrated all 11 of the secondary cancers (100%), whereas MRI demonstrated only 10/11 (91%). The index cancers not demonstrated on CEM were a 10 mm grade 2 invasive ductal carcinoma and 7 mm intermediate-grade ductal carcinoma in situ, while the secondary cancer not seen on MRI was a 20 mm low-grade DCIS. Sixty-six of the 71 lesions demonstrated on CEM were malignant, giving a positive predictive value (PPV) of 93%, whereas 69 of the 115 lesions on MRI were malignant for a PPV of only 60%, but these values would have been highly skewed in favor of CEM due to the patient selection bias. Of the 45

false-positive findings on MR, the majority were related to benign or high-risk enhancing foci.

A Taiwanese study by Chou et al. used receiver operating curve (ROC) analysis in a multi-reader study to compare CEM, MRI, and contrast-enhanced tomosynthesis, an experimental technique in which dual-energy tomosynthesis is performed

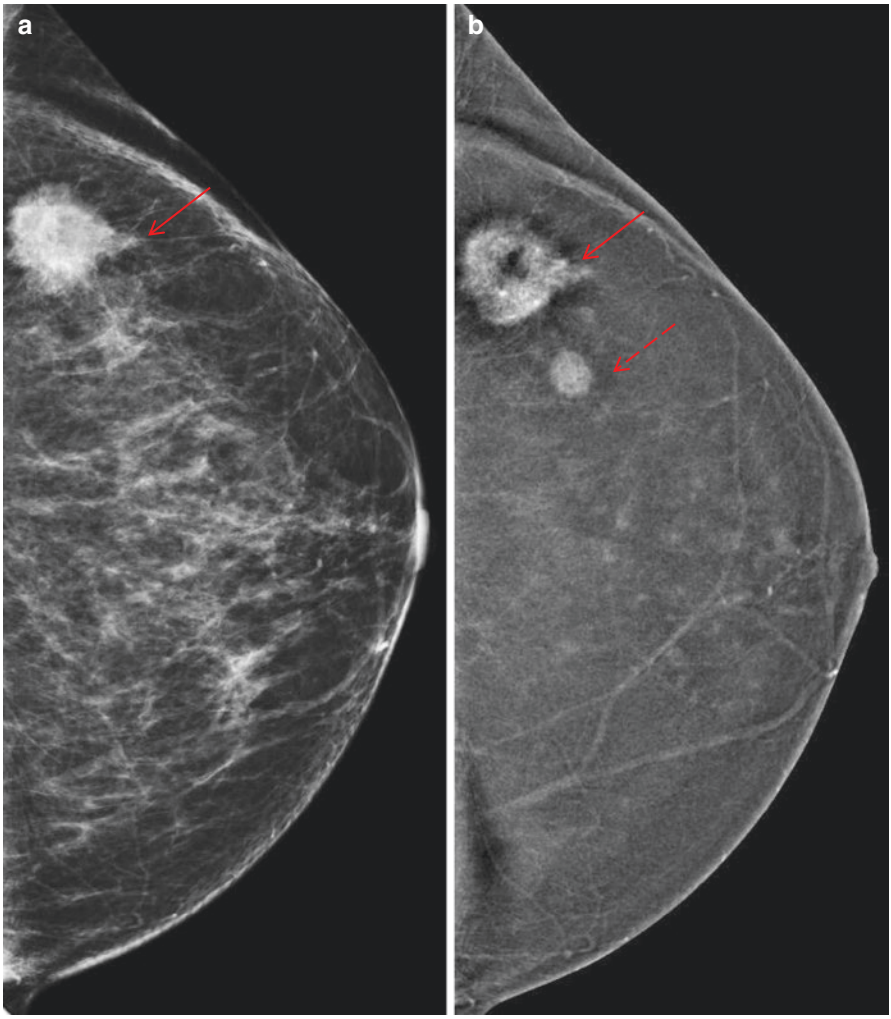

Fig. 5.1 Sixty-three year old female for diagnostic imaging. (**a**) Low energy image demonstrates 2.5 cm irregular mass (arrow) in outer posterior left breast. (**b**) Subtracted images shows index mass with second satellite lesion (dotted arrow) anteromedial to the primary mass, otherwise mammographically occult on low energy images. Both underwent US guided biopsy demonstrating IDC. (**c**) Post contrast axial delayed MR imaging following image guided biopsy also demonstrate both primary mass (arrow) and secondary satellite lesion (dotted arrow) in a similar fashion

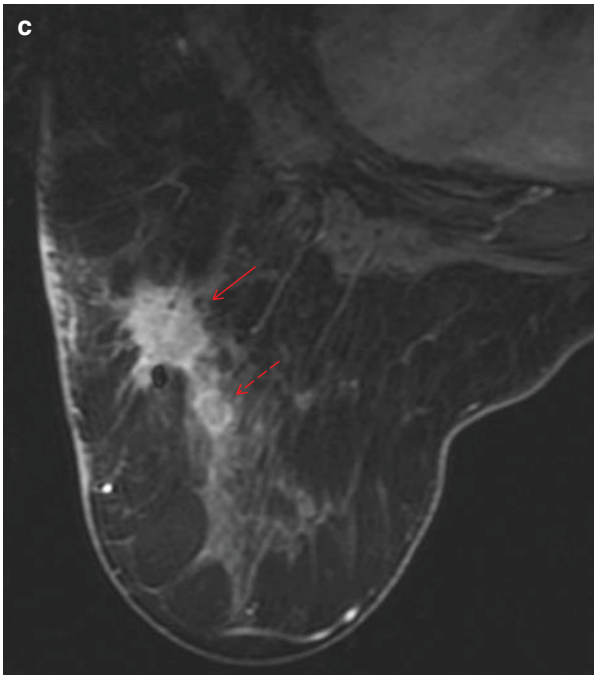

Fig. 5.1 (continued)

following a contrast injection, as well as standard mammography and tomosynthesis [15]. The study population included a mixture of 81 malignant and 144 benign lesions that were imaged on all five modalities. The study found no statistically significant difference among the three contrast-enhanced techniques in area under the ROC curve (AUC). As expected from previously published results, each of the three contrast-enhanced techniques performed significantly better than the combination of the mammography and tomosynthesis. The addition of contrast-enhanced tomosynthesis to CEM did not improve clinical performance. As of this writing, there have been no further clinical studies published on contrast-enhanced tomosynthesis.

All studies to date are promising and have concluded CEM is potentially as sensitive as MR imaging in the evaluation of extent of disease in newly diagnosed breast cancer, with a higher PPV and fewer false positives than MR. The higher specificity of CEM thus far is promising for treatment planning [16]. Specifically, in a more recent prospective, two-center study by Fallenberg comparing mammography, MRI, and CEM, the specificity of MRI was significantly worse than that of the other two modalities (all $P < 0.001$) [16].

Studies shown similar sensitivities of CEM and MRI for detection of the index cancer in the setting of newly diagnosed breast cancer. In regards to the rates of secondary cancers, however, the Lee-Felker study, the rates of secondary cancer detection were also similar between CEM and MRI (despite selection bias favoring

MRI). In the Jochelson study, however, CEM depicted only 56% of the secondary cancers versus 88% for MR imaging, albeit at the expense of more false positives. Reasons may be due to more DCIS in Jochelson's study and the use of outside MR imaging limiting the reproducibility and consistency of their imaging protocols.

A recent meta-analysis including 18 studies demonstrated a pooled sensitivity and specificity of 89% and a pooled specificity of 84% for CEM [17]. The authors concluded that CEM seems to have about the same sensitivity as MRI. Unfortunately, they did not compute the pooled values for MRI with which to form a direct comparison.

Most studies show CEM to at least have a trend toward higher PPV and, correspondingly, fewer false positives than MRI. A higher PPV for CEM would be helpful for acceptance by surgeons of CEM as a local staging tool for newly diagnosed cancers since enhancing lesions on staging MRI can delay surgical treatment. These lesions typically need to undergo targeted biopsy to confirm malignancy before any change in surgical management is agreed upon [18]. Indeed, such acceptance has been noted anecdotally at centers performing CEM. At Mayo Arizona, breast surgeons published their highly positive experience with the technique on a series of 351 patients, noting that it was "highly sensitive, had size measurements that correlated well with histologic size, and produced a relatively low rate of false-positive additional biopsy findings" [19] (Fig. 5.1).

The small study populations and nonstandardized timing of the imaging studies in relation to menstrual cycle, as well as potential selection biases, should be noted as limitations in generalizing results. Most importantly, the results in cohorts with newly diagnosed cancers may or may not be applicable to the performance of the modalities in a screening population. Specific screening studies, as discussed below, are needed to evaluate CEM for that purpose.

5.3.2 Accuracy of Size Estimation of Index Lesion

A number of studies comparing CEM to MRI in cases of known cancer included evaluation of lesion size estimation. In the 2014 European study referenced above [12], Fallenberg et al. found that CEM was superior to MRI in lesion size accuracy, although both modalities underestimated lesion size relative to pathology. In contrast, MRI slightly outperformed CEM in lesion size estimation in her 2017 reader study [15]. In a retrospective study of 66 lesions in 48 patients, Li et al. found no significant difference between CEM and MRI in tumor size estimation [19]. Lobbes et al. looked specifically at tumor size assessment by CEM in 87 cases, 57 of which had also been imaged by MRI. Both MRI and CEM were found to be highly accurate in determining lesion size, using correlation with histopathology as the gold standard (Fig. 5.2). There was no significant difference between MRI and CEM, using correlation coefficient with histopathology as the metric. The trend in mean diameter difference with histopathology favored CEM over MRI, however (0.03 mm vs. 2.12 mm) [18]. Minimal overestimation of lesion sizes on acquired images had no influence on treatment because overestimation was small and safety margins

were always included for surgical excision. The authors concluded that there was no advantage in performing an additional breast MRI when CEM was available.

These results show the potential of CEM as an alternative for tumor size measurements, especially in patients with limited MR access or contraindications. Given that CEM offers staging information that is comparable to MRI, in patients unable to undergo MRI, it is gaining favor in the staging evaluation. The 2017

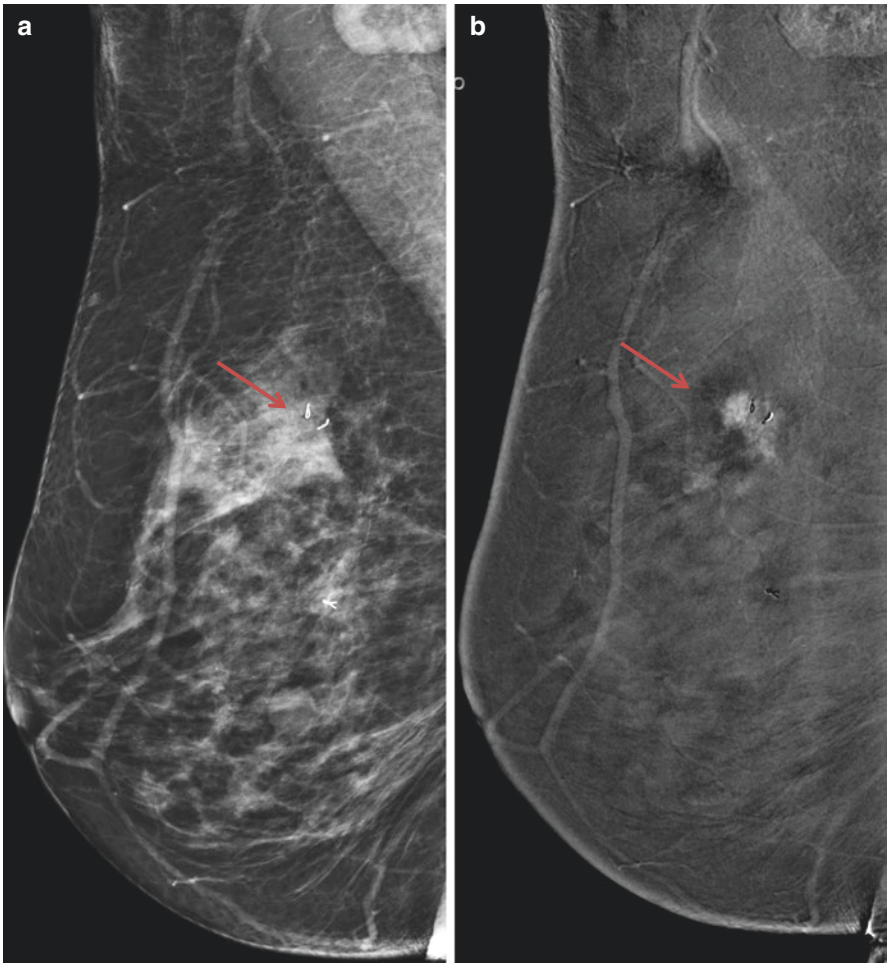

Fig. 5.2 Fifty-four year old female with a previously biopsied grade 2 invasive ductal carcinoma of the left breast. (**a**) Low- energy MLO mammogram (equivalent to a standard unenhanced mammogram) shows the ribbon-shaped marker at the cancer site (arrow), but the cancer is not discernible. (**b**) Corresponding dual-energy subtraction image clearly depicts the cancer (arrow) to measure 17 mm. Note that the background non-enhancing fibroglandular tissue is subtracted out. (**c**) Image from a contrast-enhanced MRI performed the following day shows the lesion as an enhancing mass to measure 19 mm. At surgical resection, there was 17 mm of IDC and DCIS. Note the similarity of the appearance on the CEM and MRI studies

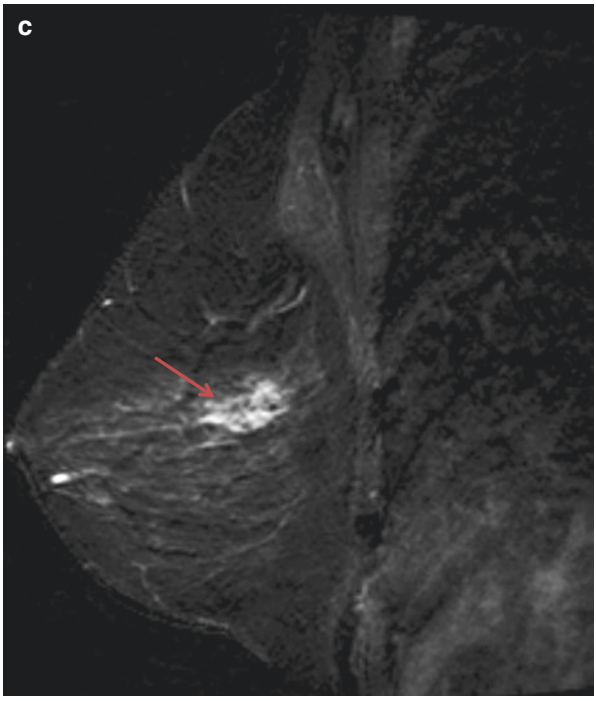

Fig. 5.2 (continued)

European Society Of Breast Imaging (EUSOBI) [20] recommendations state that CEM can be considered *as an alternative to contrast-enhanced MRI* in the case of contraindications to MRI (including the presence of MRI-unsafe devices in the patient's body, claustrophobia, and obesity preventing the patient from entering the magnet) or to gadolinium-based contrast injection as well as local conditions of difficult MRI [20].

5.4 Background Parenchymal Enhancement

Physiological, benign background parenchymal enhancement can be seen with CEM in a similar manner to that observed in breast MRI. In a retrospective study of 278 women who underwent both CEM and MRI, authors demonstrated substantial agreement between readers for BPE detected on CEM and MR images (Fig. 5.3). Similar to breast MR BPE, CEM BPE demonstrated significant association with menopausal status, prior breast radiation therapy, hormonal treatment, breast density on CEM low-energy mammographic images, and amount of fibroglandular tissue on MR images ($P < 0.001$ for all) [21]. Another small study demonstrated that CEM BPE did not significantly fluctuate during the menstrual cycle, suggesting that timing the examination with the menstrual cycle is unlikely to be such an issue for

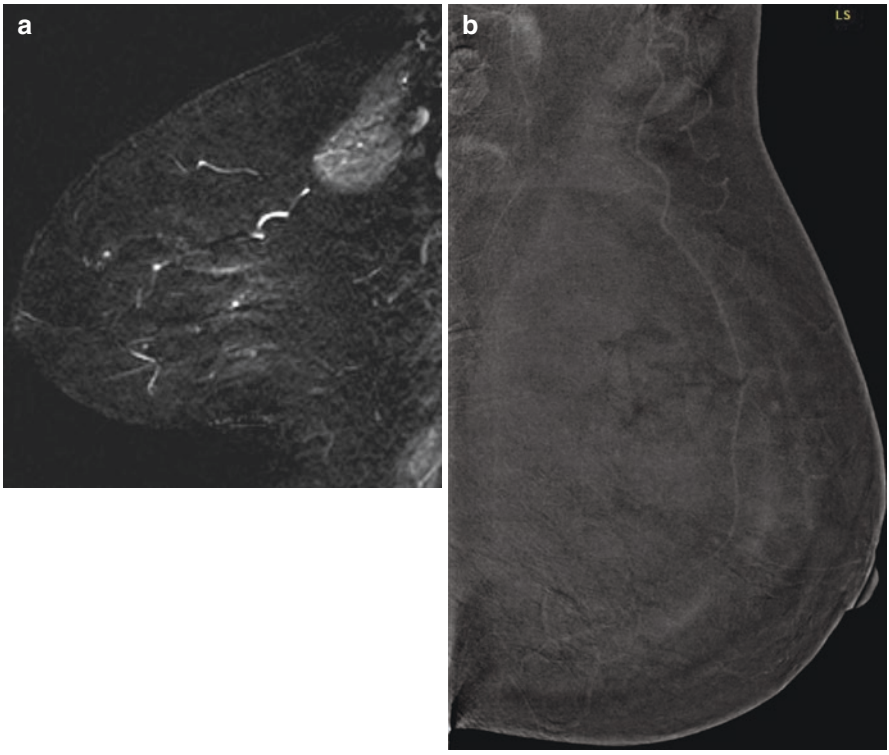

Fig. 5.3 Fifty-eight year old, post-menopausal female. Biopsy proven contralateral cancer, MRI and CEDM for staging. BPE on Sagittal post-contrast MRI (**a**) and CEM (**b**) were both reported as minimal, symmetric background parenchymal enhancement in both breasts

a CEM study as it is with MRI [22]. While grading the degree of BPE on CEM could be a useful addition to breast cancer risk assessment tools, further studies of CEM BPE as an imaging biomarker for breast cancer risk are necessary.

5.4.1 Tumor Response

CEM is currently being compared to MRI in larger, ongoing prospective clinical trials for assessment of tumor response. In small pilot studies, CEM has been compared to MR in the assessment of tumor response in breast cancer patients undergoing neoadjuvant systemic therapy. Findings in preliminary studies have concluded CEM is comparable in accuracy in assessing complete response versus residual disease [23, 24]. In a study of 65 patients, equivalence tests demonstrated that mean tumor size measured by CEM ($P = 0.009$) or by MRI ($P = 0.01$) was equivalent to the mean tumor size measured by pathology within −1 and 1 cm range [24]. Larger studies with subgroup analyses by tumor molecular subtypes are warranted and ongoing. The use of CEM with neoadjuvant chemotherapy is explored in depth in another chapter.

5.4.2 Screening Studies

CEM has recently been evaluated in a purely screening setting as well. A pilot study was performed screening supplemental CEM with supplemental MRI in 307 women at increased risk for breast cancer in which three cancers were detected on MRI and two on CEM; none of which were visible on conventional mammography. This study demonstrated a comparable PPV3 of 15% for CEM and 14% for MRI and specificity of CEM and MRI of 94%. Authors concluded CEM may be valuable as a supplemental imaging examination for women at increased risk for breast cancer who do not otherwise meet criteria for MRI or for whom access to MRI is limited [25]. In a subsequent study of 1197 CEM studies performed for high-risk population [26], CEDM has a PPV of biopsy of 31% and a cancer detection rate of 18/1000 screened (similar to that of high-risk screening MR studies) [27]. Larger clinical trials are necessary and underway.

5.5 Advantages and Disadvantages of CEM vs. MRI

Table 5.2 lists some of the advantages and disadvantages of CEM as compared to MRI. CEM is a less expensive test due to lower equipment costs and a shorter examination time [28, 29]. CEM is straightforward to implement into clinical practice as it requires a software upgrade to preexisting mammography units. Like breast MR, CEM does require additional resources of a radiology technologist or breast imaging nurse who is capable of preparing for and administering the IV contrast.

CEM is limited in assessment of posterior extent of masses, specifically to evaluate chest wall, and limited field of view prohibits evaluation of internal mammary adenopathy and axillary nodal disease (Fig. 5.4). MRI, on the other hand, has the advantage of being able to image the entire chest wall and axilla. CEM has the advantage of being able to detect DCIS presenting as morphologically suspicious calcifications, even with no enhancement [30]. This detection is possible because the high resolution of the low-energy image of the CEM study is equivalent to a

Table 5.2 Relative advantages of CEM and MRI

Advantages of CEM	Advantages of MRI
Lower equipment cost	No ionizing radiation
Shorter exam time	Able to image chest wall and entire axilla
	Less risk of acute contrast reaction
CEM examination includes a standard mammogram (able to detect calcifications)	
No claustrophobia or loud noise	No compression
No MRI-specific contraindications, such as from pacemakers or implanted metal	MR-guided biopsy is available
No risk of NSF or gadolinium deposition	

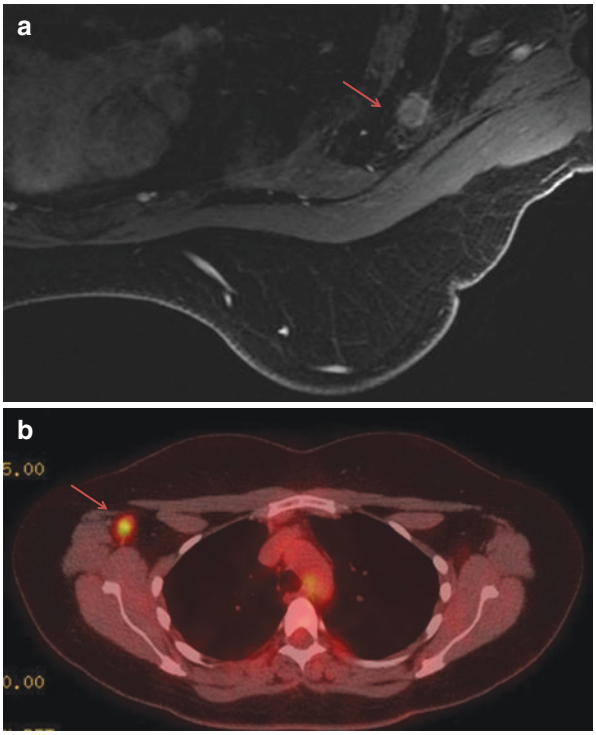

Fig. 5.4 Thirty-two year old female with biopsy proven IDC in the right breast. MR and CEM imaging demonstrated 4.2 cm of disease. (**a**) Axial MR shows a suspicious right level 3 axillary node (arrow). (**b**) PET scan obtained 2 days after MR scan confirms suspicious axillary node on PET scan. This was not included in field of view on CEM imaging but likely would have been seen on targeted axillary ultrasound, which was not performed at outside institution

standard mammogram [31, 32]. Because of this ability to detect calcifications, CEM, when validated for this purpose, would have the potential to serve as a single high-risk screening examination, as opposed to the current standard of utilizing a combination of MRI and mammography.

A disadvantage of CEM is the absence of a method to biopsy findings seen only with contrast, as is available with MRI. In practice, if a CEM finding cannot be correlated to a specific spot on unenhanced mammography or tomosynthesis and cannot be identified by ultrasound, a contrast-enhanced MRI is performed and the lesion biopsied under MRI guidance. Adding biopsy capability to CEM should be straightforward using existing upright stereotactic systems, but no commercial system is as yet available.

Unlike mammography (including CEM), MRI uses no ionizing radiation and does not require compression. On the other hand, patients with absolute contraindications to MRI, such as those with pacemakers or other implanted ferromagnetic devices, or with relative contraindications, such as claustrophobia, can undergo CEM without problem. In general, patients demonstrated significantly higher

overall preference toward CEM compared to MR [33] ($n = 49$, $P < 0.001$), with faster procedure time, greater comfort, and lower noise level cited as the commonest reasons. Participants also reported significantly lower rates of anxiety during CESM compared with CEMRI ($n = 36$, $P = 0.009$). A significantly higher rate of comfort was reported during CEMRI for measures of breast compression ($n = 49$, $P = 0.001$) and the sensation of IV contrast injection ($n = 49$, $P = 0.003$) [34].

Compared to breast MR, CEM is quicker to perform, the iodinated contrast agent is cheaper than gadolinium, and so the procedure is potentially more cost-effective. The average procedure time for CEM from contrast agent injection to compression release after the last mammographic view is 6 minutes and 30 s compared to 29 min and 39 s for breast MRI from start of first to end of last image acquisition [34]. CEM depicts the breast at only two time points, unlike commonly accepted MRI protocols which include dynamic post-contrast acquisition. For this reason, kinetics are not routinely evaluated at this time in the clinical arena. The actual effect of acquisition timing is still under investigation and may improve detection capabilities as the imaging protocols evolve.

For both CEM and MRI, the only significant risk is from the contrast. EUSOBI [20] recommendation notes: "It is important to note that iodinated contrast agents are frequently used in clinical practice, mostly intravenously injected for contrast-enhanced computed tomography. There are contraindications (history of allergic reactions, renal failure) and possible side effects that require discussion with the patient and the signature of an informed written consent. Thus, the injection of iodinated contrast agents for mammography requires the same precautions used for other contrast-enhanced X-ray-based examination. Before the examination, the radiologist will clarify the risks and benefits associated with the intravenous injection of iodinated contrast agents." This is how most clinical breast imaging centers have incorporated CEM into their practice.

Although iodinated contrast is generally considered to be significantly more hazardous than gadolinium contrast, the reported differences in frequency of adverse events, as well as the overall frequency, are small. Comparison of the two types of agents is hindered, however, by a lack of large series and a wide spread in reported outcomes, as well as variability in terminology used to describe reactions. As reported in the ACR Manual on Contrast Media, v 10.2, the frequency of "serious acute" reactions for iodinated contrast is estimated at 0.04% [35] vs. a rate of 0.001–0.01% for "severe life-threatening anaphylactic" reactions from gadolinium [35]. Other issues include the possible risk of nephrotoxicity from iodinated contrast and the proven but small risk of nephrogenic systemic fibrosis from gadolinium contrast. A more recent concern is the observed deposition of gadolinium in the brain from repeated administrations of the most common class of gadolinium contrast agents [36]. Whether this deposition has any actual consequences to human health is unknown.

5.6 Potential Applications of CEM

CEM is currently a diagnostic imaging test, to be used as an adjunct to standard mammography. Given the labeling, approved uses for CEM could include staging of newly diagnosed breast cancer, problem-solving in cases where conventional

mammography and ultrasound are inconclusive, and evaluating treatment response in patients receiving neoadjuvant chemotherapy and potentially a supplemental screening tool.

5.7 Summary

Contrast-enhanced mammography is in its early stages of development and clinical use. Diagnostic and pilot screening studies have shown similar performance to contrast-enhanced breast MRI. The technique has some cost and speed advantages over MRI and is better tolerated by most patients. Where CEM will fit in the armamentarium of imaging procedures available for detecting and diagnosing breast cancer remains to be seen.

References

1. Andersson I, Aspegren K, Janzon L, et al. Mammographic screening and mortality from breast cancer: the Malmo mammographic screening trial. BMJ (Clin Res ed). 1988;297(6654):943–8.
2. Shapiro S. Periodic screening for breast cancer : the health insurance plan project and its sequelae. Baltimore, MD: Johns Hopkins University Press; 1988. p. 1963–86.
3. Tabar L, Fagerberg CJ, Gad A, et al. Reduction in mortality from breast cancer after mass screening with mammography. Randomised trial from the Breast Cancer Screening Working Group of the Swedish National Board of Health and Welfare. Lancet. 1985;1(8433): 829–32.
4. Rosenberg RD, Hunt WC, Williamson MR, et al. Effects of age, breast density, ethnicity, and estrogen replacement therapy on screening mammographic sensitivity and cancer stage at diagnosis: review of 183,134 screening mammograms in Albuquerque, New Mexico. Radiology. 1998;209(2):511–8.
5. Kuhl CK, Schrading S, Leutner CC, et al. Mammography, breast ultrasound, and magnetic resonance imaging for surveillance of women at high familial risk for breast cancer. J Clin Oncol. 2005;23(33):8469–76.
6. Stomper PC, Herman S, Klippenstein DL, et al. Suspect breast lesions: findings at dynamic gadolinium-enhanced MR imaging correlated with mammographic and pathologic features. Radiology. 1995;197(2):387–95.
7. Weinreb JC, Newstead G. MR imaging of the breast. Radiology. 1995;196(3):593–610.
8. Lewin JM, Isaacs PK, Vance V, Larke FJ. Dual-energy contrast-enhanced digital subtraction mammography: feasibility. Radiology. 2003;229(1):261–8.
9. Cheung YC, Lin YC, Wan YL, et al. Diagnostic performance of dual-energy contrast-enhanced subtracted mammography in dense breasts compared to mammography alone: interobserver blind-reading analysis. Eur Radiol. 2014;24(10):2394–403.
10. Dromain C, Thibault F, Muller S, et al. Dual-energy contrast-enhanced digital mammography: initial clinical results. Eur Radiol. 2011;21(3):565–74.
11. Lobbes MB, Lalji U, Houwers J, et al. Contrast-enhanced spectral mammography in patients referred from the breast cancer screening programme. Eur Radiol. 2014;24(7):1668–76.
12. Fallenberg EM, Dromain C, Diekmann F, et al. Contrast-enhanced spectral mammography versus MRI: initial results in the detection of breast cancer and assessment of tumour size. Eur Radiol. 2014;24(1):256–64.
13. Jochelson MS, Dershaw DD, Sung JS, et al. Bilateral contrast-enhanced dual-energy digital mammography: feasibility and comparison with conventional digital mammography and MR imaging in women with known breast carcinoma. Radiology. 2013;266(3):743–51.

14. Lee-Felker SA, Tekchandani L, Thomas M, et al. Newly diagnosed breast cancer: comparison of contrast-enhanced spectral mammography and breast MR imaging in the evaluation of extent of disease. Radiology. 2017;285(2):389–400.
15. Chou CP, Lewin JM, Chiang CL, et al. Clinical evaluation of contrast-enhanced digital mammography and contrast enhanced tomosynthesis—comparison to contrast-enhanced breast MRI. Eur J Radiol. 2015;84(12):2501–8.
16. Fallenberg EM, Schmitzberger FF, Amer H, et al. Contrast-enhanced spectral mammography vs. mammography and MRI – clinical performance in a multi-reader evaluation. Eur Radiol. 2017;27(7):2752–64.
17. Zhu X, Huang JM, Zhang K, et al. Diagnostic value of contrast-enhanced spectral mammography for screening breast cancer: systematic review and meta-analysis. Clin Breast Cancer. 2018;18(5):e985–95.
18. Morrow M, Waters J, Morris E. MRI for breast cancer screening, diagnosis, and treatment. Lancet. 2011;378(9805):1804–11.
19. Ali-Mucheru M, Pockaj B, Patel B, et al. Contrast-enhanced digital mammography in the surgical management of breast cancer. Ann Surg Oncol. 2016;23(Suppl 5):649–55.
20. Sardanelli F, Fallenberg EM, Clauser P, et al. Mammography: an update of the EUSOBI recommendations on information for women. Insights imaging. 2017;8(1):11–8.
21. Sogani J, Morris EA, Kaplan JB, et al. Comparison of background parenchymal enhancement at contrast-enhanced spectral mammography and breast MR imaging. Radiology. 2017;282(1):63–73.
22. Savaridas SL, Taylor DB, Gunawardana D, Phillips M. Could parenchymal enhancement on contrast-enhanced spectral mammography (CESM) represent a new breast cancer risk factor? Correlation with known radiology risk factors. Clin Radiol. 2017;72(12):1085.e1081–9.
23. Iotti V, Ravaioli S, Vacondio R, et al. Contrast-enhanced spectral mammography in neoadjuvant chemotherapy monitoring: a comparison with breast magnetic resonance imaging. Breast Cancer Res. 2017;19(1):106.
24. Patel BK, Hilal T, Covington M, et al. Contrast-enhanced spectral mammography is comparable to MRI in the assessment of residual breast cancer following neoadjuvant systemic therapy. Ann Surg Oncol. 2018;25(5):1350–6.
25. Jochelson MS, Pinker K, Dershaw DD, et al. Comparison of screening CEDM and MRI for women at increased risk for breast cancer: a pilot study. Eur J Radiol. 2017;97:37–43.
26. Sung J, Lebron L, D'Alessio D, Keating D, Lee C, Morris E, Jochelson M. Utility of contrast enhanced digital mammography for breast cancer screening. Paper presented at: radiological society of North America 2017 scientific assembly and annual meeting, 26 Nov 2017 to 1 Dec 2017, Chicago, IL; 2017.
27. Kuhl C, Weigel S, Schrading S, et al. Prospective multicenter cohort study to refine management recommendations for women at elevated familial risk of breast cancer: the EVA trial. J Clin Oncol. 2010;28(9):1450–7.
28. Patel BK, Gray RJ, Pockaj BA. Potential cost savings of contrast-enhanced digital mammography. AJR Am J Roentgenol. 2017;208(6):W231–w237.
29. Phillips J, Steinkeler J, Talati K, et al. Workflow considerations for incorporation of contrast-enhanced spectral mammography into a breast imaging practice. J Am Coll Radiol. 2018;15(6):881–5.
30. Cheung YC, Juan YH, Lin YC, et al. Dual-energy contrast-enhanced spectral mammography: enhancement analysis on BI-RADS 4 non-mass microcalcifications in screened women. PLoS One. 2016;11(9):e0162740.
31. Francescone MA, Jochelson MS, Dershaw DD, et al. Low energy mammogram obtained in contrast-enhanced digital mammography (CEDM) is comparable to routine full-field digital mammography (FFDM). Eur J Radiol. 2014;83(8):1350–5.
32. Lalji UC, Jeukens CR, Houben I, et al. Evaluation of low-energy contrast-enhanced spectral mammography images by comparing them to full-field digital mammography using EUREF image quality criteria. Eur Radiol. 2015;25(10):2813–20.

33. Phillips J, Miller MM, Mehta TS, et al. Contrast-enhanced spectral mammography (CESM) versus MRI in the high-risk screening setting: patient preferences and attitudes. Clin Imaging. 2017;42:193–7.
34. Hobbs MM, Taylor DB, Buzynski S, Peake RE. Contrast-enhanced spectral mammography (CESM) and contrast enhanced MRI (CEMRI): Patient preferences and tolerance. J Med Imaging Radiat Oncol. 2015;59(3):300–5.
35. American College of Radiology. Manual on contrast media. Version 10.2. Reston, VA: American College of Radiology; 2016.
36. McDonald RJ, McDonald JS, Kallmes DF, et al. Gadolinium deposition in human brain tissues after contrast-enhanced MR imaging in adult patients without intracranial abnormalities. Radiology. 2017;285(2):546–54.
37. Li L, Roth R, Germaine P, et al. Contrast-enhanced spectral mammography (CESM) versus breast magnetic resonance imaging (MRI): a retrospective comparison in 66 breast lesions. Diagn Interv Imaging. 2017;98(2):113–23.
38. Luczynska E, Heinze-Paluchowska S, Hendrick E, et al. Comparison between breast MRI and contrast-enhanced spectral mammography. Med Sci Monit. 2015;21:1358–67.

CEM as a Problem-Solving Tool

6

Sarah L. Tennant

6.1 Introduction

Contrast-enhanced mammography (CEM) was first introduced (as a routine clinical examination) to the UK in 2013, at the Nottingham Breast Institute. At the time of writing, the technique has been adopted by approximately 20 centres throughout the UK.

The author's experience is based primarily on experience in symptomatic patients (Chap. 7 covers the use of CEM in screening populations). However, one of the advantages of CEM in the diagnostic or problem-solving setting is also an advantage in the screening setting: the ability to define the extent of any malignant tumour detected, at the same time as the diagnostic exam. This can obviate the need for MRI, for which CEM is considered an excellent alternative [1–3].

6.2 The One-Stop Clinic

The diagnostic assessment of patients with breast symptoms can be based on the multidisciplinary triple diagnostic method ("Triple Assessment") which comprises clinical assessment, imaging assessment and (where appropriate) needle biopsy. In the UK, the "one-stop" clinic is considered to be best practice—patients presenting with symptoms are seen in an environment where all appropriate tests can be carried out during the same clinic attendance [4]. CEM can work well within this setting. Work by Fallenberg et al. [5] showed that the low-energy image of a CEM exam was clinically equivalent to a full-field digital mammogram (FFDM). Technical equivalence has also been proven—Francescone et al. [6] compared various parameters in women who had undergone both CEM and standard FFDM within 6 months, concluding that the low-energy images

S. L. Tennant (✉)
Nottingham Breast Institute, Nottingham, UK
e-mail: Sarah.tennant@nuh.nhs.uk

M. Lobbes, M. S. Jochelson (eds.), *Contrast-Enhanced Mammography*,
https://doi.org/10.1007/978-3-030-11063-5_6

could be used for interpretation instead of FFDM. Importantly, an early concern regarding the visibility of calcification on the low-energy images that they might be obscured by iodinated contrast was not supported in this study—calcifications were equally well seen as on FFDM. Lalji et al. [7] corroborated this view with their 2015 publication where low-energy images were compared to FFDM using European reference criteria. In this analysis, calcifications were significantly *more visible* on LE images than on FFDM, although this was thought to be related to post-processing of the images. However, a subsequent study focusing solely on the use of CEM in calcifications did not confirm this earlier observation, showing no clinically relevant increase in diagnostic accuracy (source: personal communication and unpublished data).

6.3 The Nottingham Approach

As outlined above, there is good evidence to show that when a CEM is planned, there is no need to perform standard digital mammography first. The Nottingham model exploits this benefit of the technique, where, according to certain criteria, CEM is offered *as an alternative* to FFDM.

In the UK, most centres use the Royal College of Radiologists (RCR) Breast Group classification [8] (rather than BI-RADS [9]) to record the level of imaging suspicion. Mammographic (M1–5) and ultrasound (U1–5) scores are graded thus:

1. Normal.
2. Benign findings.
3. Indeterminate/probably benign findings.
4. Findings suspicious of malignancy.
5. Findings highly suspicious of malignancy.

A 5-point scale is also used to record the level of clinical suspicion (P for palpation):

P1. Normal.
P2. Benign.
P3. Uncertain.
P4. Suspicious.
P5. Malignant.

Figure 6.1 demonstrates the pathway used for symptomatic patients in Nottingham. In Nottingham, the lower age limit for first-line mammography in patients with suspicious clinical findings is 35 years. However, it is appreciated that other centres (both nationally and internationally) will have different approaches.

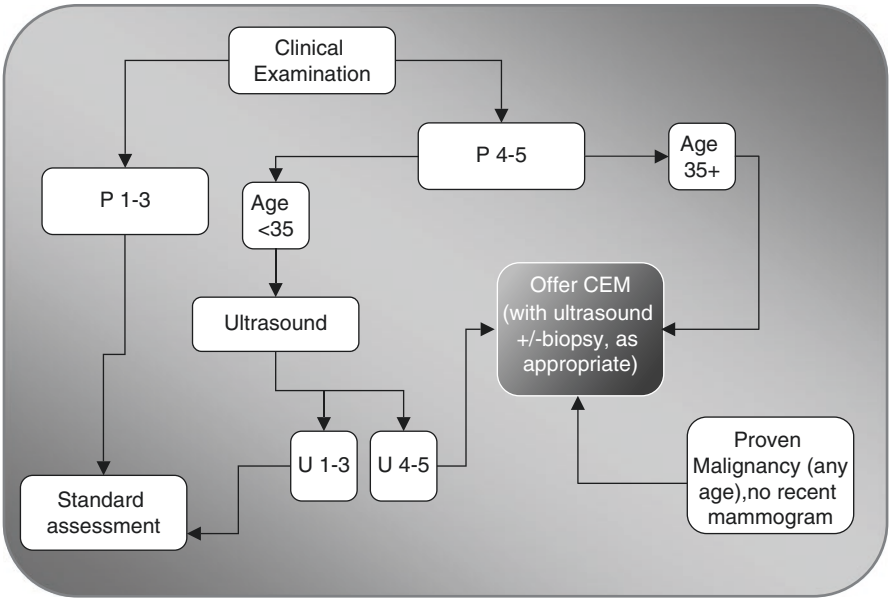

Fig. 6.1 The Nottingham approach—CEM as an alternative to FFDM in symptomatic patients. P is the clinical score (P1 = normal, P2 = benign; P3 = uncertain; P4 = suspicious; P5 = malignant) and U is the ultrasound score (U1: normal; U2: benign findings; U3: indeterminate/probably benign findings; U4: findings suspicious of malignancy U5: findings highly suspicious of malignancy)

The majority (approx. 2/3) of lesions assessed as clinically suspicious or malignant in our centre are proven malignant at subsequent biopsy [10]. Offering CEM as first-line imaging in these patients means that accurate staging is available immediately, with no significant increase in radiation dose. (Although the dose from a CEM examination is higher than that of a FFDM, it is still within European guidelines for digital mammography [11].) In patients who do not have cancer, the examination provides additional reassurance (for both patients and staff). With reported negative predictive value (NPV) of up to 100% [12, 13], a negative CEM effectively rules out a tumour, providing the lesion is within the mammographic field, although the full triple-assessment process should always be followed.

The most common explanation for a palpable breast lump with subsequent benign/normal CEM, in our centre, is a cyst [10]. Figure 6.2 shows an example of a cyst—an incidental finding in a patient with a clinically suspicious mass in the right breast. The typical appearance of a cyst on CEM is a rounded, well-defined area (which may be visible on the low-energy images, depending on lesion size and breast density) with a *lack of enhancement* compared to the surrounding tissue on the recombined images. It may have a thin rim of enhancement.

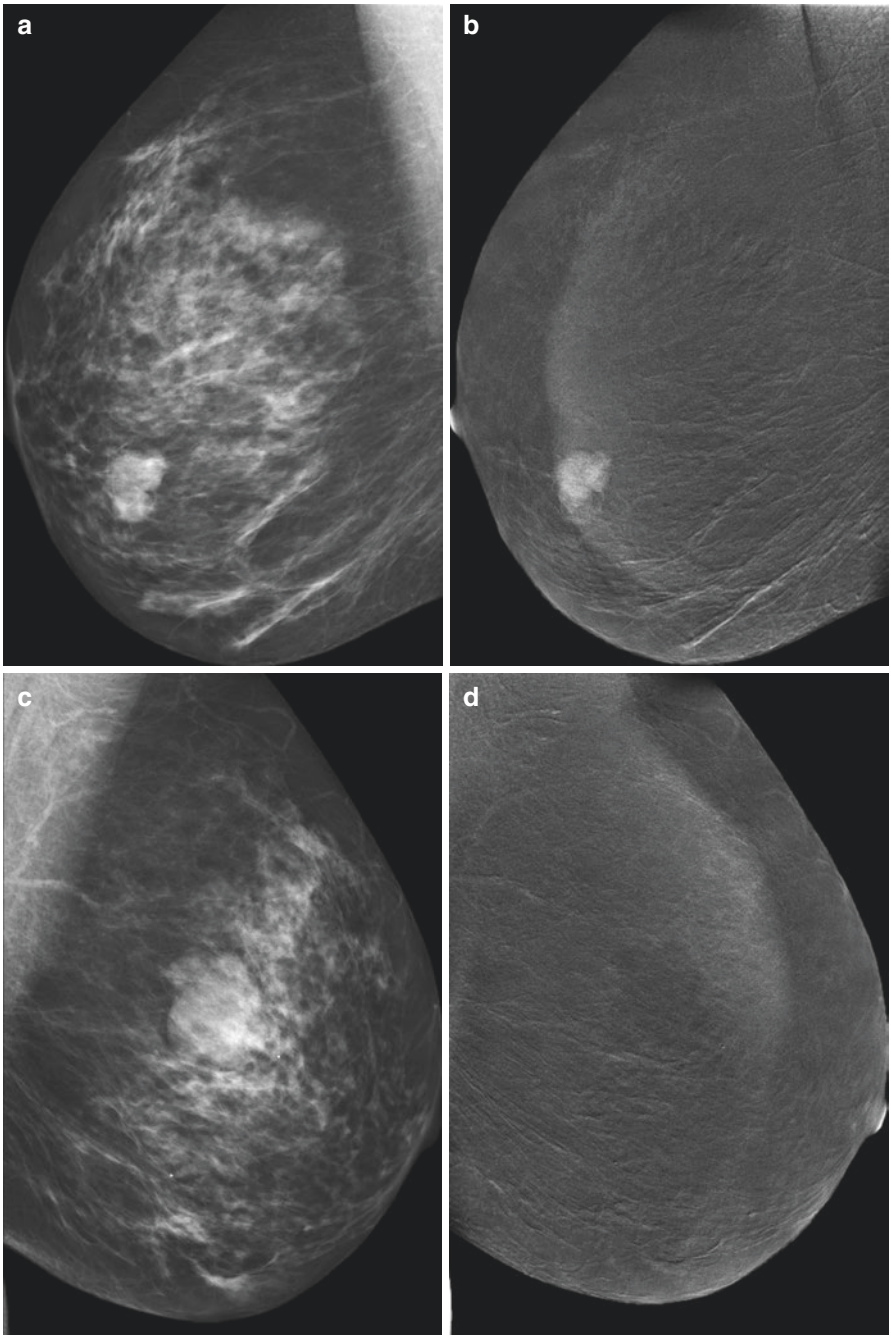

Fig. 6.2 Clinically suspicious mass in the right breast. Low energy images (**a**, **c**, **e**, **g**) show bilateral masses—well-defined on the left, slightly ill-defined on the right. Recombined images (**b**, **d**, **f**, **h**) show a focal lack of enhancement on the left, consistent with a cyst. The mass in the right breast shows homogeneous enhancement. Needle core biopsy showed a papilloma (with no atypia), and this was subsequently treated with vacuum excision. Final pathology—intraductal papilloma

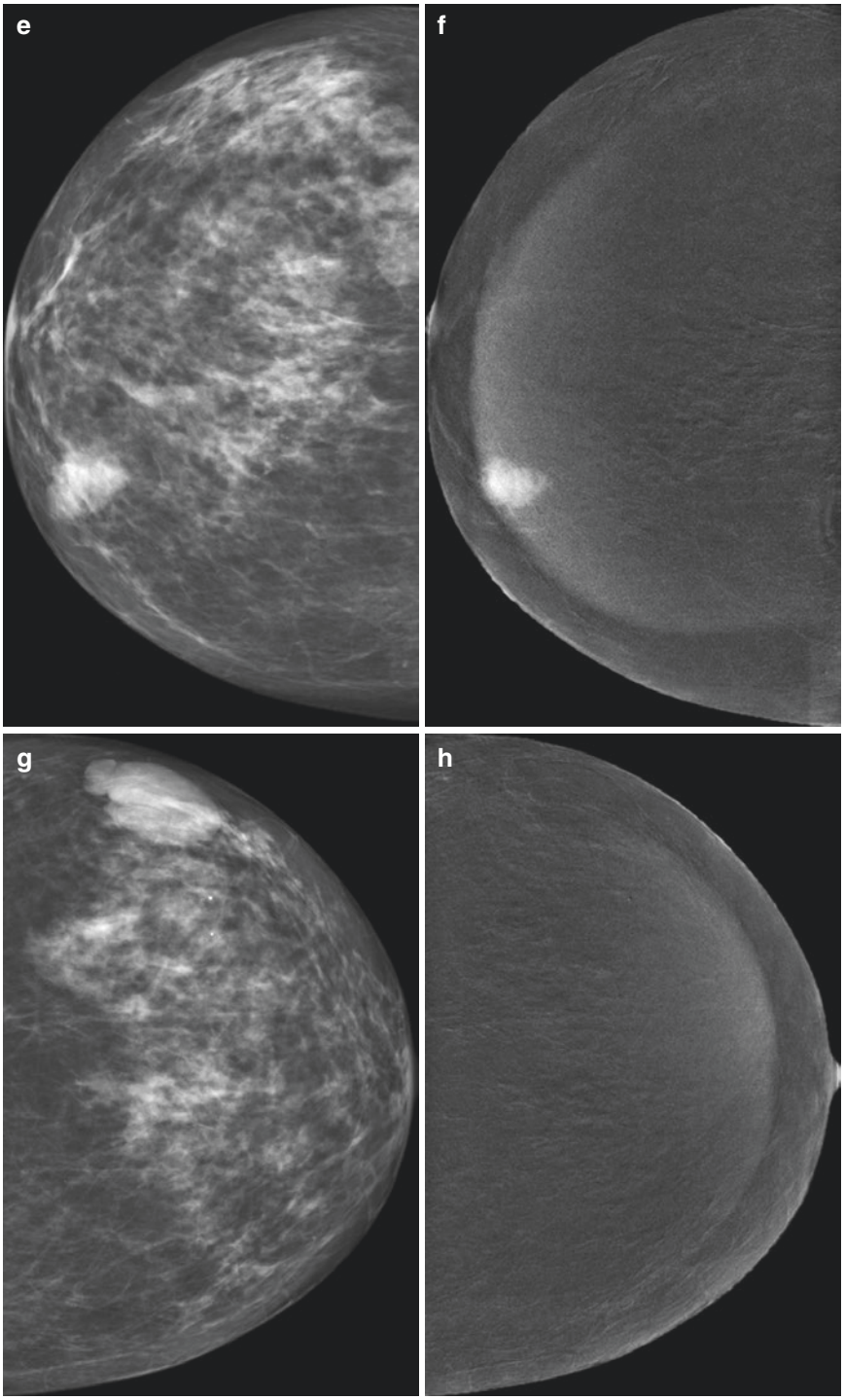

Fig. 6.2 (continued)

6.4 Negative Predictive Value

One of the great strengths of CEM in an uncertain clinical situation is its high negative predictive value. In Tagliafico et al.'s [14] systematic review and meta-analysis, CEM was shown to have an extremely high sensitivity—98% overall sensitivity was estimated across the eight papers included (95% CI 0.96–1.00). The studies included in this review were a mixture of both retrospective and prospective analyses and, as the authors noted, were heterogeneous for eligibility of included patients. Nevertheless, the lowest reported sensitivity amongst the groups (Cheung et al. [15] was 91%, and this was in a highly selected group of patients where CEM was being used to evaluate suspicious calcifications. The sensitivity reported by Cheung et al. was for *enhancement* of the lesions being assessed. Sensitivity for invasive breast cancer in this group was (7/7) (100%), but the larger group of malignant lesions in this paper was ductal carcinoma in situ (DCIS), where only 13/15 (86.7%) showed enhancement. Of the two non-enhancing lesions subsequently diagnosed as DCIS, one was low-grade, and the other was high-grade.

Other groups have also reported very high NPVs in patients called back from abnormal screening exams: Lobbes et al. [12], 100% in 113 women recalled from mammographic screening; Lalji et al. [16], 98.2% in 199 women recalled from screening; and Luczynska et al. [17], 100% in 102 women with suspicious conventional mammography.

Tardivel et al. [18] reported a lower NPV of 81% in 195 women with suspicious or indeterminate findings on conventional imaging—although did clarify that this was only considering enhancement criteria.

6.5 Assessment of Calcifications

There is some debate regarding just how the "sensitivity" of CEM is interpreted in the assessment of calcifications. Whilst the lack of enhancement of a malignant lesion has been considered a false negative by some, the detection of malignant calcifications on the low-energy image is a true positive. In practice, the two components are complementary and should never be assessed separately. Therefore, the final RCR or BI-RADS score is a combination read and determinations of sensitivity, specificity, accuracy, etc. should be based on that combined interpretation.

Cheung et al. [19] looked at CEM in 94 patients with screen-detected calcifications (that were not associated with a mass) and were classified as BI-RADS 4 [9]. 33/94 (35%) enhanced on CEM. Of these, 24/33 (73%) were malignant, and 9/33 (27%) were benign. All 8 invasive ductal cancers (100%) and 16/19 DCIS (84.2%) showed enhancement. This paper did not specify the grade of DCIS. It seems plausible that high-grade DCIS would enhance more at CEM than low or intermediate grade—we know that this is true at MRI—98% of high-grade DCIS enhances at MRI, but low- and intermediate-grade DCIS is less likely to enhance [20]. However, there are currently limited data on the role of CEM in detection of DCIS—and even less data looking at patterns of enhancement according to grade.

Houben et al. [21] studied 147 women recalled from the screening programme for suspicious calcifications, who underwent CEM as part of their diagnostic workup. Most of these cases (82/147 (55.7%)) were benign—invasive cancers (32/147 (21.7%)) and pure DCIS (33/147 22.4%)) made up the rest. Enhancement was seen in 84.4% (27/32) of invasive breast cancer and 81.1% (27/33) of DCIS. This group did consider the grade of DCIS—enhancement was noted in 16/18 (88.9%); 10/14 (71.4%) and 1/1 (100%) of high, intermediate and low-grade disease, respectively. Interestingly, using CEM, a BI-RADS 5 score was assigned more frequently than BI-RADS 4 (66.2% vs 27.6%). Using LE images only, scores were 16.9% and 77.8%, respectively. This implies that the availability of enhancement characteristics increases reader confidence in assessment of calcifications—even though it would not alter management.

As the debate regarding overdiagnosis and overtreatment in screening continues, it remains to be seen what the recommended management of low-grade DCIS will be. At the time of writing, the UK LORIS trial [22] is recruiting patients with low-risk DCIS (low/intermediate grade without comedo necrosis). The primary objective is to assess whether active monitoring is non-inferior to surgery, in terms of ipsilateral invasive breast cancer-free survival time. Unfortunately, it seems that CEM does not currently offer an easy solution for identification of low-risk calcification. Although CEM may improve reader confidence, it is important to remember that calcifications deemed worthy of a biopsy on the low-energy images should still be biopsied, even if they do not enhance.

Figure 6.3 shows an example of suspicious calcifications, with malignant enhancement on the recombined views, in this case enabling accurate assessment of disease extent.

6.6 Cancer of Unknown Primary Site/Metastatic Axillary Adenopathy

MRI is currently the problem-solving tool of choice in the assessment of clinically and mammographically occult cancers, both in patients with malignant axillary adenopathy and in systemic metastatic disease where the pathology is suggestive of a breast primary. In this setting, MRI identifies over 2/3 of tumours, most of which are then detected at targeted ultrasound [23]. CEM can also be considered in the workup of patients with cancer of unknown primary origin. Due to its superior sensitivity and specificity compared to FFDM, a diagnosis of breast cancer can be confirmed or excluded with reasonable confidence during a single clinic visit. In centres where mammography and MRI are not situated in the same facility, CEM can expedite the diagnostic pathway.

In these particular situations (the hunt for a primary lesion), one may wish to review any prior mammography available, to assess background density. The "added value" of CEM in a fatty mammogram is lower than in a dense background pattern [24, 25]. It may therefore be deemed unnecessary to perform a CEM (with the inherent risks of iodinated contrast)—as always in medicine, the risks and benefits need to be balanced.

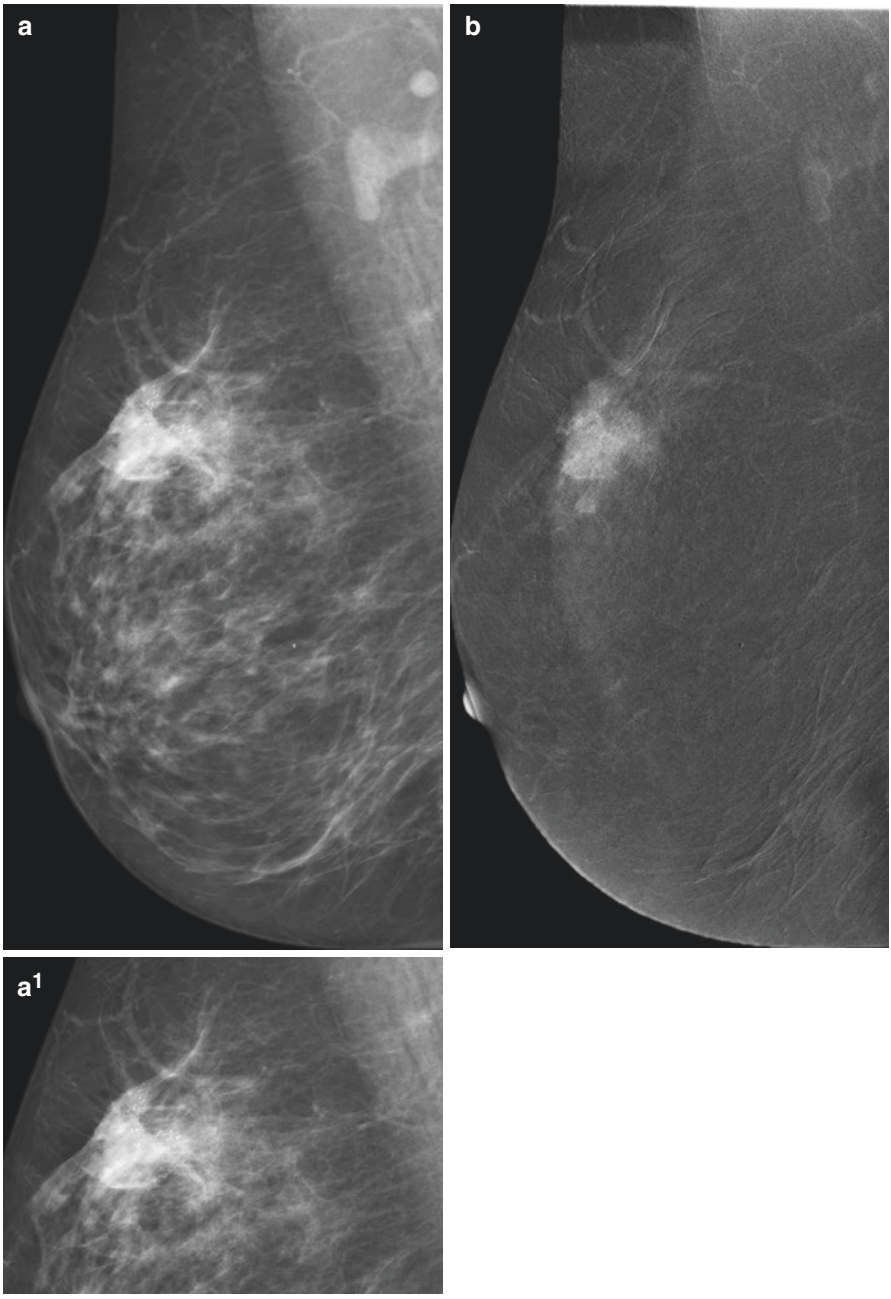

Fig. 6.3 Suspicious mass in the right breast. Low energy images (**a**, **a1** (zoomed) **c**, **c1** (zoomed)) show pleomorphic calcification in the right upper outer quadrant. Recombined images (**b**, **d**) show focal enhancement measured at 36 mm. Final pathology—ductal carcinoma, grade 3—invasive disease measured 24 mm, whole tumour size (to include DCIS) 35 mm

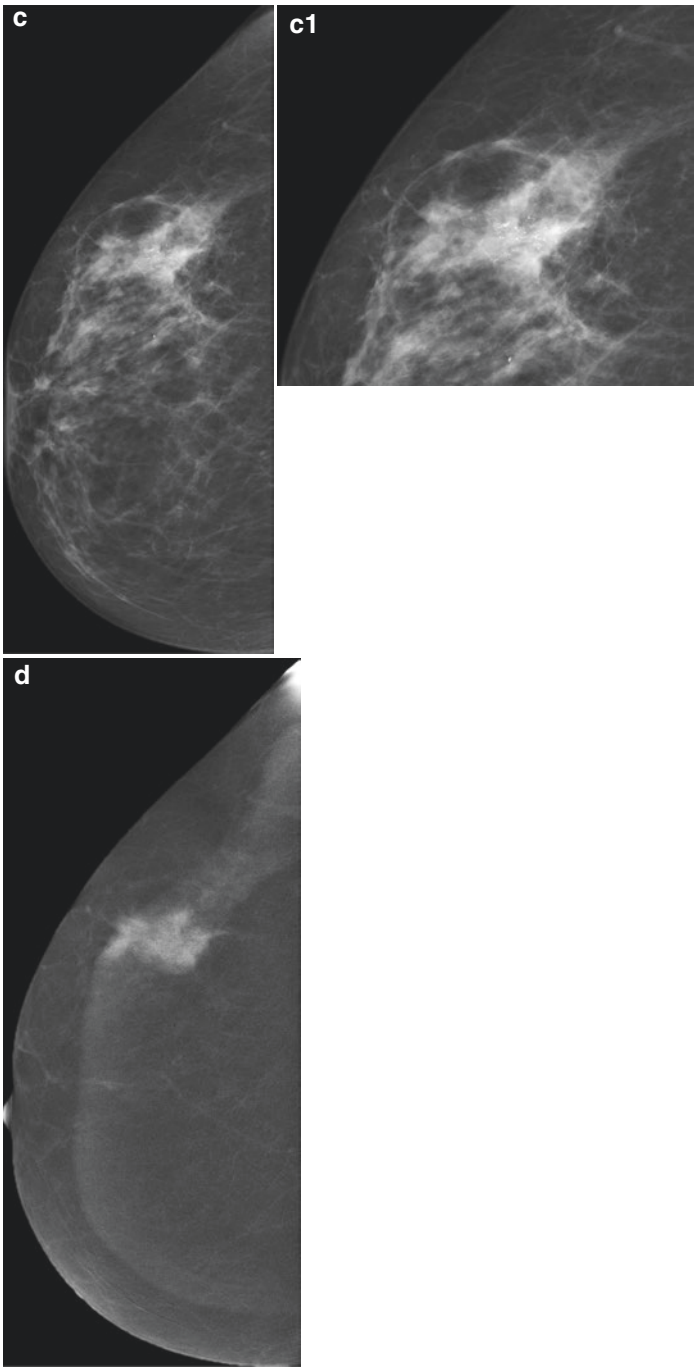

Fig. 6.3 (continued)

6.7 Staging/Surgical Planning

Mammography is generally performed in all women diagnosed with breast cancer, regardless of age. Even in tumours which are mammographically occult, the examination acts as a "baseline" for future follow-up and allows assessment of calcifications, which no other imaging modality evaluates so effectively. Modern mammography has a sensitivity of up to 88% [26], but this is lower in dense breasts [27, 28], and tumour extent can be difficult to evaluate with conventional imaging. In the UK, current guidance states that MRI should be offered if there is discrepancy (between clinical assessment and imaging) regarding the extent of disease; if breast density precludes accurate mammographic assessment or to assess tumour size if breast-conserving surgery is being considered in invasive lobular cancer [29].

With the increasing availability of oncoplastic surgical techniques, it has never been more important to stage primary breast cancer accurately. Multifocal/multicentric disease, traditionally defined as additional tumour foci in the same/different quadrants of the breast, respectively, would historically have been treated with mastectomy. This multifocal/multicentric definition has lately fallen out of favour—modern surgical planning is much more reliant on the location, volume and relationship of tumour foci than an arbitrary definition of whether they lie in the same quadrant. CEM can provide an accurate map of disease, in a format familiar to the breast surgeon (i.e. standard mediolateral oblique and craniocaudal views). Although the information acquired is very similar to that obtained from an MRI, it is much simpler to display two mammographic images in the operating room—a practice to which many breast surgeons are accustomed.

Several studies have demonstrated the benefits of CEM in women with dense breasts—in terms of sensitivity and tumour sizing. Fallenberg et al. [5] reported 118 patients with newly diagnosed invasive or in situ breast cancer. The sensitivity of CEM was higher than mammography in both dense and non-dense breasts, but the increase in sensitivity was much higher for dense breasts—from 71.6% to 93.3% and from 85.8% to 96.5% for dense and non-dense breasts, respectively.

Patel et al. [24] also looked at 88 women with newly diagnosed breast cancer. Tumour size correlation (with histopathology) correlated well (better than ultrasound or FFDM) in patients with both dense (BI-RADS categories C and D) and non-dense (BI-RADS categories A and B) breasts. Size correlation was highest for CEM in patients with invasive ductal carcinoma—tumour size was overestimated more for invasive lobular carcinoma. The added value of CEM (as a supplement to FFDM) in determining tumour size was shown to be greater in patients with dense breasts.

Mori et al. [30] studied 72 Japanese women who had undergone CEM. The group consisted of patients with BI-RADS 3 or above abnormalities, discovered at mammography or ultrasound. Ninety percent of 143 breasts (one patient had previously undergone mastectomy) were classed as heterogeneously dense (79%) or extremely dense (11%)—equivalent to BI-RADS categories C and D, respectively. CEM demonstrated increased accuracy when compared to standard mammography (90.9% vs 72.7%). Sensitivity (86.2% vs 53.4%), specificity (94.1% vs 85.9%), positive predictive value (PPV) (90.9 vs 72.1%) and NPV (90.9% vs 73%) were all improved.

Figures 6.4, 6.5, 6.6, 6.7, and 6.8 show examples where the recombined imaging aids in the diagnosis and assessment of disease extent.

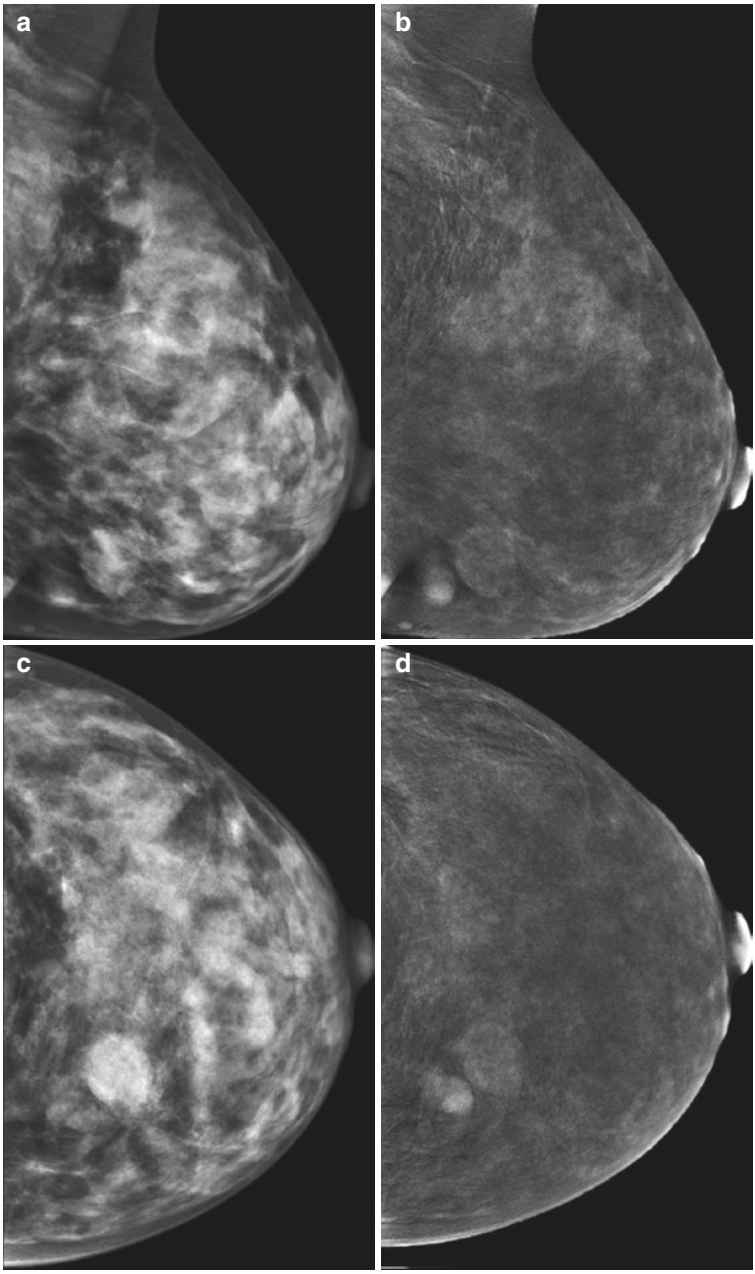

Fig. 6.4 Patient presents with a lump in the left breast. History of previous fibroadenoma (biopsy-proven). Low energy images (**a**, **c**) show a predominantly dense background pattern, with a relatively well-defined mass in the lower inner quadrant. Recombined images (**b**, **d**) show the mass enhances only faintly—this is the longstanding fibroadenoma. There is a separate mass posterior to the fibroadenoma, showing more intense enhancement. Ultrasound guided core-biopsy of the posterior mass showed invasive carcinoma, no special type, grade 2. Note the background glandular enhancement in the left upper breast on the oblique view—this was symmetrical (right sided images not shown)

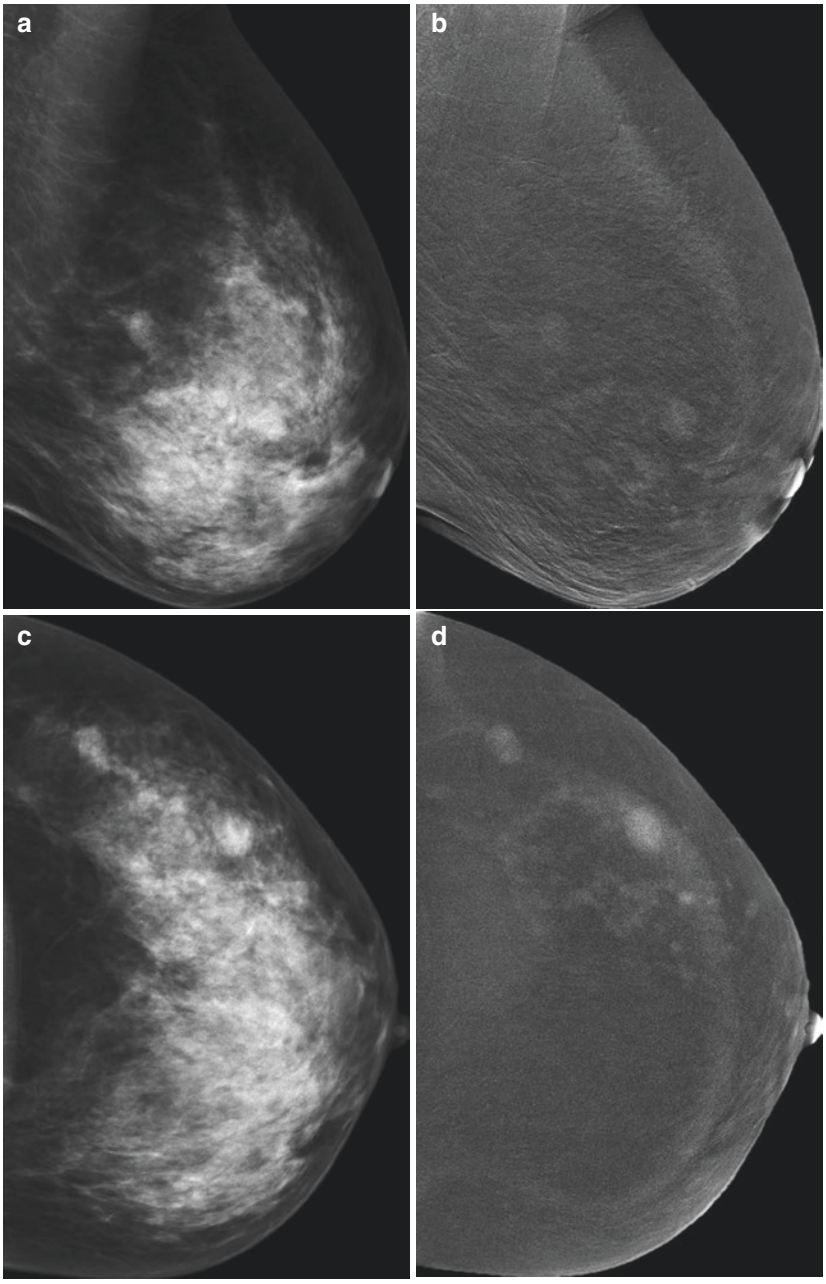

Fig. 6.5 Patient with bloody nipple discharge and lumpy area left breast. Low energy images (**a**, **c**) show two relatively well defined masses in the left breast. Recombined images (**b**, **d**) demonstrate extensive (although relatively low-grade) enhancement throughout the left lower outer quadrant. Ultrasound guided biopsy showed high nuclear grade encapsulated papillary carcinoma (B5c). Extensive abnormality was confirmed at MRI (not shown) and the patient underwent mastectomy

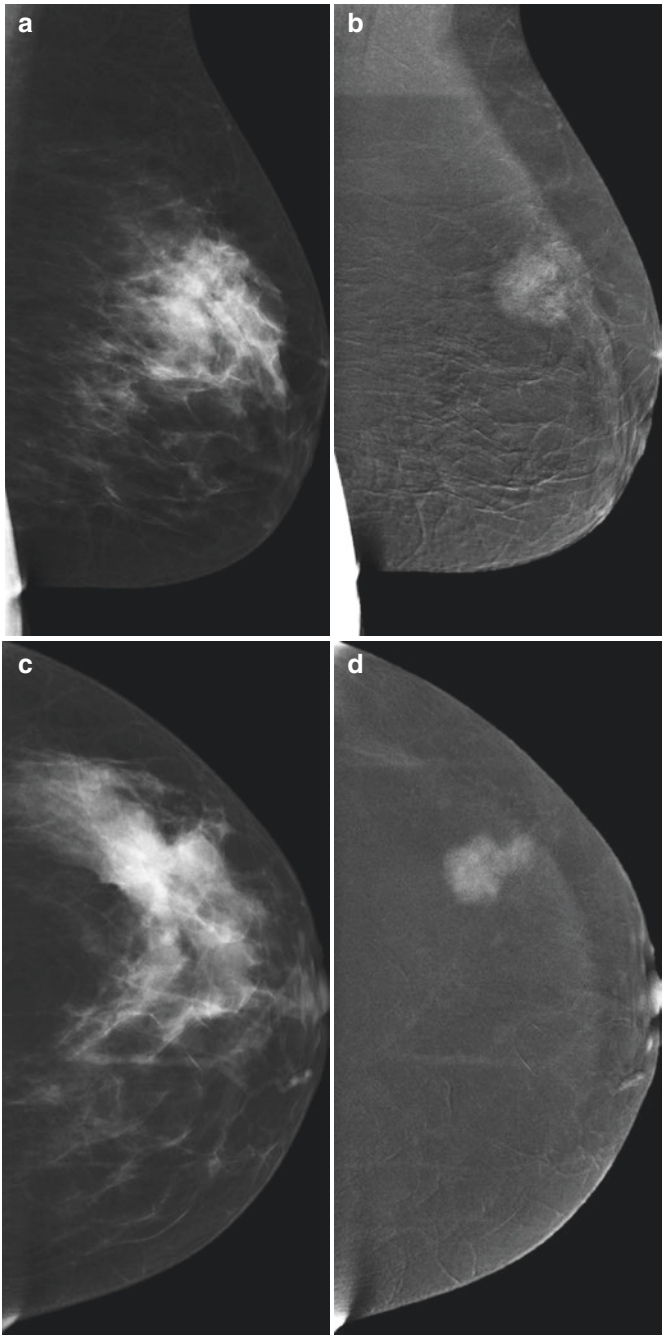

Fig. 6.6 Patient with a mass in the left breast. Abnormality is difficult to appreciate on the low-energy images (**a**, **c**). Recombined views (**b**, **d**) show focal suspicious enhancement. CEM size reported as 34 mm. Final pathology—30 mm grade 2 invasive carcinoma, no special type

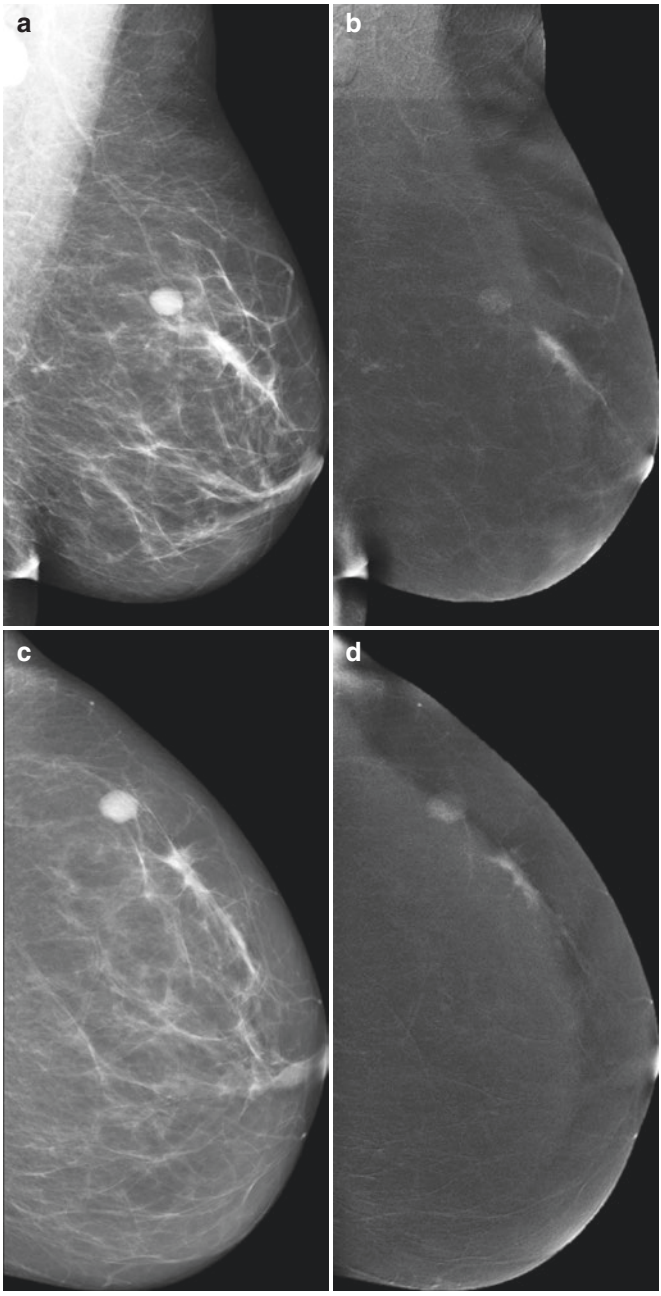

Fig. 6.7 Small ovoid mass palpable in left breast. Low energy images (**a**, **c**) show a well-defined mass in the upper outer quadrant. Some linear soft-tissue density anterior to this appears benign. Recombined views (**b**, **d**) demonstrate focal suspicious enhancement in this area. Final pathology—grade 2 tumour of no special type, adjacent malignant intramammmary lymph node

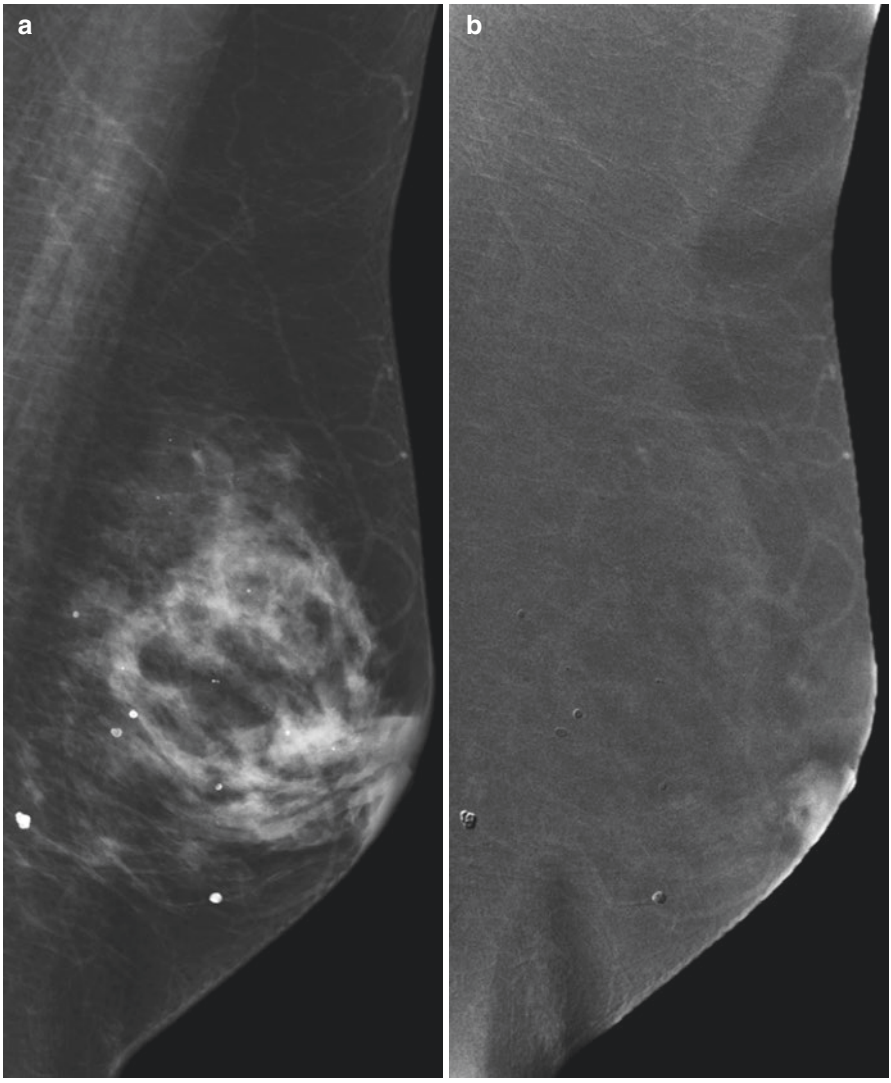

Fig. 6.8 Patient reported changes to left nipple. Low energy images (**a**, **c**) show no abnormality. Recombined views (**b**, **d**) demonstrate focal suspicious enhancement in the retroareolar region. Biopsy showed invasive tumour with lobular features, grade 2

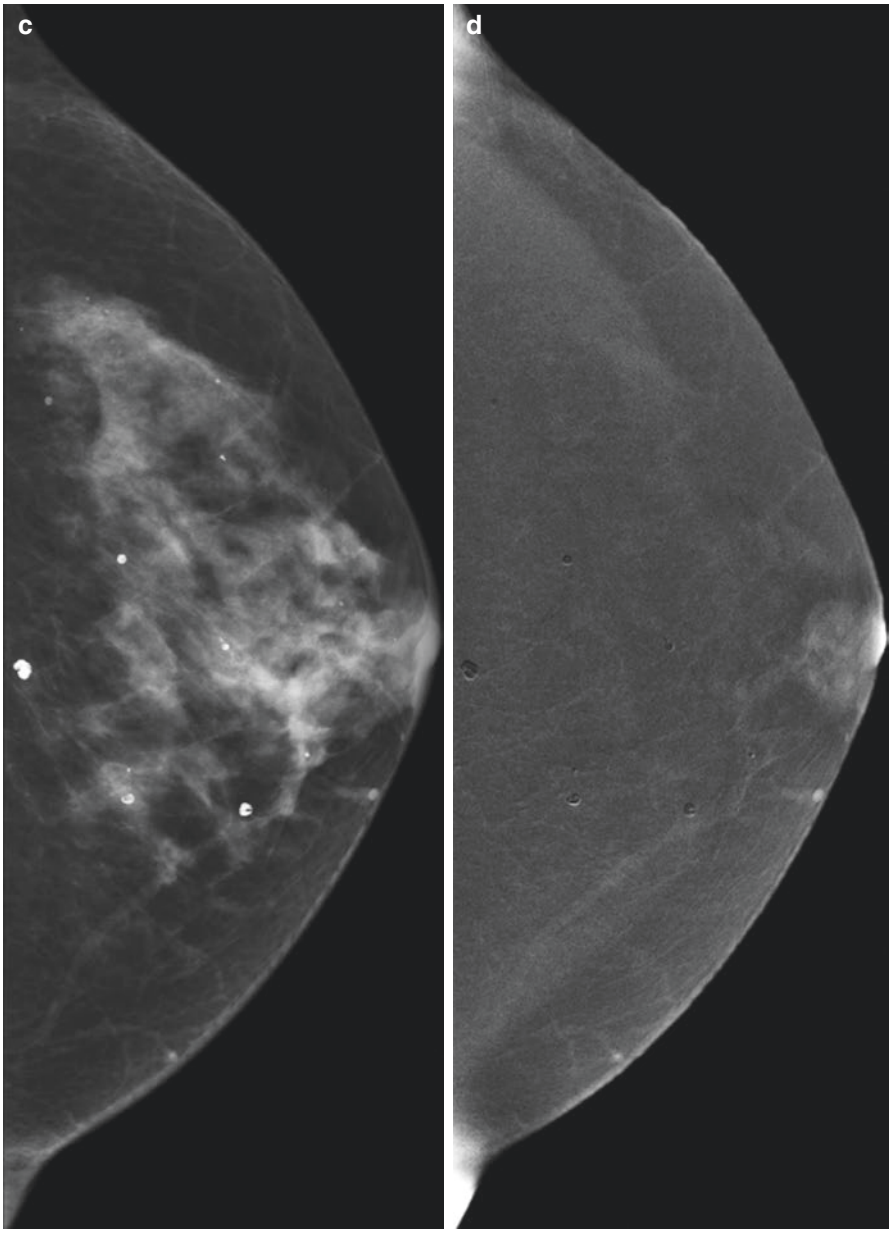

Fig. 6.8 (continued)

6.8 False Negatives

Although the sensitivity of CEM is extremely high, at >90% [2, 5, 25], false negatives do occur. Amongst the causes of false-negative exams are lesions which are outside the mammographic field. This may be due to patient factors (e.g. pectus excavatum) or radiographic technique. This is less of an issue with breast MRI due to the larger field of view.

Another potential cause for a false-negative exam is in lesions which are below the resolution of the exam. The contrast resolution of both low- and high-energy images is primarily a function of detector element size. The focal spot size and geometry also contribute. These are all the same as for a standard mammogram, so the spatial resolution for both components of a CEM (and the recombined image) would be expected to be approximately equivalent to FFDM (and better than that of MRI). However, what is more important is the smallest enhancing lesion that one can detect. This is more complex, as one needs to consider the concentration of iodine within the lesion, as well as lesion morphology.

Baldelli et al. [31] showed that a 5 mm spherical void, filled with 5.75 mg/ml of iodine, was visible in phantom studies. Hill et al. [32] considers a 5 mm diameter void filled with 1 mg/ml to be a difficult test for a system. Based on the work of these two investigators, one might expect to see enhancing lesions of approximately 5 mm. However, one might in fact see smaller lesions if there is sufficient contrast uptake and miss larger lesions if there is a lack of contrast uptake. This seems to correlate well with clinical experience—the smallest lesion detected in our own practice has been approximately 5 mm, but a 4 mm lobular tumour confirmed at surgical excision was not evident at CEM [10]. Li et al. [33] reported a smallest lesion size of 4 mm in their study comparing CEM and MRI in 66 breast lesions, as did Jochelson et al. [2] in 52 women with newly diagnosed breast cancer.

6.9 False Positives

Localised increase in vascularity and/or capillary permeability are not specific for malignancy, and various benign lesions can enhance at CEM, just as with MRI. There are also enhancing lesions that are not evident at all on low-energy images. As the PPV of CEM is so high (ranging from 76% [12], to >90% [18, 33, 34]), it is important to biopsy unexplained enhancing lesions.

Badr et al. [35] noted enhancement in 9/27 (33%) benign lesions. Jochelson et al. [2] observed two false-positive findings in 52 cases (3.8%) (although 13 (25%) false-positive findings were observed at MRI), and Lobbes et al. [12] described five false-positive findings in 113 women recalled from screening (4.4%).

A variety of benign lesions can enhance at CEM, including fat necrosis, radial scars and fibroadenomas. False-positive results are important, as not only do they generate additional biopsies (with the potential for complications), they can delay definitive care (in patients already known to have breast cancer) and increase patient anxiety. In a symptomatic patient, additional lesions (that may represent false

positives) can be biopsied at the same visit. If CEM is utilised in a screening setting (e.g. strong family history), then false positives from longstanding lesions such as fibroadenomas are likely to be much less problematic in incident rounds. An enhancing lesion evident at CEM is significantly more likely to be malignant than one seen on MR images [2, 34], so in patients where the alternative screening test is MRI, this should be borne in mind.

Examples of benign enhancing lesions are shown in Figs. 6.2 and 6.4.

6.10 Clarification of Inconclusive Conventional Imaging

Reader confidence is improved by the addition of recombined imaging to standard mammographic views. In the Nottingham series, where five radiologists independently reviewed 100 CEM examinations [10], the addition of the recombined imaging to the low-energy views was rated as a useful or significant aid to diagnosis in 75% of cases. From a clinical perspective, the benefits of CEM include identification/verification of malignancy, ability to size malignancy accurately and reassurance/downgrading in benign cases.

If a potential abnormality has been identified at conventional imaging, but there is diagnostic uncertainty, CEM can be a useful discriminating tool—with the potential to downgrade false positives or verify true malignant lesions. Whilst this may be particularly helpful in screening populations, its value in this regard is equally applicable to incidental findings in symptomatic patients. In Lobbes et al.'s 2014 paper [12], CEM was performed in 113 women recalled from the mammographic screening programme. A retrospective review of the CEM images compared to FFDM was undertaken by two readers. Results showed increases in both sensitivity and specificity—PPV was improved at 76.2% (vs. 39.7%) and NPV to 100% (vs. 97.1%).

6.11 Biopsy of CEM-Detected Lesions

Most lesions identified at CEM are likely to be found at targeted "second-look" ultrasound. Other lesions may be identified on the low-energy images and be candidates for stereotactic biopsy. But what does one do when a lesion is indeterminate or suspicious at CEM and cannot be located with ultrasound or stereotactic biopsy? There is currently no commercially available equipment that combines contrast-enhanced images with biopsy capability. Until biopsy capability is developed, contrast-enhanced MRI provides an alternative method of assessment.[1] Additional information obtained by MRI in the form of enhancement profiles of any visualised lesions may be sufficient to downgrade the level of suspicion. If the lesion remains

[1] Gadolinium-induced signal intensity increase in TW1 MRI is not exactly proportional to the concentration of contrast material that accumulates in a lesion [36]. In iodinated contrast-based imaging (e.g. CT and ostensibly CEM), there is a direct correlation between density measurements (in Hounsfield units) and contrast concentration.

indeterminate, or becomes more suspicious at MRI, then MRI biopsy can be arranged. Although the sensitivity of MRI is exquisite, there are a small number of false negatives. Therefore, if a lesion is deemed highly suspicious at CEM, but not seen on MRI, further investigation is required. This may include an attempt at localization by anatomy on mammography (to facilitate surgery) or 6 months follow-up of CEM.

6.12 The Patient Experience

Patient feedback regarding CEM is generally positive—women who already attend mammographic screening are accustomed to the procedure, and, apart from the injection of contrast, the mammographic experience is identical.

CEM has several advantages compared to MRI. It is potentially more widely available and significantly less expensive. The examination is much quicker to perform and report than a standard MRI—in the author's own practice, CEM is usually "hot-reported," so that second-look ultrasound and biopsy can be performed at the same attendance.

Hobbs et al. [37] compared the patient experience of CEM with that of MRI in patients with breast cancer who had undergone both tests. There was a significantly higher preference for CEM—faster procedure time, greater comfort and lower noise levels were the most common reasons cited. Patients also described significantly lower rates of anxiety during CEM, although comfort of both breast compression and the sensation of IV contrast injection scored significantly worse than for MRI.

The preferences/tolerances of women undergoing screening may differ from those who are known to have breast cancer. These are women who may need to undergo tests on an annual basis, for many years, often during the busiest periods of their lives, in terms of family and career. Phillips et al. [38] surveyed 43 women undergoing both CEM and MRI as part of a larger study assessing performance in the high-risk screening setting. When asked of their preference (assuming both tests had an equal chance of finding breast cancer), 79% of the 38 women responding chose CEM. The length of the screening test was also important to these women—97% indicated that the duration of CEM was about right (neither too long nor too short), whereas only 46% felt that MRI duration was about right—this was statistically significant ($p < 0.0001$). Although 89% reported that they would be comfortable receiving contrast as part of an annual screening test, 100% patients agreed (34.25%) or strongly agreed (65.8%) that they would be willing to accept the small risk of a contrast reaction if the CEM found their breast cancer.

Although patients' concerns regarding the risk of contrast reaction were examined, Phillips et al. [38] did not discuss the specific issue of gadolinium deposition. Gadolinium-based contrast agents have been widely used since the late 1980s to enhance the quality of MRI in a variety of clinical scenarios. These agents are well-tolerated and have an excellent safety profile (in those with normal renal function), with a significantly lower rate of adverse reactions than iodinated contrast. However, it has recently become apparent that gadolinium can be deposited in the bone and

brain tissues, even in individuals with normal renal function [39]. The long-term consequences of this deposition are not known. In 2017, the European Medicines Agency concluded a review, subsequently restricting the use of some linear agents and recommending that *healthcare professionals should use gadolinium contrast agents only when essential diagnostic information cannot be obtained with unenhanced scans, at the lowest dose that provides sufficient enhancement for diagnosis* [40]. In women undergoing annual breast MRI, potentially over many years, this is an important consideration.

Acknowledgements With thanks to:
- Staff and patients of the Nottingham Breast Unit, Nottingham University Hospitals NHS Trust, England.
- David Whitwam, Medical Physics Department, Northampton General Hospital, Northampton, UK.

References

1. Sardanelli F, Fallenberg EM, Clauser P, et al. Mammography: an update of EUSOBI recommendations on information for women. Insights Imaging. 2017;8:11–8.
2. Jochelson MS, Dershaw DD, Sung JS, et al. Bilateral contrast-enhanced dual-energy digital mammography: feasibility and comparison with conventional digital mammography and MR imaging in women with known breast carcinoma. Radiology. 2013;266:743–51.
3. Fallenberg EM, Schmitzberger FF, Amer H, et al. Contrast-enhanced spectral mammography vs. mammography and MRI – clinical performance in a multi-reader evaluation. Eur Radiol. 2017;27:2752–64.
4. Willett AM, Michell MJ, Lee MJR, editors. Best practice guidelines for patients presenting with breast symptoms. London: Department of Health; 2010.
5. Fallenberg EM, Dromain C, Diekmann F, et al. Contrast-enhanced spectral mammography: does mammography provide additional clinical benefits or can some radiation exposure be avoided? Breast Cancer Res Treat. 2014;146:317–81.
6. Francescone MA, Jochelson MS, Dershaw DD, et al. Low energy mammogram obtained in contrast-enhanced digital mammography (CEDM) is comparable to routine full-field digital mammography (FFDM). Eur J Radiol. 2014;83:1350–5.
7. Lalji UC, Jeukens CR, Houben I, et al. Evaluation of low-energy contrast-enhanced spectral mammography images by comparing them to full-field digital mammography using EUREF image quality criteria. Eur Radiol. 2015;25:2813–20.
8. Maxwell AJ, Ridley NT, Rubin G, et al. The Royal College of Radiologists Breast Group breast imaging classification. Clin Radiol. 2009;64:624–7.
9. D'Orsi CJ, Sickles EA, Mendelson EB, et al. ACR BI-RADS Atlas, breast imaging reporting and data system. Reston, VA: American College of Radiology; 2013.
10. Tennant SL, James JJ, Cornford EJ, et al. Contrast-enhanced spectral mammography improves diagnostic accuracy in the symptomatic setting. Clin Radiol. 2016;71:1148–55.
11. European Reference Organisation for Quality Assured Breast Screening and Diagnostic Services. European guidelines for quality assurance in breast cancer screening and diagnosis. 4th ed. Nijmegen: EUREF; 2013. http://www.euref.org/european-guidelines
12. Lobbes MB, Lalji U, Houwers J, et al. Contrast-enhanced spectral mammography in patients referred from the breast cancer screening programme. Eur Radiol. 2014;24:1668–76.
13. Luczyńska E, Heinze-Paluchowska S, Dyczek S, et al. Contrast-enhanced spectral mammography: comparison with conventional mammography and histopathology in 152 women. Korean J Radiol. 2014;15:689–96.

14. Tagliafico AS, Bignotti B, Rossi F, et al. Diagnostic performance of contrast-enhanced spectral mammography: systematic review and meta-analysis. Breast. 2016;28:13–9.
15. Cheung YC, Tsai H, Lo YF, et al. Clinical utility of dual-energy contrast-enhanced spectral mammography for breast microcalcifications without associated mass: a preliminary analysis. Eur Radiol. 2016;26:1082–9.
16. Lalji UC, Houben IP, Prevos R, et al. Contrast-enhanced spectral mammography in recalls from the Dutch breast cancer screening program: validation of results in a large multireader, multicase study. Eur Radiol. 2016;26:4371–9.
17. Łuczyńska E, Heinze-Paluchowska S, Hendrick E, et al. Comparison between breast MRI and contrast-enhanced spectral mammography. Med Sci Monit. 2015;21:1358–67.
18. Tardivel AM, Balleyguier C, Dunant A, et al. Added value of contrast-enhanced spectral mammography in postscreening assessment. Breast J. 2016;22:520–8.
19. Cheung YC, Juan YH, Lin YC, et al. Dual-energy contrast-enhanced spectral mammography: enhancement analysis on BI-RADS 4 non-mass microcalcifications in screened women. PLoS One. 2016;9:e0162740.
20. Kuhl CK, Schrading S, Bieling HB, et al. MRI for diagnosis of pure ductal carcinoma in situ: a prospective observational study. Lancet. 2007;370:485–92.
21. Houben IPL, Vanwetswinkel S, Kalia V et al. Contrast-Enhanced Spectral Mammography in the evaluation of suspicious breast calcifications: diagnostic accuracy and impact on surgical management. Acta Radiol. 2019 Jan 24. https://doi.org/10.1177%2F0284185118822639.
22. University of Birmingham. [Online] https://www.birmingham.ac.uk/research/activity/mds/trials/crctu/trials/loris/index.aspx. Accessed 16 Jul 2018.
23. de Bresser J, de Vos B, van der Ent F, et al. Breast MRI in clinically and mammographically occult breast cancer presenting with an axillary metastasis: a systematic review. Eur J Surg Oncol. 2010;36:114–9.
24. Patel BK, Garza SA, Eversman S, et al. Assessing tumor extent on contrast-enhanced spectral mammography versus full-field digital mammography and ultrasound. Clin Imaging. 2017;46:78–84.
25. Cheung YC, Lin YC, Wan YL, et al. Diagnostic performance of dual-energy contrast-enhanced subtracted mammography in dense breasts compared to mammography alone: interobserver blind-reading analysis. Eur Radiol. 2014;24:2394–403.
26. Sprague BL, Arao RF, Miglioretti DL, et al. National performance benchmarks for modern diagnostic digital mammography: update from the breast cancer surveillance consortium. Radiology. 2017;283:59–69.
27. Carney PA, Miglioretti DL, Yankaskas BC, et al. Individual and combined effects of age, breast density, and hormone replacement therapy use on the accuracy of screening mammography. Ann Intern Med. 2003;138:168–75.
28. Kolb TM, Lichy J, Newhouse JH. Comparison of the performance of screening mammography, physical examination, and breast US and evaluation of factors that influence them: an analysis of 27,825 patient evaluations. Radiology. 2002;225:165–75.
29. National Institute for Health and Care Excellence. Early and locally advanced breast cancer: diagnosis and management. NICE guideline (NG101). London: NICE; 2018. https://www.nice.org.uk/guidance/ng101
30. Mori M, Akashi-Tanaka S, Suzuki S, et al. Diagnostic accuracy of contrast-enhanced spectral mammography in comparison to conventional full-field digital mammography in a population of women with dense breasts. Breast Cancer. 2017;24:104–10.
31. Baldelli P, Bravin A, Di Maggio C, et al. Evaluation of the minimum iodine concentration for contrast-enhanced subtraction mammography. Phys Med Biol. 2006;51:4233–51.
32. Hill ML, Bloomquist AK, Shen SZ, et al. Contrast-enhanced digital mammography lesion morphology and a phantom for performance evaluation. In: Hara T, Muramatsu C, Fujita H, editors. International workshop on digital breast imaging. New York, NY: Springer; 2014.
33. Li L, Roth R, Germaine P, et al. Contrast-enhanced spectral mammography (CESM) versus breast magnetic resonance imaging (MRI): a retrospective comparison in 66 breast lesions. Diagn Interv Imaging. 2017;98:113–23.

34. Lee-Felker SA, Tekchandani L, Thomas M, et al. Newly diagnosed breast cancer: comparison of contrast-enhanced spectral mammography and breast MR imaging in the evaluation of extent of disease. Radiology. 2017;285:389–400.
35. Badr S, Laurent N, Régis C, et al. Dual-energy contrast-enhanced digital mammography in routine clinical practice in 2013. Diagn Interv Imaging. 2014;95:245–58.
36. Kuhl CK. Dynamic breast magnetic resonance imaging. Breast MRI. New York, NY: Springer; 2005. p. 79–139.
37. Hobbs MM, Taylor DB, Buzynski S, et al. Contrast-enhanced spectral mammography (CESM) and contrast enhanced MRI (CEMRI): patient preferences and tolerance. J Med Imaging Radiat Oncol. 2015;59:300–5.
38. Phillips J, Miller MM, Mehta TS, et al. Contrast-enhanced spectral mammography (CESM) versus MRI in the high-risk screening setting: patient preferences and attitudes. Clin Imaging. 2017;42:193–7.
39. Layne KA, Dargan PI, Archer JRH, et al. Gadolinium deposition and the potential for toxicological sequelae – a literature review of issues surrounding gadolinium-based contrast agents. Br J Clin Pharmacol. 2018;84(11):2522–34.
40. European Medicines Agency. http://www.ema.europa.eu/ema/index.jsp?curl=pages/medicines/human/referrals/Gadolinium-containing_contrast_agents/human_referral_prac_000056.jsp&mid=WC0b01ac05805c516f. [Online].

7 Use of Contrast-Enhanced Mammography in Breast Cancer Screening

Maxine S. Jochelson

7.1 Introduction

Breast cancer is the leading cause of cancer death among women throughout the world. Breast cancer survival has improved, in part because of a wide variety of new and improved treatments. However, it remains clear that even with these superior treatments, outcomes are better in women with smaller, node-negative cancers and the detection of these smaller cancers is the result of breast cancer screening.

Screening mammography and physical examination remain the mainstay of breast cancer screening programs. Multiple randomized studies have demonstrated that screening mammography reduces breast cancer mortality by approximately 30% [1–4]. However, mammography has its limitations. The sensitivity of mammography overall is 70–85%, but this drops significantly in high-risk women with dense breasts in whom it is no higher than 50% [5, 6]. Specificity of mammography is approximately 89% [7]. Women are frequently called back for additional imaging after they have had their screening mammogram which leads to additional radiation, cost, and patient anxiety. Call backs may occur in up to 20% of women at baseline mammogram [8] and slightly less frequently on subsequent examinations. Biopsies are also frequently recommended after screening with a positive predictive value (PPV) of only approximately 28.6% [7]. Additionally, some believe there is a great deal of "overdiagnosis" by screening mammography.

These limitations are frequently cited as a reason to decrease or avoid screening altogether [9, 10]. With these limitations, improved imaging techniques are needed, both to detect a greater number of cancers when screening and decrease the number of women called back from screening and the number of benign biopsies. As was so aptly stated by Oeffinger et al. at the publication of the most recent American Cancer Society Guidelines, "Given the weight of the evidence that mammography

M. S. Jochelson (✉)
Department of Radiology, Memorial Sloan Kettering Cancer Center, New York, NY, USA
e-mail: jochelsm@mskcc.org

M. Lobbes, M. S. Jochelson (eds.), *Contrast-Enhanced Mammography*,
https://doi.org/10.1007/978-3-030-11063-5_7

screening is associated with a significant reduction in the risk of dying from breast cancer after age 40 year, a more productive discussion would be focused on how to improve the performance of mammographic screening" [11].

To elaborate on Dr. Oeffinger's apt statement, this chapter will discuss various options for improved screening with a focus on contrast-enhanced mammography (CEM). The ideal new or supplemental screening examination needs to improve cancer detection, reduce recall rates, improve the PPV of recommended biopsies, be inexpensive, be widely available, and not add significant radiation.

7.2 Improved Screening: Purely Anatomic Techniques

7.2.1 Digital Breast Tomosynthesis

Digital breast tomosynthesis (DBT), while used occasionally as a supplemental imaging tool, is increasingly being used as a primary screening examination. It uses multiple low-dose projections of the compressed breast obtained with a moveable X-ray source—essentially like a computed tomography scan of the breast. The image slices are reconstructed in a plane parallel to the detector. Using DBT allows overlying breast tissue to be peeled away, enabling easier detection of primarily soft tissue lesions. This leads to an improvement in detection rates over full-field digital mammography (FFDM), sometimes also detecting additional lesions over those seen on FFDM. While DBT is sometimes incorrectly referred to as 3D imaging, it does lead to better lesion localization. Margin analysis is also improved with DBT. Using DBT through an area of a suspected mass may also clarify that the apparent mass is merely overlapping breast tissue. The latter two improvements over FFDM improve specificity and reduce the number of patients called back. PPV is also improved as a result.

Every study comparing the use of DBT to routine mammography has demonstrated slight improvement in cancer detection in addition to a reduction in the rate of call backs. DBT allows detection of approximately 1.5 additional cancers per 1000 women over FFDM: Skaane et al. performed a prospective trial involving nearly 13,000 women and demonstrated that adding DBT to FFDM improved cancer detection rates from 6.1/1000 to 8.0/1000 examinations with a 15% decrease in false-positive findings. The additional cancers detected were invasive cancers [12]. In a multicenter retrospective study that included both academic and private practices, Friedenwald et al. also showed a similar improvement in detection rate from 4.2/1000 to 5.4/1000 examinations and signwificant decrease in recall rates [13]. Improvement in cancer detection with DBT has been demonstrated with all breast densities except in the 10% of women with extremely dense breasts. Kim et al. found that DBT compared favorably to screening ultrasound except in women with extremely dense breasts [14].

While the slight increase in detection rate is certainly an advantage, the real advantage of DBT is in the reduction of call backs. Rafferty et al. demonstrated that

using DBT + FFDM significantly reduced call back rates in patients with nonmalignant findings without a significant change in those women subsequently found to have cancer [15]. McDonald et al. evaluated 25,000 women having baseline mammography and showed a significant reduction in call back rates from 20.5% to 16.0% [8].

In the United States, DBT is increasingly replacing FFDM as a primary screening modality because of the combination of improved detection and decreased call back rates. In countries where call backs are less frequent, DBT may not be used as much. Its limitations include high costs, increased need for data storage, and significant increase in reading time. Since 2D images remain important for an overview of the breast, doing DBT and FFDM doubles the radiation dose to the breast. Vendors have developed synthetic views to replace the FFDM which will lower the radiation dose of DBT back to that of a FFDM alone, but synthetic view software carries a high additional cost. Additionally, DBT does not improve breast cancer detection in women with extremely dense breasts, a population who are at particularly higher risk of developing cancer [16] and in whom cancers are masked and therefore missed on mammography.

7.2.2 Screening Whole-Breast Ultrasound

The most commonly used method of supplemental breast imaging, particularly in women with dense breasts, is screening whole-breast ultrasound. It is relatively inexpensive, does not expose the patient to additional radiation, and is widely available. Multiple investigators have demonstrated additional detection rates of approximately 3.5 cancers/1000 women [17–19]. The cancers detected are more frequently early-stage invasive cancers and therefore less likely to be considered "overdiagnosis." While there is no arguing that this additional detection is a substantial improvement, ultrasound also has its limitations. The ACRIN 6666 trial was a prospective trial to evaluate the utility of ultrasound screening in a population of 2637 women with normal mammograms, dense breasts, and at least one other risk factor. In the process of detecting the additional cancers, 8% of the women received a biopsy recommendation, and only 7.4% of those biopsies were malignant. An additional 9% of women were recommended to return for 6-month follow-up examinations. In the J-START study involving 72,998 Japanese women from 40 to 49 years old, ultrasound added to mammography improved the sensitivity of mammography alone but decreased its specificity significantly [20]. It should be noted that in patients who are screened for several years, there are fewer unnecessary biopsies with an improvement of PPV from approximately 7% to 20% [21].

This lack of specificity of screening whole-breast ultrasound defeats one of the main purposes of supplemental screening, i.e., to reduce call backs, and adds to the cost of ultrasound screening. With the increasing use of screening ultrasound in women with dense breasts, two studies determined that due to the large number of additional biopsies, the cost of detecting one cancer was $50,000–60,000.00 [19, 22].

Interim results of a prospective trial (ASTOUND trial) comparing DBT with screening ultrasound were performed in 3231 women with dense breasts and negative FFDM. Twenty-four additional cancers were detected; 13/24 (54%) were detected by DBT corresponding to 4/1000 screens. Ultrasound detected 23/24 (96%) or 7.1/1000 screens [23]. Kim et al. compared the performance of these two examinations in a population of 698 women with dense breasts who had 140 cancers. They demonstrated comparable performance of the two except in women with extremely dense breasts in whom DBT was inferior [14].

However, additional results from the ACRIN trial follow-up demonstrate further limitations of supplemental imaging with whole-breast screening ultrasound. At the end of the trial, 612 women who had had three rounds of negative screening mammography and ultrasound were offered a screening MRI. There were 16 cancers detected, 9 of which (56%) were seen only on MRI. MRI added 14.7 additional cancers per 1000 women screened; 75% of these cancers were invasive [24]. Kuhl et al. demonstrated similar findings with the EVA trial [25]. These latter studies suggest that performing only purely anatomic studies such as FFDM, DBT, and ultrasound remains limited for cancer detection and in fact negative examinations may give women a false sense of security when they receive negative results.

7.3 Imaging of Neovascularity

7.3.1 Contrast-Enhanced Breast MRI

Breast MRI has long been acknowledged to be the most sensitive screening examination for the detection of breast cancer. By using contrast to enhance tumor neovascularity, the sensitivity of MRI approaches 97%, sometimes detecting early cancers before a discrete mass can be detected. Specificity was initially poor but over the years has improved to be comparable to that of mammography. Because of the high sensitivity of MRI, in 2007 the American Cancer Society provided guidelines for the annual use of breast MRI for women who are at greater than 20% lifetime risk for development of breast cancer. As a result, not only has it been shown that cancers detected by MRI in the patient population are smaller and less likely to be node positive [26], but there is also a survival benefit in mutation carriers who are screened with annual MRI [27, 28].

In a review of 18,064 screening MRIs and mammography in 7519 women at high risk for developing breast cancer, Sung et al. demonstrated that cancers detected by MRI are more likely to be invasive cancers, whereas those detected by mammography are more likely to be ductal carcinomas in situ. Additionally, they showed that interval cancers which account for more than 20% of all breast cancers are reduced to 5% with screening MRI [29].

With these superb results with screening MRI, it would be ideal to offer MRI to a larger population of women or even all women. There is a large population of women at intermediate risk for developing breast cancer (15–20% lifetime risk) including in the United States alone over three million breast cancer survivors and approximately 15,000 women with high-risk lesions and 25 million women with

dense breasts. However, the cost of this would be prohibitive, and it is not realistic to think there is enough availability of MRI to accommodate these women.

Abridged (or abbreviated) MRI is a technique that has been proposed to lower costs and increase available time on MRI scanners by reducing the number of sequences performed. This technique was first performed by Kuhl et al. who prospectively evaluated results of screening MRI with only three sequences which would take 3 min to perform compared with their routine 17 min for 606 screening MRIs in 443 women at intermediate or slightly increased risk for developing breast cancer. Reading the full number of sequences required 28 s per examination and yielded a sensitivity of 100% and specificity of 94.3%. Reading a single maximum intensity projection image required 2.8 s with a sensitivity of 90.9% with a negative predictive value of 99.8% [30]. Mango et al. retrospectively reviewed three sequences from a complete MRI in 100 women with known breast cancer to include the first post-contrast, subtraction, and maximum intensity projection images. Over 95% of the cancers were visualized on a single (first post-contrast) image when read without prior examinations or history. Once prior examinations and history were available, the sensitivity of these abridged examinations was 100% [31]. Harvey et al. reviewed both abbreviated and full MRI protocols in 568 women and demonstrated no difference in cancer detection, while the abbreviated protocol reduced scan times by 18.8 min per examination and interpretation times by 4.9 min per interpretation [32]. Van Zelst et al. also demonstrated non-inferiority of MRI scans performed in 2 min compared with full diagnostic MRI scans [33].

The premise of abbreviated MRI has been so well accepted that there is currently an ECOG-ACRIN trial comparing it with DBT where the primary goal is to compare invasive cancer detection rates between the two techniques and secondary goals are to compare tumor biology, PPV of biopsies, call back rates and short-term follow-up rates, and interval cancer rates and to undertake a comparative cost analysis.

However, despite the promise of abbreviated MRI, it is still not likely that we can accommodate such large populations of women for breast MRI. Additionally, women who are claustrophobic and have certain metallic implants or allergy to gadolinium are unable to undergo MRI.

The success of MRI for the detection of early breast cancers is large because of its ability to image the neovascularity associated with most invasive breast cancers. Contrast-enhanced mammography (CEM) is a relatively new technique which was developed to utilize enhancement of neovascularity in a fashion like MRI for the earlier detection of breast cancer using an upgraded platform of digital mammography. The remainder of this chapter will focus on CEM and its potential for use in the screening setting.

7.3.2 Contrast-Enhanced Mammography

As has been described previously, CEM is performed after bolus injection of iodinated contrast material at a dose of 1.5 ml/kg. Imaging begins approximately 2.5–3 min after the injection is complete. Standard craniocaudal and mediolateral oblique views

are obtained within 5 min, and additional views can also be obtained since the contrast remains present for up to 10 min. Two nearly simultaneous images are performed with each exposure: a low-energy image below the *k*-edge of iodine (33 keV) and a high-energy image above the *k*-edge of iodine. Post-processing subtracts out non-enhancing tissue, yielding an image of any enhancing lesions. Since there is only one image done per view, kinetic information is not obtained. The low-energy images are the equivalent of a routine mammogram [34–36]. The radiation dose is of course increased with CEM, with the range of increase quoted between 20% and 80% depending on the breast thickness and vendors [37, 38]. Nevertheless, even with the additional radiation, the dose falls within the Mammography Quality Standards Act guidelines.

The report of a CEM combines the results of the low-energy images with the post-contrast images to provide a single Breast Imaging Reporting and Data System (BI-RADS) classification. Early experience utilizing CEM has been in the diagnostic setting where it has consistently been shown to be superior to digital mammography. In patients called back from abnormal screening mammography or in patients with clinical symptoms, Dromain et al. evaluated 120 women with unilateral CEM and demonstrated significantly improved sensitivity: 93% for CEM compared with 78% for FFDM and a trend toward improved sensitivity when compared with FFDM plus ultrasound [39]. In a similar population of 113 women called back from screening, Lobbes et al. showed sensitivity of 100% vs. 96.9% (all patients had mammographic abnormalities to begin with) and significantly improved specificity and PPV with CEM compared with FFDM [40].

In 52 women with known cancers, Jochelson et al. demonstrated significant superiority of CEM compared with FFDM in the detection of the index lesion (96% vs. 81%) and similar detection compared to MRI [41]. Fallenberg et al. did a similar comparison of these three techniques in 80 women with breast cancer and demonstrated significantly better sensitivity of CEM compared with mammography. They also found that of the 14 patients whose cancers were not detected on FFDM, ten women had extremely dense breasts and three had heterogeneously dense breasts [42].

CEM has been shown to be superior to FFDM in women with dense breasts (Fig. 7.1) in multiple other studies. In a multireader trial using temporal technique to perform contrast mammography in 70 women with dense breasts and at least 1 suspicious lesion on mammography, Diekmann et al. showed sensitivity improving from 35% to 59% [43]. In Taiwan, Cheung et al. prospectively evaluated CEM compared with FFDM in 89 women with 100 lesions and dense breasts. The low-energy images were read blinded to the post-contrast images. Sensitivity improved from 71.5% to 92.7%, and specificity improved from 51.8% to 67.9% with the use of contrast [44].

Cheung et al. also showed that the one area in which CEM was not as reliable was in women presenting with suspicious microcalcifications. They reported results in 59 women with suspicious calcifications in whom the negative predictive value of contrast mammography was only 93.9% which is comparable to MRI in the same setting [45] (Fig. 7.2).

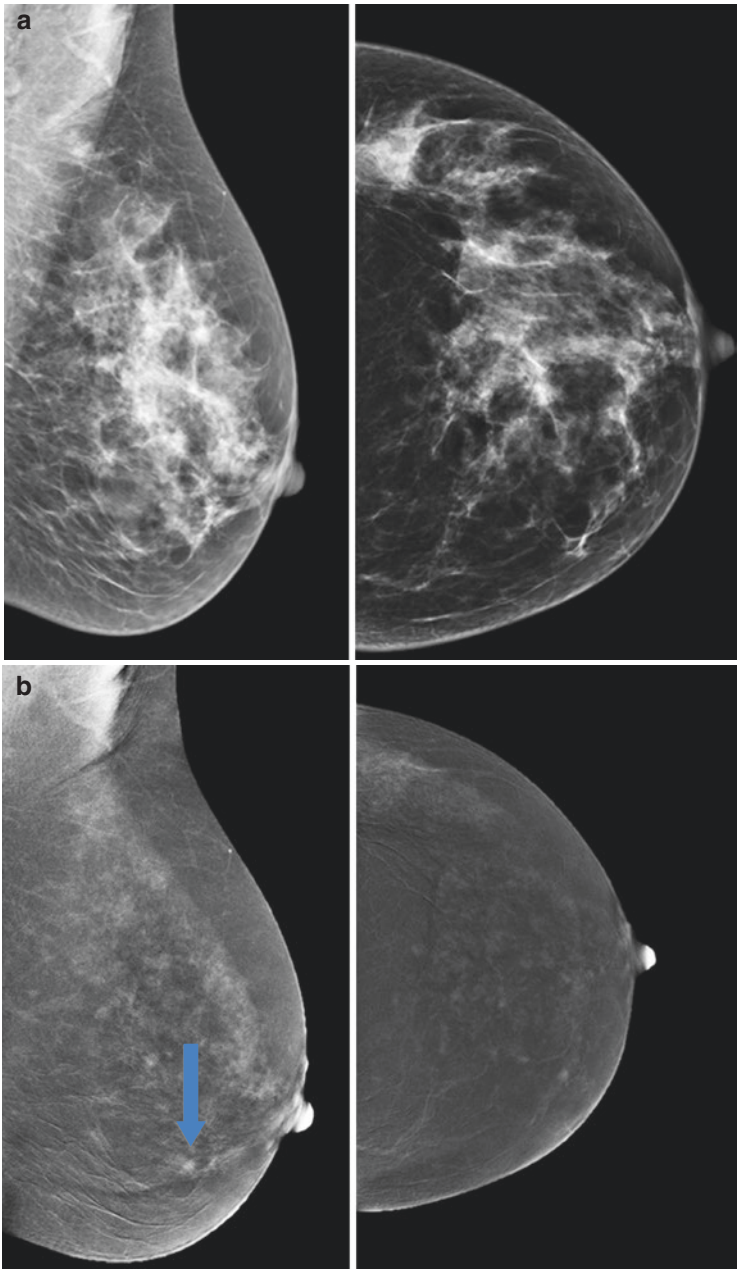

Fig. 7.1 A 62-year-old woman with a family history of breast cancer and dense breasts. (**a**) Low-energy images of the left breast demonstrate no suspicious abnormalities. (**b**) Post-contrast images demonstrate a 5 mm irregular mass in the lower inner quadrant of the left breast. (**c**) Targeted ultrasound demonstrates 5 mm mass left breast corresponding to CEM finding. Biopsy demonstrated infiltrating ductal carcinoma

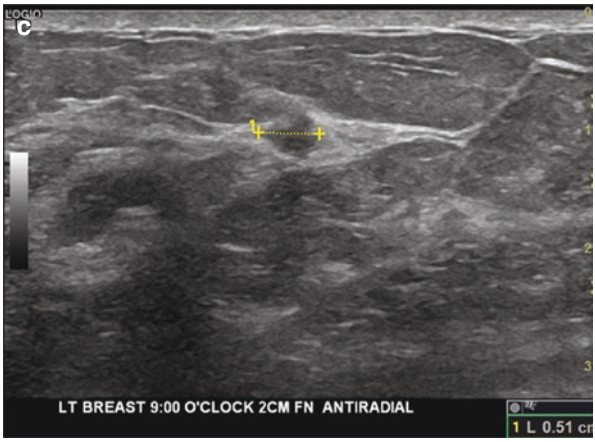

Fig. 7.1 (continued)

Considering the success of CEM in the diagnostic setting, it appears that it could have potential to improve cancer detection in the screening setting, potentially filling the need for better supplemental imaging for those patients at increased risk for breast cancer who do not meet the American Cancer Society criteria for annual breast MRI. This concept has been met with some resistance primarily due to fear of contrast reactions in healthy women. Therefore, only a small number of papers have been published on this topic.

Jochelson et al. performed the first prospective trial comparing CEM with FFDM and screening MRI in women at increased risk for developing breast cancer. Three hundred and seven heavily prescreened patients with increased breast cancer risk underwent CEM and MRI within 30 days of each other. No cancers were detected by FFDM (the low-energy images). MRI and CEM each detected two invasive lobular cancers. One patient had a sub-centimeter area of enhancement on MRI not seen on CEM which was upgraded to DCIS when she returned 9 months later with a new contralateral invasive cancer as well. At 1-year follow-up, there were no interval cancers but two screen-detected cancers. Specificity of CEM was equal to that of MRI. However, the patients had all had multiple prior MRIs, while only one patient had a prior CEM. It is well known that having prior examinations for comparison improves specificity. Therefore, it is expected that CEM will ultimately be more specific than MRI [46] as was demonstrated in earlier diagnostic trials [40, 41] (Fig. 7.3).

After this study, CEM has been used routinely in women at increased risk due to either family history with lifetime risk under 20% or personal history especially in women with dense breasts (Fig. 7.4); women with a history of high-risk lesions diagnosed at biopsy (Fig. 7.5); women receiving high-risk screening with yearly MRI as the alternating mammographic study; and women who cannot undergo MRI due to severe claustrophobia, gadolinium allergy, or metallic implants. There are

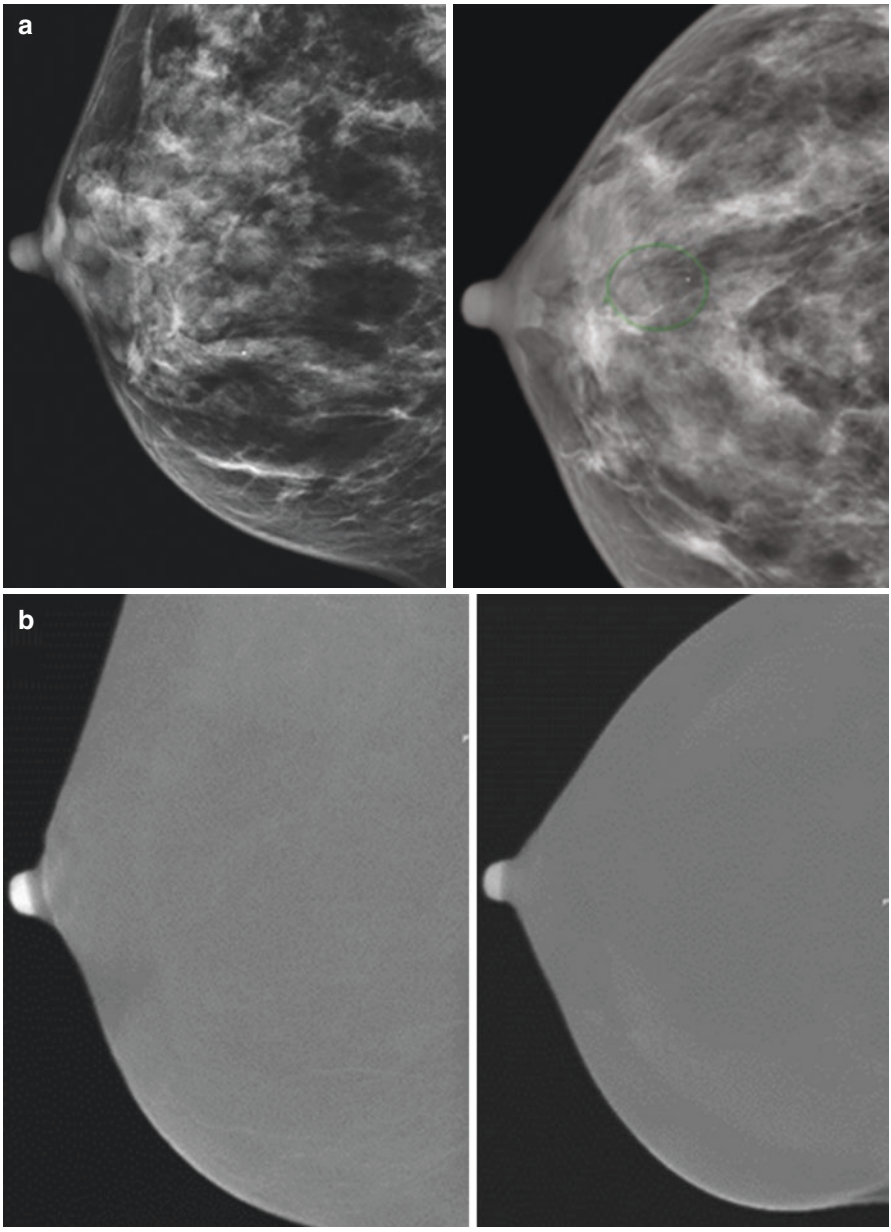

Fig. 7.2 False-negative CEM. A 51-year-old woman with a family history of breast cancer and dense breasts for screening. (**a**) Low-energy images demonstrate a new 0.9 cm group of pleomorphic calcifications, suspicious for malignancy. (**b**) Contrast images demonstrate minimal background parenchymal enhancement. No abnormal enhancement was seen in the area of microcalcifications or elsewhere. Calcifications were biopsied and yielded intermediate-grade ductal carcinoma in situ with necrosis

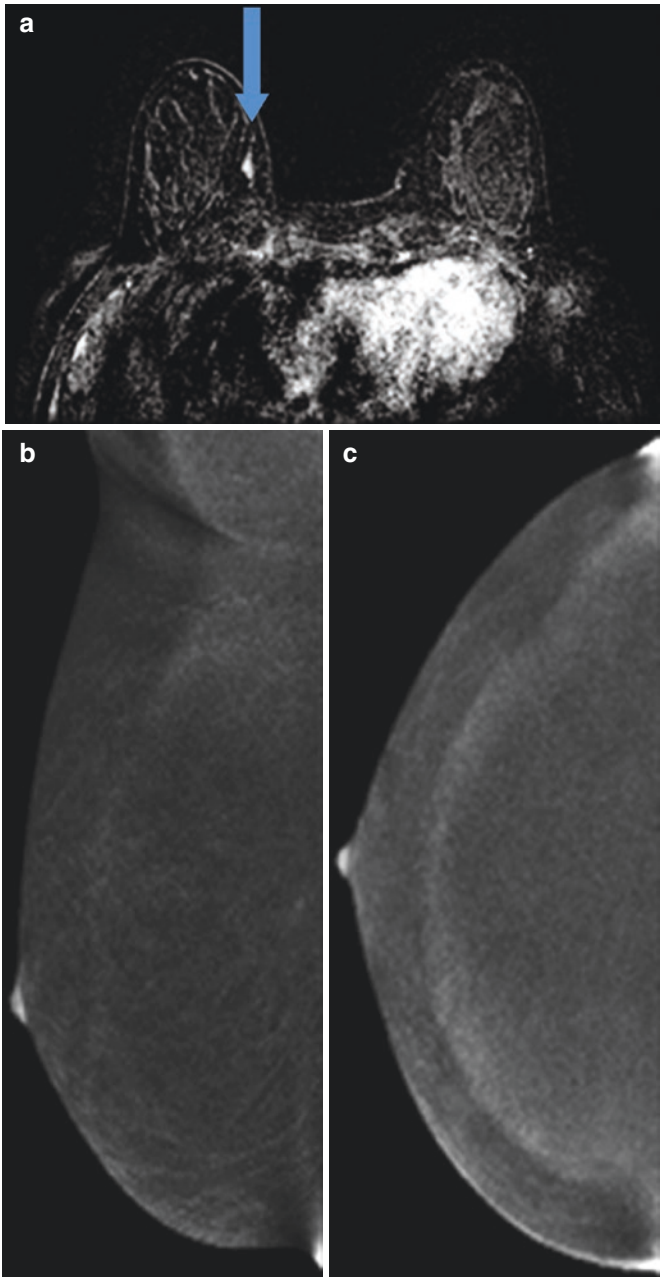

Fig. 7.3 False-positive MRI/true negative CEM. A 28-year-old with a strong family history of breast cancer and dense breasts. (**a**) Axial subtraction images from MRI demonstrate 1.2 cm area of linear non-mass enhancement in the lower inner quadrant. (**b**, **c**) Contrast-enhanced mammography shows mild background parenchymal enhancement with no suspicious enhancement. MRI-guided biopsy yielded stromal fibrosis and fibroadenomatoid changes with no evidence for malignancy

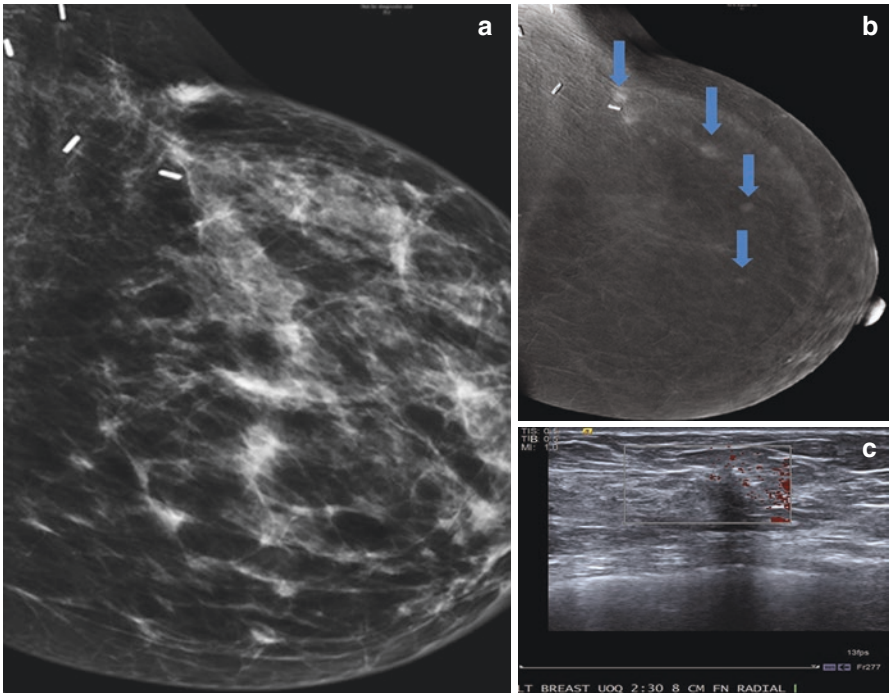

Fig. 7.4 A 45-year-old woman 1 year after lumpectomy with clear margins, radiation therapy, and 1 year of tamoxifen for routine follow-up: (**a**) heterogeneously dense breast showing post-lumpectomy change but no other abnormality. (**b**) Multiple enhancing masses at the lumpectomy site and extending toward the nipple. (**c**) Targeted ultrasound of a representative mass demonstrating an irregular hypoechoic lesion. Biopsy demonstrated infiltrating ductal carcinoma

also a growing number of patients who are concerned about gadolinium deposits in the brain who are choosing not to undergo MRI and are therefore having CEM.

Sung et al. have prospectively compared CEM with whole-breast screening ultrasound. Preliminary results are available in 250 intermediate-risk patients. Five cancers were detected: one by FFDM, two on ultrasound, and five on CEM [47]. If these early results hold, CEM may be more sensitive than whole-breast ultrasound in the screening setting (Fig. 7.6). Klang et al. have reported their experience comparing CEM to ultrasound in a retrospective study of 953 women who underwent 87 biopsies, 43% of which were malignant. CEM sensitivity was 97% compared to 92% for ultrasound. CEM specificity was 40% compared to 8% for ultrasound [48].

Sumkin et al. compared MRI with CEM and molecular breast imaging in 79 women with 80 breast cancers. They demonstrated that while MRI was slightly more sensitive than CEM, MRI had significantly more false positives [49]. It should be noted that at this time, MBI does not meet the American College of Radiology appropriateness criteria for breast cancer screening due to its high total body radiation dose.

In a retrospective review of screening CEM compared with FFDM, Sung et al reported the results of 904 screening contrast mammograms, 77% in women with dense breasts and over 90% had other risk factors including family history or personal history of breast cancer. Fourteen cancers were detected corresponding to a

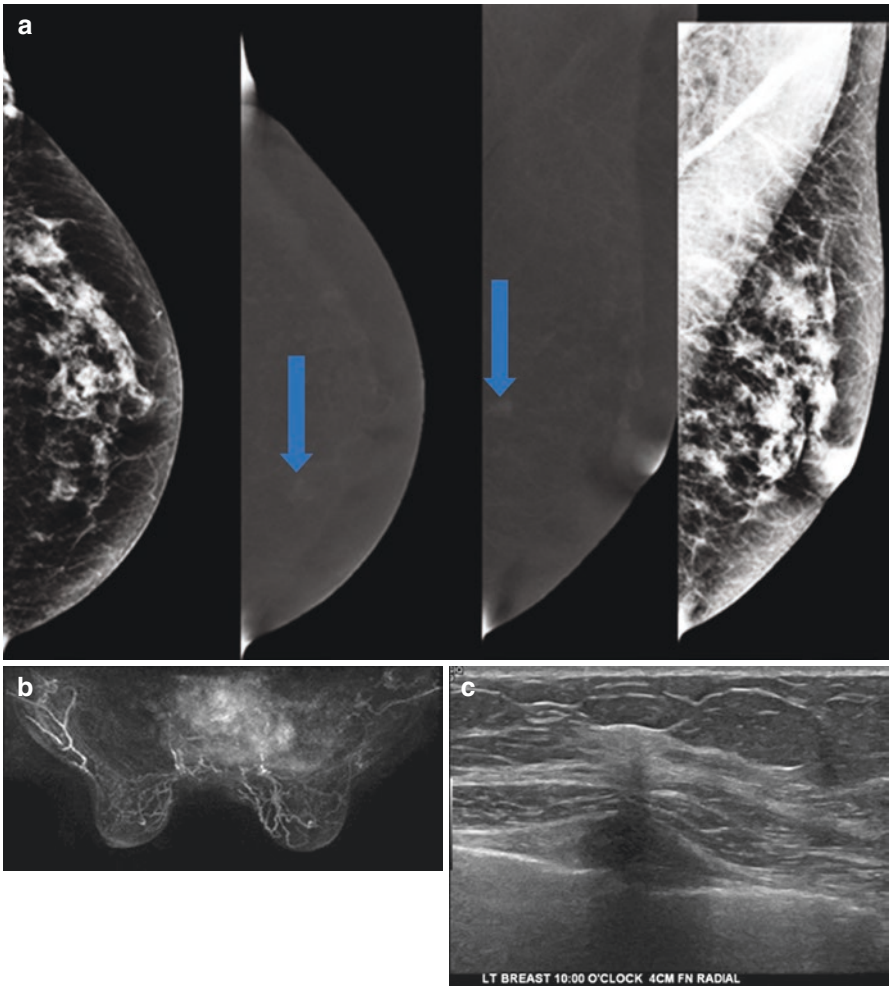

Fig. 7.5 A 61-year-old woman with a history of lobular carcinoma in situ for screening. False-negative MRI (**a**) Left low-energy and contrast images in the mediolateral oblique and craniocaudal projections show heterogeneously dense breast tissue and no abnormalities on the low-energy images. Post-contrast images demonstrate an area of non-mass enhancement in the upper inner breast posterior third. (**b**) Axial subtraction MIP MRI images demonstrated no abnormality. (**c**) Targeted ultrasound was performed and detected a 4 mm hypoechoic mass with posterior shadowing. Ultrasound-guided biopsy yielded invasive lobular carcinoma. (**d**) Post-biopsy mammogram demonstrates a ribbon-shaped marker corresponding to the area of non-mass enhancement

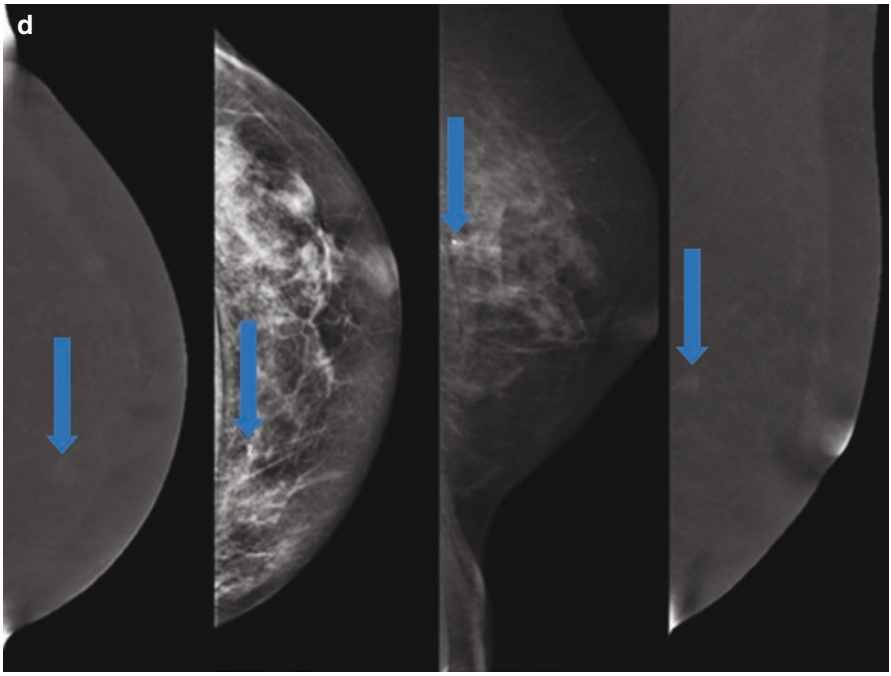

Fig. 7.5 (continued)

cancer detection rate of 15/1000 examinations. Six of the 14 (43%) cancers were detected due to contrast enhancement alone (in review).

Chou et al. performed a study comparing vascular with nonvascular imaging in 185 women with BI-RADS 4 or 5 lesions. In this population there were 81 cancers and 144 benign lesions. Not surprisingly, MRI, contrast mammography, and contrast tomosynthesis were more sensitive than FFDM or non-contrast DBT. The authors found no significant difference between MRI, CEM, and contrast tomosynthesis. Specifically, contrast tomosynthesis was no better than CEM without DBT [50].

CEM is well tolerated by patients. Hobbs et al. interviewed 49 women regarding their preference of CEM compared with MRI. These women significantly preferred CEM because it was faster and more comfortable and there was less noise ($p < 0.001$) [51]. In a prospective screening trial, Phillips et al. reported that 79% of women preferred contrast mammography to MRI if the examinations had equal sensitivity [52].

There are several limitations to the use of CEM. Probably the most significant limitation to adoption of CEM for screening is fear of contrast reaction. As with CT scanning, a small percentage of patients may have contrast reactions, generally mild, but there is the potential for a life-threatening reaction. In the screening study by Jochelson et al., 1.3% of patients had predominantly mild reactions after contrast administration. One woman who had had a reaction to gadolinium the day before had a moderate reaction but did well [46]. Houben et al. reported five minor reactions when performing 839 CEM examinations (0.6%) for patients recalled from

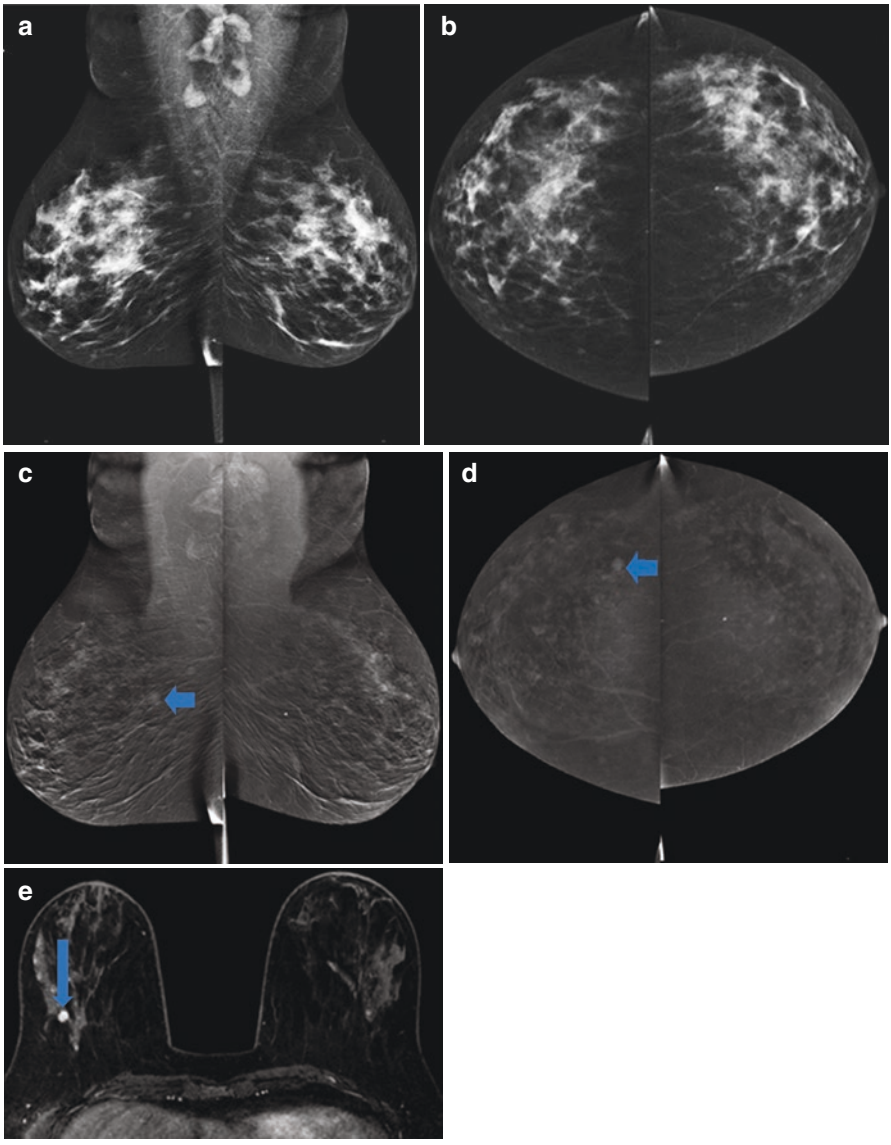

Fig. 7.6 A 55-year-old woman undergoing screening. History of lobular carcinoma in situ. False-negative ultrasound. (**a**, **b**). Bilateral mediolateral oblique and craniocaudal views demonstrate heterogeneously dense breast tissue with no abnormalities. (**c**, **d**). Subtraction images show mild background parenchymal enhancement and a small enhancing mass (arrows) in the upper outer quadrant of the right breast posteriorly. This could not be seen on ultrasound. (**e**) Axial post-contrast MRI demonstrates 1.5 cm enhancing mass (arrow) corresponding to CEM finding. MRI-guided biopsy yielded invasive ductal carcinoma

screening [53]. It is critical to carefully screen patients for any contrast allergy history. It is our practice to exclude any woman with any history of reaction to iodine from screening with CEM. Even though type A reactions officially do not require premedication or avoidance of contrast administration, it is our belief that due to the idiosyncratic nature of contrast reactions, it is not worth taking a chance when there are alternative methods of screening.

The potential for renal toxicity is another minor concern when doing CEM. Iodine is rarely toxic in the setting of normal renal function. Nevertheless, in older women or women with diabetes, multiple myeloma, or other risks for renal injury, renal function must be assessed before administering iodinated contrast. Again, if there are any abnormalities, contrast should not be used.

Radiation dose is increased when performing CEM. While use of as little radiation as possible is the goal, the limited additional dose is less than that of FFDM plus DBT and falls well within the Mammography Quality Standards Act guidelines.

7.4 Conclusions

Preliminary data for the use of CEM in the screening setting are promising. From both studies of its use in the diagnostic setting and early screening studies, it is quite clear that CEM is more sensitive and specific than mammography alone, probably more sensitive than mammography and ultrasound, and more specific than mammography plus ultrasound. CEM approaches the sensitivity of breast MRI and is likely more specific. However, the total number of patients studied in the screening setting thus far is small and performed as single-institution studies. What is needed now are prospective multicenter trials which will compare sensitivity, specificity, PPV, negative predictive value, and accuracy of CEM with that of standard screening studies such as FFDM, DBT, whole-breast screening ultrasound, combinations of FFDM or DBT with screening ultrasound, and breast MRI (complete or abbreviated). Additionally, since mammography is currently the only examination which has been demonstrated to reduce breast cancer mortality, as with all potential screening studies, it is critical to evaluate not only improvement in sensitivity but also if that improvement in sensitivity translates into decreased number of interval cancers and increases mortality reduction over that of mammography.

References

1. Tabar L, Fagerberg CJ, Gad A, Baldetorp L, Holmberg LH, Grontoft O, et al. Reduction in mortality from breast cancer after mass screening with mammography. Randomised trial from the Breast Cancer Screening Working Group of the Swedish National Board of Health and Welfare. Lancet. 1985;1(8433):829–32.
2. Andersson I, Aspegren K, Janzon L, Landberg T, Lindholm K, Linell F, et al. Mammographic screening and mortality from breast cancer: the Malmo mammographic screening trial. BMJ. 1988;297(6654):943–8.
3. Shapiro S. Screening: assessment of current studies. Cancer. 1994;74(1 Suppl):231–8.

4. Siu AL, U.S. Preventive Services Task Force. Screening for breast cancer: U.S. Preventive Services Task Force recommendation statement. Ann Intern Med. 2016;164(4):279–96.
5. Buist DS, Porter PL, Lehman C, Taplin SH, White E. Factors contributing to mammography failure in women aged 40–49 years. J Natl Cancer Inst. 2004;96(19):1432–40.
6. Carney PA, Miglioretti DL, Yankaskas BC, Kerlikowske K, Rosenberg R, Rutter CM, et al. Individual and combined effects of age, breast density, and hormone replacement therapy use on the accuracy of screening mammography. Ann Intern Med. 2003;138(3):168–75.
7. Lehman CD, Arao RF, Sprague BL, Lee JM, Buist DS, Kerlikowske K, et al. National performance benchmarks for modern screening digital mammography: update from the breast cancer surveillance consortium. Radiology. 2017;283(1):49–58.
8. McDonald ES, McCarthy AM, Akhtar AL, Synnestvedt MB, Schnall M, Conant EF. Baseline screening mammography: performance of full-field digital mammography versus digital breast tomosynthesis. AJR Am J Roentgenol. 2015;205(5):1143–8.
9. Siu AL, U.S. Preventive Services Task Force. Screening for breast cancer: U.S. Preventive Services Task Force recommendation statement. Ann Intern Med. 2009;151(10):716–26. W-236.
10. Welch HG, Black WC. Overdiagnosis in cancer. J Natl Cancer Inst. 2010;102(9):605–13.
11. Oeffinger KC, Fontham ET, Etzioni R, Herzig A, Michaelson JS, Shih YC, et al. Breast cancer screening for women at average risk: 2015 guideline update from the American Cancer Society. JAMA. 2015;314(15):1599–614.
12. Skaane P, Bandos AI, Gullien R, Eben EB, Ekseth U, Haakenaasen U, et al. Comparison of digital mammography alone and digital mammography plus tomosynthesis in a population-based screening program. Radiology. 2013;267(1):47–56.
13. Friedewald SM, Rafferty EA, Rose SL, Durand MA, Plecha DM, Greenberg JS, et al. Breast cancer screening using tomosynthesis in combination with digital mammography. JAMA. 2014;311(24):2499–507.
14. Kim WH, Chang JM, Lee J, Chu AJ, Seo M, Gweon HM, et al. Diagnostic performance of tomosynthesis and breast ultrasonography in women with dense breasts: a prospective comparison study. Breast Cancer Res Treat. 2017;162(1):85–94.
15. Rafferty EA, Park JM, Philpotts LE, Poplack SP, Sumkin JH, Halpern EF, et al. Assessing radiologist performance using combined digital mammography and breast tomosynthesis compared with digital mammography alone: results of a multicenter, multireader trial. Radiology. 2013;266(1):104–13.
16. Boyd NF, Guo H, Martin LJ, Sun L, Stone J, Fishell E, et al. Mammographic density and the risk and detection of breast cancer. N Engl J Med. 2007;356(3):227–36.
17. Kolb TM, Lichy J, Newhouse JH. Occult cancer in women with dense breasts: detection with screening US—diagnostic yield and tumor characteristics. Radiology. 1998;207(1):191–9.
18. Berg WA, Blume JD, Cormack JB, Mendelson EB, Lehrer D, Bohm-Velez M, et al. Combined screening with ultrasound and mammography vs mammography alone in women at elevated risk of breast cancer. JAMA. 2008;299(18):2151–63.
19. Weigert J, Steenbergen S. The connecticut experiment: the role of ultrasound in the screening of women with dense breasts. Breast J. 2012;18(6):517–22.
20. Ohuchi N, Suzuki A, Sobue T, Kawai M, Yamamoto S, Zheng YF, et al. Sensitivity and specificity of mammography and adjunctive ultrasonography to screen for breast cancer in the Japan Strategic Anti-cancer Randomized Trial (J-START): a randomised controlled trial. Lancet. 2016;387(10016):341–8.
21. Weigert JM. The Connecticut txperiment; the third installment: 4 years of screening women with dense breasts with bilateral ultrasound. Breast J. 2017;23(1):34–9.
22. Hooley RJ, Greenberg KL, Stackhouse RM, Geisel JL, Butler RS, Philpotts LE. Screening US in patients with mammographically dense breasts: initial experience with Connecticut Public Act 09-41. Radiology. 2012;265(1):59–69.
23. Tagliafico AS, Calabrese M, Mariscotti G, Durando M, Tosto S, Monetti F, et al. Adjunct screening with tomosynthesis or ultrasound in women with mammography-negative dense breasts: interim report of a prospective comparative trial. J Clin Oncol. 2016;34(16):1882–8.

24. Berg WA, Zhang Z, Lehrer D, Jong RA, Pisano ED, Barr RG, et al. Detection of breast cancer with addition of annual screening ultrasound or a single screening MRI to mammography in women with elevated breast cancer risk. JAMA. 2012;307(13):1394–404.
25. Kuhl C, Weigel S, Schrading S, Arand B, Bieling H, Konig R, et al. Prospective multicenter cohort study to refine management recommendations for women at elevated familial risk of breast cancer: the EVA trial. J Clin Oncol. 2010;28(9):1450–7.
26. Warner E, Hill K, Causer P, Plewes D, Jong R, Yaffe M, et al. Prospective study of breast cancer incidence in women with a BRCA1 or BRCA2 mutation under surveillance with and without magnetic resonance imaging. J Clin Oncol. 2011;29(13):1664–9.
27. Heijnsdijk EA, Warner E, Gilbert F, et al. Difference in natural history between breast cancers in BRCA1 and BRCA2 mutation carriers and effects of MRI screening-MRISC, MARIBS, and Canadian studies combined. Cancer Epidemiol Biomark Prev. 2012;21(9):1458–68.
28. Rijnsburger AJ, Obdeijn IM, Kaas R, Tilanus-Linthorst MM, Boetes C, Loo CE, et al. BRCA1-associated breast cancers present differently from BRCA2-associated and familial cases: long-term follow-up of the Dutch MRISC Screening Study. J Clin Oncol. 2010;28(36):5265–73.
29. Sung JS, Stamler S, Brooks J, Kaplan J, Huang T, Dershaw DD, et al. Breast cancers detected at screening MR imaging and mammography in patients at high risk: method of detection reflects tumor histopathologic results. Radiology. 2016;280(3):716–22.
30. Kuhl CK, Schrading S, Strobel K, Schild HH, Hilgers RD, Bieling HB. Abbreviated breast magnetic resonance imaging (MRI): first postcontrast subtracted images and maximum-intensity projection-a novel approach to breast cancer screening with MRI. J Clin Oncol. 2014;32(22):2304–10.
31. Mango VL, Morris EA, David Dershaw D, Abramson A, Fry C, Moskowitz CS, et al. Abbreviated protocol for breast MRI: are multiple sequences needed for cancer detection? Eur J Radiol. 2015;84(1):65–70.
32. Harvey SC, Di Carlo PA, Lee B, Obadina E, Sippo D, Mullen L. An abbreviated protocol for high-risk screening breast MRI saves time and resources. J Am Coll Radiol. 2016;13(4):374–80.
33. van Zelst JCM, Vreemann S, Witt HJ, Gubern-Merida A, Dorrius MD, Duvivier K, et al. Multireader study on the diagnostic accuracy of ultrafast breast magnetic resonance imaging for breast cancer screening. Investig Radiol. 2018;53(10):579–86.
34. Lalji UC, Jeukens CR, Houben I, Nelemans PJ, van Engen RE, van Wylick E, et al. Evaluation of low-energy contrast-enhanced spectral mammography images by comparing them to full-field digital mammography using EUREF image quality criteria. Eur Radiol. 2015;25(10):2813–20.
35. Fallenberg EM, Dromain C, Diekmann F, Renz DM, Amer H, Ingold-Heppner B, et al. Contrast-enhanced spectral mammography: does mammography provide additional clinical benefits or can some radiation exposure be avoided? Breast Cancer Res Treat. 2014;146(2):371–81.
36. Francescone MA, Jochelson MS, Dershaw DD, Sung JS, Hughes MC, Zheng J, et al. Low energy mammogram obtained in contrast-enhanced digital mammography (CEDM) is comparable to routine full-field digital mammography (FFDM). Eur J Radiol. 2014;83(8):1350–5.
37. Jeukens CR, Lalji UC, Meijer E, Bakija B, Theunissen R, Wildberger JE, et al. Radiation exposure of contrast-enhanced spectral mammography compared with full-field digital mammography. Investig Radiol. 2014;49(10):659–65.
38. James JR, Pavlicek W, Hanson JA, Boltz TF, Patel BK. Breast radiation dose with CESM compared with 2D FFDM and 3D tomosynthesis mammography. AJR Am J Roentgenol. 2017;208(2):362–72.
39. Dromain C, Thibault F, Muller S, Rimareix F, Delaloge S, Tardivon A, et al. Dual-energy contrast-enhanced digital mammography: initial clinical results. Eur Radiol. 2011;21(3):565–74.
40. Lobbes MBILU, Houwers J, et al. Contrast-enhanced spectral mammography in patients referred from the breast cancer screening program. Eur Radiol. 2014;24(7):1668–76.
41. Jochelson MSDDD, Sung J, Heerdt AS, Thornton C, Moskowitz CS, Ferrara J, Morris EA. Bilateral contrast-enhanced dual-energy digital mammography: feasibility and comparison with conventional digital mammography and MR imaging in women with known breast carcinoma. Radiology. 2013;266(3):743–51.

42. Fallenberg EM, Dromain C, Diekmann F, Engelken F, Krohn M, Singh JM, et al. Contrast-enhanced spectral mammography versus MRI: initial results in the detection of breast cancer and assessment of tumour size. Eur Radiol. 2014;24(1):256–64.
43. Diekmann F, Freyer M, Diekmann S, Fallenberg EM, Fischer T, Bick U, et al. Evaluation of contrast-enhanced digital mammography. Eur J Radiol. 2011;78(1):112–21.
44. Cheung YC, Lin YC, Wan YL, Yeow KM, Huang PC, Lo YF, et al. Diagnostic performance of dual-energy contrast-enhanced subtracted mammography in dense breasts compared to mammography alone: interobserver blind-reading analysis. Eur Radiol. 2014;24(10):2394–403.
45. Cheung YC, Tsai HP, Lo YF, Ueng SH, Huang PC, Chen SC. Clinical utility of dual-energy contrast-enhanced spectral mammography for breast microcalcifications without associated mass: a preliminary analysis. Eur Radiol. 2016;26(4):1082–9.
46. Jochelson MS, Pinker K, Dershaw DD, Hughes M, Gibbons GF, Rahbar K, et al. Comparison of screening CEDM and MRI for women at increased risk for breast cancer: a pilot study. Eur J Radiol. 2017;97:37–43.
47. Sung JS, Jochelson MS, Lee CH, Bernstein JL, Reiner AS, Morris EA, et al. SSJ01-05 comparison of contrast enhanced digital mammography and whole breast screening ultrasound for supplemental breast cancer screening. RSNA, Chicago, IL, 2016.
48. Klang E, Krosser A, Amitai MM, Sorin V, Halshtok Neiman O, Shalmon A, et al. Utility of routine use of breast ultrasound following contrast-enhanced spectral mammography. Clin Radiol. 2018;73(10):908.e11–6.
49. Sumkin JH, Berg WA, Houshmand G, Chough DM, Hakim CM, Zuley ML, et al. Comparison of MRI, CEM and MBI for staging breast cancer in women with a newly diagnosed breast cancer. RSNA scientific assembly and annual meeting, McCormick Place, Chicago, IL. Oral presentation. 2017.
50. Chou CP, Lewin JM, Chiang CL, Hung BH, Yang TL, Huang JS, et al. Clinical evaluation of contrast-enhanced digital mammography and contrast enhanced tomosynthesis—comparison to contrast-enhanced breast MRI. Eur J Radiol. 2015;84(12):2501–8.
51. Hobbs MM, Taylor DB, Buzynski S, Peake RE. Contrast-enhanced spectral mammography (CESM) and contrast enhanced MRI (CEMRI): patient preferences and tolerance. J Med Imaging Radiat Oncol. 2015;59(3):300–5.
52. Phillips J, Miller MM, Mehta TS, Fein-Zachary V, Nathanson A, Hori W, et al. Contrast-enhanced spectral mammography (CESM) versus MRI in the high-risk screening setting: patient preferences and attitudes. Clin Imaging. 2017;42:193–7.
53. Houben IPL, Van de Voorde P, Jeukens C, Wildberger JE, Kooreman LF, Smidt ML, et al. Contrast-enhanced spectral mammography as work-up tool in patients recalled from breast cancer screening has low risks and might hold clinical benefits. Eur J Radiol. 2017;94:31–7.

8 Contrast-Enhanced Mammography in Neoadjuvant Therapy Response Monitoring

Valentina Iotti and Paolo Giorgi Rossi

8.1 Introduction

1.67 million new cases of breast cancer were diagnosed in 2012 [1], and each year 522,000 women die of breast cancer worldwide [1]. Five-year breast cancer survival in the United States and Western Europe has improved over the last 30 years and now ranges from 80% to 90% [2, 3]. This improvement has been due to a combination of early diagnosis and improved treatments [4]. As most of the cancers in industrialized countries are diagnosed early, they are more frequently amenable to breast-conserving surgery. In the last two decades, neoadjuvant systemic therapies (NST) have been introduced with the aim of further reducing the proportion of nonsurgically treatable cancers and to decrease the proportion of women needing mastectomy. The achievement of pathological complete response (pCR) is associated with favorable disease-free and, in some tumors, overall survival, equivalent to those for adjuvant therapy in operable breast cancer [5–8].

In addition, neoadjuvant chemotherapy is increasingly being used for women presenting with axillary adenopathy to downstage their cancers with the goal of reducing the requirement for axillary lymph node dissection.

8.1.1 Neoadjuvant Systemic Therapies

Recent guidelines worldwide [5, 6, 9] recommend NST for locally advanced nonmetastatic cancers: some stages II and IIIA (operable but needing mastectomy)

V. Iotti (✉)
Radiology Unit, Azienda USL—IRCCS di Reggio Emilia, Reggio Emilia, Italy
e-mail: valentina.iotti@ausl.re.it

P. Giorgi Rossi
Epidemiology Unit, Azienda USL—IRCCS di Reggio Emilia, Reggio Emilia, Italy
e-mail: paolo.giorgirossi@ausl.re.it

M. Lobbes, M. S. Jochelson (eds.), *Contrast-Enhanced Mammography*,
https://doi.org/10.1007/978-3-030-11063-5_8

and stages IIIB and IIIC (inoperable). In women below the age of 65, large stages IIA (T2, N0) and IIB, IIIA, IIIB, and IIIC account for about 20% of breast cancers, about one third of whom receive NST [10]. Approximately one fourth of stage II and two thirds of stage III cancers are treated with NST, more so in larger urban hospitals [10]. NST is recommended in most triple-negative (TNBC), HER2-positive, and high-risk luminal HER2-negative tumors [5, 6, 9]. Anthracyclines and/or taxanes are frequently part of NST chemotherapy regimens, and trastuzumab (sometimes with pertuzumab) is administered in addition to chemotherapy in HER2-positive breast cancer [9]. Endocrine therapy is used in all patients with detectable hormone receptor (HR) expression, regardless of whether chemotherapy and/or targeted therapy is used [5, 9]. The type of treatment may affect response assessment as drugs such as taxanes have been noted to decrease enhancement yielding false-negative results on magnetic resonance (MRI) [11]. According to Von Minckwitz [12], achievement of pCR defined as the absence of residual invasive and in situ cancer (ypT0) can best discriminate between patients with favorable and with unfavorable outcomes. The occurrence of pCR ranges from 3% to 40% [13], less frequently in women who are hormone receptor positive compared with women who have HER2-positive or triple-negative disease [12, 14]. The absence of pCR in hormone receptor-positive patients is less of a poor prognostic sign than in women with more aggressive tumors.

8.1.2 Response Assessment

Accurate in vivo response assessment during and/or after treatment is required to provide predictive and prognostic information and enable accurate surgical planning. Two definitions of pCR have been recognized by the Food and Drug Administration (FDA) [6]: the absence of residual invasive cancer (ypT0/is) and the absence of residual invasive and in situ cancer (ypT0). Several studies have reported no difference in survival between patients with residual ductal carcinoma in situ (DCIS) after NST and those without residual DCIS [7, 15], while others have reported that patients with residual DCIS had worse event-free survival than did patients with no remaining disease whatsoever [16].

Response to NST is currently assessed by combining physical examination and conventional imaging techniques such as full-field digital mammography (FFDM), ultrasound (US), and, frequently, with contrast-enhanced MRI. Croshaw et al. [17] reported that all these tests are good at predicting the presence of residual disease on final pathology (with an accuracy, respectively, of 57% for physical examination, 74% for FFDM, 79% for US, and 84% for MRI), but none can reliably predict pathologic complete response.

FFDM is widely available and allows the evaluation of calcifications but has reduced sensitivity in defining residual disease, mainly due to the masking effect of fibroglandular tissue and the absence of functional information. The primary advantages of US are real-time capability and the relatively low cost and widespread availability [18]. However, limitations include the restricted field of view for large tumors, high operator dependence and low reproducibility, and again the absence of functional information, mainly relying on morphological-based changes in tumor

size. To overcome these limitations, three-dimensional US, elastography, and dynamic contrast-enhanced US after the injection of intravascular microbubble contrast agents have been recently studied [19, 20].

Breast dynamic contrast-enhanced MRI is currently considered the most reliable diagnostic method for both the initial assessment of tumor extent and for monitoring the response to NST, demonstrating superiority over physical examination, FFDM, and US in identifying the extent of any residual disease and predicting pathological complete response [8, 20–22]. Reported sensitivity, specificity, positive predictive value, and negative predictive value for predicting pCR with MRI ranged from 25% to 100%, 50% to 97%, 47% to 73%, and 71% to 100%, respectively, observing both overestimation and underestimation [20]. Multiparametric MRI has been investigated as a method to improve the accuracy of the routine MRI sequences. This includes diffusion-weighted imaging (DWI) with calculating the apparent diffusion coefficient (ADC) and potentially MRI spectroscopy [23–26]. The meta-analysis published by Gao et al. [24] evaluating DWI in the detection of pCR reported a sensitivity of 89% (95% CI 86–91) and a specificity of 72% (95% CI 68–75). Radiomics also have the potential to improve upon the utility of MRI in the prediction of response to NST [27].

As mentioned previously, combined modality imaging both prior to and after neoadjuvant chemotherapy allows for better surgical planning and theoretically fewer re-excisions. Jochelson et al. [28] demonstrated that the use of MRI after NST allowed accurate prediction of the ability of breast conservation after chemotherapy in 88% of women and MRI plus mammography improved this to 92% primarily because of improved delineation of calcifications on mammography.

Access to MRI, however, may be limited even in industrialized countries, and MRI exams are expensive and time-consuming, both in the image acquisition and in radiologist interpretation time. Furthermore, MRI is precluded in patients with metallic implants, claustrophobia, or who cannot tolerate MRI because of the prolonged prone position. Although the rate of adverse gadolinium (Gd) reactions in MRI examinations is low (0.001–0.01%), patients with Gd allergies may be better served by using a different examination. A recent study has shown that repeated Gd administration may result in Gd deposition in the brain [29]. Additional studies are needed to investigate the clinical significance of these findings, but it is an important consideration in women receiving multiple doses of gadolinium-based contrast agents. As mentioned earlier in this chapter, combining MRI with FFDM is necessary to depict the presence and extent of residual calcifications to enable more accurate response assessment and for surgical planning. It should be noted that even in patients with benign residual calcifications in the tumor bed after NST, the standard of care is complete excision making post-treatment mammography a necessity [12, 20, 30].

8.1.3 Imaging Technique

CEM is a dual-energy exam performed by acquiring a pair of low- (LE) and high-energy (HE) images during each exposure after intravenous administration of contrast medium. A low-osmolar iodinated contrast agent is administered using a power injector at a rate of 2–3 mL/s. Contrast agents with concentration between 300 and 370 mgI/ml

and a volume of 1.5 mL/kg of body weight are typically used [31]. Approximately 2 min after the injection, the patient is positioned, and conventional mammographic cranio-caudal (CC) and mediolateral oblique (MLO) views are taken. The performance of a routine four-view CEM ranges from 4 to 10 min after injection (less than 6 s for the acquisition of each image pair) [31–33] with contrast enhancement persisting for up to 10 min [34]. Various orders of acquisition of views (CC and MLO) and of the two breasts (with or without the known tumor) have been reported to all be essentially equivalent [33]. Occasionally, additional views may be added to better visualize lesions that were only partially visible from standard ones.

8.2 CEM in Therapy Monitoring

Conceptually similar to contrast-enhanced breast MRI, CEM potentially has similar indications, but as it is a relatively new technique, the scientific evidence supporting its accuracy in treatment monitoring is limited compared to MRI.

8.2.1 Imaging Analysis

In NST monitoring, accurate definition of disease extent is critical to decide if conservative surgery will be possible even after successful treatment. In the initial assessment, CEM enables accurate tumor size measurement that matches the quality of the same measurement assessed by breast MRI [35–39]. Direct comparison with histopathology, without NST, confirmed the good correlation for both CEM and MRI, as reported in several studies [35–39]. Lobbes et al. [36] found a small systematic overestimation of the tumor diameter measured on MRI, whereas CEM did not overestimate the size, while Łuczyńska et al. [35] described an overestimation of lesion size both in CEM and in MRI. Fallenberg et al. [38] instead found an underestimation of the tumor size using MRI compared to CEM and pathology, describing an increasing discrepancy between the pathological lesion size and the dimensions measured with imaging methods for larger breast tumors. This consideration is relevant in NST monitoring, since this treatment is recommended for locally advanced breast carcinomas.

The accuracy of CEM in staging the breast is still debated. Jochelson et al. [33] reported a detection rate of 88% for additional cancers in MRI and 56% for additional cancer foci in CEM. Fallenberg et al. [37] also reported that MRI performed 10% better than CEM regarding additional lesions, concluding nevertheless that CEM is also helpful in the detection of multifocal breast cancers, knowing it is inferior to MRI regarding the detection rate but providing better specificity. On the other hand, Łuczyńska et al. [35] described that CEM detected multifocal breast cancers in all cases studied. In the initial pretreatment assessment, it is also necessary to report the enhancement of any concomitant benign lesions to subsequently avoid misinterpretation of loss of enhancement after treatment [40] (Fig. 8.1).

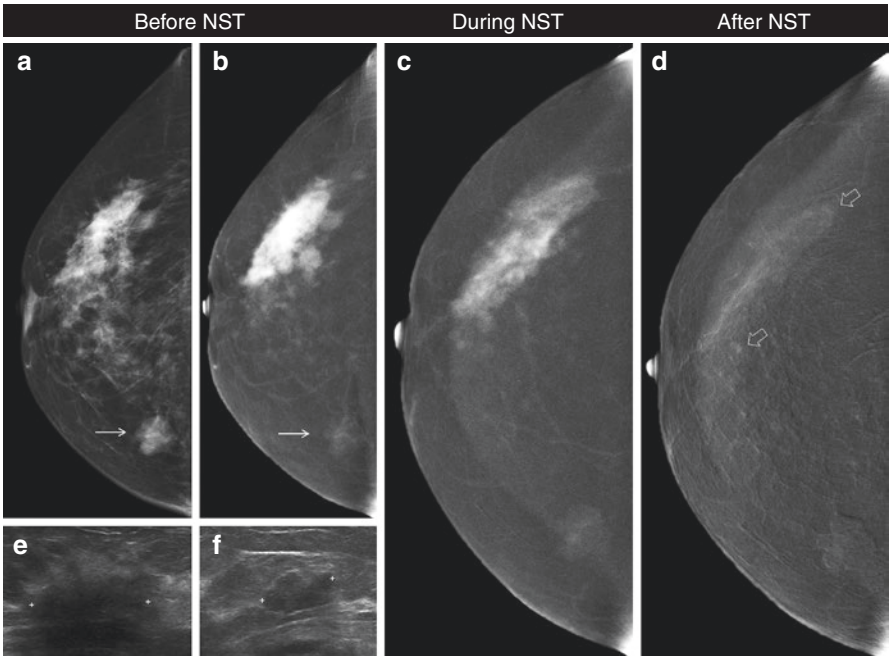

Fig. 8.1 Patchy enhancement in ILC showing partial response. Partial response to NST in a 72-year-old woman with 50 mm invasive lobular carcinoma (luminal B) in the right breast. Before NST, CEM showed an opacity with intense enhancement in the outer quadrants (**a**, CC-view LE image; **b**, recombined image). In the inner quadrants, a smaller opacity with regular margins was also visible in the LE image (**a**: white arrow), with faint enhancement on recombined image (**b**: white arrow), which are benign characteristics of a fibroadenoma, confirmed also by US (**f**), clearly different from the malignant area of the outer quadrants (**e**). During NST, a patchy shrinkage and loss of enhancement intensity was detectable (**c**: CC-view recombined image), becoming more heterogeneous, while the faint enhancement of the fibroadenoma remained stable. After NST (**d**: CC-view recombined image), very faint spots of enhancement were detectable in the whole tumor bed (**d**: delimited by the black arrows with white profile). The patient underwent breast-conserving surgery; on the surgical specimen, a partial response was described due to the persistence of small foci of invasive lobular carcinoma spread throughout the entire 50 mm of the primary tumor bed

In NST monitoring, in cases with multifocal breast cancers, the maximum dimension of the largest invasive tumor is used to determine the degree of response [36].

The assessment of response during and after NST with CEM is based on the analysis of both the LE image and the post-processing recombined image, evaluating both the CC and MLO views. LE image allows the evaluation of calcifications, while the tumor size measurements require the matched examination of enhancement on the recombined images.

Like what has been proposed with MRI [41], different response patterns may occur: complete radiologic response, tumor shrinkage, and stable or progressive disease. Combining the evaluation of LE images and recombined images and

following what has been done with MRI [20–22] in the analysis of enhancement, the possible response patterns are:

- *Complete radiologic response*: no contrast enhancement in the entire tumor bed and any other sites of biopsy-proven disease, not always accompanied by disappearance of the tumor opacity on LE images due to persistence of fibrous stroma despite the loss of viable cells [30, 32, 42].
- *Shrinkage*: progressive loss of enhancement and/or tumor shrinkage has been observed among responders (Fig. 8.2) [30, 32, 43].
- *Stable or progressive disease*: stable tumor size and enhancement, increase in tumor size, or new lesions, associated with the persistence of contrast enhancement that denotes resistance to chemo- or hormonal therapy [30, 32].

In the measurement of residual enhancement among responders, most authors that have dealt with the topic of NST monitoring with CEM [30, 44, 45] have considered any minimum detectable enhancement within the tumor bed after NST as the expression of viable residual neoplastic cells, i.e., residual disease. Drugs used in the NST regimen frequently have antiangiogenic activity (taxanes have been reported to have greater antiangiogenic activity compared to anthracyclines [11])

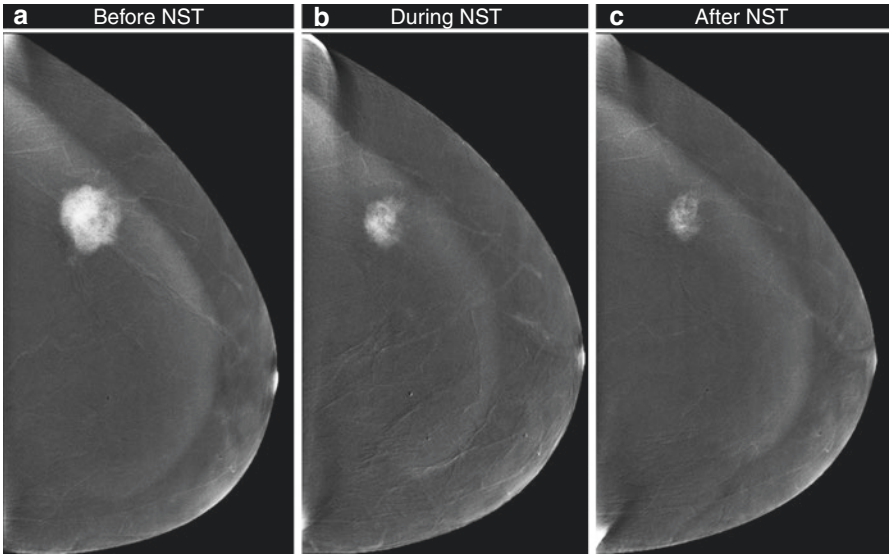

Fig. 8.2 Concentric shrinkage in TNBC partial responder. Partial response to NST in a 62-year-old woman with 35 mm invasive ductal carcinoma (G3, TNBC) in the left breast. Before NST, CEM showed a mass-like, intense enhancement in the outer quadrants (**a**: CC-view recombined image). During NST, a concentric shrinkage and loss of enhancement intensity were detectable (**b**: CC-view recombined image), which became fainter and more heterogeneous after NST (**c**: CC-view recombined image) though still clearly delimited (2 cm). The patient underwent breast-conserving surgery; on the surgical specimen, a partial response was described due to the persistence of 2 cm of invasive ductal carcinoma

that, combined with changes in tumor microvessel functionality, decreases the enhancement on residual tumor tissue on MRI. Enhancing foci inside the tumor bed may indicate residual active disease [30, 44]. Considering all the area as a lesion gave good correlation between imaging and pathology in the measurement of lesion dimension [30, 44].

CEM has some intrinsic limitations, however. Unlike MRI, CEM does not assess lesion kinetics, even though this enhancement characterization is not so important in the assessment of residual disease. MRI also has a larger field of view and can therefore depict the chest wall, axilla, and internal mammary lymph nodes, which are not available with CEM [33].

Patients who have impaired renal function or an iodine contrast allergy cannot undergo this exam or need to be premedicated before the procedure. Consisting of two image acquisitions (i.e., the low- and high-energy image), the radiation dose of CEM is higher than that of FFDM, although the overall dose is still within internationally accepted radiation dose limits. Furthermore, radiation dose of imaging techniques is not really an issue in patients that frequently also have indications for radiotherapy, which usually includes a total dose of 45 Gy on the target, i.e., about 10,000 times the dose of a CEM.

The presence of a clip as marker in the tumor bed could cause a focal metal artifact on the recombined image of CEM, which could potentially obscure a small amount of residual enhancement yielding a false-positive result like MRI.

8.2.1.1 Calcifications

After NST the number and extent of calcifications may remain stable, decrease, or increase. When the index lesions initially present with calcifications, residual DCIS is more likely to be observed after NST [46]. An increase in malignant calcifications is more frequently observed in patients with poor response and a decrease in calcifications in patients with better response [16, 46, 47]. Residual or new calcifications have also been noted in patients with pCR (ypT0) sometimes due to dystrophic calcifications. Indeed, residual calcifications are not always an expression of the residual tumor but may represent treated cancer with calcified or necrotic tissue and sloughed cells in the tumor bed [46, 47]. Feliciano et al. [48] described that calcifications post-NST were associated with DCIS or invasive ductal carcinoma (IDC) on final pathology in 34/90 (37.8%) patients and were benign in 56/90 (62.2%) patients. Patients with benign calcifications after treatment were significantly more likely to have HER2+ tumors.

Among conventional imaging, FFDM is the main diagnostic tool for evaluating the extent of calcifications, while the DCIS component tends to be misdiagnosed by MRI [38, 49]. However, several studies showed a lower correlation between the extent of pathologic residual cancer and the extent of calcifications on FFDM after NST, compared to the assessment with MRI [16, 47–49]. This suggests the fundamental contribution of enhancement in monitoring the response to NST, even for the in situ component.

In the evaluation of both the extension and characterization of calcifications (on the LE image), CEM combines the advantage of FFDM resolution and of enhancement in

a single examination. In the past, concerns were raised regarding potential obscuration of calcifications on the LE images due to the administration of contrast agent [50]. Actually, the visualization of calcifications on LE images is non-inferior when compared to FFDM [51–53].

Calcifications may be obvious on the LE images, but the intraductal neoplastic component most frequently presents as calcifications with weak or no enhancement on the recombined views [40, 50]. The initial weak enhancement could be further reduced by the chemotherapeutic anti-angiogenetic effect in the post-NST assessment. The lack of contrast enhancement anyway should not be used to downgrade any lesion with suspicious morphology on LE image, including suspicious calcifications [50] (Fig. 8.3).

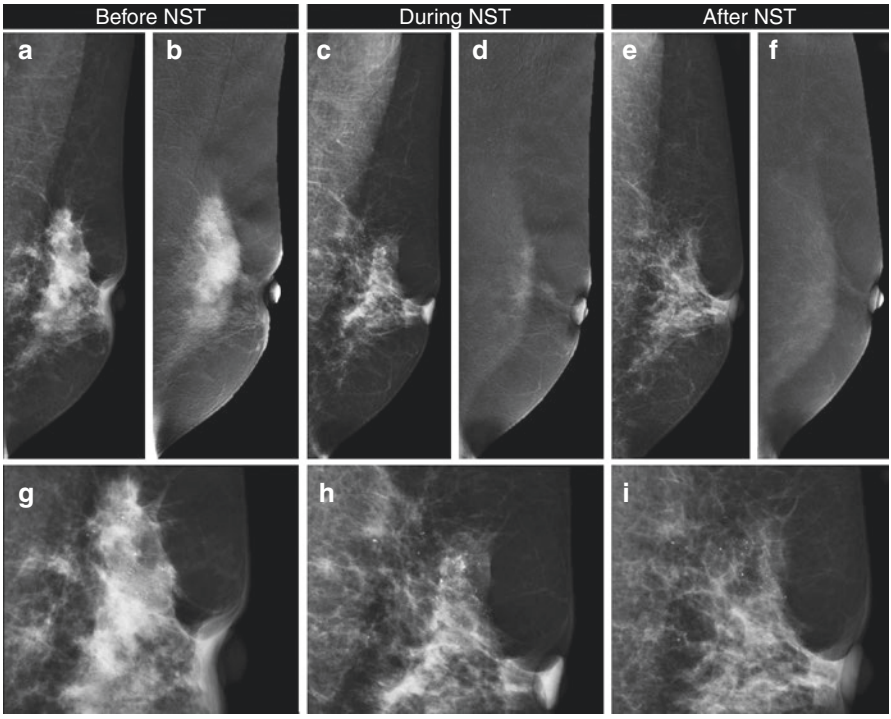

Fig. 8.3 Calcifications and DCIS residual component after NST. A 47-year-old woman with 60 mm of in situ and invasive ductal carcinoma (G3, HER2+) in the left breast, presenting before treatment as an irregular opacity with concomitant crushed stonelike calcifications on the LE image (**a**, MLO view; **g**, magnification) spread "inside" [11] 40 mm of the tumor bed, and with intense enhancement on recombined image (**b**: MLO view). During NST, the opacity on LE image (**c**, MLO view; **h**, magnification) and the concomitant enhancement (**d**: MLO-view recombined image) regressed, while calcifications remained substantially stable. After NST, "inside" calcifications were minimally decreased on LE image (**e**, MLO view; **i**, magnification), while no significant residual concomitant enhancement was detectable on recombined image (**f**: MLO view). The patient underwent non-conservative surgery; on the surgical specimen, a partial response was described due to the persistence of ductal in situ foci spread in the area of 35 mm of tumor bed

Regardless of the degree of response, all suspicious calcifications inside the tumor bed must be removed. With this aim, CEM could be more precise than MRI allowing the direct visualization of both the tumor bed and the concomitant suspicious calcifications. Further focused studies are encouraged.

8.2.1.2 Influence of Breast Cancer Histological and Molecular Subtypes

Breast cancer molecular subtypes influence the choice of chemotherapeutic agent, response to chemotherapy, and risk of recurrence. Patients with TNBC and HER2-positive breast cancer have the highest rates of pCR after NST (in the range of 60%) and the strongest correlation between pathologic response and long-term outcomes [5, 12, 14, 54, 55].

Several studies have shown that breast cancer subtype also affects imaging performance, with the highest accuracy in TNBC and HER2-positive disease [13, 14]. In these studies, among patients who presented complete response with conventional imaging, especially MRI, HR-positive status and low tumor grade were most commonly associated with residual disease at surgery, suggesting that a complete response on preoperative MRI in these patients should be interpreted with caution [14]. The underlying reason for the higher accuracy of MRI in TNBC than in HR-positive can be explained by the typical well-delineated smooth mass margin, rim enhancement due to the intratumoral necrosis, and higher capillary permeability [47, 56]. In treatment monitoring with MRI, several pre-chemotherapy phenotypes have been characterized, ranging from solitary and well-defined to diffuse disease [42, 57–59]. Mukhtar et al. [57] described how the response to NST varied not only by breast cancer subtype ($p = 0.005$) but also by MRI phenotype ($p = 0.037$), with a higher concordance between tumor size on MRI and surgical pathology in well-defined tumors, especially those with a TNBC subtype.

In pretreatment evaluation, heterogeneities in the contrast uptake may reflect underlying molecular intratumor heterogeneity, typical in aggressive tumors [25].

The presentation of HER2-positive cancers varies, both appearing as smooth mass margins with tumor extension around the mass [56] and as architectural distortion.

An irregular mass margin has been observed to be associated with luminal A cancers, which are generally slow growing and histologically rich in fibrous components [56]. Women with luminal disease are significantly less likely to achieve pCR and therefore to have conservative surgery. This is particularly a problem in patients with invasive lobular carcinomas. In fact, lobular tumors have higher rates of re-excision after NST due to positive margins, compared with the ductal tumors in the same subgroup [10, 60, 61].

As CEM is a relatively new technique, the literature available is still limited. Travieso-Aja et al. [62] evaluated the factors affecting the precision of lesion sizing with CEM and found no significant differences in relation to the histological type, subtype, or tumor grading. The few articles regarding CEM evaluation of response to

NST have also reported the molecular subtypes while describing the population, but none could associate them with accuracy of assessment due to the small sample size.

A subpopulation analysis performed by Iotti et al. [30, 63, 64] confirmed that the correlation (r = Pearson's correlation coefficient) between imaging and pathology on surgical specimen was stronger for IDC ($r = 0.934$ for CEM and $r = -0.893$ for MRI), for TNBC ($r = 0.946$ for CEM and $r = -0.864$ for MRI), and for HER2+ ($r = 0.979$ for CEM and $r = -0.975$ for MRI) than for ILC ($r = 0.628$ for CEM and $r = -0.298$ for MRI) and luminal B ($r = 0.750$ for CEM and $r = -0.003$ for MRI). Furthermore, CEM accuracy in determining tumor size seemed to be less influenced by tumor morphology (Figs. 8.1 and 8.4), confirming that these lesions are more challenging than are IDC, TNBC, and HER2+ cancers (Figs. 8.2 and 8.5), but suggesting as well that CEM accuracy could be less affected than MRI accuracy by cancer type. However, these results have no statistical relevance due to the very small population.

8.2.1.3 Shrinkage Patterns

The aim of pre- and post-NST imaging is to assess how the tumor mass regresses; in this assessment, characterizing different shrinkage patterns may help interpret findings. Several variables influence the tumor shrinkage and its evaluation with imaging, including primary tumor size, edema, necrosis, obstruction of lymphatics or blood vessels exerted by growing tumors, destruction of the existing lymphatics

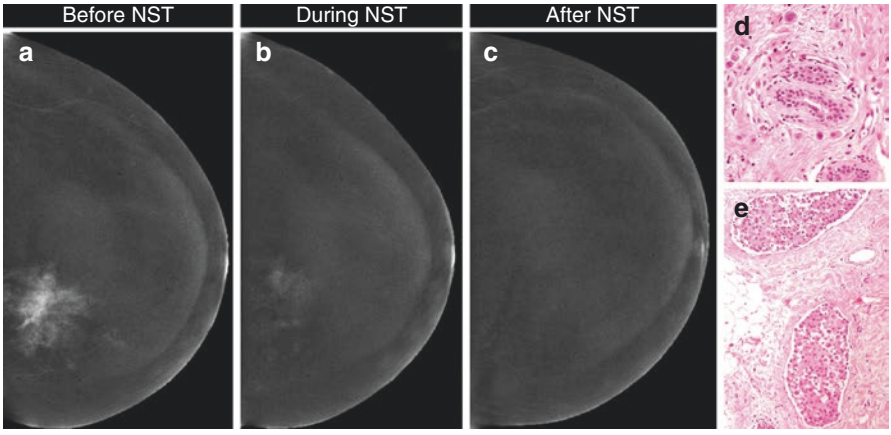

Fig. 8.4 Pathological residual disease misinterpreted as complete response with CEM (false negative). Pathological partial response to NST in a 69-year-old woman with 43 mm invasive lobular carcinoma, luminal A, in the left breast, misinterpreted as complete responder by CEM. Before NST, CEM showed a non-mass enhancement in the inner quadrants (**a**: CC-view recombined image). During NST, a patchy shrinkage and loss of enhancement intensity were detectable (**b**: CC-view recombined image), while after NST, no enhancement was detectable in the tumor bed (**c**: CC-view recombined image). The patient underwent breast-conserving surgery; on the surgical specimen, a partial response was described due to the persistence of small foci of invasive lobular carcinoma within the primary tumor bed (**d**: H&E, high magnification). Interestingly, a lot of lymphovascular spaces stuffed with neoplastic cells were present (**e**: H&E, high magnification)

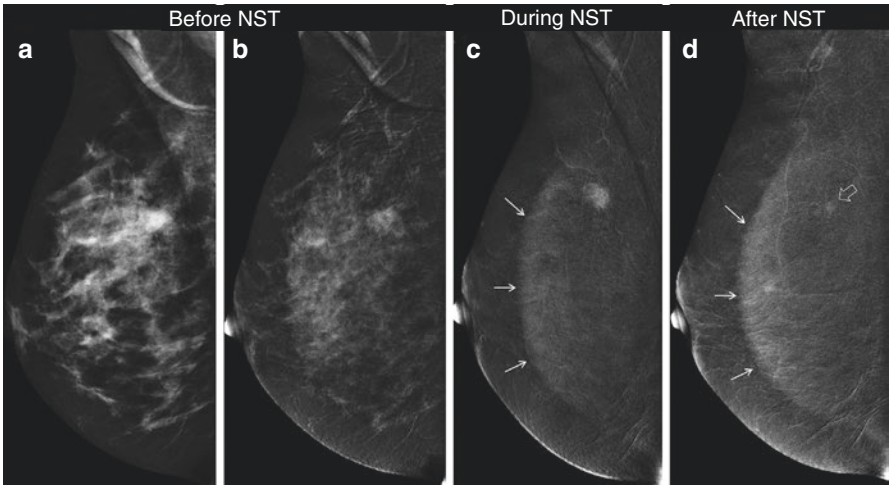

Fig. 8.5 Background parenchymal enhancement in TNBC. Partial response to NST in a 48-year-old woman with 20 mm invasive ductal carcinoma (G2, TNBC) in the right breast. Before NST, CEM showed a scattered dense breast (**a**: MLO-view LE image) with BPE (**b**: MLO-view recombined image). The known TNBC appeared as an opacity in the LE image corresponding on the recombined image to an area of enhancement more intense than the surrounding BPE. During NST, a concentric shrinkage and loss of enhancement intensity were detectable (**c**: MLO-view recombined image). Both during (**c**) and after NST (**d**: MLO-view recombined image) "halo" or "rim" artifact (*breast within breast* [49]) occurred (white arrows on **c** and **d**), without any significant effect on the measurements of the residual lesion. After NST, a focal faint enhancement was still visible in the tumor bed (**d**: black arrow with white profile), measuring 4 mm. The patient underwent breast-conserving surgery; on the surgical specimen, a partial response was described due to the persistence of focal invasive residual component (3 mm)

or lack of tumor lymphangiogenesis [65], and subjective variation in tumor measurement methods [66]. Also, each chemotherapeutic drug contributes differently to the variation of the primitive lesion. For example, taxanes have been reported to have greater antiangiogenic activity compared to that of anthracyclines. In the literature, different regression patterns have been described for treatment monitoring with MRI [41, 58, 59, 67, 68] and CT [42]. Aside from the direct disappearance of the lesion, these can be summarized as [59]:

– *Concentric pattern*: solitary nodule, a more regular shape, and with a clear boundary (Figs. 8.2 and 8.5).
– *Patchy pattern (non-concentric)*: multiple nodules, irregular shapes, and unclear boundaries (Figs. 8.1, 8.3, and 8.4).

Li et al. [59] reported a correlation between these tumor regression patterns and some molecular subtypes: TNBC more frequently presented a concentric pattern while HR+ and HER2+ a patchy pattern ($p = 0.028$).

Kim et al. [67] described a correlation between shrinkage patterns and pathological response: concentric shrinkage was more frequently observed among the

responders, while a diffuse contrast enhancement was more frequently noted in non-responders. The volume of tumor enhancement measured by MRI also showed to be a strong predictor of recurrence-free survival as described by Hylton et al. [69]. Goorts et al. [41] confirmed this evaluation, describing though a better correlation among response pattern and the pathological response when assessed halfway through NST than after NST, possibly due to taxanes, only administered during the second half of treatment. Interestingly, patients with diffuse enhancement showed chemoresistance, but in these cases, correlation between sizes obtained by MRI and histology was good. Instead, patients presenting a shrinkage with residual multinodular lesions showed better chemo-responsiveness, but the correlation between sizes obtained by MRI and histology was poor. Fukada et al. [70], evaluating MRI response to NST in low-grade luminal early breast cancers, reported that only the concentric pattern had a significant independent association with disease-free survival ($p = 0.001$) and overall survival ($p = 0.009$) rate. Esserman et al. [71] reported that the likelihood of response as measured by change in longest diameter was 77% for circumscribed mass and 20% for patchy enhancement. MRI has been observed to have limitations in detecting non-concentric shrinkage mainly composed by scattered, microscopic tumor foci after NST [14, 58, 61]. Therefore, the concern of leaving microscopic residual tumor surrounding the surgical area after NST has given rise to a dilemma concerning how much breast tissue to excise, leading to a higher rate of non-conservative surgery in non-concentric regressions [42, 58, 61].

The precision of size estimation with CEM is more accurate in large tumors that frequently exhibit strong contrast enhancement [62]. Lesions in NST responders progressively shrink and lose enhancement. Ambicka et al. [72] described a statistically significant association between tumor margin on CEM and macroscopic border on histological examination only when strong enhancement was present, while the assessment of the tumor margin might not be precise in cases showing weak enhancement. The high spatial resolution of CEM (ten times higher than breast MRI [35]) facilitates the depiction of tiny foci of residual enhancing lesion inside the tumor bed.

The shrinkage pattern differentiation proposed by Li et al. [59] was adopted by Iotti et al. to categorize shrinkage patterns seen on CEM [64]. Forty-eight percent of tumors presented a concentric shrinkage, 33% presented a patchy shrinkage, and 19% presented complete direct disappearance of the lesion. Focusing on the most challenging subtypes, 75% of ILC presented a patchy shrinkage and 25% a direct disappearance, while 50% of luminal B presented concentric shrinkage, 44% patchy, and 6% direct disappearance. The largest differences in predicting the residual tumor size between CEM and MRI as measured by pathology were observed in the patchy shrinkage (mean underestimation of 30 mm for CEM and 56 mm for MRI in ILC; 2 mm for CEM and 18 mm for MRI in luminal B). Instead, the precision of the two imaging techniques was similar among concentric (mean underestimation of 3 mm for both CEM and MRI in luminal B) and direct disappearance (mean underestimation of 7 mm for both CEM and MRI in ILC; 5 mm for both CEM and MRI in luminal B).

8.2.1.4 Background Parenchymal Enhancement

Background parenchymal enhancement (BPE) refers to the uptake of contrast medium by normal fibroglandular breast tissue and is affected by age, hormonal status, and breast density [62, 73]. Controversy exists as to whether BPE negatively affects the sensitivity of image interpretation by obscuring enhancing malignancies and the specificity of the same by causing enhancement patterns that mimic cancerous lesions [74]. This could be a partial limitation principally in the initial evaluation before the beginning of NST. The degree of BPE has been shown to be reduced by hormonal or chemotherapy treatment [70, 74, 75]; its impact on tumor measurements should therefore diminish during and after NST in women with HR-positive neoplasm and receiving those therapies (Fig. 8.5).

Nonetheless, BPE and its variation during NST are related to the response: patients with a higher pre-treatment BPE who showed a significant decrease on MRI after starting NST were more likely to achieve pCR [74]. Since BPE is an indicator of blood perfusion, which delivers both contrast agents and chemotherapy agents, a higher BPE theoretically may allow more delivery of therapeutic agents into the breast, leading to a better response [74, 76]. This would require more study.

8.2.2 Accuracy of CEM in Assessing Response to NST

In this paragraph, we report the findings of studies that investigated the accuracy of CEM in NST monitoring. To ensure a complete and unbiased presentation, we conducted a systematic review of the literature. The methods are reported in the box, and the protocol can be found in the Prospero database n° CRD42018100393.

PubMed and Google Scholar were searched for studies evaluating the accuracy of CEM in assessing residual disease extent after NST in patients with breast cancer from 2000 to June 5, 2018. We included both studies evaluating only CEM and studies comparing CEM with other imaging techniques, i.e., MRI. The pathology was the standard. Article titles were reviewed by order of publication date (oldest to newest), and two independent reviewers (VI and PGR) screened the title and abstract. For relevant papers according to one of the two reviewers, the full text was analyzed. The following information was extracted from each article: (1) basic information, including the year of publication and the first author's name; (2) study information, including study design, number of patients, histological and molecular characteristics of tumor, stage at diagnosis, and the diagnostic tools considered; (3) treatment information; (4) outcomes of interest, such as number of women with residual disease on pathology, mean size measured on imaging and pathology, and the accuracy in assessing the presence of residual disease with imaging (TP, FP, TN, FN); (5) the correlation and concordance between imaging and pathology; and (6) final surgical treatment.

We searched the main trial registries for ongoing trials evaluating the accuracy of CEM in assessing residual disease extent after NST.

We defined as positive CEM for residual disease all patterns of enhancement in the tumor bed, minimum detectable, considered as the expression of viable residual neoplastic cells. Drugs used in the NST regimen frequently have antiangiogenic activity that, added to changes in tumor microvessel functionality, lowers the enhancement on residual tumor tissue. Measurements were obtained considering the maximum dimension of enhancement (focal or multiple enhancing foci spread inside the tumor bed considered as the same pathologic area) on recombined images, in the cranio-caudal and mediolateral oblique. Suspicious calcifications detectable in the LE images and considered as part of the tumor bed in the pre-NST evaluation were included in the measurements.

We considered as positive MRI for residual disease the enhancing lesion detectable on post-contrast T1-weighted or subtracted images at peak enhancement, measuring the largest dimension in either plane.

The literature reports different criteria adopted in the definition of pCR. Here we decided to consider the absence of residual invasive and in situ cancer (ypT0), since the residual DCIS component could be still visible on imaging after NST, for example, as persistent calcifications in the tumor bed, impacting the surgical planning. Obtaining clear resection margins with accurate preoperative evaluation helps decrease operation time and reduces the chances of repeating surgery or early local recurrence.

We assessed the risk of bias for each outcome and each study, and then we synthetized it as level of the evidence according to the GRADE criteria (www.gradeworkinggroup.org).

Statistical analysis: We present pooled results of the sensitivity and specificity, positive predictive value, and negative predictive value for CEM and MRI, with relative 95% confidence interval computed according to random effects model. We also report the pooled relative sensitivity and relative specificity through a meta-analysis of only studies with direct comparison. For the correlation between diameter at imaging and pathology, we present a narrative synthesis of each paper's results. Analyses were performed with RevMan 5.3; when > = 4 studies were found, pooled estimates were calculated with Stata 13.0, metandi command.

Research question: To evaluate the accuracy of CEM in assessing residual disease extent after NST in patients with breast cancer.

Inclusion and exclusion criteria:

- **P** ***Patient, population, problem***: women with breast cancer and indication to NST.
- **I** ***Intervention of interest***: measuring residual tumor size after NST with CEM.

- **C *Comparison***: measuring residual tumor size after NST measured with MRI or FFDM.
- **O *Outcomes***: primary outcome: accuracy, i.e., sensitivity and specificity, positive predictive value, and negative predictive value, in identifying the residual disease, using as reference test the pathology after surgery. Secondary outcome: accuracy in measuring residual tumor size after NST (reference pathology).

Database(s):

- PubMed—Free, MeSH.
- Google Scholar—Free.

Terms used in the search:

Breast cancer AND (neoadjuvant OR neoadjuvant OR (primary chemotherapy)) AND (contrast-enhanced mammography OR CESM OR CEDM).

8.2.2.1 Characteristics of the Studies, Methodological Challenges, Endpoints, and Risk of Bias

As shown in Table 8.1, four recently published studies were included in this review.

Barra et al. [45] performed a retrospective feasibility study on eight patients reviewed by three radiologists, comparing the pathological response to CEM, which was analyzed by independently evaluating the recombined image and the LE image, considered as a FFDM. Specific objectives were to evaluate the accuracy of CEM in determining residual tumor size using pathology results as the gold standard, to compare the performance of recombined images with that of low-energy images, and to analyze interobserver agreement. Sensitivity and specificity for residual disease were reported. The reported sensitivity, specificity, PPV, and NPV were higher for CEM than for FFDM (83.33%, 100%, 100%, and 66% vs. 50%, 50%, 50%, and 25%, respectively). CEM measurements showed a strong, consistent correlation with the pathological findings (correlation coefficient 0.76–0.92; intraclass correlation coefficient 0.692–0.886), while the correlation between FFDM and pathology was not statistically significant, with questionable consistency (intraclass correlation coefficient 0.488–0.598).

El Said et al. [32] published a prospective study involving 21 patients in whom CEM was done at the end of the last cycle of NST to evaluate its ability to predict the final pathological response and residual tumor size. The lesions were analyzed by the radiologist for the presence, morphology, and pattern of enhancement of residual lesions after NST. The specificity of the CEM in predicting the tumor response to NST was 91%, sensitivity was 40%, and the NPV and PPV were 80% and 62.5%, respectively. The sensitivity of this technique for complete response detection was 100% with a specificity 83% and lowered sensitivity in detecting chemoresistant tumors (33.3%). In the definition of pathological response, they considered minimal residual disease as pCR (ypT < mic). These criteria are not

Table 8.1 Characteristics of the studies included in the meta-analysis

Author	*Year*	*Country*	*Study period*	*Study methodology*	*Diagnostic tools*	*Population, n*	*Mean age, years (range)*	*Postmenopausal status, n (%)*	*Neoadjuvant systemic therapy*	*Histology, n (%)*	*Biologic subtypes, n (%)*	*T stage at diagnosis pre-NST, n (%)*	*N+ at diagnosis pre-NST, n (%)*
Barra et al. [45]	2017	Brazil	2011–2013	Retrospective	CEM FFDM	8	46 (22–76)	–	–	–	–	–	–
El Said et al. [32]	2017	Egypt	–	Prospective	CEM	21	50 (30–77)	–	21 chemo-tp	IDC 18 (86) ILC 2 (9) mixed IDC/ILC 1 (5)	ER+ 13 (68) PgR+ 12 (63) HER2+ 10 (53) TNBC 2 (10) n.a. 2	–	–
Iotti et al. [30]	2017	Italy	2012–2014	Prospective	CEM MRI	46	54 (33–72)	20 (43)	46 chemo-tp	IDC 40 (87) ILC 4 (9) other 2 (4)	ER+ 31 (67) PgR+ 23 (50) HER2+ 18 (39) TNBC 12 (26)	T2 30 (65) T3 14 (31) T4 2 (5)	28 (61)
Patel et al. [44]	2018	USA	2014–2017	Retrospective	CEM MRI	65	53 (30–76)	33 (51)	53 chemo-tp 12 endocrine tp	IDC 56 (86) ILC 5 (8) mixed IDC/ILC 2 (5) other 1 (1)	ER+ 41 (63) PgR+ 39 (60) HER2+ 25 (38) TNBC 16 (25)	T1c 12 (19) T2 35 (54) T3 15 (23) T4 2 (3) TX 1 (1)	24 (37)

Author	*Surgical treatment, n (%)*	*Residual disease on pathology, n (%)*	*Mean size of RD on pathology, mm (range)*	*Mean underestimation of diagnostic tools vs pathology, mm (SD)*	*Lin's concordance coefficient of diagnostic tools vs. pathology, (95% CI)*	*Pearson correlation of diagnostic tools vs. pathology*	*CEM TP for RD, n*	*CEM FP for RD, n*	*CEM TN for RD, n*	*CEM FN for RD, n*	*MRI TP for RD, n*	*MRI FP for RD, n*	*MRI TN for RD, n*	*MR FN for RD, n*
Barra et al. [45]	–	6 (75)	17 (0–40)	–	–	CEM 0.64–0.92 FFDM 0.57–0.64	5	0	2	1	–	–	–	–
El Said et al. [32]	Mastectomy 16 (76) Lumpectomy 5 (24)	15 (71)	–	–	–	–	14	1	5	1	–	–	–	–
Iotti et al. [30]	Mastectomy 18 (39) Lumpectomy 28 (61)	38 (83)	18.6 (0–95)	CEM 4.1 (12.3) MRI 7.5 (17.1)	CEM 0.81 MRI 0.59	CEM 0.85 MRI 0.67	32	0	8	6	23	1	7	15
Patel et al. [44]	Mastectomy 34 (52) Lumpectomy 31 (48)	45 (69)	19.6 (0–100)	CEM 5 (16.8) MRI 5.4 (15.5)	CEM 0.75 (0.62–0.83) MRI 0.76 (0.65–0.84)	CEM 0.77 MRI 0.8	30	1	19	15	31	1	19	14

– not applicable, *RD* residual disease, *TP* true positive, *FP* false positive, *TN* true negative, *FN* false negative

consistent with those of the other studies. The paper reported data in detail, allowing us to recompute false positive and false negative with ypT0 as threshold for pCR. Therefore, sensitivity and specificity values reported in this review are different from those reported in the original paper.

Iotti et al. [30] published a prospective study on 46 women who underwent both CEM and MRI before, during, and after neoadjuvant chemotherapy; no multicentric or multifocal cancers were included. The objective of the study was to compare post-treatment measurements on CEM and MRI with the pathological measurement on surgical specimens. Correlation between measurements using CEM and MRI at each step of the study (pre-, during, and post-NST) and the variation in the largest dimension of the tumor on imaging was also assessed. Sensitivity and specificity for complete response were also evaluated (pCR = ypT0). The agreement between measurements using CEM and MRI was 0.96, 0.94, and 0.76 before, during, and post-NST, respectively. In the assessment of complete response, sensitivity and specificity were 100% and 84%, respectively, for CEM, and 87% and 60% for MRI.

Patel et al. [44] retrospectively evaluated the accuracy of CEM in assessing residual disease extent compared to MRI for 65 patients after completion of NST. All patients had both CEM and MRI performed pre- and post-NST. NST included both neoadjuvant chemotherapy (82%) and endocrine therapy alone (18%). The authors also presented agreement between the two techniques. Including patients treated with endocrine therapy only led to possible heterogeneity in drug influence on imaging compared to the other three studies. Equivalence tests demonstrated that mean tumor size measured by CEM ($p = 0.009$) or by MRI ($p = 0.01$) was equivalent to the mean tumor size measured by pathology within −1 and 1-cm range. Comparing CEM vs. MRI for the assessment of complete response, the sensitivity was 95% vs. 95%, specificity 66.7% vs. 68.9%, PPV 55.9% vs. 57.6%, and NPV 96.7% vs. 96.9%, respectively.

There is an ongoing trial (clinicaltrials.gov number: NCT03070340) at Memorial Sloan Kettering Cancer Center. This is a prospective study comparing the ability of CEM to MRI to determine whether there is residual disease as well as the extent of that residual disease. The study will accrue 125 patients.

8.2.2.2 Sensitivity and Specificity for Residual Disease

In this meta-analysis, 140 patients were included, 36 (26%) of whom showing pCR (Fig. 8.6). Pooled sensitivity for the detection of residual disease estimate for CEM was 80.7% (95% CI 65.5–90.2). The heterogeneity between studies was substantial, ranging from 67% to 93%, and the 95% CI of the estimate from one study [43] does not include the estimates from the other three. Only two studies [30, 44] also reported MRI sensitivity in the same cases, and none reported FFDM accuracy. MRI sensitivity was 61% (95% CI 43–76) [30] and 69% (95% CI 53–82) [44]. Considering only the two studies with direct comparison, sensitivity was slightly higher for CEM than for MRI in the study by Iotti et al. [30] and almost identical in the study by Patel et al. [44]; pooled relative sensitivity of CEM vs. MRI was 1.15 (95% CI 0.939–1.404; $p = 0.18$).

Pooled specificity estimate for CEM was 94.0% (95% CI 78.3–98.6), with very limited heterogeneity, ranging from 83% to 100%. MRI specificity was 88% (95%

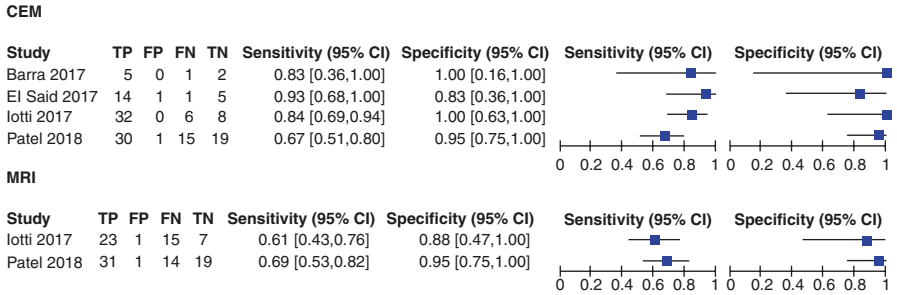

Fig. 8.6 Forest plot. Forest plot of study-specific estimates of CEM and MRI sensitivity and specificity. The blue squares and black horizontal lines represent the estimate and 95% confidence interval (CI) for each study

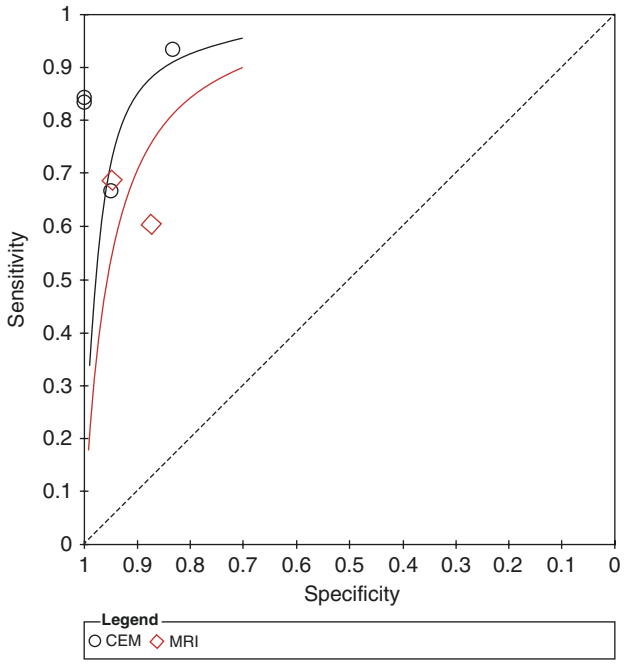

Fig. 8.7 Hierarchical summary receiver-operating characteristic (HSROC) plot for CEM and MRI

CI 47–100) [30] and 95% (95% CI 75–100) [44]. Direct comparison with between CEM and MRI resulted in slightly better specificity than MRI in the study by Iotti et al. [30] and identical specificity in the study by Patel et al. [44]; pooled relative specificity of CEM vs. MRI was 1.04 (95% CI 0.916–1.177; $p = 0.55$).

The estimated ROC curves are reported in Fig. 8.7. Although the estimated area under ROC curve is evidently larger for CEM, the difference between the two accuracy estimates is compatible with random fluctuations.

8.2.2.3 Agreement of CEM with Pathology and MRI in Measuring Lesion Diameter

Patel et al. [44] reported that CEM accurately showed final tumor size to within 1 cm in 72.3% of patients, underestimated tumor size by more than 1 cm in 20.0% of patients, and overestimated disease in 7.7%. MRI accurately showed final tumor size to within 1 cm in 69.2% of patients, underestimated tumor size by more than 1 cm in 23.1% patients, and overestimated tumor size by more than 1 cm in 7.7% of patients. Compared with histopathological results, CEM underestimated tumor size by 5.0 mm [standard deviation (SD) = 16.8], whereas MRI underestimated tumor size by 5.4 mm (SD = 15.5).

Iotti et al. [30] described that measurements on CEM agreed strongly with those on MRI, especially before (Lin's coefficient 0.96, CI 0.94–0.98) and during (Lin's coefficient 0.94, CI 0.89–0.97) NST, while after treatment, the agreement decreased (Lin's coefficient 0.76, CI 0.61–0.86), revealing considerable divergence, which reflects a different correlation with pathological assessment. After NST, 28% of patients had no residual pathological enhancement on CEM vs. 46% who did not on MRI. Comparing the post-NAC measurements with the pathological response in surgical specimens, CEM had stronger agreement with pathology than did MRI (Lin's coefficient 0.81 and 0.59, respectively; PCC 0.85 and 0.67, respectively). Both methods tended to underestimate the real extent of the residual tumor, with a mean underestimation of 4.1 mm (SD = 12.3) in CEM and of 7.5 mm in MRI (SD = 17.1).

8.2.2.4 Inter-reader Agreement of CEM

Barra et al. [45] described perfect agreement among readers regarding the presence or absence of residual tumors as determined by FFDM and CEM. In the assessment of residual tumor size compared to pathology, although inter-reader agreement was very good for both CEM and FFDM, it was slightly better for CEM. Three readers were involved in the study: a radiologist with 3 years of experience in CEM, a breast radiologist with over 10 years of practice, and a breast imaging fellow. As indirect evidence, in the diagnostic setting, the use of CEM increased the diagnostic performance of all readers, as was also reported by Dromain et al. [77] and Cheung et al. [53].

8.2.2.5 Other Outcomes and Resource Consumption

The practical aspects of the imaging technique have shown clinical advantages with respect to patient preferences. Claustrophobia and time constraints are the two most common complaints for breast MRI. Patients who undergo CEM often report lower rates of anxiety and higher rates of comfort compared to MRI. Time saving can be substantial, because MRI acquisition in most institutions lasts approximately 30–60 min, whereas CEM requires 7–10 min. Additionally, the potential for substantial cost savings compared with MRI makes CESM an appealing option in a stringent healthcare economy [44].

8.3 Prospective Vision

8.3.1 Possible Impact in Practice

In summary, in small numbers of patients, CEM has shown similar, or even better, accuracy than MRI for evaluation after neoadjuvant chemotherapy. The advantages of CEM over breast MRI include the short examination time, easy accessibility, and lower costs (about 80% less than for breast MRI) [78, 79]. Additionally, the low-energy mammogram that is part of the exam replaces the need for an additional mammogram and is useful for detection of the presence and extent of posttreatment calcifications [35]. The faster, lower-cost procedure, greater comfort, and significantly lower rates of anxiety [80, 81] must be taken into consideration when deciding what exams should be used in this population although some are concerned about the use of an iodine-based contrast agent instead of a gadolinium-based agent. Another limitation is that CEM does not include other anatomic details (i.e., chest wall and regional lymph nodes), which are captured by MRI, and no percutaneous biopsy technique exists yet to sample enhancing lesions on CEM [79].

The high PPV and specificity of CEM could be influenced by considering pCR no evidence of invasive or in situ disease. Including in the definition of pCR, the in situ (ypTis) or microinvasive (ypTmic) residual component (the so-called near-pCR), which remains debatable in terms of overall survival and disease-free survival, would probably decrease specificity and increase sensitivity. Nevertheless, such an extension of pCR definition would also require a redefinition of the criteria for defining pathological vs. non-pathological residual enhancement of the tumor bed after NST. In a meta-analysis about MRI in treatment monitoring, Marinovic et al. [21] described that near-pCR may plausibly overestimate accuracy relative to standard pCR definitions, and given the impact of residual malignancy on prognosis, the use of near-pCR as an outcome in the preoperative post-NST setting is not recommended.

On the other hand, no enhancement after NST remains the most challenging assessment. The lack of enhancement could be the effect of several situations: procedural (late acquisition after complete washout), pathologic (neoplastic invasion or obstruction of tumor blood vessels), and/or therapeutic (complete response). These factors affect MRI as well, which in this meta-analysis showed a sensitivity and NPV of 65.1% (with a relative sensitivity of 1.15, 95% CI 0.939–1.404; $p = 0.18$) and 47.3%, respectively. The higher spatial resolution and intrinsic different characteristics of contrast media may be the reason there are fewer false-negative CEM exams.

CEM is now a mature enough technique in terms of standardization of procedures, feasibility, promising accuracy results, and availability in practice to be considered as an alternative to MRI and FFDM.

8.3.2 Impact on Surgical Planning

The high pCR rates based on modern NST regimens lead to improved overall survival and disease-free survival outcomes [54]. NST effect on surgical planning

varies according to the volume of disease at presentation, response to treatment, tumor subtype, pre- and post-NST imaging and clinical assessment, and patient/surgeon preferences [54]. Breast-conserving surgery after NST is associated with improved cosmetic outcomes and improved aspects of quality of life compared to non-conservative surgery, and when associated with radiotherapy and the achievement of clear margins, it provides equivalent survival outcomes [14, 54, 58]. Arlow et al. [82] recently described even better survival with conservative surgery than non-conservative surgery without radiation. Van la Parra [14] even suggested that given high response rates in defined subgroups among exceptional responders (especially in HER2+ and TNBC), it should be questioned whether surgery is now a redundant procedure in their overall management, particularly when patients will often routinely be treated with adjuvant radiotherapy. However, the recent meta-analysis published by the Early Breast Cancer Trialists' Collaborative Group (EBCTCG) [83] described an increase in breast-conserving surgery in women who underwent NST worryingly associated with a significant increase in local recurrence 15 years after treatment (5.5%) [83]. The influence of breast cancer subtypes (especially HER2+ and TNBC) varies differently in these studies, affecting the results.

There is an urgent need to improve tumor assessment after NST based on better imaging and pathological analysis of specimens to more accurately predict which patients can be safely considered candidates for conservative surgery. Based on current data, there is no evidence supporting a positive effect of NST on clear margins and thus on a reduction of secondary surgery [61]. In several contemporary reports, neither FFDM, US, nor MRI can predict pCR (ypT0) with sufficient accuracy to replace the pathologic diagnosis of a surgical excision specimen [15].

In this scenario, CEM, an inexpensive, simple technique that has the potential to enhance sensitivity and specificity, could provide information on whether and how surgery should be done after neoadjuvant therapy.

8.3.3 Research Priorities

8.3.3.1 Dedicated Protocol

To improve a protocol for CEM dedicated to NST monitoring, further studies are encouraged, especially ones focusing on the optimal timing in CEM acquisition after NST. The antivascular effect of chemotherapeutic drugs slows the diffusion of contrast enhancement, as described both for Gd in MRI [67] and for iodinated agents for CT in breast assessment after NST [42]. Indeed, contrast agents move both via perfusion and via diffusion, and the latter has been described to be the preferential track when the residual disease is present as small foci or scattered cells [67]. When contrast agents move via diffusion, the amount of contrast reaching the tissue is time-dependent [67]. Evaluating iodinated contrast on CT for breast assessment after NST, Tozaki [42] described that late phase images were excellent for the depiction of the residual disease. Since a contrast agent moves to the ducts by diffusion, the amount of contrast reaching the tissue is time-dependent, which could be important in the

evaluation after NST, when the tumor tissue is affected by the antivascular effect of chemotherapeutic drugs, thus slowing the spread of enhancement [39]. Kim et al. [67] also described that when the residual disease is present as small foci or scattered cells, nutrients are received via diffusion rather than from vascular perfusion. Evaluating iodinated contrast on CT for breast assessment after NST, Tozaki [42] described that late phase images were excellent for the depiction of the residual disease.

For post-NAC CEM evaluation, a "delayed acquisition" should be considered, referring to the standard performed 2 and 4 min after injection. However, since iodine enhancement lasts at least 10 min, we should balance the advantage of delaying acquisition with the risk of false-negative artifacts due to washout [43]. This is a topic for a research on the technology.

8.3.3.2 Influence of Different Subtypes

The studies conducted so far on this topic have had small sample sizes [32, 45]. Nevertheless, results are encouraging and sufficient to have an initial judgment of CEM's overall accuracy but too small for the subgroup analysis that has been done with MRI. In this era of precision medicine, women are receiving personalized therapies; personalized protocols could also be defined to monitor the treatment itself. Cancer subtype is a known determinant of accuracy of the imaging in predicting complete response with MRI, and with larger populations of women undergoing CEM, there will be more evidence emerging on this point which could led to different monitoring protocols based on different cancer types. Another future source of research with CEM as is currently being done with MRI will include consideration of using posttreatment imaging (possibly with biopsy of non-enhancing tumor bed) to avoid post-NST surgery all together.

8.3.3.3 Early Response

Another potential research aim could be to determine if there is any clinical value in re-imaging at earlier time points after initiation of treatment with the theoretical advantage of changing suboptimal treatment to improve outcomes. The need for this remains disputed in the medical oncology community but may be worth pursuing as we learn more about this technology.

References

1. GLOBOCAN cancer fact sheets. http://globocan.iarc.fr/old/FactSheets/cancers/breast-new.asp. Accessed 28 Jul 2018.
2. SEER Surveillance, Epidemiology and End Results Program. https://seer.cancer.gov/statfacts/html/breast.html. Accessed 28 Jul 2018.
3. Sant M, Chirlaque Lopez MD, Agresti R, Sánchez Pérez MJ, Holleczek B, Bielska-Lasota M, et al. Survival of women with cancers of breast and genital organs in Europe 1999–2007: results of the EUROCARE-5 study. Eur J Cancer. 2015;51(15):2191–205. https://doi.org/10.1016/j.ejca.2015.07.022.
4. Plevritis SK, Munoz D, Kurian AW, Stout NK, Alagoz O, Near AM, et al. Association of screening and treatment with breast cancer mortality by molecular subtype in US women, 2000–2012. JAMA. 2018;319(2):154–64. https://doi.org/10.1001/jama.2017.19130.

5. NCCN clinical practice guidelines in oncology, breast cancer, version 1.2018, 20 Mar 2018.
6. FDA Food and Drug Administration. http://www.fda.gov/downloads/Drugs/GuidanceComplianceRegulatoryInformation/Guidances/UCM305501.pdf. Accessed 28 Jul 2018.
7. Hennigs A, Riedel F, Marmé F, Sinn P, Lindel K, Gondos A, et al. Changes in chemotherapy usage and outcome of early breast cancer patients in the last decade. Breast Cancer Res Treat. 2016;160(3):491–9. https://doi.org/10.1007/s10549-016-4016-4.
8. Cortazar P, Zhang L, Untch M, Mehta K, Costantino JP, Wolmark N, et al. Pathological complete response and long-term clinical benefit in breast cancer: the CTNeoBC pooled analysis. Lancet. 2014;384(9938):164–72. https://doi.org/10.1016/S0140-6736(13)62422-8.
9. Senkus E, Kyriakides S, Ohno S, Penault-Llorca F, Poortmans P, Rutgers E, et al. Primary breast cancer: ESMO clinical practice guidelines for diagnosis, treatment and follow-up. Ann Oncol. 2015;26(Suppl 5):v8–30. https://doi.org/10.1093/annonc/mdv298.
10. Mohiuddin JJ, Deal AM, Carey LA, Lund JL, Baker BR, Zagar TM, et al. Neoadjuvant systemic therapy use for younger patients with breast cancer treated in different types of cancer centers across the United States. J Am Coll Surg. 2016;223(5):717–728.e4. https://doi.org/10.1016/j.jamcollsurg.2016.08.541.
11. Schrading S, Kuhl CK. Breast cancer: influence of taxanes on response assessment with dynamic contrast-enhanced MR imaging. Radiology. 2015;277(3):687–96. https://doi.org/10.1148/radiol.2015150006.
12. Von Minckwitz G, Untch M, Blohmer JU, Costa SD, Eidtmann H, Fasching PA, et al. Definition and impact of pathologic complete response on prognosis after neoadjuvant chemotherapy in various intrinsic breast cancer subtypes. J Clin Oncol. 2012;30(15):1796–804. https://doi.org/10.1200/JCO.2011.38.8595.
13. Semiglazov V. RECIST for response (clinical and imaging) in neoadjuvant clinical trials in operable breast cancer. J Natl Cancer Inst Monogr. 2015;2015(51):21–3. https://doi.org/10.1093/jncimonographs/lgv021.
14. van la Parra RF, Kuerer HM. Selective elimination of breast cancer surgery in exceptional responders: historical perspective and current trials. Breast Cancer Res. 2016;18(1):28. https://doi.org/10.1186/s13058-016-0684-6. Review.
15. Mazouni C, Peintinger F, Wan-Kau S, et al. Residual ductal carcinoma in situ in patients with complete eradication of invasive breast cancer after neoadjuvant chemotherapy does not adversely affect patient outcome. J Clin Oncol. 2007;25:2650–5.
16. Yim H, Ha T, Kang DK, Park SY, Jung Y, Kim TH. Change in microcalcifications on mammography after neoadjuvant chemotherapy in breast cancer patients: correlation with tumor response grade and comparison with lesion extent. Acta Radiol. 2018;1:284185118776491. https://doi.org/10.1177/0284185118776491.
17. Croshaw R, Shapiro-Wright H, Svensson E, Erb K, Julian T. Accuracy of clinical examination, digital mammogram, ultrasound, and MRI in determining postneoadjuvant pathologic tumor response in operable breast cancer patients. Ann Surg Oncol. 2011;18(11):3160–3. https://doi.org/10.1245/s10434-011-1919-5.
18. Athanasiou A, Latorre-Ossa H, Criton A, Tardivon A, Gennisson JL, Tanter M. Feasibility of imaging and treatment monitoring of breast lesions with three-dimensional shear wave elastography. Ultraschall Med. 2017;38(1):51–9. https://doi.org/10.1055/s-0034-1398980.
19. Hoyt K, Umphrey H, Lockhart M, Robbin M, Forero-Torres A. Ultrasound imaging of breast tumor perfusion and neovascular morphology. Ultrasound Med Biol. 2015;41(9):2292–302. https://doi.org/10.1016/j.ultrasmedbio.2015.04.016.
20. Lobbes MB, Prevos R, Smidt M, Tjan-Heijnen VC, van Goethem M, Schipper R, et al. The role of magnetic resonance imaging in assessing residual disease and pathologic complete response in breast cancer patients receiving neoadjuvant chemotherapy: a systematic review. Insights Imaging. 2013;4(2):163–75. https://doi.org/10.1007/s13244-013-0219-y.
21. Marinovich ML, Houssami N, Macaskill P, Sardanelli F, Irwig L, Mamounas EP, et al. Meta-analysis of magnetic resonance imaging in detecting residual breast cancer after neoadjuvant therapy. J Natl Cancer Inst. 2013;105(5):321–33.

22. Marinovich ML, Macaskill P, Irwig L, Sardanelli F, Mamounas E, von Minckwitz G, et al. Agreement between MRI and pathologic breast tumor size after neoadjuvant chemotherapy, and comparison with alternative tests: individual patient data meta-analysis. BMC Cancer. 2015;15:662. https://doi.org/10.1186/s12885-015-1664-4.
23. Bufi E, Belli P, Costantini M, Cipriani A, Di Matteo M, Bonatesta A, et al. Role of the apparent diffusion coefficient in the prediction of response to neoadjuvant chemotherapy in patients with locally advanced breast cancer. Clin Breast Cancer. 2015;15(5):370–80. https://doi.org/10.1016/j.clbc.2015.02.002.
24. Gao W, Guo N, Dong T. Diffusion-weighted imaging in monitoring the pathological response to neoadjuvant chemotherapy in patients with breast cancer: a meta-analysis. World J Surg Oncol. 2018;16(1):145. https://doi.org/10.1186/s12957-018-1438-y.
25. Ashraf A, Gaonkar B, Mies C, DeMichele A, Rosen M, Davatzikos C, et al. Breast DCE-MRI kinetic heterogeneity tumor markers: preliminary associations with neoadjuvant chemotherapy response. Transl Oncol. 2015;8(3):154–62. https://doi.org/10.1016/j.tranon.2015.03.005.
26. Lee J, Kim SH, Kang BJ. Pretreatment prediction of pathologic complete response to neoadjuvant chemotherapy in breast cancer: perfusion metrics of dynamic contrast enhanced MRI. Sci Rep. 2018;8(1):9490. https://doi.org/10.1038/s41598-018-27764-9.
27. Hilal T, Covington M, Kosiorek HE, Zwart C, Ocal IT, Pockaj BA, Northfelt DW, Patel BK. Breast MRI phenotype and background parenchymal enhancement may predict tumor response to neoadjuvant endocrine therapy. Breast J. 2018; https://doi.org/10.1111/tbj.13101.
28. Jochelson MS, Lampen-Sachar K, Gibbons G, Dang C, Lake D, Morris EA, et al. Do MRI and mammography reliably identify candidates for breast conservation after neoadjuvant chemotherapy? Ann Surg Oncol. 2015;22(5):1490–5. https://doi.org/10.1245/s10434-015-4502-7.
29. McDonald RJ, McDonald JS, Kallmes DF, Jentoft ME, Murray DL, Thielen KR, et al. Intracranial gadolinium deposition after contrast-enhanced MR imaging. Radiology. 2015;275(3):772–82. https://doi.org/10.1148/radiol.15150025.
30. Iotti V, Ravaioli S, Vacondio R, Coriani C, Caffarri S, Sghedoni R, et al. Contrast-enhanced spectral mammography in neoadjuvant chemotherapy monitoring: a comparison with breast magnetic resonance imaging. Breast Cancer Res. 2017;19(1):106. https://doi.org/10.1186/s13058-017-0899-1.
31. Patel BK, Lobbes MBI, Lewin J. Contrast enhanced spectral mammography: a review. Semin Ultrasound CT MR. 2018;39(1):70–9. https://doi.org/10.1053/j.sult.2017.08.005.
32. ElSaid NAE, Mahmoud HGM, Salama A, Nabil M, ElDesouky ED. Role of contrast enhanced spectral mammography in predicting pathological response of locally advanced breast cancer post neo-adjuvant chemotherapy. Egypt J Radiol Nucl Med. 2017;48(2):519–27.
33. Lewis TC, Pizzitola VJ, Giurescu ME, Eversman WG, Lorans R, Robinson KA, et al. Contrast-enhanced digital mammography: a single-institution experience of the first 208 cases. Breast J. 2017;23(1):67–76. https://doi.org/10.1111/tbj.12681.
34. Jochelson MS, Dershaw DD, Sung JS, Heerdt AS, Thornton C, Moskowitz CS, et al. Bilateral contrast-enhanced dual-energy digital mammography: feasibility and comparison with conventional digital mammography and MR imaging in women with known breast carcinoma. Radiology. 2013;266(3):743–51. https://doi.org/10.1148/radiol.12121084.
35. Łuczyńska E, Heinze-Paluchowska S, Hendrick E, Dyczek S, Ryś J, Herman K, et al. Comparison between breast MRI and contrast-enhanced spectral mammography. Med Sci Monit. 2015;21:1358–67. https://doi.org/10.12659/MSM.893018.
36. Lobbes MB, Lalji UC, Nelemans PJ, Houben I, Smidt ML, Heuts E, et al. The quality of tumour size assessment by contrast-enhanced spectral mammography and the benefit of additional breast MRI. J Cancer. 2015;6(2):144–50. https://doi.org/10.7150/jca.10705.
37. Fallenberg EM, Schmitzberger FF, Amer H, Ingold-Heppner B, Balleyguier C, Diekmann F, et al. Contrast-enhanced spectral mammography vs. mammography and MRI – clinical performance in a multi-reader evaluation. Eur Radiol. 2017;27(7):2752–64. https://doi.org/10.1007/s00330-016-4650-6.
38. Fallenberg EM, Dromain C, Diekmann F, Engelken F, Krohn M, Singh JM, et al. Contrast-enhanced spectral mammography versus MRI: initial results in the detection of breast can-

cer and assessment of tumour size. Eur Radiol. 2014;24(1):256–64. https://doi.org/10.1007/s00330-013-3007-7.
39. Li L, Roth R, Germaine P, Ren S, Lee M, Hunter K, et al. Contrast-enhanced spectral mammography (CESM) versus breast magnetic resonance imaging (MRI): a retrospective comparison in 66 breast lesions. Diagn Interv Imaging. 2017;98(2):113–23. https://doi.org/10.1016/j.diii.2016.08.013.
40. Łuczyńska E, Niemiec J, Hendrick E, Heinze S, Jaszczyński J, Jakubowicz J, et al. Degree of enhancement on contrast enhanced spectral mammography (CESM) and lesion type on mammography (MG): comparison based on histological results. Med Sci Monit. 2016;22:3886–93.
41. Goorts B, Dreuning KMA, Houwers JB, Kooreman LFS, Boerma EG, Mann RM, et al. MRI-based response patterns during neoadjuvant chemotherapy can predict pathological (complete) response in patients with breast cancer. Breast Cancer Res. 2018;20(1):34. https://doi.org/10.1186/s13058-018-0950-x.
42. Tozaki M, Kobayashi T, Uno S, Aiba K, Takeyama H, Shioya H, et al. Breast-conserving surgery after chemotherapy: value of MDCT for determining tumor distribution and shrinkage pattern. AJR Am J Roentgenol. 2006;186(2):431–9.
43. Richter V, Hatterman V, Preibsch H, Bahrs SD, Hahn M, Nikolaou K, et al. Contrast-enhanced spectral mammography in patients with MRI contraindications. Acta Radiol. 2018;59(7):798–805. https://doi.org/10.1177/0284185117735561.
44. Patel BK, Hilal T, Covington M, Zhang N, Kosiorek HE, Lobbes M, et al. Contrast-enhanced spectral mammography is comparable to MRI in the assessment of residual breast cancer following neoadjuvant systemic therapy. Ann Surg Oncol. 2018;25(5):1350–6. https://doi.org/10.1245/s10434-018-6413-x.
45. Barra FR, de Souza FF, Camelo REFA, Ribeiro ACO, Farage L. Accuracy of contrast-enhanced spectral mammography for estimating residual tumor size after neoadjuvant chemotherapy in patients with breast cancer: a feasibility study. Radiol Bras. 2017;50(4):224–30. https://doi.org/10.1590/0100-3984.2016-0029.
46. Park S, Yoon JH, Sohn J, Park HS, Moon HJ, Kim MJ, et al. Magnetic resonance imaging after completion of neoadjuvant chemotherapy can accurately discriminate between no residual carcinoma and residual ductal carcinoma in situ in patients with triple-negative breast cancer. PLoS One. 2016;11(2):e0149347. https://doi.org/10.1371/journal.pone.0149347. eCollection 2016.
47. Kim YS, Chang JM, Moon HG, Lee J, Shin SU, Moon WK. Residual mammographic microcalcifications and enhancing lesions on MRI after neoadjuvant systemic chemotherapy for locally advanced breast cancer: correlation with histopathologic residual tumor size. Ann Surg Oncol. 2016;23(4):1135–42. https://doi.org/10.1245/s10434-015-4993-2.
48. Feliciano Y, Mamtani A, Morrow M, Stempel MM, Patil S, Jochelson MS. Do calcifications seen on mammography after neoadjuvant chemotherapy for breast cancer always need to be excised? Ann Surg Oncol. 2017;24(6):1492–8. https://doi.org/10.1245/s10434-016-5741-y.
49. Um E, Kang JW, Lee S, Kim HJ, Yoon TI, Sohn G, et al. Comparing accuracy of mammography and magnetic resonance imaging for residual calcified lesions in breast cancer patients undergoing neoadjuvant systemic therapy. Clin Breast Cancer. 2018;pii:S1526–8209(17)30614-6. https://doi.org/10.1016/j.clbc.2018.03.011.
50. Tennant SL, James JJ, Cornford EJ, Chen Y, Burrell HC, Hamilton LJ, Girio-Fragkoulakis C. Contrast-enhanced spectral mammography improves diagnostic accuracy in the symptomatic setting. Clin Radiol. 2016;71(11):1148–55. https://doi.org/10.1016/j.crad.2016.05.009.
51. Francescone MA, Jochelson MS, Dershaw DD, Sung JS, Hughes MC, Zheng J, et al. Low energy mammogram obtained in contrast-enhanced digital mammography (CEDM) is comparable to routine full-field digital mammography (FFDM). Eur J Radiol. 2014;83(8):1350–5. https://doi.org/10.1016/j.ejrad.2014.05.015.
52. Lalji UC, Jeukens CR, Houben I, Nelemans PJ, van Engen RE, van Wylick E, et al. Evaluation of low-energy contrast-enhanced spectral mammography images by comparing them to full-field digital mammography using EUREF image quality criteria. Eur Radiol. 2015;25(10):2813–20. https://doi.org/10.1007/s00330-015-3695-2.

53. Cheung YC, Lin YC, Wan YL, Yeow KM, Huang PC, Lo YF, et al. Diagnostic performance of dual-energy contrast-enhanced subtracted mammography in dense breasts compared to mammography alone: interobserver blind reading analysis. Eur Radiol. 2014;24(10):2394–403. https://doi.org/10.1007/s00330-014-3271-1.
54. Criscitiello C, Golshan M, Barry WT, Viale G, Wong S, Santangelo M, et al. Impact of neoadjuvant chemotherapy and pathological complete response on eligibility for breast-conserving surgery in patients with early breast cancer: a meta-analysis. Eur J Cancer. 2018;97:1–6. https://doi.org/10.1016/j.ejca.2018.03.023.
55. Karakatsanis A, Tasoulis MK, Wärnberg F, Nilsson G, MacNeill F. Meta-analysis of neoadjuvant therapy and its impact in facilitating breast conservation in operable breast cancer. Br J Surg. 2018;105(5):469–81. https://doi.org/10.1002/bjs.10807. Review.
56. Kawashima H, Inokuchi M, Furukawa H, Ikeda H, Kitamura S. Magnetic resonance imaging features of breast cancer according to intrinsic subtypes: correlations with neoadjuvant chemotherapy effects. Springerplus. 2014;3:240. https://doi.org/10.1186/2193-1801-3-240. eCollection 2014.
57. Mukhtar RA, Yau C, Rosen M, Tandon VJ, I-SPY 1 TRIAL and ACRIN 6657 Investigators, Hylton N, Esserman LJ. Clinically meaningful tumor reduction rates vary by prechemotherapy MRI phenotype and tumor subtype in the I-SPY 1 TRIAL (CALGB 150007/150012; ACRIN 6657). Ann Surg Oncol. 2013;20(12):3823–30. https://doi.org/10.1245/s10434-013-3038-y.
58. Tomida K, Ishida M, Umeda T, Sakai S, Kawai Y, Mori T, et al. Magnetic resonance imaging shrinkage patterns following neoadjuvant chemotherapy for breast carcinomas with an emphasis on the radiopathological correlations. Mol Clin Oncol. 2014;2(5):783–8.
59. Li M, Xu B, Shao Y, Liu H, Du B, Yuan J. Magnetic resonance imaging patterns of tumor regression in breast cancer patients after neo-adjuvant chemotherapy, and an analysis of the influencing factors. Breast J. 2017;23(6):656–62. https://doi.org/10.1111/tbj.12811.
60. Boughey JC, McCall LM, Ballman KV, Mittendorf EA, Ahrendt GM, Wilke LG, et al. Tumor biology correlates with rates of breast-conserving surgery and pathologic complete response after neoadjuvant chemotherapy for breast cancer: findings from the ACOSOG Z1071 (Alliance) prospective multicenter clinical trial. Ann Surg. 2014;260(4):608–14.; discussion 614–6. https://doi.org/10.1097/SLA.0000000000000924.
61. Volders JH, Negenborn VL, Spronk PE, Krekel NMA, Schoonmade LJ, Meijer S, et al. Breast-conserving surgery following neoadjuvant therapy-a systematic review on surgical outcomes. Breast Cancer Res Treat. 2018;168(1):1–12. https://doi.org/10.1007/s10549-017-4598-5.
62. Travieso-Aja MDM, Naranjo-Santana P, Fernández-Ruiz C, Severino-Rondón W, Maldonado-Saluzzi D, Rodríguez Rodríguez M, et al. Factors affecting the precision of lesion sizing with contrast-enhanced spectral mammography. Clin Radiol. 2018;73(3):296–303. https://doi.org/10.1016/j.crad.2017.10.017.
63. Iotti V, Ravaioli S, Sghedoni R, Coriani C, Vacondio R, Caffarri S, et al. Monitoring neoadjuvant chemotherapy: comparison of contrast-enhanced spectral mammography (CESM) and MRI versus breast cancer characteristics. ECR. 2016. https://doi.org/10.1594/ecr2016/B-1062
64. Iotti V, Ravaioli S, Levrini G, Marchesi V, Coriani C, Caffarri S, et al. Breast cancer characteristics and shrinkage patterns in neo-adjuvant chemotherapy monitoring: comparison between contrast-enhanced spectral mammography and breast-MRI. RSNA. 2016.
65. Luczynska E, Niemiec J, Heinze S, Adamczyk A, Ambicka A, Marcyniuk P, et al. Intensity and pattern of enhancement on CESM: prognostic significance and its relation to expression of podoplanin in tumor stroma – a preliminary report. Anticancer Res. 2018;38(2):1085–95.
66. Ah-See ML, Makris A, Taylor NJ, Harrison M, Richman PI, Burcombe RJ, et al. Early changes in functional dynamic magnetic resonance imaging predict for pathologic response to neoadjuvant chemotherapy in primary breast cancer. Clin Cancer Res. 2008;14(20):6580–9. https://doi.org/10.1158/1078-0432.CCR-07-4310.
67. Kim TH, Kang DK, Yim H, Jung YS, Kim KS, Kang SY. Magnetic resonance imaging patterns of tumor regression after neoadjuvant chemotherapy in breast cancer patients: correlation with pathological response grading system based on tumor cellularity. J Comput Assist Tomogr. 2012;36(2):200–6. https://doi.org/10.1097/RCT.0b013e318246abf3.

68. Ballesio L, Gigli S, Di Pastena F, Giraldi G, Manganaro L, Anastasi E, et al. Magnetic resonance imaging tumor regression shrinkage patterns after neoadjuvant chemotherapy in patients with locally advanced breast cancer: correlation with tumor biological subtypes and pathological response after therapy. Tumor Biol. 2017;39(3):1010428317694540. https://doi.org/10.1177/1010428317694540.
69. Hylton NM, Gatsonis CA, Rosen MA, Lehman CD, Newitt DC, Partridge SC, et al. Neoadjuvant chemotherapy for breast cancer: functional tumor volume by MR imaging predicts recurrence-free survival-results from the ACRIN 6657/CALGB 150007 I-SPY 1 TRIAL. Radiology. 2016;279(1):44–55. https://doi.org/10.1148/radiol.2015150013.
70. Fukada I, Araki K, Kobayashi K, Shibayama T, Takahashi S, Gomi N, et al. Pattern of tumor shrinkage during neoadjuvant chemotherapy is associated with prognosis in low-grade luminal early breast cancer. Radiology. 2018;286(1):49–57. https://doi.org/10.1148/radiol.2017161548.
71. Esserman L, Kaplan E, Partridge S, Tripathy D, Rugo H, Park J, et al. MRI phenotype is associated with response to doxorubicin and cyclophosphamide neoadjuvant chemotherapy in stage III breast cancer. Ann Surg Oncol. 2001;8(6):549–59.
72. Ambicka A, Luczynska E, Adamczyk A, Harazin-Lechowska A, Sas-Korczynska B, Niemiec J. The tumor border on contrast-enhanced spectral mammography and its relation to histological characteristics of invasive breast cancer. Pol J Pathol. 2016;67(3):295–9. https://doi.org/10.5114/pjp.2016.63783.
73. Chen JH, Yu HJ, Hsu C, Mehta RS, Carpenter PM, Su MY. Background parenchymal enhancement of the contralateral normal breast: association with tumor response in breast cancer patients receiving neoadjuvant chemotherapy. Transl Oncol. 2015;8(3):204–9. https://doi.org/10.1016/j.tranon.2015.04.001.
74. Sogani J, Morris EA, Kaplan JB, D'Alessio D, Goldman D, Moskowitz CS, et al. Comparison of background parenchymal enhancement at contrast-enhanced spectral mammography and breast MR imaging. Radiology. 2017;282(1):63–73. https://doi.org/10.1148/radiol.2016160284.
75. Savaridas SL, Taylor DB, Gunawardana D, Phillips M. Could parenchymal enhancement on contrast-enhanced spectral mammography (CESM) represent a new breast cancer risk factor? Correlation with known radiology risk factors. Clin Radiol. 2017;72(12):1085.e1–9. https://doi.org/10.1016/j.crad.2017.07.017.
76. Hattangadi J, Park C, Rembert J, Klifa C, Hwang J, Gibbs J, et al. Breast stromal enhancement on MRI is associated with response to neoadjuvant chemotherapy. AJR Am J Roentgenol. 2008;190(6):1630–6. https://doi.org/10.2214/AJR.07.2533.
77. Dromain C, Thibault F, Diekmann F, Fallenberg EM, Jong RA, Koomen M, et al. Dual-energy contrast enhanced digital mammography: initial clinical results of a multireader, multicase study. Breast Cancer Res. 2012;14:R94.
78. Patel BK, Gray RJ, Pockaj BA. Potential cost savings of contrast-enhanced digital mammography. AJR Am J Roentgenol. 2017;208(6):W231–7. https://doi.org/10.2214/AJR.16.17239.
79. Ali-Mucheru M, Pockaj B, Patel B, Pizzitola V, Wasif N, Stucky CC, et al. Contrast-enhanced digital mammography in the surgical management of breast cancer. Ann Surg Oncol. 2016;23(Suppl 5):649–55.
80. Hobbs MM, Taylor DB, Buzynski S, Peake RE. Contrast-enhanced spectral mammography (CESM) and contrast enhanced MRI (CEMRI): patient preferences and tolerance. J Med Imaging Radiat Oncol. 2015;59(3):300–5. https://doi.org/10.1111/1754-9485.12296.
81. Phillips J, Miller MM, Mehta TS, Fein-Zachary V, Nathanson A, Hori W, et al. Contrast-enhanced spectral mammography (CESM) versus MRI in the high-risk screening setting: patient preferences and attitudes. Clin Imaging. 2017;42:193–7. https://doi.org/10.1016/j.clinimag.2016.12.011.
82. Arlow RL, Paddock LE, Niu X, Kirstein L, Haffty BG, Goyal S, et al. Breast-conservation therapy after neoadjuvant chemotherapy does not compromise 10-year breast cancer-specific mortality. Am J Clin Oncol. 2018. https://doi.org/10.1097/COC.0000000000000456.
83. Early Breast Cancer Trialists' Collaborative Group (EBCTCG). Long-term outcomes for neoadjuvant versus adjuvant chemotherapy in early breast cancer: meta-analysis of individual patient data from ten randomised trials. Lancet Oncol. 2018;19:27–39.